

**THE IMPACT OF CONTAINER CARRIER HEAVY
GOODS VEHICLES ON ROAD TRANSPORTATION
OPERATION, SAFETY, AND LOGISTICS**

AHMED ADNAN MAKKI

**A thesis submitted in partial fulfilment of the requirements of Liverpool
John Moores University for the degree of Doctor of Philosophy**

June 2021

CONTENTS

LIST OF FIGURES.....	VIII
LIST OF TABLES	XVIII
ABSTRACT.....	XXII
DECLARATION OF AUTHOR’S RIGHT	XXIII
ACKNOWLEDGEMENTS	XXIV
LIST OF ABBREVIATIONS.....	XXV
LIST OF GLOSSARIES	XXX
VAIRIABLES’ DEFINITIONS, UNITS, INITIAL VALUES, AND CONSTRIANS.....	XXXIII
CHAPTER ONE: INTRODUCTION	1
1.1 BACKGROUND	1
1.2 INTERMODAL TRANSPORTATION.....	1
1.2.1 Freight rail	1
1.2.2 Inland Waterway Freight	2
1.2.3 Road freight	2
1.2.4 Urban Consolidation Centres.....	6
1.3 PASSENGER CAR EQUIVALENT	7
1.4 SYSTEM DYNAMICS.....	8
1.4.1 Causal Loop Diagram.....	10

1.4.2	Stock and Flow	12
1.5	RESEARCH MOTIVATION	14
1.6	RESEARCH OBJECTIVES	15
1.7	RESEARCH LIMITATION	16
1.8	RESEARCH CONTRIBUTIONS.....	16
1.9	RESEARCH APPLICATIONS.....	17
1.10	THESIS OUTLINES.....	18
1.11	PUBLICATIONS.....	19
	CHAPTER TWO: LITERATURE REVIEW	20
2.1	INTRODUCTION	20
2.2	LITERATURE REVIEW.....	21
2.2.1	PCE Estimation Methods.....	21
2.2.1.1	PCE based on Traffic Flow and Vehicle Proportion.....	22
2.2.1.2	PCE based on Speed, Travel Time, and Delay	25
2.2.1.3	PCE Based Queue Discharge	29
2.2.1.4	PCE based on Vehicle's Headway	30
2.2.1.5	PCE at Tunnels and Roundabouts.....	33
2.2.2	Acceleration and Deceleration.....	35
2.2.3	Deceleration Forces	37
2.2.5	Reaction Time and Braking Competency Level.....	41
2.2.6	Stopping Distance.....	44

2.2.7	Road Capacity Estimation	46
2.2.8	Effective Green Ratio	48
2.2.9	Automatic Traffic Counters	50
2.2.9.1	Intrusive ATC Technologies	51
2.2.9.2	Non-intrusive ATC Technologies	52
2.2.10	System Dynamics	53
2.3	SUMMARY OF LITERATURE REVIEW	54
CHAPTER THREE: PASSENGER CAR EQUIVALENT AND ROAD CAPACITY ESTIMATION		55
3.1	INTRODUCTION	55
3.2	METHODOLOGY	56
3.2.1	Deceleration Component	59
3.2.2	Acceleration Component	66
3.2.3	Effective Green Ratio	72
3.2.4	Deceleration and Acceleration Space Capacity Method	73
3.2.5	Rescheduling HGVa	74
3.3	FINDINGS AND ANALYSIS	77
3.3.1	Vehicle's Headway	77
3.3.2	Passenger Car Equivalent	79
3.3.3	Volume to Capacity Ratio and Capacity	85
3.3.4	Passenger Car Equivalent Methods	89
3.3.5	Rescheduling HGVa	94

3.3.5	Annual TEU.....	95
3.4	SUMMARY, CONTRIBUTION AND NOVELTY.....	96
CHAPTER FOUR: TRAFFIC SPEED FLOW PREDICTION		98
4.1	INTRODUCTION	98
4.2	FLOW SPEED ESTIMATION METHODS.....	99
4.2.1	Greenshields Method.....	99
4.2.2	Greenberg Method.....	100
4.2.3	Underwood Method.....	101
4.2.4	Two Regime Method.....	102
4.2.5	Pipes’s Method	102
4.2.6	Drew’s Method.....	103
4.2.7	Drake’s Method.....	103
4.2.8	Kinetic wave speed Method	104
4.2.9	Logistic curve method	104
4.2.10	Gaddam’s method.....	105
4.3	SPEED PREDICTION PARAMETERS	105
4.3	FLOW SPEED ANALYSIS	107
4.3.1	Flow Speed Parameters.....	107
4.3.2	Flow Speed Methods’ Analysis	109
4.3.3	New Flow Speed Methodology	120
4.4	ESTIMATING INDIVIDUAL VEHICLE’S SPEEDS	121

4.5	RESCHEDULING ARTICULATED HGV	125
4.6	LOGISTICS AND ROAD PLANNING OPTIONS	126
4.7	SUMMARY AND CONTRIBUTION AND NOVELTY	132
CHAPTER FIVE: LEVEL OF SERVICE		133
5.1	INTRODUCTION	133
5.2	LEVEL OF SERVICE	135
5.3	METHODOLOGY	139
5.3.1	Available reaction time and available stopping distance	140
5.3.2	Risk of sustaining severe injuries or death	143
5.4	FINDINGS	146
5.5	SUMMARY	156
5.6	CONTRIBUTION AND NOVELTY	156
CHAPTER SIX: MODEL's system and data VALIDATION		158
6.1	INTRODUCTION	158
6.2	THE BUILDING OF THE SYSTEM DYNAMICS MODEL	158
6.2.1	Conceptualization	158
6.2.1.1	Purpose	159
6.2.1.2	Variable's Relationship	159
6.2.1.3	Mechanism	159
6.2.2	Model Structure	165
6.3	DATA VALIDATION	172

6.3.1	Data Evaluation	172
6.3.2	ATC Data Imputation.....	174
6.3.3	Headway Measurement	174
6.3.4	Manual Count and Observation.....	175
6.3.5	Traffic Flow Data Validation and Analysis.....	176
6.4	MODEL SYSTEM VALIDATION.....	183
CHAPTER SEVEN: CONCLUSIONS AND FUTURE WORK.....		200
7.1	CONCLUSIONS	200
7.2	FUTURE WORK	201
REFERENCES.....		203
APPENDIX A: INTRODUCTION		215
A.1	AUTOMATIC RAIL TIMETABLE.....	215
A.2	INLAND WATERWAY FREIGHT OPERATIONAL BARRIERS.....	216
APPENDIX B: ATC IMPUTED DATA.....		218

LIST OF FIGURES

FIGURE 1-1: Option A is to upgrade the existing A5036 road with junction improvements (HE 2017)..... 4

FIGURE 1-2: Option B is to build a new dual carriageway bypass through the Rimrose Valley (HE 2017)..... 5

FIGURE 1-3: Option C is several improvement options for both the existing A5036 and bypass were considered and discounted for a variety of reasons (HE 2017) 6

FIGURE 1-4: A demonstration of the vehicle’s length effect on the PCE value (The author has created this image) 8

FIGURE 1-5: Cause and Effect Relationship (The author has created this image)..... 10

FIGURE 1-6: A causal loop for population, birth, and death cause and effect (The author has created this image) 11

FIGURE 1-7: A representation of functions for population-birth has exponential growth function (Kirkwood 2013) 11

FIGURE 1-8: A representation of functions for population-death has a goal-seeking function (Kirkwood 2013) 12

FIGURE 1-9: Stock and flow diagram (Kirkwood 2013) 12

FIGURE 1-10: The stock and flow diagram of the system in FIGURE 1-6 (Kirkwood 2013)..... 13

FIGURE 1-11: Stock and flow diagram (The author has created this image)..... 13

FIGURE 2-1: Average PCE of all non-PC vehicles on the DBR A5036 of link A5038-B5207.....23

FIGURE 2-2: F_{hv} with a linear increase of P_T (0 to 0.3) and PCE_T (1 to 4) 23

FIGURE 2-3: F_{hv} with a linear increase of PCE_T (1 to 4) and constant P_T of 0.1 23

FIGURE 2-4: F_{hv} with constant PCE_T of 3 and linear increase in P_T 23

FIGURE 2-5: Average PCE of all non-PC vehicles using methods of Saturation flow, Huber (1982), and St. John (1976) as in (2-6), (2-7),..... 24

FIGURE 2-6: Average PCE value of all non-PC vehicles using Sumner’s formula (2-10) by Sumner (1984).....	25
FIGURE 2-7: The composite PCE value of non-PC of 14 non-PC vehicle types by Cunagin (1983).....	26
FIGURE 2-8: The composite of non-PC vehicles’ PCE by Rahman (2005).....	28
FIGURE 2-9: Estimated PCE at tunnels by Ahmed (2017).....	33
FIGURE 2-10: Illustration of the wind aerodynamics	38
FIGURE 2-11: A queue of N vehicles at the intersection (TRB 2000) (Mathew 2014)	49
FIGURE 2-12: The start-up lost time and saturation headway (TRB 2000) (Mathew,2014)	49
FIGURE 2-13: Inductive Loop traffic flow detector (the has created this image).....	50
FIGURE 3-1: Vehicles’ headways at ABCL of 50%, 75%, and 100% and ATS of DBR.....	77
FIGURE 3-2: The ATS obtained from ATCs at ATS of DBR.....	78
FIGURE 3-3: HGVa headway before and after adding an extra space at ABCL of 50%, 75%, and 100% and ATS of DBR	78
FIGURE 3-4: Impact of changing the HGVs’ GM on their safe headways at ABCL of 50%, 75%, and 100% and ATS of DBR.....	78
FIGURE 3-5: PCE_{DASi} values for LGV, HGVR, and HGVa (no extra space) vehicles at an ABCL of 50%, 75%, and 100% and ATS of DBR.....	80
FIGURE 3-6: PCE_{DAS} values for HGVa after adding an extra space at an ABCL of 50%, 75%, and 100% and ATS of DBR	80
FIGURE 3-7: Composite proportions of non-PCE traffic flow volumes and ATS of DBR	81
FIGURE 3-8: Vehicles’ proportions of traffic flow using PCE converted traffic flow volumes at ABCL of 50% and ATS of DBR.....	82

FIGURE 3-9: Vehicles' proportions of traffic flow using PCE converted traffic flow volumes at ABCL of 75% and ATS of DBR.....	82
FIGURE 3-10: Vehicles' proportions of traffic flow using PCE converted traffic flow volumes at ABCL of 100% and ATS of DBR.....	83
FIGURE 3-11: PC, LGV, HGVr, HGVa, TF, and TF_{PCE} flow volumes at ABCL of 50%, 75%, and 100% and ATS of DBR.....	84
FIGURE 3-12: Impact of GM (as a percentage of MAM) level on the PCE_{DAS} and ATS of DBR.....	84
FIGURE 3-13: Impact of ATS level on the PCE_{DAS} and TF of DBR.....	85
FIGURE 3-14: Impact of changes in ABCL on the $VtCR_{SF}$ of DBR.....	85
FIGURE 3-15: Impact of changes in ABCL on the C_{SF} of DBR.....	86
FIGURE 3-16: Impact of changes in ATS on the C_{SF} of DBR.....	86
FIGURE 3-17: Impact of changes in GM on the C_{SF} of DBR.....	86
FIGURE 3-18: Impact of changes in ABCL on the $VtCR_{DAS}$ of DBR.....	87
FIGURE 3-19: Impact of changes in ABCL on the C_{DAS} of DBR.....	87
FIGURE 3-20: Impact of changes in GM on the $VtCR_{DAS}$ of DBR.....	88
FIGURE 3-21: Impact of changes in GM on the C_{DAS} at an ABCL of 50% of DBR.....	88
FIGURE 3-22: Impact of changes in ATS on the $VtCR_{DAS}$ at an ABCL of 50% of DBR.....	88
FIGURE 3-23: Impact of changes in ATS on the C_{DAS} at an ABCL of 50% of DBR.....	89
FIGURE 3-24: The results of the SF and St Johns methods of estimating the PCE at ABCL of 50%, 75%, and 100% by utilising vehicle's traffic flow proportion.....	90
FIGURE 3-25: The results of the Gwynn (1968) method of estimating the PCE at ABCL of 50%, 75%, and 100% by utilising vehicle's traffic flow proportion and vehicles' headways.....	90

FIGURE 3-26: The results of the Benekohal (2000) and Sumner (1984) methods of estimating the PCE at ABCL of 50%, 75%, and 100%.....	91
FIGURE 3-27: Huber (1982) PCE estimation method at ABCL of 50%, 75%, and 100%	91
FIGURE 3-28: Chandra (2000) PCE estimation method at ABCL of 50%, 75%, and 100%.....	91
FIGURE 3-29: Greenshields (1935), Seguin (1982), Cunagin (1982), and Fan (1990) PCE estimation methods at ABCL of 50%, 75%, and 100%	92
FIGURE 3-30: Molina (1987) PCE estimation method at ABCL of 50%, 75%, and 100%.....	92
FIGURE 3-31: Krammes (1986) PCE estimation method at ABCL of 50%, 75%, and 100%.....	93
FIGURE 3-32: ATS and average FFS.....	93
FIGURE 3-33: Lu (2020) PCE estimation method at ABCL of 50%, 75%, and 100%.....	93
FIGURE 3-34: Keller (1984) PCE estimation method at ABCL of 50%, 75%, and 100%	94
FIGURE 3-35: Rahman (2005) PCE estimation method at ABCL of 50%, 75%, and 100%	94
FIGURE 3-36: Impact of the two rescheduling approaches on the VtCR at ABCL of 50%, 75%, and 100%	95
FIGURE 3-37: Impact of the two approaches of rescheduling on the HGVa PCE _{DAS} at ABCL of 50%, 75%, and 100%	95
FIGURE 4-1: Speed-Density curve for a single lane and interrupted traffic flow.....	107
FIGURE 4-2: Speed-Capacity curve for uninterrupted traffic flow.....	108
FIGURE 4-3: Traffic jam gap at standstill vehicle (Carwow Ltd 2020).....	108
FIGURE 4-4: Jam gap calculation method (the author has created this figure).....	109
FIGURE 4-5: Results of the Greenshields (1935) speed prediction method for non-PCE and PCE converted flow	112
FIGURE 4-6: Results of the Greenberg (1959) speed prediction method for non-PCE and PCE converted flow.....	112

FIGURE 4-7: Results of the Underwood (1961) speed prediction method for non-PCE and PCE converted flow	112
FIGURE 4-8: Results of the Edie (1961) speed prediction method for non-PCE and PCE converted flow	113
FIGURE 4-9: Results of the Drew (1965) speed prediction method for non-PCE and PCE converted flow.....	113
FIGURE 4-10: Results of the Pipes (1967) speed prediction method for non-PCE and PCE converted flow.....	113
FIGURE 4-11: Results of the Drake (1967) speed prediction method for non-PCE and PCE converted flow....	114
FIGURE 4-12: Results of the Easa (1982) speed prediction method for non-PCE and PCE converted flow	114
FIGURE 4-13: Results of the Del Castillo (1995) speed prediction method for non-PCE and PCE converted flow	114
FIGURE 4-14: Results of the Lee (1998) speed prediction method for non-PCE and PCE converted flow	115
FIGURE 4-15: Results of the Wang (2011) speed prediction method for non-PCE and PCE converted flow	115
FIGURE 4-16: Results of the Del Castillo (2012) speed prediction method for non-PCE and PCE converted flow	115
FIGURE 4-17: Results of the Gaddam (2018) speed prediction method for non-PCE and PCE converted flow	116
FIGURE 4-18: VtCR values of non-PCE and PCE converted traffic flow volume	119
FIGURE 4-19: The modified Del Castillo prediction method for PCE converted traffic flow.....	121
FIGURE 4-20: Estimated speed of PC (ES_1) at ABCL of 50%, 75%, and 100%.....	123
FIGURE 4-21: Estimated speed of LGV (ES_2) at ABCL of 50%, 75%, and 100%.....	123
FIGURE 4-22: Estimated speed of HGVr (ES_3) at ABCL of 50%, 75%, and 100%.....	123
FIGURE 4-23: Estimated speed of HGVa (ES_4) at ABCL of 50%, 75%, and 100%.....	124
FIGURE 4-24: Average Estimated Speed (AES) for a composite of all four types of vehicles at ABCL of 50%, 75%, and 100% with comparison to ATS	124

FIGURE 4-25: The change HGVa vehicle’s flow volume AR at an ABCL of 100%	125
FIGURE 4-26: The predicted ATS before and AR at an ABCL of 100%	126
FIGURE 4-27: ATS for Scenario one in comparison to the current ATS.....	127
FIGURE 4-28: ATS for Scenarios two and three in comparison to the current ATS	128
FIGURE 4-29: ATS for Scenarios four and five in comparison to the current ATS.....	129
FIGURE 4-30: ATS for Scenario six in comparison to the ATS of Scenario four	130
FIGURE 4-31: ATS for Scenario 7 in comparison to the ATS of Scenario 5.....	131
FIGURE 5-1: VtCR for non-PCE traffic flow.....	136
FIGURE 5-2: Traffic flow density of non-PCE traffic flow	137
FIGURE 5-3: Travel delay for controlled intersections	137
FIGURE 5-4: The average gap between following and leading vehicles.....	137
FIGURE 5-5: LoS based on travel delay, traffic density, VtCR, and gap BR.....	138
FIGURE 5-6: LoS based on travel delay, traffic density, VtCR, and gap AR	138
FIGURE 5-7: Vehicles types and their stopping time, RT, and braking time according to the drivers’ competency levels (Makki 2019c).....	144
FIGURE 5-8: Diagram of the pedestrian position from the approaching vehicle and the available stopping time based on the pedestrian’s position (Makki 2019c).....	145
FIGURE 5-9: Four scenarios of pedestrians’ crossing position based on the PDR value (the author has created this figure) (Makki 2019c).....	146
FIGURE 5-10: The LoS based on the ART at an average flow speed of BR.....	147
FIGURE 5-11: The LoS based on the ART at an average flow speed AR.....	148
FIGURE 5-12: ART values BR and AR at the hours of 8.00-19.00	149

FIGURE 5-13: LoS based on the ASD at an ATS BR	149
FIGURE 5-14: LoS based on the ASD at an average flow speed AR.....	150
FIGURE 5-15: SDR values BR and AR HGVa	150
FIGURE 5-16: LoS based on the risk of a pedestrian sustaining a severe injury for PCs and LGVs at a variable PDR.....	151
FIGURE 5-17: LoS based on the risk of a pedestrian sustaining a severe injury by an HGVR at a variable PDR BR	151
FIGURE 5-18: LoS based on the risk of a pedestrian sustaining a severe injury for HGVa at a variable PDR BR	152
FIGURE 5-19: LoS based on the risk of a pedestrian sustaining a severe injury by an HGVR at a variable PDR AR	152
FIGURE 5-20: LoS based on the risk of a pedestrian sustaining a severe injury for HGVa at a variable PDR AR	153
FIGURE 5-21: LoS based on the risk of a pedestrian death for HGVR at a variable PDR BR.....	154
FIGURE 5-22: LoS based on the risk of a pedestrian death for HGVa at a variable PDR BR	154
FIGURE 5-23: LoS based on the risk of a pedestrian death for HGVR at a variable PDR AR	155
FIGURE 5-24: The LoS based on the risk of a pedestrian death for HGVa at a variable PDR AR.....	155
FIGURE 6-1: The developed system dynamics qualitative assessment's main causal loops due to HGVa rescheduling.....	160
FIGURE 6-2: Variables that contribute to the prediction of ATS_{SDE} method AR (The author has extracted this image from the SDM software, Vensim)	162
FIGURE 6-3: The variables that the ATS contribute to AR (The author has extracted this image from the SDM software, Vensim)	162

FIGURE 6-4: The variables that contribute to the calculation of the headway of a PC AR (The author has extracted this image from the SDM software, Vensim).....	163
FIGURE 6-5: The variables that the headway of a PC contribute to AR (The author has extracted this image from the SDM software, Vensim).....	163
FIGURE 6-6: The variables the contribute to the rescheduling estimation of FV_{4a} (The author has extracted this image from the SDM software, Vensim)	164
FIGURE 6-7: Estimating the vehicle’s headway that represents the deceleration impact (The author has created this image).....	166
FIGURE 6-8: Estimating HGV_{di} and $THGV_f$ that represent the acceleration impact (The author has created this image).....	167
FIGURE 6-9: Deceleration and acceleration space PCE and capacity (The author has created this image).....	168
FIGURE 6-10: The two estimation methods of ATS using speed-density and acceleration performance.....	169
FIGURE 6-11: The rescheduling of HGV_a vehicles (The author has created this image).....	170
FIGURE 6-12: Estimation of all four LoS methods (The author has created this image).....	171
FIGURE 6-13: Vehicle classification in the AADF data set and overlap between the proposed vehicle categories in the ATC data set.....	177
FIGURE 6-14: C_{DAS} estimation BR in comparison to C_{SF} at the hours of 1.00-24.00 at an ABCL of 50% and RT of 1.46s.....	187
FIGURE 6-15: C_{DAS} estimation BR in comparison to C_{SF} at the hours of 1.00-24.00 at an ABCL of 75% and RT of 1.55s.....	187
FIGURE 6-16: C_{DAS} estimation in comparison to C_{SF} at the hours of 1.00-24.00 BR at an ABCL of 100% and RT of 1.68s.....	187

FIGURE 6-17: C_{DAS} estimation BR and AR in comparison to C_{SF} at the hours of 8.00-19.00 at an ABCL of 50% and RT of 1.46s 189

FIGURE 6-18: C_{DAS} estimation BR and AR in comparison to C_{SF} at the hours of 8.00-19.00 at an ABCL of 75% and RT of 1.55s 189

FIGURE 6-19: C_{DAS} estimation BR and AR in comparison to C_{SF} at the hours of 8.00-19.00 at an ABCL of 100% and RT of 1.18-1.68s 190

FIGURE 6-20: $VtCR_{DAS}$ estimation BR in comparison to $VtCR_{SF}$ at the hours of 1.00-24.00 at an ABCL of 100% and RT of 1.46s 190

FIGURE 6-21: $VtCR_{DAS}$ estimation BR and AR in comparison to $VtCR_{SF}$ at the hours of 1.00-24.00 at an ABCL of 75% and RT of 1.1s 191

FIGURE 6-22: $VtCR_{DAS}$ estimation in comparison to $VtCR_{SF}$ at the hours of 1.00-24.00 BR and AR at an ABCL of 100% and RT of 1.18s 191

FIGURE 6-23: $VtCR_{DAS}$ estimation in comparison to $VtCR_{SF}$ at the hours of 8.00-19.00 BR and AR at an ABCL of 50% and RT of 1.46s 194

FIGURE 6-24: $VtCR_{DAS}$ estimation BR and AR in comparison to $VtCR_{SF}$ at the hours of 8.00-19.00 at an ABCL of 75% and RT of 1.1s 194

FIGURE 6-25: $VtCR_{DAS}$ estimation BR and AR in comparison to $VtCR_{SF}$ at the hours of 8.00-19.00 at an ABCL of 100% and RT of 1.18s 195

FIGURE 6-26: ATS_{SDE} and ATS_{APE} estimation BR and AR fit in comparison to ATS obtained from the ATC at the hours of 1.00-24.00 at an ABCL= 50% and an RT=1.46s for the ATS_{SDE} and an RT=2.41-2.81s for the ATS_{APE} 195

FIGURE 6-27: ATS_{SDE} and ATS_{APE} estimation BR and AR in comparison to ATS obtained from the ATC at the hours of 1.00-24.00 at an ABCL= 75% and an RT=1.1s for the ATS_{SDE} and an RT=2.45s for the ATS_{APE} 196

FIGURE 6-28: ATS_{SDE} estimation BR in comparison to ATS obtained from the ATC at the hours of 1.00-24.00 at an ABCL=100% and an RT=0.73s for the ATS_{SDE} 197

FIGURE 6-29: ATS_{SDE} estimation BR in comparison to ATS obtained from the ATC at the hours of 8.00-19.00 at an ABCL= 50% and an RT=1.46s for the ATS_{SDE} and an RT=1.46s for the ATS_{APE} 197

FIGURE 6-30: ATS_{SDE} estimation BR in comparison to ATS obtained from the ATC at the hours of 8.00-19.00 at an ABCL= 75% and an RT=1.1s for the ATS_{SDE} 198

FIGURE 6-31: ATS_{SDE} estimation BR in comparison to ATS obtained from the ATC at the hours of 8.00-19.00 at an ABCL= 1000% and an RT=0.73s for the ATS_{SDE} 199

LIST OF TABLES

TABLE 1-1: Causal loop relationship.....	11
TABLE 2-1: Literature Review formulas and their description	21
TABLE 2-2: Results of Sumner (1983) measurements.....	29
TABLE 2-3: The PCE Estimation Methods and their variable components	35
TABLE 2-4: Various Driving scenarios and their effect on RT.....	43
TABLE 2-5: BD for PCs and LGVs conducted by different studies	45
TABLE 2-6: BD for HGVs conducted by different studies	45
TABLE 3-1: Categorisation of the vehicle types.....	60
TABLE 3- 2: Composite vehicles’ weights and dimensions.....	61
TABLE 3- 3: Composite vehicles and weather parameters	61
TABLE 3-4: Tfi ratio values for various types of vehicles	68
TABLE 3-5: SD, BD, and RD for PC, LGV, HGVr, and HGVa at a BCL of 50%-100% when utilising an ATS of 64.37km/h	79
TABLE 3-6: ST, BT, and RT for PC, LGV, HGVr, and HGVa at a BCL of 50%-100% when utilising an ATS of 64.37km/h	79
TABLE 3-7: ST and RT values for PC, LGV, HGVr, and HGVa at ABCL of 50%-100% when utilising an ATS 64.37km/h after adding the RT required for manoeuvring and unexpected situations	79
TABLE 3-8: PCE _{DAS} and H values for HGVr, and HGVa at BCL of 50%-100% when utilising an ATS of 64.37km/h	80
TABLE 3-9: Annual TEU Capacity for 35% of HGVa that are Container Carriers originated from the container terminal variable Speed, RT, and EGR dual carriageway data of DBR.....	96

TABLE 4-1: Flow speed prediction parameters for microscopic modelling.....	110
TABLE 4-2: Flow speed prediction parameters for macroscopic modelling.....	110
TABLE 4-3: The average maximum error of the ATCs utilised to obtain the ATS data.....	116
TABLE 4-4: Results of the goodness of fit for all thirteen methods using non-PCE traffic flow density for 24 hours period	117
TABLE 4-5: Results of the goodness of fit for all thirteen methods using PCE converted traffic flow density for 24 hours period.....	118
TABLE 4-6: Results of only five-speed estimation methods test using PCE traffic flow density at peak hours of 8.00-19.00	120
TABLE 4-7: Results of analysis of the improvement provided by the new method.....	121
TABLE 4-8: Reduction of ATS due to the increase of HGVA vehicles in scenario one.....	127
TABLE 4-9: Change in ATS due to building an extra two-lane road in scenarios two and three.....	128
TABLE 4-10: Change in ATS due to building a third lane in scenarios four and five	129
TABLE 4-11: Change in ATS due to reducing lanes' width in scenario six in comparison to scenario four	130
TABLE 4-12: Change in ATS due to reducing lanes' width in scenario seven in comparison to scenario five ..	131
TABLE 5-1: Total Annual Cost In million £ (DfT Accidents 2018).....	134
TABLE 5-2: Average Cost in £ (DfT Accidents 2018).....	134
TABLE 5-3: Current main LoS methods' criteria.....	136
TABLE 5-4: The change in LoS due to rescheduling, LoS levels of A-F refer to section 5.1	139
TABLE 5-5: The change in LoS _{art} for four types of vehicles BR and AR	148
TABLE 5-6: The change in LoS _{asd} for four types of vehicles BR and AR	150
TABLE 5-7: The number of hours that each LoS _{rsi} level for all-day, LoS levels of A-F refer to section 5.1	153

TABLE 5-8: The number of hours that each LoS _{rdi} level for all-day, LoS levels of A-F refer to section 5.1	155
TABLE 6-1: Model variables that are part of loops and the count of these loops BR and AR.....	161
TABLE 6-2: Information on the fields of the ATC data table	172
TABLE 6-3: The data file content' fields and description	172
TABLE 6-4: Maximum allowed vehicle' length (DfT-Maximum Length of Vehicles used in Great Britain, 2017)	173
TABLE 6-5: Registration data of vehicle proportion of NW and GB.....	178
TABLE 6-6: AADF data for road A5038	178
TABLE 6-7: Regression Analysis for GB, NW, and A5038 data results.....	180
TABLE 6-8: SSE results based on existing GB and NW data as \hat{y}	180
TABLE 6-9: Correlation analysis by Pearson, Spearman, and Kendall's tau_b methods	181
TABLE 6-10: Annual average traffic flow for the year 2015 by ATC data for road A5036 at road link of A5038- A5207.....	181
TABLE 6-11: Annual Average Day for the year 2015 by AADF for road A5036 at road link of A5038-A5207 and road A5038 at road link of A566-A5036	182
TABLE 6-12: Results for curve fitting by utilising four different regression methods with no constant (no line interception)	182
TABLE 6-13:Change in ATC traffic flow composite daily traffic volumes because of overlapping for road A5036 (link A5038-A5207).....	182
TABLE 6-14: ATC data correction by compensating for the overlap effect	183
TABLE 6-15: Model scenarios of RT and GM.....	185
TABLE 6-16: Results of the goodness of fit of the C _{DAS} estimation at the hours of 1.00-24.00 BR and AR	186

TABLE 6-17: Results of the goodness of fit of the C_{DAS} estimation at the hours of 8.00-19.00 BR and AR	188
TABLE 6-18: Results of the goodness of fit of the $VtCR_{DAS}$ estimation at the hours of 1.00-24.00 BR and AR	192
TABLE 6-19: Results of the goodness of fit of the $VtCR_{DAS}$ estimation at the hours of 8.00-19.00 BR and AR	193
TABLE 6-20: Results of the goodness of fit of the ATS estimation methods at the hours of 1.00-24.00 BR	196
TABLE 6-21: Results of the goodness of fit of the ATS estimation methods at the hours of 8.00-19.00 BR	198

ABSTRACT

The purpose of this research is to investigate the impact of heavy goods vehicles that are carrying intermodal shipping containers on the traffic flow. The objective is to estimate the available capacity for HGVs on the road at every hour to accommodate the increasing demand due to the expansion of Liverpool container terminal. The author has developed a passenger car equivalent estimation method and a road traffic capacity estimation methods by considering the deceleration and acceleration performances of vehicles, and the methods consider the speed, reaction time, braking competency level of the driver, and road safety.

The author has developed an average traffic speed prediction method to facilitate the rescheduling and planning of the traffic operation. The proposed prediction method provides higher accuracy than all other speed prediction methods and facilitates highly efficient rescheduling and planning operations. The author has proposed four level of service methods that consider the safety, prevention of accidents by available reaction time, stopping distance, and the risk of pedestrians sustaining severe injuries or death, and they unique method because they measure the level of service not from the prospective of the user but from the prospective the traffic management and local authority. The methods target the individual type of vehicle and drivers' behaviour and competency level.

The results showed that the required time gap to maintain a safe gap between the following vehicle and the leading vehicle ranges from 2.59 to 3.32s for passenger cars and from 2.94 to 4.89s for heavy goods vehicles. The results also showed that the passenger car equivalent for heavy goods vehicles with braking competency level of 100%-50% is 1.32-2.77 that depends on vehicle parameters. The results also showed that the passenger car equivalent for heavy goods vehicles at 64.4km/h with braking competency level of 100%-50% is 1.32-1.65, and 2.41- 2.77 for rigid heavy goods vehicle, and articulated heavy goods vehicles, respectively.

The rescheduling results show how that it is possible to meet both of Mersey ports' targets for Liverpool's container port by either building an extra lane of an heavy goods vehicle access only two-lane road in parallel to the current road. However, to improve the traffic flow operation and safety, the second choice will be better because it will keep the average traffic speed above the optimum speed of the road at all times.

DECLARATION OF AUTHOR'S RIGHT

I declare that no portion of the work referred to in the thesis has been submitted in support of an application for another degree or qualification of this or any other university or other institute of learning;

The copyright of this thesis belongs to the author under the terms of the United Kingdom Copyright Acts as qualified by the Liverpool John Moores University Regulation. The due acknowledgement must always be made of the use of any material contained in or derived from this thesis.

Alakki

11/06/2021

Signed: _____ Date: _____

ACKNOWLEDGEMENTS

I wish to gratefully acknowledge the technical and financial support of Liverpool John Moores University that allowed me to carry out this research. I would also like to express my appreciation to my director of studies Dr Trung Thanh Nguyen, Prof. Dhiya Al-Jumeily, and Dr Jun Ren, and Dr William Hurst for their professional advice and guidance throughout this research. Finally, I would like to thank my wife and parents, especially my father that who wished to celebrate my graduation before he passed away, for their great love, guidance and support. Without them, I would not have been able to get this far, and they are the reason behind my patience and hard work. No matter what happens, I know that they are always standing by my side to share my happiness and accompany me with my every achievement.

LIST OF ABBREVIATIONS

a	Acceleration Rate
AADF	Annual Average Daily Flow
AAG	Average Available Gap
AASHTO	American Association of State Highway and Transportation Officials
ABCL	Average Braking Competency Level
ABD	Available Braking Distance
AD	Air Density
AF	Area of the Front Surface of the vehicle
AEB	Autonomous Emergency Braking
AFFS	Average Free Flow Speed
Al	Alcohol Level
AR	After Rescheduling
ART	Available Reaction Time
ARTT	Automatic Rail Timetable
AS	Acceleration Space
ASD	Available Stopping Distance
ASO	Acceleration Space Occupied
ATC	Automatic Traffic Counters
ATS	Average Traffic Speed
ATS _{APE}	ATS Prediction Method based on Vehicle's Acceleration Performance
ATSo	Optimum Average Traffic Speed
ATS _{SDE}	ATS Prediction Method based on Speed-Density
BAC	Blood Alcohol Concentration
BCL	Braking Competency Level
BD	Braking Distance
BE	Braking efficiency
BF	Braking force

BP	Braking Pressure
BPL	Braking Pad's Length
BPW	Braking Pad's Width
BR	Before Rescheduling
BSA	Braking Surface Area
BT	Braking Time
C	Traffic Signal Cycle
CC-HGVa	Container Carrier HGVa
Cd	Drag Coefficient
C _{DAS}	Deceleration and Acceleration Space Capacity
Chi-Sq-GF	Chi-Square Goodness of Fit
CLD	Causal Loop Diagram
Cr	Rolling Resistance Coefficient
C _{SF}	Saturation Flow Capacity
d	Deceleration Rate
DAS	Deceleration and Acceleration Space Method
DBR	Dunnings Bridge Road
DES	Discrete Event Simulation
DfT	Department for Transport
EGR	Effective Green Ratio
EGT	Effective Green Time
EM	Basic Eye Movement
ENE	Expected and Not Expected Situation
EP	Engine Power
f _A	Access Point Adjustment Factor
FB	Force due to Braking
FD	Deceleration Force
FFS	Free Flow Speed
F _{hv}	Heavy Vehicle Factor
f _{LW}	Lane Width Adjustment Factor
f _p	Population Factor

FR	Rolling Friction Force
f_w	Lane Width Correction Factor
FW	Deceleration or Acceleration Force due to Wind
FV	Vehicle's Flow Volume
g	Acceleration due to Gravity
G	Green Light Time
GB	Great Britain
GM	Gross Mass
G_{min}	Minimum Green Time
H	Vehicle's Headway
HC	Highway Code
HCM	Highway Capacity Manual
HE	Highway England
HGV	Heavy Goods Vehicles
HGV _a	Articulated HGV
HGV _r	Rigid HGV
HGV _d	HGV Acceleration Performance Delay
H_{PC}	Headway of PC
h_s	Saturation Headway
H_T	Headway of Trucks
IF	Ratio of the impact pressure of a vehicle to the impact pressure of a PC
IS	Impact Speed
ISO	International Organisation of Standardisation
k	Traffic Flow Density
KE	Kinetic Energy
k_j	Traffic Jam Density
k_m	Maximum Traffic Flow Density
L	Vehicle's Length
LD	Length of Vehicle's Displacement
LGV	Light Goods Vehicle
LoS	Level of Service

LoS _{art}	LoS Method based on Available Reaction Time
LoS _{asd}	LoS Method based on Available Stopping Distance
LoS _{rd}	LoS Method based on the Risk of Pedestrian Death
LoS _{rsi}	LoS Method based on the Risk of Pedestrian Sustaining a Severe Injury
LW	Lane Width
MAM	Maximum Authorised Mass
ME	Mean Error
MPE	Mean Percent Error
MTBF	Mean Time Between Failure
NHTSA	National Highway Traffic Safety Administration
NL	Number of Lanes
NW	North-West England
PC	Passenger Car
PCE	Passenger Car Equivalent
PCE _{DAS}	PCE using Deceleration and Acceleration Space Method
PCE _T	PCE of Trucks
PDR	Pedestrian Distance Ratio
P _T	Traffic Flow Volume Proportion
PWR	Power to Weight Ratio
QDF	Queue Discharge Flow
RD	Reaction Distance
R _{LL}	Road Link Length
RMSE	Root Mean Square Error
RMSPE	Root Mean Square Percent Error
RT	Reaction Time
SA	Space Available
SBT	Safe Braking Time
SD	Stopping Distance
SDM	System Dynamics Model
SF	Saturation Flow Method
SF _{DAS}	Saturation Flow using the DAS method

SF _{SF}	Saturation Flow using the SF method
SSE	Sum of Square Error
SST	Safe Stopping Time
ST	Stopping Time
T	Air Temperature
t _{cl}	Clearance Lost Time
TEU	Twenty-foot Equivalent Unit
Tf	Traction Factor
TF	Heterogeneous Composite Traffic Flow Volume
TF _{PCE}	PCE Converted Traffic Flow Volume
t _L	Start-up Lost Time (t _L)
THGV _d	Total HGV Acceleration Delay
THGV _f	Total HGV Acceleration Performance Factor
t _s	Start-up Time
U ₁	Theil's inequality coefficient
U ₂	Theil's suitability test
U _C	Theil's covariance inequality coefficient
UCC	Urban Consolidation Centre
U _M	Theil's inequality coefficient
U _S	Theil's variance inequality coefficient
VtCR	Volume to Capacity Ratio
VtCR _{DAS}	Volume to Capacity Ratio of the DAS method
VtCR _{SF}	Volume to Capacity Ratio of the SF method
VVF	Vehicle's Vertical Force
WF	Weather Factor
WS	Wind Speed
Y	Yellow Light Time

LIST OF GLOSSARIES

1 MEASUREMENTS OF TRAFFIC:

1.1 Annual Average Daily Flow (AADF): The average over a full year of the number of vehicles passing a point in the road network each day.

1.2 **Vehicle mile/kilometre:** One vehicle time one mile/km travelled (we can calculate the vehicle miles/km by multiplying the AADF by the corresponding length of road). For example, one vehicle travelling 1 mile a day for a year would be 365 vehicle miles. It is sometimes known as the volume of traffic.

2 VEHICLE DEFINITIONS

2.1 **All motor vehicles:** All vehicles except pedal cycles

Pedal cycles: Includes all non-motorised cycles.

Cars and taxis: Include passenger vehicles with nine or fewer seats, three-wheeled cars and four-wheel drive 'sports utility vehicles. The count of cars towing caravans or trailers is as one vehicle.

2.2 **Motorcycles:** Includes motorcycles, scooters and mopeds and all motorcycle or scooter combinations.

2.3 **Buses and coaches:** Includes all public service vehicles and works buses which have a gross weight higher than 3.5 tonnes.

Light vans: Goods vehicles not exceeding 3.5 tonnes gross vehicle weight, includes all car-based vans and those of the next largest carrying capacity such as transit vans. Also included are ambulances, pickups and milk floats.

Heavy goods vehicles (HGV): Includes all goods vehicles over 3.5 tonnes gross vehicle weight Rigid HGV with two axles: Includes all rigid heavy goods vehicles with two axles, includes tractors (without trailers), road rollers, box vans and similar large vans, and also includes a two-axle motor tractive unit without a trailer.

2.4 **Rigid HGV with three axles:** Includes all non-articulated goods vehicles with three axles irrespective of the position of the axles. Excludes two-axle rigid vehicles towing a single axle caravan or trailer, and also includes three axle motor tractive units without a trailer. Rigid HGV with four or more axles: Includes all non-articulated

goods vehicles with four axles, regardless of the position of the axles, excludes two or three-axle rigid vehicles towing a caravan or trailer.

2.5 Articulated heavy goods vehicles: For articulated heavy goods vehicles, When the vehicle is travelling by one or more axles raised from the road, classifying the vehicle by the number of axles on the road, and not by the total number of axles. Articulated goods vehicles with three and four axles are in one category, and there is no differentiation between three and four axles vehicles during manual traffic counts.

B.2.6 Articulated HGV with three axles (or with trailer): Includes all articulated goods vehicles with three axles. The motor tractive unit will have two axles and the trailer one. Also included in this class are two-axle rigid goods vehicles towing a single axle caravan or trailer.

2.7 Articulated HGV with four axles (or with trailer): Includes all articulated vehicles with a total of four axles regardless of the position of the axles, i.e. two on the tractive unit with two on the trailer, or three on the tractive unit with one on the trailer. Also includes two-axle rigid goods vehicles towing two-axle close-coupled or drawbar trailers.

2.8 Articulated HGV with five axles (or with trailer): This includes all articulated vehicles with a total of five axles regardless of the position of the axles. Also includes rigid vehicles drawing close-coupled or drawbar trailers where the total axle number equals five and articulated vehicles where the motor tractive unit has more than one trailer, and the total axle number equals five.

2.9 Articulated HGV with six or more axles (or with trailer): This includes all articulated vehicles with a total of six or more axles regardless of the position of the axles. Also includes rigid vehicles drawing close-coupled or drawbar trailers where the total axle number equals six or more and articulated vehicles where the motor tractive unit has more than one trailer, and the total axle number equals six or more.

3 ROAD DEFINITIONS

The road definitions included in the traffic estimates are as follows:

Major roads include motorways and all class ‘A’ roads: These roads usually have high traffic flows and are often the main arteries to major destinations. Motorways (built under the enabling legislation of the Special Roads Act 1949, now consolidated in the Highways Acts of 1959 and 1980): Includes major roads of regional and urban

strategic importance, often used for long-distance travel. They are usually three or more lanes wide in each direction and generally have the maximum speed limit of 70 mile/h.

3.1 'A' Roads: these can be trunk or principal roads. They are often described as the 'main' roads and tend to have heavy traffic flows though generally not as high as motorways. Trunk roads (designated by the Trunk roads Acts 1936 and 1946): Most motorways and many of the long-distance rural 'A' roads are trunk roads. The responsibility for their maintenance lies with the Secretary of State, and they are managed by Highways England (formerly the Highways Agency) in England, the Welsh Government and the Scottish Government (National Through Routes). Principal roads: these are major roads which are maintained by local authorities. They are mainly 'A' roads, though some local authorities do have responsibility for some motorways.

3.2 Minor Roads: these are 'B' and 'C' classified roads and unclassified roads (all of which are maintained by the local authorities), as referred to above. Class III (later 'C') roads were created in April 1946. 'B' roads in urban areas can have relatively high traffic flows but are not regarded as being as significant as 'A' roads, though in some cases may have similarly high flows. They are useful distributor roads often between towns or villages. 'B' roads in rural areas often have markedly low traffic flows compared with their 'A' road counterparts. 'C' Roads are regarded as of lesser importance than either 'B' or 'A' roads, and generally, have only one carriageway of two lanes and carry less traffic. They can have low traffic flows in rural areas. Unclassified roads include residential roads both in urban and rural situations and rural lanes, the latter again usually having shallow traffic flows. Most unclassified roads will have only two lanes, and in rural areas may only have one lane with "passing bays" at intervals to allow for two-way traffic flow

3.3 Urban roads: these are major and minor roads that sit within a built-up area, with a population of 10,000 or more in England and Wales or 3,000 in Scotland.

3.4 Rural roads: These are major and minor roads that sit outside urban areas (these urban areas have a population of more than 10,000 people in England and Wales or 3,000 in Scotland)

3.5 Private Roads: For this publication, private roads are considered to be the road not maintained at public expense. For major roads, private roads (usually toll roads, tunnels and bridges) are included in the road length figures as they are accessible to the general public. For minor roads, private roads are not included in the road length figures as they are not usually accessible to the general public.

VAIRIABLES' DEFINITIONS, UNITS, INITIAL VALUES, AND CONSTRIANS

Component	Definition	Unit	Initial Value	Constrains (Variable x)
a	Vehicle's acceleration rate	m/s ²	0	-
AAG	Average available gap	m	0	$x \leq 1$
ABCL	Average Braking Competency Level	kg/kg	0.5	0.5-1
AD	Air Density	kg/m ³	1.225	-
AFFS	Average Free Flow Speed	km/h	-	-
A _f	Vehicle's Frontal Area	m ²	{2.734,3.854, 9.05,9.05}	$x > 0$
AS	Acceleration Space	m	1.973	-
ASO	Acceleration Space Occupied	m	1	$x \leq 1$
ATS	Average Flow Speed	km/h	1	$x \geq 0$
ATSo	Optimum Speed	km/h	36.34	-
AVR	Average articulated HGV hourly traffic volume	HGV _a /h	90	-
BA	Braking pad area	m ²	-	-
BCL	Braking Competency Level	-	0.5	0.5-1
BD	Braking distance	m	-	-
BP	Braking Pressure	Pa	689500	$x \leq 1000000$
C	Traffic Light Cycle length	s	90	120
CCP	Container Carrier HGVs Proportion	CCHGV _a /HGV _a	0.35	0-1
C _d	Articulated HGV Aerodynamic drag constant	-	{1,0.95,0.91,0.8}	-
C _{DAS}	Deceleration and Acceleration Space Capacity	PCE/h	-	-
C _r	Coefficient friction due to rolling	-	0.002	-
d	Vehicle's deceleration rate	m/s ²	-	-
DPA	Area of Disk-Pad Contact for Articulated HGV	m ²	0.67	0.67 to 2.67
d _w	Deceleration due to the aerodynamic drag force	m/s ²	-	-
EGR	Effective Green Ratio	-	0.5	0.7
EP	Vehicle's Engine Power	HP	{138,122,400,500}	-
F _{hv}	Heavy Vehicle Factor	veh/veh	1	$x \geq 0$
FV	Vehicle type's flow volume	veh/h	0	$x \geq 0$
FV _{PC}	Traffic flow volume of PCs	veh/h	0	$x \geq 0$

Component	Definition	Unit	Initial Value	Constrains (Variable x)
fw	Lane Width Correction factor	m/m	0.94	-
g	Acceleration due to gravity	m/s ²	9.8066	9.8066
GM	Gross Mass of vehicle	Tonne	{1.87,3.325,27.3,35.2}	$x \leq \{1.87, 3.5, 36,44\}$
Grade	Road Upgrade/Downgrade	m/m	0	0.3
H	Headway for vehicle	m	7.173	$x \geq 7.173$
HASL	Height Above Sea Level	m	24	$x \geq 0$
HGV _d	HGV acceleration delay factor for vehicle	m/m	0	$1 \geq x \geq 0$
k	Traffic flow density	veh/km/ln	0	$x \geq 0$
kj	Traffic Jam Density	PC/km/ln	139	-
km	Optimum Traffic Flow Density	PC/km/ln	27	27-34
L	Vehicle's Length	m	{5.2, 6.6, 11.6,16.5}	{5.2, 6.6,12, 18.75}
MAM	Maximum Authorised Mass	Tonne	{-, -, 36, 44 }	{-, -, 36, 44 }
NL	Number of lanes	Lane	1	$x \geq 1$
PC	Passenger Car	veh/h	0	$x \geq 0$
PDR	Pedestrian Distance Ratio,	m/m	1	0-1
PCE _T	Passenger car equivalence for trucks	PC/truck	1	$x \geq 1$
PCE _{DAS}	Deceleration and Acceleration Space PCE	m/m	1	$x \geq 1$
P _T	Proportion of trucks in traffic flow (TF)	truck/TF	0	$1 \geq x \geq 0$
RF	Rescheduling factor	veh/veh	1	$1 \geq x \geq 0$
RT	Reaction Time	s	0.63	3.5
SD	Stopping Distance	m	1.973	-
T	Air Temperature	°C	15	-27.2 to +38.5
Tf	Vehicle's Traction Factor	-	0.3636, 0.2,0.5, 0.6	$x < 1$
TF	Traffic Composite Flow	veh/h	0	$x \geq 0$
TF _{PCE}	PCE Traffic Flow Volume	PC/h	0	$x \geq 0$
THGV _d	Total HGV acceleration delay factor	m/m	0	$1 \geq x \geq 0$
THGV _f	Total HGV acceleration factor	m/m	1	$1 \geq x \geq 0$
TP	Tire inflation pressure for vehicle	bar	{2,2,5.5,9}	{2,2,5.5,9}
VtCR	Volume to Capacity Ratio	veh/veh	1	$x \geq 0$
WF	Weather Factor	N/N	1	0.1-1
WS	Wind Speed	m/s	1	$x \geq 0$

CHAPTER ONE: INTRODUCTION

1.1 BACKGROUND

The expansion of the Liverpool container terminal increases the demand for road freight, and roads that connect the terminal with the city and the nearby cities will suffer from congestion. Therefore, local authorities either try to overcome this problem by building new roads, tunnels, adding extra lanes to existing roads, Urban Consolidation Centre (UCC) or utilising other modes of transport for freight transportation. To reach a feasible solution, the planners would require an accurate and efficient method of estimating the effect of Heavy Goods Vehicles (HGV) on road traffic flow.

Traffic operators and planners determine the effect of non-PC vehicle on the traffic flow by estimating the Passenger Car Equivalent (PCE) of these vehicles compared to passenger cars. The PCE value is the equivalent effect of a Light Goods Vehicle (LGV), Rigid HGV (HGVr) or Articulated HGV (HGVa) on traffic flow in comparison to Passenger Car (PC) vehicles. The determination of HGVs' effect requires estimating the PCE of the various vehicle types that make the traffic flow composition at different hours of the day. The PCE represents the equivalent effect of non-PC vehicles on the traffic flow, and the PCE value representing the effect of a non-PC vehicle as an equivalent to the effect of a number of PCs on the road.

1.2 INTERMODAL TRANSPORTATION

Intermodal freight transport involves the transportation of freight in an intermodal container, using multiple modes of transportation. The author has discussed the intermodal modes in the following subsections: rail, containership, and container carrier HGVs.

1.2.1 Freight rail

The purpose of utilising freight rail is to distribute the transportation workload over several transportation modes. The Liverpool port's rail freight line has a maximum length of 380m (63 Twenty-foot Equivalent Unit (TEU)) for every dispatch. The routes' availability depends on the weight of the freight axle and the strength of underline

bridges. Therefore, the freight rail will not have enough capacity to accommodate the increase in delivery demand unless the dispatch frequency and rail lines increase (Network Rail 2018).

Many issues can affect the maximum capacity of freight rail (Meadows 2018):

- Unloading/loading times for a ship and associated trains
- Available storage area for transferring the containers
- Number of cranes or grab stackers (big fork-lifts)

The maximum capacity of trains handling may or may not have commercial customers. For example, the port terminal's rail plan may handle five trains a day, but there may be only enough commercial traffic for one. The freight operating companies will bid for train paths to/from the port based on their commercial requirements. There is also a proposed approach to increase freight rail flow by utilising an Automatic Rail Timetable (ARTT). However, it is far from reach due to many challenges and barriers, as in Appendix A.

1.2.2 Inland Waterway Freight

The inland waterway freight destinations are limited to the North West region and share the same freight rail issues. In addition, the tide and weather conditions affect the inland waterway freight operation and limit the number of deliveries. Besides, there are other operational barriers (IWA 2013), as shown in Appendix A.

1.2.3 Road freight

The North West region suffers from road congestion because of freight deliveries and the continuous yearly increase of PC traffic flow. Urban congestion is one of the main issues, especially in Liverpool, whereas the rise in demand for road freight is due to the expansion of the Liverpool container terminal. For example, the traffic flow at Church street and Dunning's Bridge Road (DBR) (A5036) has increased by 26% from May-2016-May-2017.

The increase in HGV access puts pressure on the traffic flow and limits the maximum available space for HGVs on this road. More specifically, the HGVs will increase congestion and the number of times vehicles require to stop for every road link. Therefore, there is a plan by local authorities to create a new two-lane road to reduce congestion and pave the way to meet the 2020 and 2030 targets.

The author has chosen the road under investigation because of the ongoing expansion of the container terminal of Liverpool. The data collection is from (HE-ATC 2017), conducted by Automatic Traffic Counters (ATC). The utilised data contains traffic flow of vehicles with a length of ≤ 5.2 m, 5.21-6.6 m, 6.61-11.6 m, and ≥ 11.6 m and their average speed for every hour.

The proposal's target for expanding Mersey ports aims to process an annual 2MTEUs by 2020 and 3MTEUs by 2030. The proposed targets by Mersey ports are that the freight rail and inland waterway would transport 10% and 5% of these containers, respectively (Peel Ports 2011).

The number of existing Annual TEUs (ATEU) processed in the year 2017 was 760kTEU, and the TEUs are entering the UK through the port account for 48.5% of the yearly TEUs in both directions. Therefore, the author can assume that the annual TEUs that leave the container terminal to the UK mainland by utilising intermodal transportation is 369kTEUs.

The author's method of estimating the number of TEUs is by considering the number of the daily HGVA vehicles, number of working days, number of weeks, percentage of CC-HGVA, road share split, percentage of HGVs going to the motorway, and the share of containers going to the Liverpool, as in (1-1).

$$ATEU = \frac{FV_4 \times NoWD \times NoW \times PCC}{RSS \times PtM \times (1 - PL)} \quad (1-1)$$

where,

ATEU is the annual TEUs transported through road

FV₄ is the traffic flow volume of articulated HGVs

NoWD is the number of working days in the week (maximum five days)

NoW is the number of working weeks in the year (maximum 52 weeks)

PCC is the proportion of CC-HGVA from the total HGVA vehicles (The author's field survey, 0.35)

RSS is the target road freight share (Mersey ports target, 0.85)

PL is the proportion of freight going to Liverpool (literature review, 0.22)

PtM is the proportion of HGVs going to the motorway (the author's estimation, 0.48)

Of all the road freight TEUs going to the UK through Liverpool container terminal, 22% go to Liverpool while 78% go to Manchester, North West Region, and the rest of the UK (LTP Support Unit 2011). By deducting the TEUs transported by rail and inland water modes (Peel Ports 2018; Merseytravel 2018), the TEUs transported by

road passing through the port's inland access of DBR should be 244kTEU by now, 643kTEU by 2020, and 965kTEU by 2030.

However, for the year 2017, the inland waterway freight transported just 2.39% of TEUs and freight rail transported just 1.642% of TEUs, which leaves 95.968% of TEUs delivered by road freight transportation using Container Carrier HGVa (CC-HGVa). Therefore, the author has considered in this thesis the target for Mersey port's intermodal split share of 85%, and it is equal to 636.48kTEU and 954.72kTEU for 2020 and 2030 targets, respectively, for the UK inbound road freight to the North-West and the rest of the UK.



FIGURE 1-1: Option A is to upgrade the existing A5036 road with junction improvements (HE 2017)

Highway England (HE) planned to invest in developing road A5036 because A5036 is the main road linking the port to the motorway network, and it is already congested and has a poor safety record. HE proposed three development options and discounted one of them, as shown in FIGURE 1-1 and FIGURE 1-2 chosen and FIGURE 1-3 that was discounted (HE 2017). The road link under investigation is A5038-A5307, illustrated with an arrow in FIGURE 1-1, and the author has obtained the ATC data and the Annual Average Daily Flow (AADF) data from this road link. The road link has shown high congestion, delays, and safety issues for many years.

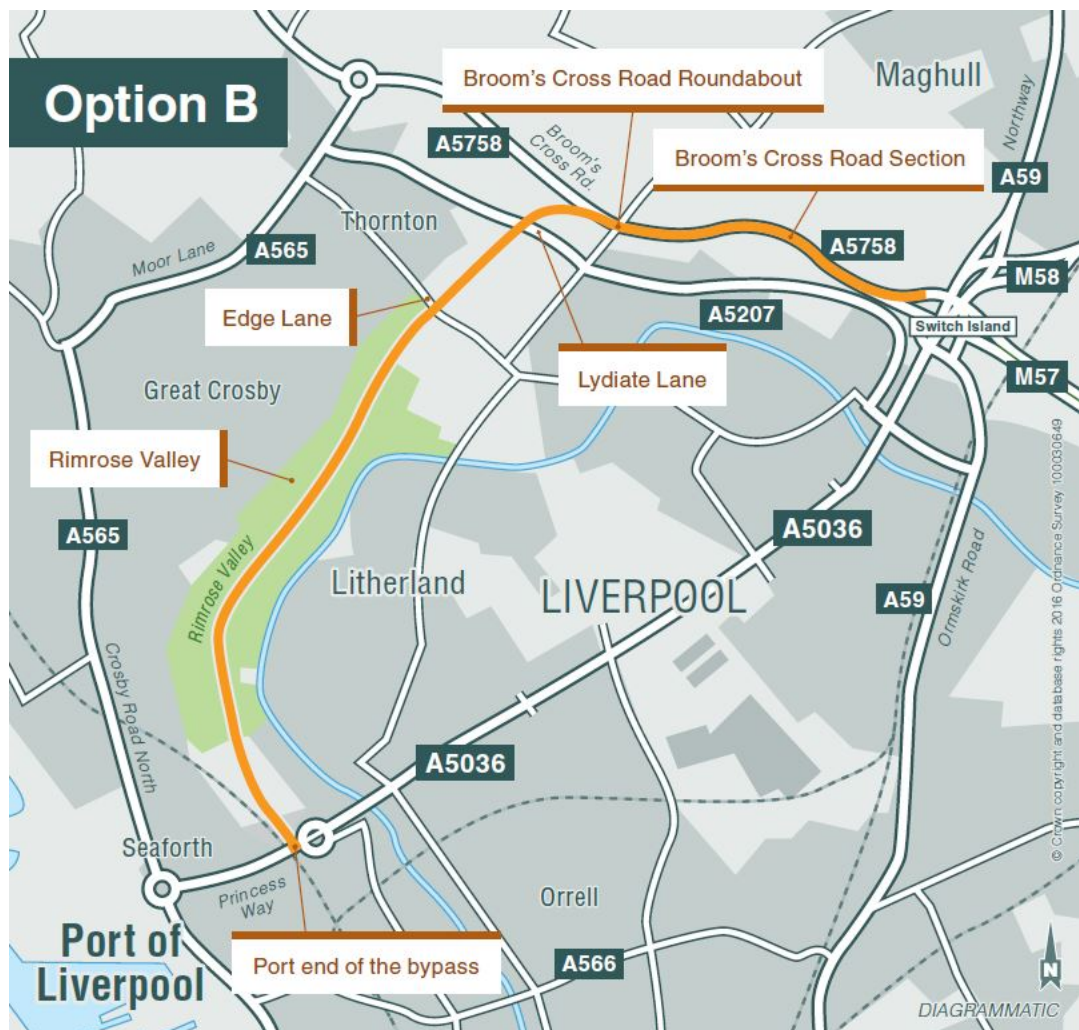


FIGURE 1-2: Option B is to build a new dual carriageway bypass through the Rimrose Valley (HE 2017)

A5036 Port of Liverpool Access Scheme

Discounted Options

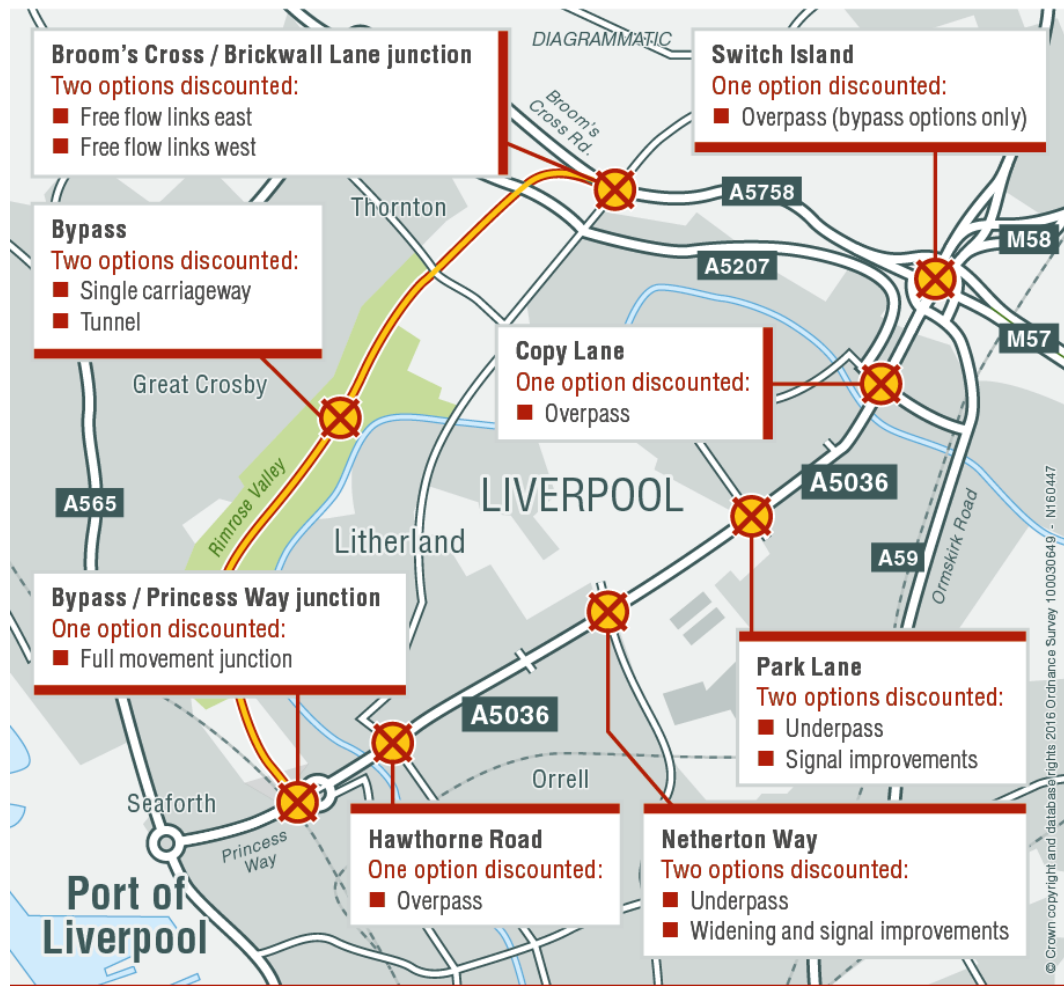


FIGURE 1-3: Option C is several improvement options for both the existing A5036 and bypass were considered and discounted for a variety of reasons (HE 2017)

1.2.4 Urban Consolidation Centres

The utilisation of UCC will reduce the number of heavy and prolonged vehicles flowing on city roads during peak hours by processing large containers at consolidation centres and making several smaller deliveries by using smaller trucks of 2-3 axles and a maximum gross weight of 18 tonnes (Browne 2007). Making deliveries with smaller trucks will reduce their effect on the traffic flow and make it easier to access roads, parking areas, unloading goods, and reduce noise (Rooijen 2010).

It will solve the last mile problem during the last mile of the delivery where the city's delivery location is inside. The last mile problem is one of the most expensive and challenging parts of urban freight distribution as it holds over 50% of the logistics cost (Allen 2012; Allen 2014). The UCC will collaborate with the port, logistic companies, freight rail companies, local authorities, retailers, end users, and traffic control. As a result, the UCC would provide seamless deliveries that contribute to the urban economy by reducing costs, delivery delays, congestion, pollution, and noise, and will increase the reliability of deliveries, and reduce the number of freight journeys, journey time, pollution, noise, cost of delivery, road congestion, and the number of HGVs utilised.

Besides, it will reduce the weight and length of the trucks used for delivery, thereby reducing their effect on road congestion, traffic flow speed, and increase their access and manoeuvring ability to make quick and efficient deliveries in the city centre (Johansson 2017).

Collaboration with local authorities and traffic control will significantly benefit the centre's functioning and enable the centre to fulfil its objectives. Collaboration with the rail network regarding the train timetable will facilitate seamless deliveries with minimum delay and no extra cost. Besides, it would be possible to avoid the knockout effect of rail operation. Collaboration with logistic companies and ports will provide an accurate delivery time with less cost to the end-user by knowing the transport mode availability and ability at remote rail freight destination to distribute freight to their final destinations or other UCCs.

Working with local authorities will help create a better life for locals and be in touch with all the cities' construction, development, and problems. Working with ports will determine the final destinations, weight, number of TEUs, and number and type of items. In addition, it will provide information about the location and the deadline of the delivery, the alternative modes of transport, and alternative routes that can deliver the products to end users. However, the UCC lifespan is usually 2-3 years, and this makes it an unreliable long-term solution and limits its benefits to the short-term only (Allen 2012; Allen 2014).

1.3 PASSENGER CAR EQUIVALENT

The PCE value represents the effect of non-PCs vehicles on the traffic flow compared to the impact of an average PC on the traffic flow. The utilisation of PCE value is essential in determining the road capacity because it provides

the actual effect of a non-PC on the road and leads to a more realistic modelling solution. The estimation of PCE depends on several variables, such as the vehicle's dimensions, headway, gross weight, Engine Power (EP), traffic volume, braking forces, flow speed, and the driver's Reaction Time (RT) and Braking Competency Level (BCL). For example, an HGV can be equivalent to 2-3 passenger cars in length, as shown in FIGURE 1-4.

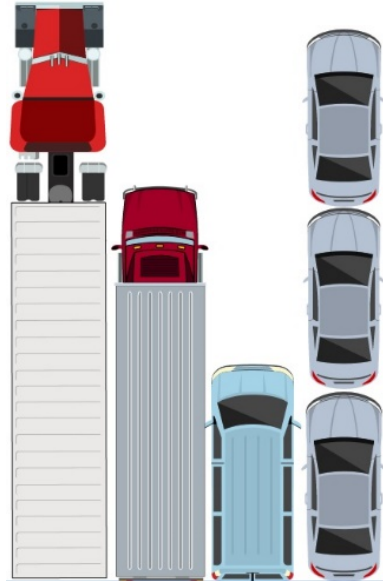


FIGURE 1-4: A demonstration of the vehicle's length effect on the PCE value (The author has created this image)

1.4 SYSTEM DYNAMICS

Solving a system's problem would require a full understanding of that system's mechanism and identify the variables that influence the system, and therefore determine the cause of the problem.

One of the popular tools to understand this causal relationship between complex systems is system dynamics. Hence, a System Dynamics Model (SDM) design for the system under investigation is vital. The design development starts by generalising from the specific events associated with our problem and drawing a Causal Loop Diagram (CLD) that contains all the variables that influence this behaviour that is causing the problem (Fishwick 1995; Kirkwood 1998).

The design of the SDM involves two parts, a qualitative assessment and a quantitative assessment. The qualitative assessment describes the causal relationships between the systems' variables through a causal loop model, and the

quantitative assessment presents the mathematical relationship between the system's variables in a stock and flow model. Qualitative models are useful in describing the system structure for decision-makers to form the necessary strategy to improve system behaviour (Roberts 1983; Sterman 2000). However, qualitative assessment alone is not enough to obtain all the necessary facts to design a new strategy. Usually, decision-makers would require quantitative results to support the qualitative assessment (Shepherd 2012).

Many researchers explored utilising system dynamics in the supply chain, logistics and transport. In the 1990s, Abbas (1990) introduced SDM to solve transportation problems, evaluated the strengths and weaknesses and identified 12 advantages of using the dynamic system approach (Abbas 1990). Abbas (1994) set the terms for qualitative and quantitative assessments when compared to traditional transport modelling (Abbas 1994)

Tako (2011) reviewed 127 papers in logistics and supply chain management for the years 1996-2006, and from 15 papers on freight transportation (Tako 2011), only one that used SDM by Disney (2003) (Disney 2003). Shepherd (2012) reviewed papers that utilised SDM in transportation for the years 1994-2013 and found only five papers that used SDM in freight transportation (Shepherd 2012).

Sterman (2000) used system dynamics in the supply chain to determine the sources of demand oscillation, demand amplification, and phase lag. Georgiadis (2005) used SDM to reduce the number of owned trucks and minimise transportation costs for a fast-food chain company. Potter (2008) determined that the demand amplification and bullwhip effect increased transportation costs and determined that a demand amplification will improve transport performance when a vehicle capacity is less than average demand.

Disney (2003) investigated the effect of the Vendor Management Inventory strategy on transport operations in the supply chain by focusing on batching orders to utilise vehicles efficiently. Nielsen (2003) assessed the driving forces behind mobility influence the transport industry (Nielsen 2003). Finally, Wilson (2007) investigated the effect of transportation disruption on supply chain performance (Wilson 2007).

Solving a system problem would require a full understanding of the mechanism and behaviour of the variables that system thereby; the investigators would require identifying the variables that influence the system and, therefore, determine the cause of the problem. Hence, a system dynamic model design for the system under investigation is vital. The design development starts by generalising from the specific events associated with the problem and

drawing a CLD that contains all of the variables that influence the behaviour that is causing the problem (Fishwick 1995; Kirkwood 1998). The system in question is for supply chain, logistics or intermodal transportation; it always has internal and external influences. The challenge is identifying the structure variables connecting these systems and influencing the behaviour of those systems. For example, an intermodal transportation system model can be influenced by some factors of logistics. Logistics can be affected by the supply chain management system, which influences the logistics policies, such as Just-In-Time manufacturing (Nielsen 2003; Aschauer 2015).

1.4.1 Causal Loop Diagram

SDM is an approach to understanding complex systems' nonlinear behaviour over time using stocks, flows, internal feedback loops, table functions, and time delays. The building of a CLD is for the system's qualitative assessment, and it consists of variables connected by causal links. The illustrations of causal links are in arrows and are associated with polarities of positive (+) or negative (-) and delay (||). If the polarity is positive, there is a positive relationship between the two variables. Hence, if the first variable increase, the second variable will increase as well, and if the first variable decreases, the second variable will decrease as well. Simultaneously, a minus sign denotes a negative relationship would mean that, unlike the positive causal relationship, the second variable's reaction will be the opposite to the change direction of the first variable, as shown in FIGURE 1-5.



FIGURE 1-5: Cause and Effect Relationship (The author has created this image)

For example, the relationship between supply and demand is positive because the supply will increase if demand increases. In some CLDs, the denotation of a positive relationship is either supporting “S” or reinforcing “R” or “+” for positive, and the denotation of a negative relationship is either opposite “O” or “B” for balance or “-“ for negative.

The classification of a causal loop will be positive either when there are no negative causal links or when the number of the negative causal links is even, and the classification of a causal loop will be negative when the number

of negative causal links is odd as in TABLE 1-1 and FIGURE 1-6. The positive causal loop is uncontrollable, has an exponential function, as shown in FIGURE 1-7, while the negative causal loop is controllable and has a goal-seeking function, as shown in FIGURE 1-8 (Kirkwood 2013; Forrester 1961).

TABLE 1-1: Causal loop relationship

CAUSAL RELATIONSHIP	1 st	2 nd	3 rd	CAUSAL LOOP
+ * + = +	+	+	NONE	POSITIVE
- * - = +	-	-	NONE	POSITIVE
+ * - = -	+	-	+	NEGATIVE
- * + = -	-	+	+	NEGATIVE
- * - * - = -	-	-	-	NEGATIVE
+ * + * + = +	+	+	+	POSITIVE

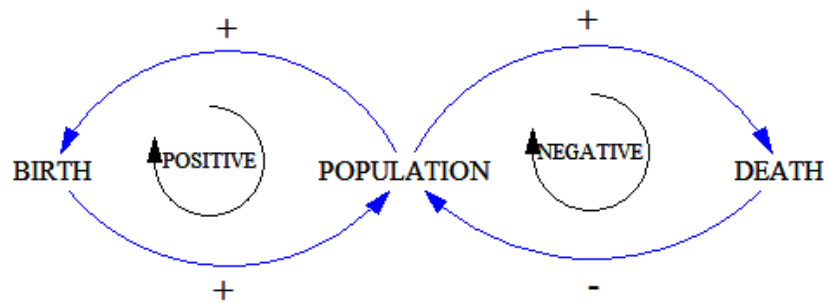


FIGURE 1-6: A causal loop for population, birth, and death cause and effect (The author has created this image)

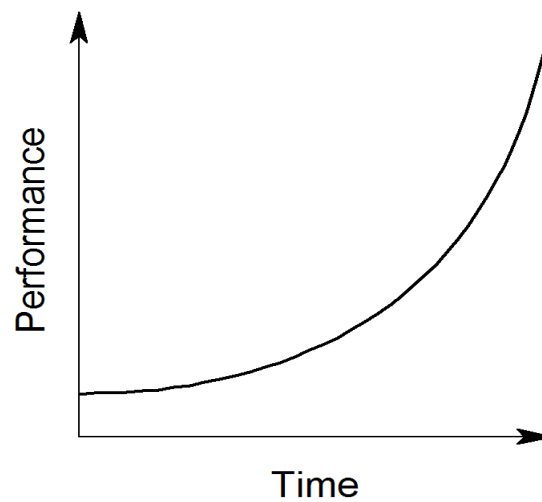


FIGURE 1-7: A representation of functions for population-birth has exponential growth function (Kirkwood 2013)

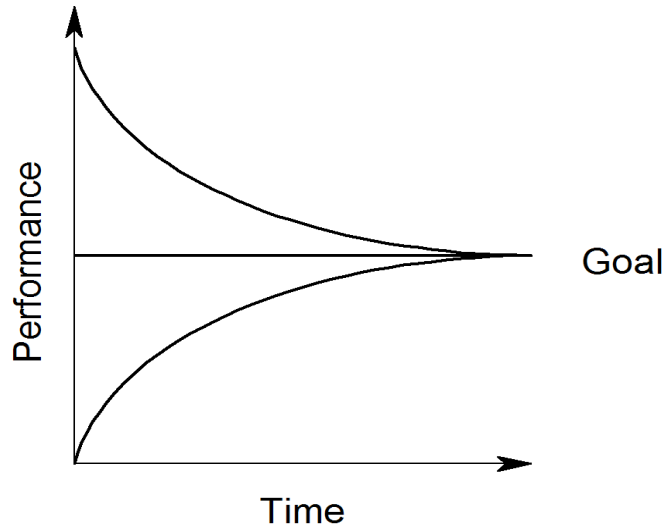


FIGURE 1-8: A representation of functions for population-death has a goal-seeking function (Kirkwood 2013)

1.4.2 Stock and Flow

Quantitative assessments in SDM requires building a stock and flow diagram. As with a causal loop diagram, the stock and flow diagram shows the relationships between variables that can change over time due to changes that occur to other variables (Kirkwood 2013). However, unlike the causal loop diagram, the stock or flow functions contain constants or formulas that describe the relationship between mathematical formulation variables. For example, FIGURE 1-9 shows a stock and flow diagram, and FIGURE 1-10 shows the stock and flow diagram of the system in FIGURE 1-6.

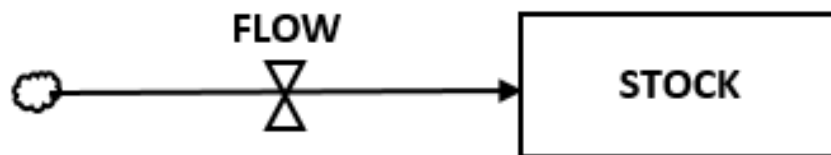


FIGURE 1-9: Stock and flow diagram (Kirkwood 2013)

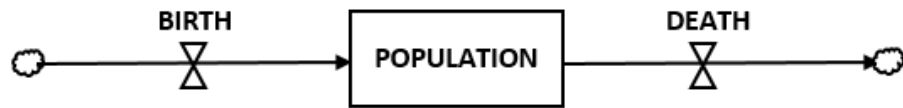


FIGURE 1-10: The stock and flow diagram of the system in FIGURE 1-6 (Kirkwood 2013)

The population-birth relationship is positive, and it means that when the births increase, the population increases and when the population increases, the births will increase as in (1-2). On the other hand, the population-death relationship is negative because when the death rate increases, the population decreases, as in (1-3), and if the death rate exceeds the birth rate, the negative relationship effect overcomes the positive relationship effect (1-4). Therefore, the stock and flow diagram shown in FIGURE 1-10 has been presented in a mathematical relationship between population, birth, and death in FIGURE 1-11.

$$\text{Pop}\Delta 1 = \text{Pop}1 \times \text{Br} \tag{1-2}$$

$$\text{Pop}\Delta 2 = -\text{Pop}1 \times \text{Dr} \tag{1-3}$$

$$\text{Pop}2 = \text{Pop}1 + \text{Pop}\Delta 1 + \text{Pop}\Delta 2 \tag{1-4}$$

where,

Pop Δ 1 is the number increase in the population due to births

Pop Δ 2 is the number decrease in the population due to deaths

Pop1 is the number population before the increase and decrease due to births and deaths

Pop2 is the number population after the increase and decrease due to births and deaths

Br is the birth rate in percentage

Dr is the death rate in percentage

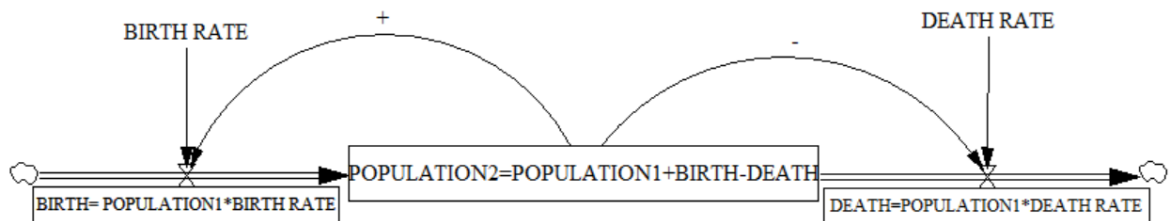


FIGURE 1-11: Stock and flow diagram (The author has created this image)

1.5 RESEARCH MOTIVATION

The motivation behind the research was the expansion of the Liverpool container terminal, and the future demand increase of shipment containers flow on the road congestion and safety. The gradual increasing demand for road freight is reducing traffic flow speed and increasing congestion. Hence, it is essential to determine the effect of intermodal CC-HGVs on the traffic flow and estimate the impact of reaching the maximum capacity at the Liverpool container terminal on the traffic flow operation. Besides, it is vital to have a quantitative tool to estimate the HGV's effect, predict future demand increase, and provide developers, planners, and traffic operators options on an hourly basis. Furthermore, the ongoing increase in congestion has caused a poor record of safety. Therefore, the main issue is to improve the safety of the road that will help reduce accidents, save lives, and avoid unnecessary obstructions and blocked roads.

In the year 2011, the Mersey ports have set the first target for the years 2020 and 2030 for growth to accommodate the expansion of the Liverpool container terminal (Peel Ports 2011), and the target was to transport 85% of intermodal containers by road and 10% by rail, and 5% by inland waterways by 2030. However, the freight rail and inland waterway freight in the UK are underdeveloped in comparison to European countries and demand increase targets. Therefore, currently, over 90% of intermodal container transportation is conducted by road freight. Currently, the Liverpool container terminal processes 1.101M TEUs annually, while the target for the years 2020 and 2030 requires processing and transporting 2MTEU and 3MTEU, respectively.

For the last ten years, the Peel Ports have been developing the Mersey ports to meet the targets by providing new service lines, new HGV refuelling site, and new rail container service (Maritime UK, 2019) (Peel Ports, 2018). However, the actual increase in container processing has not taken place yet, and the increased demand rate is not related to the targets because the growth of demand requires a build-up of contracts and deals with international logistic and manufacturing organisations.

In the year 2019, reports have been published by the National Infrastructure Commission (NIC) (NIC, 2019) and the Government Office of Science (GOS) (GOS, 2019) have stated that the new road freight policy up to the year 2050 is to keep things the way they are and focus on reducing road pollution by electrifying HGVs and reduce cost

by switching to autonomous HGVs. (National Infrastructure Commission, 2019) (Government Office of Science, 2019)

1.6 RESEARCH OBJECTIVES

The aim of the research is to determine the impact of increasing HGVs on the road traffic operation and safety.

The research objectives are as follows:

- 1- To determine the impact of CC-HGVs on traffic flow operation and safety to improve the traffic operation safety and road freight deliveries by developing PCE and capacity estimation methods that consider drivers and pedestrians' safety and improve the desired traffic operation and logistics of the road.
- 2- To derive an efficient estimation method of PCE of HGVs that is effective in oof-peak as well as off-peak hours of the day
- 3- To develop a dynamic model that considers all the variables that correspond to vehicle's parameters, average traffic flow speed, loading rate, traffic flow volumes of the composite traffic flow and the four main types of vehicles' volumes. Also, the braking competency level and reaction time of drivers.
- 4- To determine the feasibility of building new roads, lanes or reschedule shipments to accommodate the demand increase for road freight.
- 5- To develop a capacity estimation method that considers average flow speed and safe headway to determine CC-HGVs' effect on the traffic flow speed before and after rescheduling or rerouting.
- 6- To assess the headway of a vehicle according to the required driving safety and not according to the random driving competency and behaviour because part of road planning is to improve the level of service of the road, reduce congestion, and reduce accidents.
- 7- To develop a highly accurate average traffic speed prediction method to facilitate rescheduling and routing and develop a speed prediction method for individual vehicle's speed to assess the effect of the proportion of a single type of vehicle in the traffic flow on the average traffic speed.
- 8- To assess the space required to decelerate to bring the vehicle to a standstill and the space required for the driver to accelerate up to the average traffic speed of the road.

- 9- To develop a level of service methods that estimate the risk of having an accident and the risk of sustaining a severe injury or death to pedestrians and consider the available reaction time and available stopping distance to determine the impact of HGVs on the available gap between vehicles and its impact on safety.
- 10- To determine the impact of increasing HGVs on the road on the average traffic speed and explore scenarios of road planning.

1.7 RESEARCH LIMITATION

The research covers the impact of HGVs on traffic flow speed, congestion, safety, and seamless products' flow for all urban roads and streets in the UK and the USA that have controlled intersections. The research also covers traffic speed flow prediction, accident prevention, pedestrian fatality and severe injury prevention, and the level of service assessment. The model design is microscopic, and in further work, the authors can develop it to assess a wider area by connecting road links.

The method is not suitable for roundabouts, tunnels, minor roads, rural roads, and uncontrolled intersections. It does not cover drivers' behaviour of large vehicles such as long HGVs and high Q container carriers, tankers, and cryogenic container tank carriers, it is because, in such conditions, drivers can face some issues in loss of balance when turning at intersections and roundabouts or due to crosswind. Research only covers basic aerodynamics, driver behaviour, and environmental impact on the traffic flow (Makki 2020).

1.8 RESEARCH CONTRIBUTIONS

The author has developed eight original methodology contributions in this research, as follows:

- 1- The Deceleration and Acceleration Space PCE estimation method (PCE_{DAS}) (in chapter three)
- 2- The Deceleration and Acceleration Space capacity estimation method (C_{DAS}) (in chapter three)
- 3- The Average Traffic Speed prediction method based on the Speed-Density relationship and Acceleration Delay Impact (ATS_{SDE}) (in chapter four)
- 4- The Average Traffic Speed prediction method based on Acceleration Performance and Vehicle types Proportions in the traffic flow (ATS_{APE}) (in chapter four)

- 5- The Level of Service method based on Available Reaction Time (LoS_{art}) (in chapter five)
- 6- The Level of Service method based on Available Stopping Distance (LoS_{asd}) (in chapter five)
- 7- The Level of Service method based on the risk of a pedestrian sustaining a severe injury (LoS_{rsi}) (in chapter five)
- 8- The Level of Service method based on the risk of a pedestrian's death (LoS_{rd}) (in chapter five)

1.9 RESEARCH APPLICATIONS

There are several applications for the proposed method (Makki 2020):

- 1- The container terminal managers and logistic transportation companies have access to trucks' dimensions and drivers' records, and the load's weight and volume. They can utilise the new method to determine the available road space for HGVs to apply a dynamic rescheduling calculation to determine the efficient combination for HGVs and loading factors that help ship dry and cryogenic intermodal containers in the most effective logistic routing.
- 2- The container terminal managers and logistic companies, local and national travel authorities, and councils can access vehicle registration, drivers' license, load factor, and routing. Hence, they can coordinate and integrate the new method's algorithms with the existing traffic operation and logistics systems and determine the optimum intermodal logistics network operation.
- 3- The local and national travel authorities and councils can utilise the new traffic operations and road construction and development planning methods.
- 4- The developers can utilise big data to improve the model outcome and obtain detailed and commercialised projections that help plan for road development.
- 5- The method contributes to road level of service estimation that can help to reduce road accidents' casualties and costs
- 6- The level of service method can be utilised to control access to roads with a poor safety record and to improve the safety of roads near schools by applying access charges to drivers with penalty points or a record of bad behaviour. The decision can also be related to the materials that the driver is transporting or the operating conditions of the vehicle, such as the braking system.

- 7- The new method also contributes to automated braking and cruising systems by estimating the safe stopping distance.

1.10 THESIS OUTLINES

CHAPTER 1: INTRODUCTION

This chapter contains a background of this research's central issue, motivations, objectives, limitations, applications, contributions, and a list of publications.

CHAPTER 2: LITERATURE REVIEW

This chapter contains a literature review of the primary PCE estimation methodologies, braking system, stopping distance, reaction time, capacity, automatic traffic counting, and system dynamics.

CHAPTER 3: PASSENGER CAR EQUIVALENT AND ROAD CAPACITY ESTIMATION METHODS

This chapter contains the development of two main contributions of this research. The author presented the methodologies of estimating PCE and road's capacity and the rescheduling of HGVa.

CHAPTER 4: TRAFFIC FLOW SPEED PREDICTION METHODS

This chapter contains the literature review of the current speed prediction methodologies and the development of two speed-prediction methods method of predicting the average flow speed and an assessment of the impact of several logistics and transportation scenarios on the average traffic speed

CHAPTER 5: LEVEL OF SERVICE ESTIMATION METHODS

This chapter contains the development of four methods of road Level of Service with consideration to available reaction time, available stopping distance, the risk of sustaining a severe injury, and risk of death,

CHAPTER 6: MODAL DATA AND SYSTEM VALIDATION

This chapter contains the variables' relationships, model structure, mechanism, data validation, and system validation and calibration

CHAPTER 7: CONCLUSIONS AND FUTURE WORK

This chapter contains the conclusions and future work.

1.11 PUBLICATIONS

Based on the results of the research work reported in this thesis, the following PhD publications have been published:

1. A. A. Makki, T. T. Nguyen, J. Ren, D. Al-Jumeily and W. Hurst, "Estimating Road Traffic Capacity," in IEEE Access, vol. 8, pp. 228525-228547, 2020, doi: 10.1109/ACCESS.2020.3040276 (Open Access).
2. A. A. Makki, T. T. Nguyen, J. Ren, W. Hurst and D. Al-jumeily, "Utilising Automatic Traffic Counters to Predict Traffic Flow Speed," 2019 12th International Conference on Developments in eSystems Engineering (DeSE), Kazan, Russia, 2019, pp. 823-830, doi: 10.1109/DeSE.2019.00153.
3. A. A. Makki, T. T. Nguyen and J. Ren, "A New Level of Service Method for Roads Based on Available Perception Time and Risk of Sustaining Severe Injury or Death," 2019 5th International Conference on Transportation Information and Safety (ICTIS), Liverpool, United Kingdom, 2019, pp. 1031-1036, doi: 10.1109/ICTIS.2019.8883572. (Awarded for best paper)
4. Ahmed Adnan Makki, Trung Thanh Nguyen, Jun Ren, William Hurst, "The effect of the increase of container carrier heavy goods vehicles on traffic flow operation and congestion," Research week conference in Liverpool John Moores University May-2019 (Internally published: Awarded for best paper, first place)
5. Danial Yazdani, Mohammad Nabi Omidvar, Igor Deplano, Charly Lersteau, Ahmed Makki, Jin Wang, Trung Thanh Nguyen, "Real-time seat allocation for minimising boarding/alighting time and improving quality of service and safety for passengers," Transportation Research Part C: Emerging Technologies, Volume 103, 2019, Pages 158-173, ISSN 0968-090X, <https://doi.org/10.1016/j.trc.2019.03.014>.

CHAPTER TWO: LITERATURE REVIEW

2.1 INTRODUCTION

The PCE of HGVs has to be estimated to determine HGVs' effect on the traffic flow operation. Many factors affect the PCE value, and some of the critical factors affecting the accuracy of the traffic flow analysis are the vehicular types and proportions of the traffic flow (Al-Kaisy 2006). The proportions of non-PC vehicles have a negative effect on the capacity and Level of Service (LoS) of roads, mainly when roads are located near container ports or industrial areas, due to the relatively high traffic volume and percentage of HGV in traffic flow. Hence, it is essential to obtain a realistic PCE of HGVs, which show the equivalent effect of an HGVr or HGVA on traffic flow compared to PC vehicles. Over the last 80 years, researchers have developed PCE estimation methodologies that utilise vehicle's proportion, traffic volume, length, speed, delay, travel time, EP, or a combination of two to three of these variables.

The PCE Converted Traffic Flow Volume (TF_{PCE}) calculation converts non-PC vehicles to their PCE values. For example, by assuming that there are only two types of vehicles on the road of PCs and HGVs, then the Heterogeneous Composite Traffic Flow Volume (TF) is as in (2-1), and the TF_{PCE} is as in (2-2). Therefore, converting a TF to a TF_{PCE} is by deducting the number of HGVs on the road from the TF and converting the HGVs to their PCE value and adding them to the number of PC vehicles (2-3). The author chose to use the expression flow volume rather than flow rate because according to (TRB 2000), the flow rate in transport terminology is for periods of less than an hour and volume is for an hour, day, week, month, or year. Therefore, although the ATC data are for every 15 minutes, the author has compiled it and converted it to an hourly rate.

$$TF=PC+HGV \quad (2-1)$$

$$TF_{PCE}=PC+HGV \times PCE \quad (2-2)$$

$$TF_{PCE}=TF-HGV+HGV \times PCE \quad (2-3)$$

where,

TF is the total composite traffic flow volume in veh/h

TF_{PCE} is the total PCE converted traffic flow volume in PC/h

PC is the PC vehicles traffic flow volume in PC/h

HGV is the HGV traffic flow volume in HGV/h

2.2 LITERATURE REVIEW

This section holds a review of the current PCE estimation methods, vehicle's acceleration performance effect, the effect of the RT and BCL on vehicle Stopping Distance (SD), and the vehicle's braking performance effect on SD.

TABLE 2-1 shows the literature review formulas and description.

TABLE 2-1: Literature Review formulas and their description

Author	Formulas	Description	Author	Formulas	Description
TRB (2000) TRB (2010) TRB (2020)	$F_{bv} = \frac{1}{1 + P_T \times (PCE_T - 1)}$	Heavy vehicle factor	Molina (1987)	$PCE_T = 1 + \frac{DT_T - DT_{PC}}{HT_{PC}}$	Based on vehicle delay
TRB (2000) TRB (2010) TRB (2020) Huber (1982)	$PCE_T = \left(\frac{1}{P_T}\right) \times \left(\frac{TF_{PCE}}{TF} - 1\right) + 1$	Saturation Flow	Greenshields (1935) Seguin (1982) Cunagin (1982)	$PCE_T = \frac{H_T}{H_{PC}}$	Vehicle headway
John (1976)	$PCE_T = \left(\frac{1}{2 * P_T}\right) \times \left(\left(\frac{TF_{PCE}}{TF}\right)^2 - 1\right) + 1$	Non-linear relationship	Gwynn (1968) Werner (1976)	$PCE_T = \frac{\frac{H_{Total}}{H_{PC}} - P_{PC}}{P_T}$	Headway
Sumner (1984)	$PCE_T = \frac{1}{P_T} \times \left(\frac{TF_{PCE}}{Truck} - \frac{TF_{PCE}}{TF}\right) + 1$	Based on traffic volumes	Krammes (1986)	$PCE_T = \frac{PCE_T \times (1 - P_T) \times (H_{pt} + H_{tp} - H_{pp}) + P_T \times H_{tt}}{H_{pp}}$	Impact of trucks' position on the road
Cunagin (1983)	$PCE_i = \frac{D_i}{D_{PC}}$	Based on vehicle delay	Rahman (2005)	$PCE_T = 1 + \frac{S_b - S_m}{S_b}$	Impact of trucks on average speed
Benekohal (2000)	$PCE_T = 1 + \frac{D_T - D_{PC}}{P_T \times AD_{PC}}$	Based on vehicle delay	Guiffre' (2017) Guiffre' (2018) Guiffre' (2019)	$PCE_T = \left(\frac{1}{P_T}\right) \times \left(\frac{C_{PC}}{C_M} - 1\right) + 1$	Capacity and proportion
Keller (1984)	$PCE_T = \frac{TT_T}{TT_{PC}}$	Based on travel time	Macioszek (2019)	$PCE_r = \frac{t_f}{t_{fc}} \quad \text{and} \quad PCE_a = \frac{t_a}{t_{fa}}$	
Chandra (2000)	$PCE_T = \frac{S_{PC} \times A_T}{S_T \times A_{PC}}$	vehicle speed and footprint	Lu (2020)	$PCE_T = \frac{D_T}{D_{PC}} = \frac{Q_T + H_T}{Q_{PC} + H_{PC}}$	Based on vehicle delay
Huber (1982)	$PCE_T = \frac{S_{PC} \times L_T}{S_T \times L_{PC}}$	vehicle speed and length			

2.2.1 PCE Estimation Methods

Usually, the purpose of the PCE estimation is to assess the impact of any type of non-PC vehicles, but this research focuses on determining the impact of trucks. This section contains a review of the existing PCE estimation methods that depend on traffic flow and proportion, flow speed and travel delay, traffic light queue discharge, and vehicle's headway.

2.2.1.1 PCE based on Traffic Flow and Vehicle Proportion

The Highway Capacity Manual (HCM) (TRB 2000; TRB 2010; Ryus 2011; TRB 2020) proposed the saturation method to estimate trucks' effect on the road traffic capacity. The saturation flow method is assessed by calculating the Heavy Vehicle Factor (F_{hv}) that estimates traffic flow capacity considering the vehicle's PCE and the proportion of the vehicle's type in the traffic flow, as in (2-4). According to (2-3) and (2-4), the relationship between the F_{hv} and the traffic flow volume is shown in (2-5), where the F_{hv} is equivalent to the ratio of TF to the TF_{PCE} . The author has concluded from (2-4) that the PCE_T formula is (2-6).

$$F_{hv} = \frac{1}{1 + P_T \times (PCE_T - 1)} \quad (2-4)$$

$$F_{hv} = \frac{TF}{TF_{PCE}} \quad (2-5)$$

$$PCE_T = \frac{1 + F_{hv} \times (P_T - 1)}{F_{hv} \times P_T} \quad (2-6)$$

where,

F_{hv} is the heavy vehicle factor

PCE_T is the PCE of trucks

P_T is the proportion of trucks' flow volume in the traffic flow

TF_{PCE} is the PCE converted traffic flow volume

TF is the heterogeneous traffic flow volume

Therefore, by utilising TF of the road link under investigation and applying the formula (2-6) to estimate the average PCE of all non-PC vehicles on the DBR by using the F_{hv} and P_T of all non-PC vehicles, as shown in FIGURE 2-1. The F_{hv} is inversely proportional to trucks' traffic volume, PCE of Trucks (PCE_T) and Traffic Flow Volume Proportion (P_T), as shown in FIGURE 2-2, FIGURE 2-3, and FIGURE 2-4. If there are only PCs on the road, then the P_T equal to zero. Therefore, the F_{hv} is equal to one, as in (2-4), and if the F_{hv} equals one, then the PCE_T is equal to one, as in (2-6).

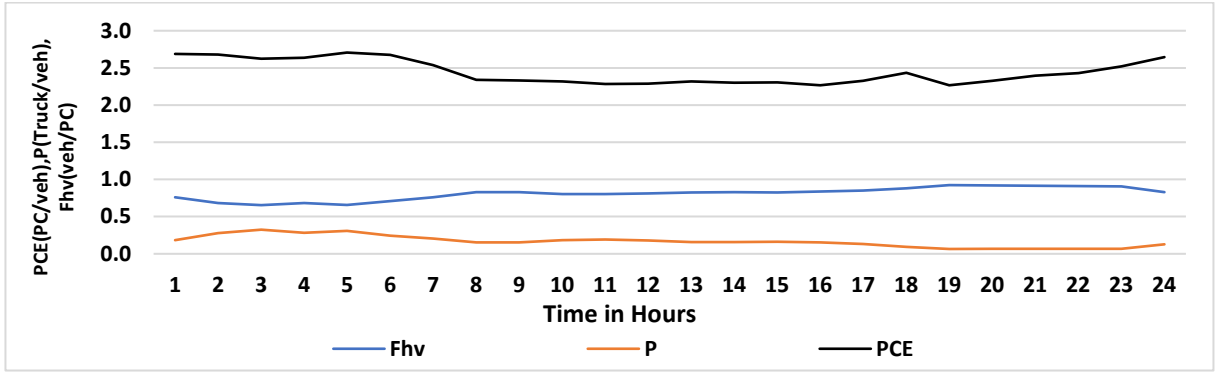


FIGURE 2-1: Average PCE of all non-PC vehicles on the DBR A5036 of link A5038-B5207

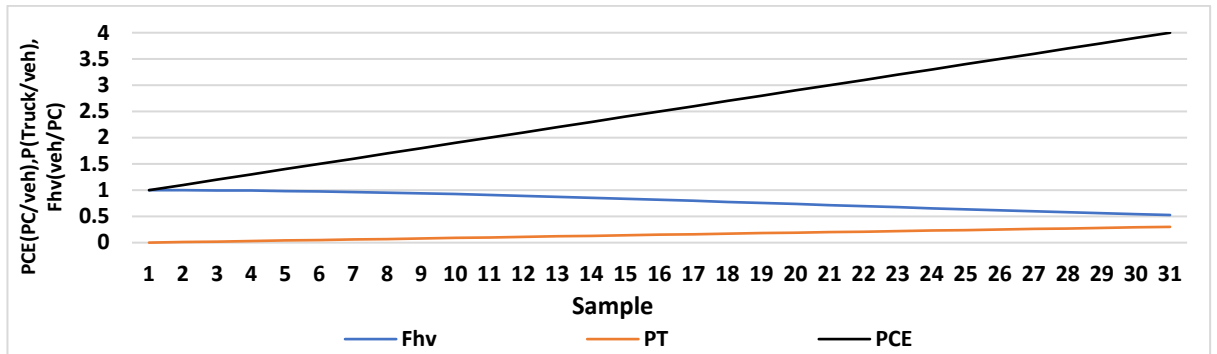


FIGURE 2-2: F_{hv} with a linear increase of P_T (0 to 0.3) and PCE_T (1 to 4)

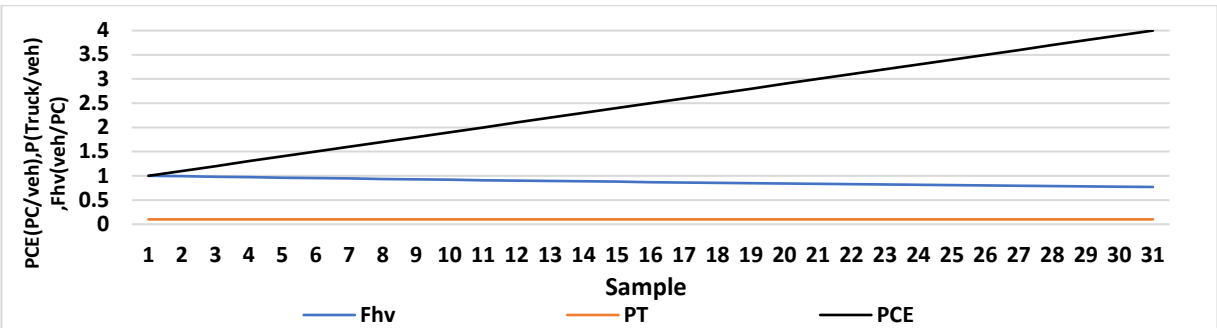


FIGURE 2-3: F_{hv} with a linear increase of PCE_T (1 to 4) and constant P_T of 0.1

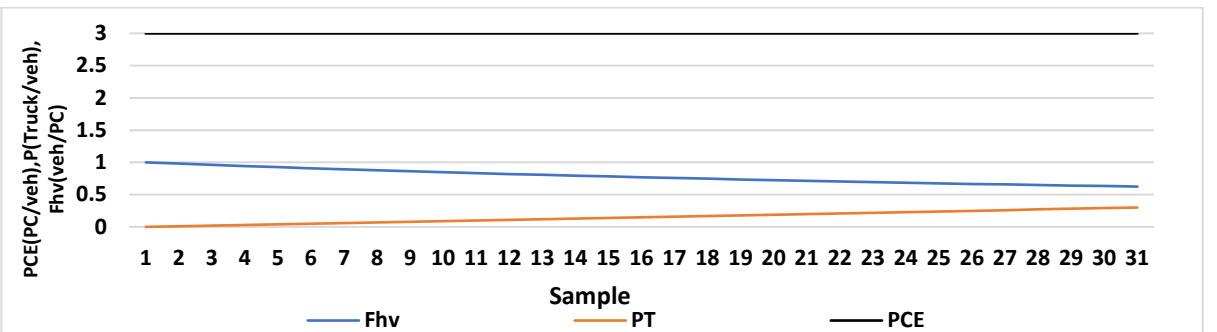


FIGURE 2-4: F_{hv} with constant PCE_T of 3 and linear increase in P_T

Some PCE estimation methods utilise the traffic flow volumes and P_T , such as the method developed by Huber (1982) as in (2-7). Also, according to (2-1), (2-2), and (2-3), the formula (2-7) is equivalent to (2-8), and by considering the same road and conditions as in Figure 2-1, the results of (2-7) are equivalent to that of (2-6).

$$PCE_T = \frac{1}{P_T} \times \left(\frac{TF_{PCE}}{TF} - 1 \right) + 1 \quad (2-7)$$

$$PCE_T = \frac{TF_{PCE} - TF \times (1 - P_T)}{TF \times P_T} \quad (2-8)$$

St John (1976) derived a nonlinear formula from equations (2-2), (2-4), and (2-5), as in (2-9) (St John 1976; St John 1978). St John (1976) claimed that his formula is suitable for estimating the PCE of a single type of vehicles and assuming that only PCs and one type of trucks are on the road.

$$PCE_T = \frac{1}{2 \times P_T} \times \left(\left(\frac{TF_{PCE}}{TF} \right)^2 - 1 \right) + 1 \quad (2-9)$$

where,

TF_{PCE} is the total PCE traffic flow volume in PC/h

TF is the heterogeneous traffic flow volume in veh/h

P_T is the proportion of trucks' flow volume in the traffic flow in truck/veh

Webster (1999) found that HGVs' PCE in (2-7) increases with the increase in traffic flow, Free Flow Speed (FFS) and grade length and decreases with the increase in the truck's proportion (Webster 1999). The estimated PCE of trucks uses the saturation flow, Huber, and St John's formulas are in FIGURE 2-5. The saturation flow and Huber methods show identical results, while the St John method shows a similar pattern with higher values.

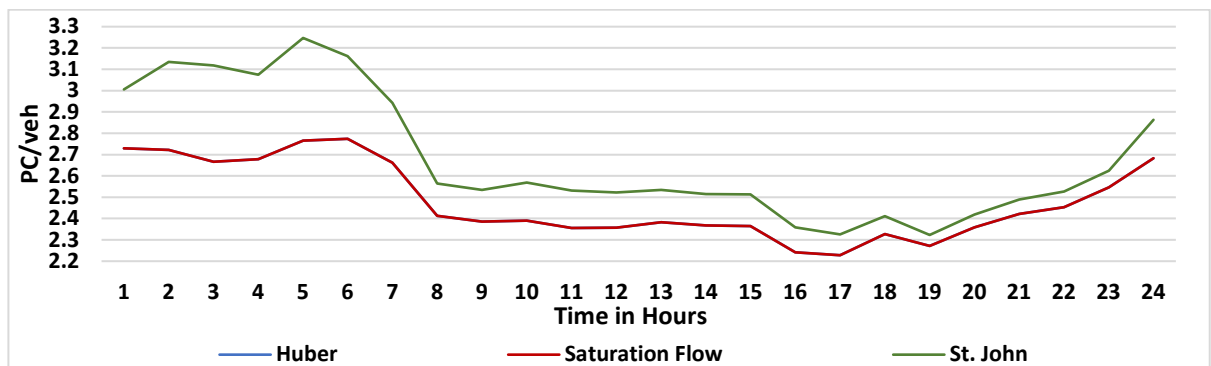


FIGURE 2-5: Average PCE of all non-PC vehicles using methods of Saturation flow, Huber (1982), and St. John (1976) as in (2-6), (2-7),

Sumner (1984) derived a formula that utilised the truck flow volume and proportion (2-10) (Sumner, 1984). The results for Sumner's formula for the DBR are in FIGURE 2-6.

$$PCE_T = \frac{1}{P_T} \times \left(\frac{TF_{PCE}}{Truck} - \frac{TF_{PCE}}{TF} \right) + 1 \quad (2-10)$$

where,

TF_{PCE} is the total PCE traffic flow volume in PC/h

TF is the heterogeneous traffic flow volume in veh/h

P_T is the proportion of trucks' flow volume in the traffic flow in truck/veh

Truck is the truck' flow volume in truck/h

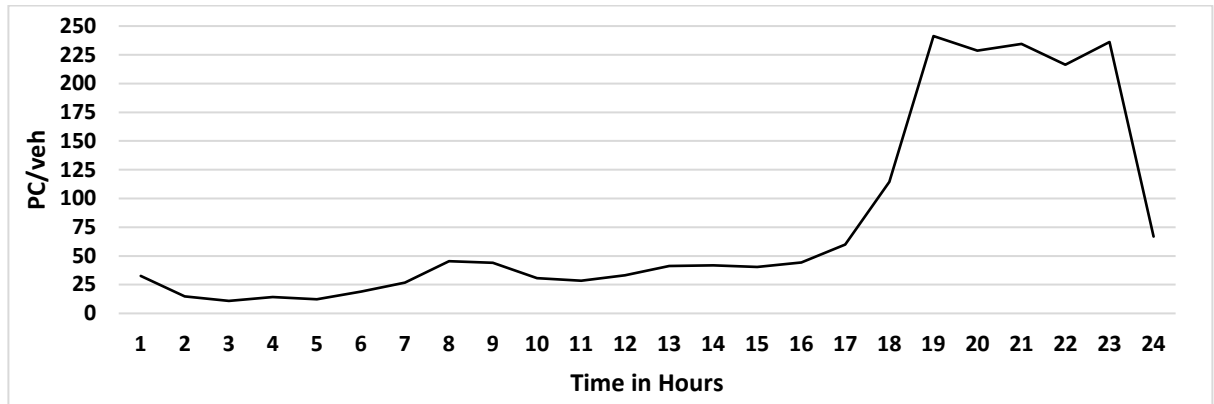


FIGURE 2-6: Average PCE value of all non-PC vehicles using Sumner's formula (2-10) by Sumner (1984)

2.2.1.2 PCE based on Speed, Travel Time, and Delay

St John (1976) also developed a PCE estimation method that uses only the type of non-PC vehicle's speed, as in (2-11). The (2-11) formula showed that the PCE_T decreases exponentially with the increase of the truck's speed.

$$PCE_T = e^{(7.440436 - 0.0749846 \times S_T)} \quad (2-11)$$

where,

S_T is the speed of the truck in km/h

St John (1976) stated that (2-11) was suitable for flows that are nearly balanced on highways where the 85th percentile speed of passenger cars is about 105 km/h (65 mi/h) and should change under different roads, speeds, and speed limits. The $PCE_T=1$ at vehicle's speed of 99.22 km/h (61.65 mi/h) and the PCE of a truck running with 88.51 km/h (55 mi/h) equals 2.23. However, the formula (2-11) is not suitable for a 64.37 km/h (40 mi/h) road.

Huber (1982) derived the formula from the formula in (2-7). Huber's method is dependent on the vehicle's length, and speed, as in (2-12), and Huber (1982) proved that the formula (2-12) is equivalent to the formula (2-7). Huber (1982) estimated the PCE_T to be 4.5 for an FFS of 48.28 km/h and 32.187 km/h for PCs and Trucks and vehicle

lengths of 7.62 m and 22.86 m for PCs and Trucks, respectively (Huber 1982). Huber (1982) used the ratio of a vehicle's speed to the vehicle's length compared to that of a PC, as in (2-12).

$$PCE_T = \frac{S_{PC}}{S_T} \times \frac{L_T}{L_{PC}} \quad (2-12)$$

where,

S_{PC} is the FFS of passenger cars in km/h

S_T is the FFS of trucks in km/h

L_{PC} is the PC's length in m

L_T is the Truck's length in m

Methodologies that depend on time delay or travel time, such as evaluating the composite PCE of 14 different non-PC vehicle types (Cunagin 1983). Cunagin (1983) estimated the composite PCE by calculating the extra delay caused to PCs by non-PC vehicles compared to the delay caused to PCs by slower PCs, as in (2-13).

$$PCE_T = (D_T - D_{PC}) / D_{PC} \quad (2-13)$$

where,

D_T is the delay caused to PC by trucks in s

D_{PC} is the delay to PCs caused by slower PC in s

Cunagin (1983) found that the composite PCE at level terrain started with 1.5 at P_T of 0.05 and a TF of 600 veh/h and started to increase at a TF of 1000 veh/h, and PCE reached its maximum value of 2 at TF of 2000 veh/h and a P_T of 0.25, as shown in FIGURE 2-7.

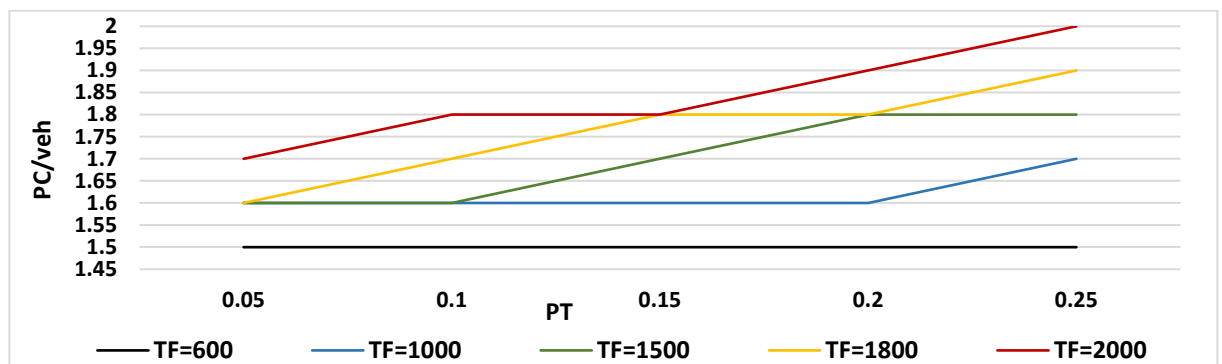


FIGURE 2-7: The composite PCE value of non-PC of 14 non-PC vehicle types by Cunagin (1983)

Keller (1984) developed an estimation method of PCE that depends on the truck's travel time compared to the average travel time of composite TF, as in (2-14), and used macroscopic traffic modelling (Keller 1984).

$$PCE_T = \frac{TT_T}{TT_{PC}} \quad (2-14)$$

where,

TT_T is the total travel time of trucks in s

TT_{PC} is the total travel time of PCs in s

The results in (Keller 1984) showed that the estimates of PCEs increase as the traffic volume exceeded capacity, larger trucks are inserted in the flow, and the traffic signal reached maximum flow. The results showed that the PCE_T was equal to 1.29 at off-peak and peak conditions except for a traffic jam condition where it reached 1.53.

Aerde (1984) developed a method for PCE estimation based on speed reduction caused by traffic in the opposite direction in two-lane rural highways (two-lane road with the unseparated two-direction flow) and explored the effect of having a group of vehicles travel very closely together. The PCE values that Aerde (1984) estimated for trucks ranged from 3.8 to 11.4 and for recreational vehicles ranged from 2.6 to 3.9. Following vehicles' PCE values for trucks and recreational vehicles at high traffic volumes were 1.20, 1.07, respectively, and 1.23 for both types at low traffic volumes, while leading vehicles' PCE for trucks and recreational vehicles are 2 and 1.55, respectively (Aerde 1984).

Chandra (2000) estimated PCE based on speed and occupied area on the road, as in (2-15), and stated that the physical size indicated its manoeuvrability and acceleration capability and estimated its footprint 7.28m² and 23m² PCs and HGVs, respectively. Chandra's method led to a PCE_T value of 4.77, and it is slightly higher than the PCE_T of Huber's method (Chandra 2000). In addition, Chandra (2000) used the ratio of vehicle's speed to the occupied area on the road compared to that of a PC, as in (2-15).

$$PCE_T = \frac{S_{PC}}{S_T} \times \frac{A_T}{A_{PC}} \quad (2-15)$$

where,

S_{PC} is the FFS of passenger cars in km/h

S_T is the FFS of trucks in km/h

A_{PC} is the area occupied by passenger cars on the road in m²

A_T is the area occupied by trucks on the road in m²

Benekohal (2000) developed a method for signalised intersections by measuring the PCE according to the additional delay caused by trucks with consideration to P_T , as in (2-16), and concluded that the P_T had less impact

on the PCE value than TF. The results showed that the PCE for single-unit trucks varied from 1 to 1.37 PC/truck while the PCE value for combination trucks varied from 1 to 2.18 PC/truck (Benekohal 2000).

$$PCE_T = 1 + \frac{D_T - D_{av}}{P_T \times D_{av}} \quad (2-16)$$

where,

D_{av} is the average vehicle delay when the traffic consists of only PCs in s

D_T is the delay of trucks in s

P_T is the truck flow volume proportion in truck/veh

Rahman (2005) utilised only PCs' speed to estimate non-PC vehicles' PCE, as in (2-17). Even though the Rahman (2005) method was for non-motorised vehicles, it resembled non-PC vehicles' effect on the traffic flow speed as a PCE measure because heavier and larger vehicles usually have lower performance (Rahman 2005) shown in FIGURE 2-8.

$$PCE_T = 1 + \frac{S_b - S_m}{S_b} \quad (2-17)$$

where,

S_b is the speed of PCs in a basic flow where there are only PCs on the road, in km/h

S_m is the speed of PCs in a mixed flow, in km/h

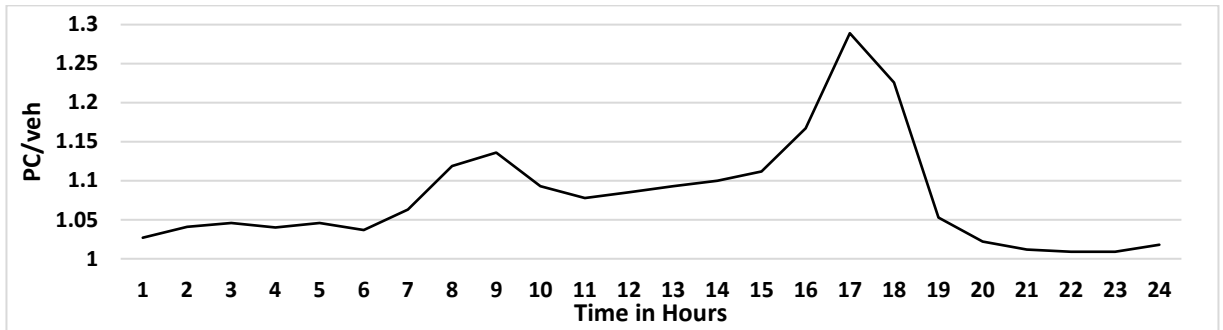


FIGURE 2-8: The composite of non-PC vehicles' PCE by Rahman (2005)

Lu (2020) developed a PCE method based on vehicle's delay for two-lane with unseparated two-way traffic flow highway, as in (2-18) (Lu 2020), and found that traffic congestion level duration time has a significant impact on PCE values. The PCE did not change with time when traffic has balanced (when traffic congestions levels are the same for both lanes), but it increased over time when traffic loses balance from 2.35 to 6.71, with the duration time increases from 5 to 120 minutes. Lu (2020) stated that TRB (2010) had underestimated the value of PCE in such a condition.

$$PCE_T = \frac{D_T}{D_{PC}} = \frac{Q_T + H_T}{Q_{PC} + H_{PC}} \quad (2-18)$$

where,

D_T is the delay caused by a truck in s

D_{PC} is the delay caused by a slow PC in s

H_T is space between the passenger car in front of the truck and the one following right behind the truck

H_{PC} is space between the passenger car in front of the slow passenger car and the one following right behind it

Q_T is the length of queue caused by the truck

Q_{PC} is the length of queue caused by the slow PC

2.2.1.3 PCE Based Queue Discharge

Sumner (1984) collected data from ten cities in the USA of 15 categories of vehicles from cameras at intersections, measured the discharge headway, acceleration, and speed of various vehicles, and estimated the PCE HGVa be a maximum of 1.59. as in TABLE 2-2. Sumner (1984) only considered the vehicles that had gaps with the leading vehicles of greater or equal to 2.5s.

TABLE 2-2: Results of Sumner (1983) measurements

Type of vehicle	Length in m	Max. Acceleration in m/s ²	Speed in km/h	Discharge headway in s	PCE at off-peak	PCE at peak
PC	3.96	2.32	57.93	2.1	-	-
HGV _a	15.85	1.25	48.28	5.5	1.25-1.52 and average of 1.36	1.48-1.78 and average of 1.59

Molina (1987) developed a PCE estimation method dependent on the vehicle's position in a traffic queue. The method is dependent on the extra delay caused by longer trucks. Molina (1987) proposed modifying the headway ratio by adding a headway behind trucks and developing a relationship between passenger cars' headway and time of discharge of passenger cars' queue and time of discharge of trucks' queue, as in (2-19) (Molina 1987). Molina (1987) estimated the PCE values to be 1.6, 2, 2.3-2.5 and 3.1-4.1 for two-axle, three axles, four-axle and five-axle trucks, respectively. Molina (1987) suggested that vehicles' positions in the queue do not significantly affect the two to three-axle trucks' PCE values. The acceleration performance of these types of trucks is close to that of passenger cars. Thus, their position in the queue has minimal effect on the PCE value.

$$PCE_T = \frac{H_T + \Delta H}{H_{PC}} \quad (2-19)$$

where,

H_T is the truck headway in s

H_{PC} is the PC headway in s

ΔH is the increased headway of the queue caused by the trucks in s

There are other methods developed based on congested conditions represented by Queue Discharge Flow (QDF) and vehicle's Power to Weight Ratio (PWR) Al-Kaisy (2002) and Al-Kaisy (2005), respectively. These two methods work during congested traffic where traffic volume has reached the capacity level and dependent on a vehicle's manufacturing characteristics that vary according to the HGV's load. For example, a fully loaded truck acceleration time is different from an empty truck, and the QDF method only considers traffic flow at full capacity (Al-Kaisy 2002; Al-Kaisy 2005).

Different factors involve estimating the effect of HGVs, such as grade, grade length and lane restriction by vehicle type. Al-Kaisy (2004) investigated HGVs' effect that ran on roads with upgrade or downgrade (non-level terrain) and suggested that the HCM's PCE recommended values may have a considerable error. Due to the acceleration and deceleration experienced during congestion, Al-Kaisy (2004) utilised the QDF method, and Al-Kaisy (2002) derived the PCE from simulation experiments based on grade lengths of 0.2-2 km, grades of +2-6% and HGV percentage of 2-25%. Al-Kaisy (2004) concluded that HGVs' effect on upgrade roads would not depend solely on the truck's length and headway and acceleration performance, depending on the PWR of the HGV (Al-Kaisy 2004).

2.2.1.4 PCE based on Vehicle's Headway

Gwynn (1968) developed a formula for estimating PCE that considered headway distance and vehicular proportions (2-20). Thus, the study of (Gwynn 1968) focused on assessing the headway distance of vehicles according to their positions in traffic and specified headways for a PC followed by a PC as PP headway, a PC followed by a truck as PT headway, a truck followed by a PC as PP headway, and a truck followed by a truck as TT headway.

$$PCE_T = \frac{H_{av} \cdot P_{PC}}{H_{PC} \cdot P_T} \quad (2-20)$$

where,

H_{av} is the average headway of all vehicle types in the composite traffic flow in s

H_{PC} is the headway for passenger cars in s

P_{PC} is the proportion of passenger cars in the traffic flow

P_T is the proportion of trucks

Gwynn (1968) found that the PCE value is proportional to the traffic flow speed and P_T and found that the PCE for a P_T of 0.8 and a traffic flow speed of 64.37 km/h is 1.86 and that instead of the TT headways being double that of

PP headways, they are only 1.32 times the PP headway. Werner (1976) conducted a study and adopted the formula (2-15) and found that the PCE value is inversely proportional to the road's ATS, and the PCE of a truck at level terrain is equal to 2 PC/truck (Werner, 1976).

Greenshields (1935) utilised the truck's headway in comparison to the PC's headway. Cunagin (1982) used the same method and stated that HGVs' presence reduced the road capacity during the peak period and found that the increase of HGVs in traffic flow would increase the mean headway. Seguin (1982) also used the headway method and found that for typical urban freeway sections, PCE values are less than 2.00 regardless of vehicle type, up to and including tractor-trailers. Fan (1990) found that the PCE values are higher in Singapore than those recommended in the USA and the UK and stated that it is due to lower speed limits for HGVs and LGVs and higher capacity per hour lane in Singapore. In addition, Fan (1990) concluded that HGVs and buses have higher PCE values than LGV even though they have the same speed limit due to the smaller size of LGVs and because LGV drivers exceed speed limits in high proportions. The formulas of Greenshields (1935), Seguin (1982), Cunagin (1982), and Fan (1990) are all the same, as in (2-21) (Greenshields 1935; Seguin 1982; Cunagin 1982; Fan 1990).

$$PCE_T = \frac{H_T}{H_{PC}} \quad (2-21)$$

where,

H_T is the headway for trucks in m

H_{PC} is the PC's headway in m

Note: Both time and distance depend on the vehicle's speed. For example, the headway time does not have a fixed distance unless the speed is constant and vice versa. Researchers or engineers can measure and present a vehicle's headway in time or distance. Different engineers have different approaches, where some of them focus on distance and others focus on time. However, researchers or engineers must be consistent in utilising only one form (either time or distance) in any single formula or model throughout their model calculation.

Krammes (1986) evaluated the merits of three approaches of constant Volume to Capacity Ratio (VtCR), equal density, and spatial headway as identified by (Roess 1980; Roess 1983) to estimate PCE. The formula in (Krammes 1986) considered truck proportion, PC headway, and average traffic headway and assessed the headways in the

same way as Gwynn (1968) approach, as in (2-20). Krammer (1986) assessed the PCE value at two sided and found that the maximum PCE value of a combination of trucks at level terrain was 1.8 PC/truck.

Krammes (1986) stated that trucks are larger than PCs and have lower operating capabilities than PCs and that the spatial headway approach was the most suitable method for basic freeway segments. In addition, Krammes (1986) found that due to the spacing between the following and leading vehicles was maintained by the following vehicle, the formula (2-22) is equivalent to (2-21). However, if the author introduced an extra gap behind HGVA vehicles, then (2-22) will be equivalent (2-23).

$$PCE_T = \frac{(1-P_T) \times (H_{pt} + H_{tp} - H_{pp}) + P_T \times H_{tt}}{H_{pp}} \quad (2-22)$$

$$PCE_T = \frac{H_T - P_T \times G_{PC}}{H_{PC}} \quad (2-23)$$

where,

- H_{pt} is the headway between a PC and a leading truck
- H_{tp} is the headway between a truck and a leading PC
- H_{pp} is the headway between the following PC and a leading PC
- H_{tt} is the headway between a truck and a leading truck
- P_T is the proportion of trucks
- H_T is the truck's headway
- H_{PC} is the PC's headway
- G_{PC} is the gap between a PC and another PC

Obiri-Yeboah (2014) showed that PCE values were higher at intersections with roadside friction (Side friction factors are defined as those activities which take place on the sides of carriageways or even on the carriageways that are likely to affect the normal traffic flowing through the carriageways (Salini 2016) than those without roadside friction. The values obtained in that study were larger than values adopted elsewhere, and it showed PCE values for medium vehicles and trucks of 1.65 and 3.05, respectively, with roadside friction and 1.35 and 2.25, respectively, without roadside friction (Obiri-Yeboah 2014). Elefteriadou (1997) stated that variables such as the percentage of trucks do not always have the expected effect on PCEs. In contrast, other variables, such as vehicle type, PWR ratio, and vehicle length, could be vital to PCE estimation, especially on roads with steep upgrade or downgrade (Elefteriadou 1997).

2.2.1.5 PCE at Tunnels and Roundabouts

The TRB (2010) recommendation on PCE value for traffic flow in tunnels and roundabouts is equal to 2 PC/truck regardless of the proportions of HGV flow volumes. However, Umama (2017) utilised the headway method, as in (2-21), and found that the PCE value measured at the entrance of a tunnel is higher than the PCE inside the tunnel, and the PCE can range of 1.9-2.6 PC/truck (Umama 2017), as shown in FIGURE 2-9.

Kang (2016) estimated the PCE of trucks at roundabouts by utilising the saturation flow method, as in (2-5) and (2-6), and found that the PCE value of the roundabout entry flow volume increased when circulating flow increased but decreased when the circulating flow exceeded 600pc/h and that the PCE of entry flow is lower than that of circulating flow (Kang 2016). Therefore, Kang (2016) stated that the TRB 2000 might have underestimated the PCE for the roundabout.

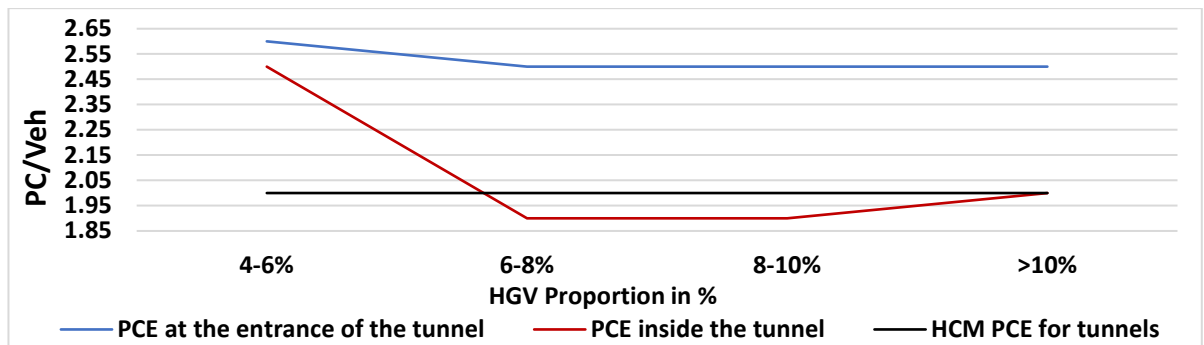


FIGURE 2-9: Estimated PCE at tunnels by Ahmed (2017)

Giuffrè (2017) estimated the PCE for trucks at a single double-lane roundabout by calculating PC-only flow capacity and the mixed flow capacity (Giuffrè 2017; Giuffrè 2018). Giuffrè (2017) and Giuffrè (2018) applied the saturation flow method in their assessment by utilising the capacity rather than traffic flow, as in (2-24) and (2-25).

$$C_{PC} = (1 - P_T) \times C_M + P_T \times PCE_T \times C_M \quad (2-24)$$

$$PCE_T = \left(\frac{1}{P_T} \right) \times \left(\frac{C_{PC}}{C_M} - 1 \right) + 1 \quad (2-25)$$

where,

P_T is the truck proportion in traffic flow volume

C_{PC} is the capacity based on only PC flow (excludes trucks)

C_M is the capacity based on mixed flow (includes trucks)

Giuffrè (2017) found that the impact of heavy vehicles suggested by HCM of PCE equals 2 PC/veh is underestimated at TF of greater than 900 veh/h because it exceeds 2 PC/truck and reaches 3 PC/truck at P_T of 30%. On the other hand, Giuffrè (2018) founded that the PCE value reached 3 PC/veh when the TF ranged from 400 to 800 veh/h and reached 4 PC/truck when the TF exceeded 800 veh/h.

Pajecki (2019) determined the PCE value for small and large HGVs at roundabout entry by using micro-traffic simulation, by applying the saturation flow method and estimated the PCE value from 1.25 to 1.75 PC/truck for small heavy vehicles, such as single-unit trucks, buses, and small semitrailers, and 1.45–2.10 PC/truck for large heavy vehicles (large semitrailers) (Pajecki 2019).

Macioszek (2019) utilised the follow-up time of vehicles to estimate the PCE for non-PC vehicles for traffic flow for two-lane roundabouts at roundabout entry, as in (2-26) and (2-27). The following time consisted of the travel time of the length of the truck and the time gap. Macioszek (2019) categorised HGVs by two types, HGVr and HGVa, and estimated their lengths by 8.2 m and 16.5 m for HGVr and HGVa, respectively, and estimated the PCE of HGVr and HGVa by 1.74 PC/truck and 1.86 PC/truck (Macioszek 2019), respectively.

$$PCE_r = \frac{tf_r}{tf_{pc}} \quad (2-26)$$

$$PCE_a = \frac{tf_a}{tf_{pc}} \quad (2-27)$$

where,

PCE_r is the PCE of an HGVr

PCE_a is the PCE of an HGVa

tf_r is the follow-up time for HGVr

tf_a is the follow-up time of an HGVa

tf_{pc} is the follow-up time of a PC

According to the current PCE estimation methods literature review, the researchers considered the vehicle's speed, dimensions, headway, flow volume proportion, flow volume, engine power, and weight. However, none of the researchers considered the RT and BCL that represent the driver's competency and alertness against unexpected situations. TABLE 2-3 shows the current PCE estimation methods authors and the parameters that they considered.

TABLE 2-3: The PCE Estimation Methods and their variable components

PCE Estimation Method	Speed	Structure	Headway	Proportion	Flow Volume	EP	Weight
Greenshields (1935)			X				
Gwynn (1968)			X	X			
Werner (1976)			X	X			
St John (1976)			X	X	X		
Seguin (1982)			X				
Cunagin (1982)	X		X			X	X
Huber (1982)	X	X		X	X		
Keller (1984)	X						
Krammes (1986)			X	X			
Molina (1987)	X		X			X	X
Chandra (2000)	X	X					
Benekohal (2000)	X			X			
Al-Kaisy (2002)						X	X
Al-Kaisy (2004)			X		X		
Al-Kaisy (2005)						X	X
Rahman (2005)	X						
Obiri-Yeboah (2014)	X	X	X			X	X
Kang (2016)				X	X		
Umama (2017)				X	X		
Giuffrè (2017)	X						
Giuffrè (2018)	X						
Pajecki (2019)				X	X		
Macioszek (2019)	X	X					
Lu (2020)	X	X					

2.2.2 Acceleration and Deceleration

Al-Kaisy (2004) stated that the average PWR of HGVs is 11.76W/kg, of which 60% of HGVs have 16.4W/kg and 40% of HGVs have 8.2 W/Kg. The PWR is also dependent on whether the truck is empty, half-loaded or fully loaded. Sharp (1972) conducted a study to assess the minimum required EP for HGVs to limit the delay caused by HGVs that have different PWRs (Sharp 1972). The assessment examined 6, 8 and 10 brake horsepower per ton of Gross Mass (GM). Sharp (1972) proposed a minimum EP of 300HP, and it is equivalent to 6.99 W/kg PWR for a GM of 32 tons and 5.086 W/kg for a 44 tons GM (Which is the Maximum Authorised Mass (MAM) in the UK). The assessment also included the change in fuel consumption due to the change in the PWR. Maurya (2012) investigated the acceleration and deceleration behaviour of various vehicle types using the global positioning system, as in (2-28) and (2-29) (Maurya 2012).

$$S_2 = S_1 + \Delta t \times d \quad (2-28)$$

$$a \text{ or } d = \pm \left(\frac{S_2 - S_1}{t_2 - t_1} \right) \quad (2-29)$$

where,

- Δt is the period of change in time where acceleration or deceleration occurred in s
- S_1 is the vehicle speed before the change in m/s
- S_2 is the speed change after change in m/s
- t_1 is the time before the change in s
- t_2 is the time after the change in s
- a is the acceleration rate in m/s^2
- d is the deceleration rate in m/s^2

Maurya (2012) proposed a method for estimating the acceleration and deceleration for trucks using statistical methods (2-30), and it was according to a truck's PWR of 5.45 W/kg.

$$a=0.666 \times e^{-0.13 \times S} \quad (2-30)$$

where,

- S is the vehicle's speed in m/s
- a is the vehicle's acceleration rate in m/s^2

The proposed model produced a relatively low a_i of $0.065m/s^2$ at a speed of 64.37km/h (40 mi/h). Mehar (2013) estimated the acceleration of HGVs based on their loading using statistical methods as well, as in (2-31), (2-32) and (2-33) (Mehar 2013). The formula in (2-30) estimates the acceleration rate of an empty truck with consideration to the speed, while (2-32) and (2-33) estimate the acceleration rate of half loaded and fully loaded truck, respectively

$$a_e = 2.19 \times e^{-0.03 \times S} \quad (2-31)$$

$$a_h = 1.65 \times e^{-0.04 \times S} \quad (2-32)$$

$$a_f = 0.98 \times e^{-0.03 \times S} \quad (2-33)$$

where,

- S is the vehicle's speed in m/s
- a_e is the acceleration rate of HGV when it is empty in m/s^2
- a_h is the acceleration rate of HGV when it is at 50% of maximum payload in m/s^2
- a_f is the acceleration rate of HGV when it is at maximum payload in m/s^2

Mehar's model shows that the truck acceleration at 100% payload is 44.75% of the acceleration when it is empty and 71.05% of the acceleration at 50% payload.

2.2.3 Deceleration Forces

The braking system's development requires the determination of the resistive forces such as braking, rolling friction, aerodynamic wind drag, road's grade, and driveline friction forces (Gillespie 1992). However, the author neglected the driveline friction force in this research. Hence, the formula for deceleration forces that reduce the vehicle's speed will consist of only four forces, as in (2-34).

$$FD=FR+FG+FW+FB \quad (2-34)$$

where,

FD is the deceleration force in N

FG is the road's grade force in N

FR is the rolling resistance force in N

FW is the wind force in N

FB is the braking force in N

The rolling resistance is one of the forces that affect vehicle speed due to very low rolling friction (GmbH 2011; Gillespie 1992). e.g., a 44tonnes HGV with a speed of 64.37km/h (40mi/h) would have a Rolling Resistance Coefficient (C_r) of 0.0048, as in (2-35).

$$d_r = \frac{\mu_r \times g \times GM}{GM} = C_r \times g \quad (2-35)$$

where,

d_r is the deceleration due to rolling friction in m/s^2

C_r is the rolling friction coefficient due to rolling

Different type of tyres and conditions lead to different rolling resistances. For example, radial tyres provide 25% less rolling friction force than bias-ply tyres (Rakha 2001). The aerodynamic drag depends on Air Density (AD), air temperature, the vehicle's frontal area, vehicle speed, Wind Speed (WS), and Cd. In the worst-case scenario where the aerodynamic resistance is the minimum, and accordingly, the author has made several assumptions:

1. No directional wind developed
2. Cd of 0.8-1 (For HGVa and HGVr with trailers=0.82) (Ando 2002; Heisler 2002; Rakha 2001; Gillespie 1992).
3. Maximum vehicle speed is 17.89 m/s (40mi/h) for DBR
4. The frontal area of a truck is 10.2 m²
5. Air Temperature (T) is 15°C and pressure=100485 Pa (pressure at 70.1m above sea level, as in (2-36)).
6. The AD will be equal to 1.214853 kg/m³, as in (2-37).

$$P_a = 101325 \times (1 - 2.25577 \times 10^{-5} \times H_s)^{5.25588} \quad (2-36)$$

$$AD = 1.225 \times \left(\frac{P_a}{101325} \right) \times \left(\frac{288.16}{273.16 + T} \right) \quad (2-37)$$

where,

AD is the air density in kg/m³

P_a is the air pressure in Pa

HASL is the height above sea level in m

T is the air temperature in °C

The author needed to calculate the AD to be able to determine the aerodynamic resistance. For example, an HGVA would be 4.39% (1931kg) of the total GM of 44tonnes. The author only considered aerodynamic forces that affect traffic flow speed. Therefore, the formula does not include the side wind drag force, and only includes the opposite and supports the traffic flow direction.

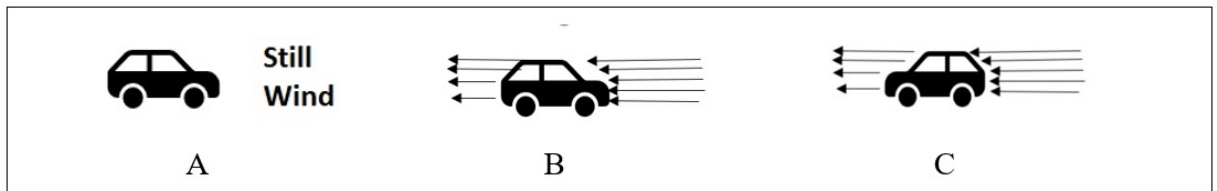


FIGURE 2-10: Illustration of the wind aerodynamics

This research's aerodynamic drag force calculation is limited to the wind's resistance force to the vehicle's frontal area. If there is a still wind (WS is equal to zero), the car speed will create a resistance force of the wind in the opposite direction of the car's flow, and the wind's speed will be equal to the car's speed, as shown in FIGURE 2-10A. However, if the wind is not still and is blowing in the opposite direction of the car's flow, as shown in FIGURE 2-10B and FIGURE 2-10C, then the aerodynamic drag force will be proportional to the square sum of the car's speed and wind's speed.

For example, if the WS is 10m/s (36km/h) and a PC speed is 17m/s (61.2km/h), then the actual resistant WS is equal to 27m/s. The aerodynamic drag force is proportional to the car's square velocity. The author utilised the aerodynamic drag force formula, as in (2-38)

$$d_w = \frac{\left(\frac{1}{2} \times C_d \times AD \times S^2 \times A_f \times g \right)}{GM} \quad (2-38)$$

where,

S is the speed of the vehicle in m/s
 d_w is the deceleration due to wind force in m/s^2
g is the acceleration due to gravity in m/s^2
 A_f is the frontal area of the vehicle in m^2
Cd is the aerodynamic drag coefficient

The rolling resistance and aerodynamic drag resistance under the excellent road and tyre conditions, still wind and an HGV speed of 64.37km/h (40mi/h) would contribute to 3.9% (1715kg) of the energy required to bring the truck to stand still. This contribution is equivalent to a deceleration rate of $0.38m/s^2$. Therefore, the braking force produced by rolling and aerodynamic resistance is deducted from the required braking force when designing the brake system.

The braking system is applied to bring the vehicle to stop within a short distance braking capability during and after exposure to the high brake temperatures affected by prolonged or severe use. Excessive use of the service brake would increase the braking pad's temperature by up to $600^\circ C$ at emergency braking. In addition, the brake oil temperature will also build up a high temperature of up to $150^\circ C$ (Podoprighora 2017). If the brake oil reaches its boiling temperature, it would adversely affect the braking system.

Therefore, having an antilock brake and air brake systems would help maintain the vehicle's control and avoid brake oil. These two braking systems could contribute to the decrease of the Braking Distance (BD). However, the air brake system response is slower than the hydraulic system response. The hydraulic system responds instantly, while the air brake system's response requires half a second. Brakes on both trucks and PCs work on the principle of friction. Usually, PCs have brake discs and pads, while HGVs have brake drums and shoes.

PCs' brakes are hydraulic systems that rely on fluid, while trucks' brakes depend on compressed air. Most of the newer heavy trucks use a dual air brake system that is not available on automobiles. The problem with the air brake system is that it has a slower response than the hydraulic system. The hydraulic system responds instantly, while the air system requires over half a second to respond. The delay is due to the time required for air to get through the lines and force the linings to contact the brake disc.

According to Thatcham Research (2016), from the 1st of November 2015, most newly registered HGVs in the UK were required to have Autonomous Emergency Braking (AEB) fitted as standard (Thatcham Research, 2016). The

problem with the AEB is that it is limited in response concerning speed range. The AEB sensor is set based on the notion that three-quarters of all collisions occur at speeds less than 20mi/h (Volvo 2017).

Hence, the AEB would help avoid crashes at speeds up to 15mi/h and mitigate those up to 25mi/h. The AEB intervenes a second before impact to reduce the effect of a collision and one second. According to the Highway Code (HC) and the American Association of State Highway and Transportation Officials (AASHTO), the AEB is sufficient to stop a PC with a speed of up to 15mi/h (excluding RT) (AASHTO 2001). However, it is not enough to prevent an accident at a vehicle speed higher than 15mi/h. For example, the AEB would only be able to reduce a vehicle's speed from 11.18 m/s to 4.472 m/s (25mi/h to 10mi/h) at the time of the crash. In such a case, the vehicle would still be 3m short of the SD for PCs (Tefft 2013).

HGVs usually require a longer time to make an emergency stop. Therefore, the AEB will not help vehicles with a speed of higher than 25mi/h. In addition, the deceleration capability of vehicles decreases with an increase in size and weight (Kutz 2004). Therefore, HGVs will require a longer distance to brake, and the stopping time for HGVs would be higher than the PCs' stopping time. Another factor considered is the braking friction that affects the braking efficiency (also called the braking ratio). The Braking Efficiency (BE) is the ratio of the Braking Force (BF) to the Vehicle's Vertical Force (VVF) as in (2-38). The BF is the force caused by the Braking Pressure (BP) applied by the braking pad/shoe on the Braking Surface Area (BSA) of the braking disc or drum, causing braking friction force as in (2-39) - (2-42).

$$BE = \frac{BF}{VVF} \tag{2-39}$$

$$BF = BP \times BSA \tag{2-40}$$

where,

BE is the braking efficiency in N/N

BF is the braking force in N

VVF is the vehicle's vertical force in N

BP is the braking pressure in Pa

BSA is the braking surface area in m²

$$BSA = BPL \times BPW \tag{2-41}$$

$$BD = \frac{S^2}{2 \times BE \times g} \equiv \frac{S^2 \times VVF}{2 \times BF \times g} \tag{2-42}$$

where,

BPL is the braking pad's length in m
BPW is the braking pad's width in m
BD is the braking distance in m
S is the vehicle speed in m/s
g is the acceleration due to gravity (9.8066m/s²)

The braking friction is far higher than the rolling resistance, which is approximately equal to 0.015 (for PCs) (GmbH, 2011). Therefore, the braking friction required to reduce the vehicle speed to stop within a specific distance depends on the BP and braking pad (or shoe) size. Most conducted brake test trials by professional drivers, where the braking pressure is assumed to be at its maximum designed level.

2.2.5 Reaction Time and Braking Competency Level

The determination of the SD should consider the worst-case scenario, and the SD value is a combination of BD and Reaction Distance (RD) of the driver during unexpected (surprise) emergencies. As proposed by the HC of the UK (DfT-Stopping Distance 2015), the thinking time for driver's reaction is a minimum of 0.67s, although the BD varies in proportion to vehicle type, speed, and braking efficiency.

The thinking time varies depending on the driver's age, health, and state of mind, and it could reach up to 2.5s as recommended by (AASHTO 2001; AASHTO 2011; Layton 2012; Geometrics and Operations Unit Traffic and Safety 2015). For example, Johansson (1971) tested the RT of a group of 321 drivers at expected situations and tested a small group of 5 at unexpected situations and found that the average RT was 0.9s and 25% of drivers have exceeded 1.2s and 10% of drivers required ≥ 1.5 s of RT, and also found that when the situation is unexpected, the RT will increase by 1s (Johanson 1971).

Chang (1985) assessed drivers' RT to a yellow traffic signal and found that the RT equal to 1.2s (Chang 1985). Lerner (1993) compared RT for unexpected situations of three drivers' age groups three age groups of 20-40, 65-69, and ≥ 70 years old and found that the younger group's RT was equal to 1.5s and the other two groups it was equal to 1.9s (Lerner 1993). Porciatti (1999) determined that the effect of ageing on the visual and decision responses led to an increase in RT of up to 75ms (Porciatti, 1999; Kroyer, 2015). Green (2000) stated that the RT to an unexpected situation was twice that of an expected situation (Green 2000).

MIT (1935) found that the average RT is 0.64s, while 5% of drivers have exceeded 1s (MIT 1935). Norman (1953) found that the RT ranges from 0.4 to 1.7s (Norman 1953). Fambro (1997) found that while a driver requires 0.2-0.3s in expected situations, it would require 1.5s in unexpected situations (Fambro 1997). Hence, the chosen RT by HC considered alert drivers, and the AASHTO recommendation considered the least alert drivers in unexpected situations.

Sivak (1982) determined that RT was within a range from 0.58 to 3s and an average RT of 1.21s and that in unexpected situations, RT would increase by a factor of 1.35 or up to 1s more (Sivak 1982). Consiglio (2003) investigated the effect of RT in conditions where drivers:

- listen to the radio
- have a conversation with a passenger
- have a conversation using a hand-held phone
- have a conversation using a hands-free phone,

Consiglio (2003) found that the RT delay is 0.016s, 0.061s, 0.072s, and 0.073s, respectively (Consiglio 2003). Zwahlen (1976) found that drivers with Blood Alcohol Concentration (BAC) of 0.088g/100ml would require up to 0.274s more RT than drivers with no alcohol consumption and up to 0.419s more for RT and information processing rate (Zwahlen, 1976; TAC-Drink Driving Statistics, 2017; TAC-Effects of Alcohol, 2017; TAC-Fatigue statistics, 2017; NHTSA 2000).

TAC (2017) also stated that if a driver is continuously awake for 17 hours and 24 hours, it is equivalent to a driver with a BAC of 0.05g/100ml and 0.1g/100ml, respectively, and this makes the driver twice and seven times likely to have an accident as a driver with zero alcohol intake respectively (TAC-Fatigue statistics 2017). In addition, Zwahlen (1976) found that drivers with a BAC of 0.088g/100ml would require up to 0.274s more RT than drivers with no alcohol consumption and up to 0.419s more RT for information processing rate (TAC-Drink Driving Statistics 2017; TAC-Effects of Alcohol 2017; NHTSA 2000).

Since the Covid-19 pandemic has started, the logistics workforce became along with the NHS on the front line of the fight against the disease to secure emergency food and medicine, and due to the lockdown, there has been a

sharp increase in online purchasing and deliveries. The average age of the logistics transportation industry's working population in the UK is increasing.

HGV driver's workforce is ageing, where HGV driver average age is 57 years old, and 13% of them are over 60 years old. The industry is keeping drivers for older ages because of their experience and competency. However, there is a shortage of HGV drivers (Johnson 2020), and the drivers are under much pressure because of long shifts of 11-15 hours, and workers are more likely to fall asleep on the wheel (HSE 2017). Therefore, it is necessary to consider an extra RT for fatigue to apply to HGV drivers, especially during the night.

Greibe (2007) conducted braking trials for 172 emergency stops and 23 comfort-braking manoeuvres, where most test drivers were non-professional (non-professional braking test drivers) (Greibe 2007).

TABLE 2-4: Various Driving scenarios and their effect on RT

Conditions	RT (s)	Unprofessional and Unexpected Situation	Unprofessional, Unexpected situation, Distraction and Alcohol intake	Unprofessional, High fatigue, Unexpected situation, and Distraction	Professional and Unexpected situation	Professional, Unexpected situation, Distraction, and Alcohol intake	Professional, High Fatigue, Unexpected situation, and Distraction
Radio	0.016	0	0.016	0	0	0.016	0
Conversation with passengers	0.061	0	0.061	0	0	0.061	0
Conversation using a handheld phone	0.072	0	0	0.072	0	0	0
Conversation using hand free phone	0.073	0	0	0	0	0	0.073
Elderly	0.075	0	0	0	0	0	0
Unexpected Situation	0.5/1	1	1	1	0.5	0.5	0.5
Eye Movement	0.63	0.63	0.63	0.63	0.63	0.63	0.63
Pressing the brakes	0.83/0.1	0.83	0.83	0.83	0.1	0.1	0.1
Alcohol intake of 0.05g/100ml	0.4	0	0.4	0	0	0.4	0
Alcohol intake of 0.1g/100ml	0.8	0	0	0	0	0	0
Low Fatigue	0.4	0	0	0	0	0	0
High Fatigue	0.8	0	0	0.8	0	0	0.8
Total max. RT	4.269	2.46	2.937	3.332	1.23	1.607	2.103

Greibe (2007) concluded that professional drivers (professional braking test drivers) press the brake pedal and reach 10kg pressure (50% of the brake pressure) in 0.05s, and non-professional drivers achieve that in 0.83s, and

the majority of non-professional drivers applied only 50% of the intended maximum pressure for the emergency brake. Hence, the author has prepared a table that shows RT for available situations according to the literature review of this section and proposed six scenarios, as in TABLE 2-4.

2.2.6 Stopping Distance

According to the Department for Transport (DfT) statistical release (DfT-FFS Statistics 2016), in the UK during 2015, 25% and 12% of HGVr and HGVA respectively left a time gap of fewer than two seconds between the following and the leading vehicle. However, the two seconds time gap will not necessarily apply to all speeds and vehicle types.

The HC (DfT-Stopping Distance 2015) stated that the safe spacing between a PC and the vehicle in front should be from 1.34s for 32.19km/h (20mi/h) to 4.69s for 112.65km/h (70mi/h), while the Braking BD varies according to vehicle type, speed, and braking efficiency. In addition, the thinking time varies according to the driver's age, health, and state of mind, and it could reach 2.5s as recommended by the AASHTO (AASHTO 2001).

The DfT has stated in its document of Design Manual for Roads and Bridges (2002) (DfT-Design Manual 2002) the BD for PCs and LGVs at a speed of 32.19 km/h (20 mi/h) should be a maximum of 24.85 m, and it is extremely high for a 20 mi/h while AASHTO (2004) (AASHTO 2004) proposed a BD that is less than 50% of the DfT's Design Manual (2002), as in TABLE 2-5. In addition, the Stopping Time (ST) calculation is in (2-43) (Fambro 1997).

$$ST=RT+\frac{S}{a} \quad (2-43)$$

where,

ST is the vehicle's stopping time in s

S is the speed of the vehicle in m/s

a is the vehicle acceleration rate in m/s²

RT is the time taken for the driver to react in s (0.67-2.5s)

The National Highway Traffic Safety Administration (NHTSA) (2005) (NHTSA 2005) conducted a laboratory test to assess light vehicle brake systems performance and found that the BD for light vehicles is 36% lower than the recommended BD values by the AASHTO (2004) while the DfT (2015) (DfT-Stopping Distance, 2015) proposed BD values that are even lower by 18% than the NHTSA (2005), as in TABLE 2-5.

TABLE 2-5: BD for PCs and LGVs conducted by different studies

Speed in km/h	DfT Design Manual (2002) BD in m	AASHTO (2004) BD in m	(NHTSA FMVSS 135, 2005) BD in m	DfT-Stopping Distance (2015) BD in m
32.19	24.85	11.43	7.33	6
48.28	55.9	25.71	16.48	14
64.37	99.3	45.716	29.305	24
80.47	155.29	71.43	45.789	38
96.56	223.61	102.86	65.85	55

The BD values proposed TABLE 2-5 show that the deceleration rate is 6.67 m/s^2 (recommended by the HC) which is 96.18% higher than the acceleration rate recommended AASHTO. Therefore, the Rolling Friction Coefficient (Cr) is higher, and it is equal to 0.68. However, the deceleration rate usually varies during the stopping period (Akelik 2001), and it is caused by the weight applied to the brake pedal and the friction between the vehicle tyres and the road.

According to Bullas (2004) and GmbH (2011), the Cr between the tyre and the road with dry asphalt is high with a coefficient of friction of 0.5-0.8, and in wet road conditions, the Cr will be as low as 0.2-0.4 (Bullas 2004; GmbH 2011). Conversely, the Cr is relatively low, with approximately 0.008-0.012 (Gillespie 1992). Both factors depend on the tyres' condition, as the tread depth can be from 8 mm at the new condition to 1.6 mm at the bold state (GmbH 2011). Therefore, the HC's BD considered perfect road and vehicle conditions and highly perceptive drivers, while the AASHTO recommended BD considered the worst-case scenario.

NHTSA (2004) tested trucks with the air brake system, as in TABLE 2-6, and another study by NHSTA (2004) in the same year tested trucks with various braking systems of all discs, standard S-cam drums, hybrid drum, hybrid disc, and air brakes, and the study aimed to reduce the BD by 30% by testing these brake types with fully and lightly loaded of two types of truck tractors and found that all the discs configuration of the braking system provides the lowest BD, as in TABLE 2-6 (NHTSA FMVSS 121 2004) (NHTSA Stopping Performance 2004).

TABLE 2-6: BD for HGVs conducted by different studies

Speed in km/h	(NHTSA FMVSS 121, 2004) standard of BD in m	(NHTSA Stopping Performance, 2004) 30% reduction in BD in m	DMV (2005) Standard of BD in m
32.19	12.01	8.41	6.91
48.28	27.03	18.92	17.2
64.37	48.05	33.64	32.05
80.47	75.08	52.55	51.49
96.56	108.23	75.91	71.84

DMV (2005) proposed slightly lower values, as in TABLE 2-6. However, the DMV (2005) stated that the truck's braking system is designed to work at best the truck is fully loaded, and the BD will be higher when the truck is lightly loaded (DMV-Driving Safely 2005) (DMV-Air Brakes 2005).

2.2.7 Road Capacity Estimation

The capacity estimation method utilised by the HCM (O'Flaherty; 2006; TRB, 2000) starts by calculating the Saturation Flow (SF_{SF}) using the saturation flow capacity estimation method for a single lane is as in (2-44):

$$SF_{SF}=3600/h_s \quad (2-44)$$

Thereby, the definition of a saturation headway in the HCM is "It is the average headway that can be achieved by a saturated, stable moving queue of vehicles passing through the signal, and the unit is (s/veh)". Therefore, the HCM determined that saturation headway (h_s) is equal to 2s/veh (second/vehicle), and since that one hour is equal to 3600s, the saturation flow should be equal to $3600/2=1800$ veh/h (vehicle/hour).

By calculating the capacity of the road by utilising the saturation flow method, the author considered the Number of Lanes (NL), F_{HV} , Lane Width Correction Factor (f_w), Effective Green Ratio (EGR), and driver' Population Factor (f_p). However, the road under investigation is a one-way two-lane road with a speed limit of 64.37km/h (40mi/h) with a signalised intersection. Therefore, the author has neglected the effect of the access ramp and two-directional flow.

The F_{HV} measures the impact of heavy vehicles on the road's capacity by utilising the vehicle's PCE and vehicle's percentage of flow from the total traffic flow composition as in section 2.1.1. Finally, the f_p is a measure of the driver's familiarity with the road, e.g., every weekday commuter has an f_p of 1 while unfamiliar drivers can have an f_p of 0.75-0.9 (Rogers 2016).

The f_w considers the width of a vehicle, lane, and distance of obstruction from each side of the road, and f_w varies from 0.66 to 1 depending on the lane's width, vehicle's width, and whether the obstruction on one side or both side as in (2-45). Therefore, the f_w for HGVs is 0.81-0.9, as in (2-45), and for PCs is 0.94-0.97 (Rogers 2016; TRB

2000). The capacity estimation formula for a multi-lane one-way road with signalised intersection (Interrupted traffic flow) is as in (2-46) (Roess 1980; TRB 2000).

$$f_w = \begin{cases} 1, & \text{if } OD \geq 1.83 \text{ AND } LW = 3.65 \\ 0.97, & \text{if } OD \geq 1.83 \text{ AND } LW = 3.36 \\ 0.91, & \text{if } OD \geq 1.83 \text{ AND } LW = 3.05 \\ 0.98, & \text{if } 1.22 \leq OD < 1.83 \text{ AND } LW = 3.65 \\ 0.95, & \text{if } 1.22 \leq OD < 1.83 \text{ AND } LW = 3.36 \\ 0.89, & \text{if } 1.22 \leq OD < 1.83 \text{ AND } LW = 3.05 \\ 0.94, & \text{if } 0.61 \leq OD < 1.22 \text{ AND } LW = 3.65 \\ 0.91, & \text{if } 0.61 \leq OD < 1.22 \text{ AND } LW = 3.36 \\ 0.86, & \text{if } 0.61 \leq OD < 1.22 \text{ AND } LW = 3.05 \\ 0.81, & \text{if } 0 \leq OD < 0.61 \text{ AND } LW = 3.65 \\ 0.79, & \text{if } 0 \leq OD < 0.61 \text{ AND } LW = 3.36 \\ 0.74, & \text{if } 0 \leq OD < 0.61 \text{ AND } LW = 3.05 \\ 0.66, & \text{else} \end{cases} \quad (2-45)$$

where,

OD is the distance between the side of the vehicle and the obstruction in m

LW is the lane width in m

$$C_{SF} = \left(\frac{3600}{2} \right) \times NL \times f_w \times f_p \times F_{hv} \times EGR \quad (2-46)$$

where,

C_{SF} is the saturation flow capacity in PC/h

NL is the number of lanes of the road in ln

f_w is the lane width correction factor

F_{hv} is the heavy vehicle factor

EGR is the effective green ratio in s/s

Britain does not adopt the HCM method in estimating road capacity. In the UK, the highways are categorised as follows:

- Motorways
- Built-up trunk roads with a speed limit of 40mi/h
- Built-up principle roads with a speed limit of 40mi/h
- Non-built-up trunk roads a speed limit of >40mi/h
- Non-built-up principle roads a speed limit of >40mi/h

In this research, the author investigates the A5036 road, and it is a built-up trunk road with a speed limit of 40mi/h. The A5036 is also a dual carriageway with two lanes for each direction. The capacity estimation methodology considers an approach based on empirical British research studies related to different discrete aspects of road operation and analysis in the UK. The result of this approach shows that the road under investigation has a capacity of 3250veh/h, and with a reduction of 100veh/h from every lane for traffic flows with 15-20% HGVs, and a reduction of 150 from every lane for traffic flows with 20-25% HGVs (Rogers 2016; O’Flaherty 2006).

2.2.8 Effective Green Ratio

The Effective Green Time (EGT) is the Green Light Time (G) plus the Yellow Light Time (Y) minus the Start-up Lost Time (t_L), as in (2-47). The EGR is the ratio of the EGT to the entire Traffic Signal Cycle (C), as in (2-48) (Mathew 2014; TRB 2000).

$$EGT = G + Y - t_L \quad (2-47)$$

$$EGR = \frac{EGT}{C} \quad (2-48)$$

The t_L is the combination of Start-up Time (t_s) and the Clearance Lost Time (t_{cl}), as in (2-49). This would require estimating the gap between vehicles in the queue (minimum gap equals 1.973m, as shown in chapter four). The author can estimate the Minimum Green Time (G_{min}) by utilising (2-50):

$$t_L = t_s + t_{cl} \quad (2-49)$$

where,

t_L is the start-up lost time, t_s is the start-up time, t_{cl} is the clearance lost time

$$G_{min} = t_L + \left[h_s \times \text{Integer} \left(\frac{d}{x} \right) \right] \quad (2-50)$$

where,

- t_L is the start-up lost time in s
- h_s is the saturation headway in s
- d is the distance between the detector and the stopping line in m
- x is the distance between the stored vehicles

The first vehicle in the queue will have the longest headway compared to other vehicles in the queue because it includes the RT of the driver and the time necessary to accelerate. The second vehicle will have shorter headway because the second driver can overlap his/her RT with that of the first driver’s. After a few vehicles, the headway

will become constant (Mathew 2014). The h_s that characterise all headways beginning with the sixth vehicle and the start-up occur only at the front five vehicles in the queue, as shown in FIGURE 2-11 and FIGURE 2-12.

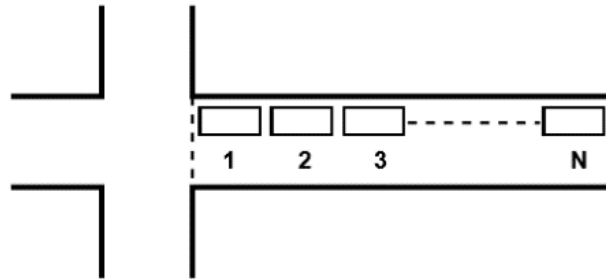


FIGURE 2-11: A queue of N vehicles at the intersection (TRB 2000) (Mathew 2014)

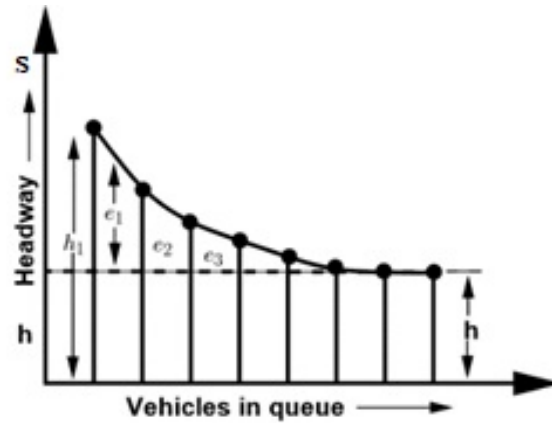


FIGURE 2-12: The start-up lost time and saturation headway (TRB 2000) (Mathew,2014)

Matsoukis (2013) found that start-up time ranges from 0.35 to 1.39s, and the average start-up lost time of 5.34s can be accounted to the first four vehicles and the average headway after the fourth vehicle was 1.82s. (Matsoukis 2013), as shown in FIGURE 2-12. Shawky (2016) estimated that the lost start-up time ranges from 0.75-3.04s with a mean of equal to 2.21s. Bester (2002) found that the start-up time can be up to 7.8s for the first six vehicles in the queue, as shown in FIGURE 2-12 (Bester 2002). Ericksen (1947) determined that the t_s starts from 2.95s for the first car in the queue and the extra time required by the first five vehicles' drivers in the queue to start-up the vehicles Ericksen (1947) also found that the headway starts with the second vehicle at 3.1s and starts decreasing until it gets to the sixth car then the headway will remain constant at 2.1s (Ericksen 1947). Caliskanelli (2017) determined that the start-up lost time ranges from 1.47-3.81s (Caliskanelli 2017).

The author required to estimate the C and the G_{\min} to clear all the vehicles to determine the EGR, Mathew (2014) stated that the minimum green time calculation depends on the vehicle's location and the type of detector (Mathew 2014). For example, a square or arrowed shaped inductive loop detector, as shown in FIGURE 2-13. The distance between the first inductive loop from the right and the traffic lights is 32m. Therefore, the author has calculated the G_{\min} by estimating the number of vehicles found between the first loop on the right and the traffic lights.

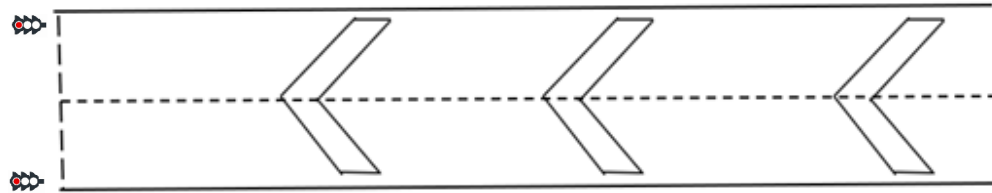


FIGURE 2-13: Inductive Loop traffic flow detector (the has created this image)

Mathew (2014) stated that distance x is equal to 6m, and it is relatively low because vehicles in a queue at the intersection leave around 2m of a gap (Mathew 2014). However, if the algorithm of (2-34) aims to count the number of queued vehicles at positions within the detection zone, as shown in FIGURE 2-13, 6m will be the headway of stored vehicles (stored vehicles means the vehicles that stop in the area between the arrowed loops, as shown in FIGURE 2-13). Therefore, for h equals 2s, x equals 6m, t_L equals 3s, and d equals 32m, results in a G_{\min} equals 13s.

This result estimates the minimum green time for only five vehicles, and by assuming a traffic volume of 1000 veh/hour/lane and a C equal to 120s, the total queued vehicles for every lane and every cycle will reach 33 vehicles. Therefore, according to (2-50), the required green time should be 86s to be enough to clear all the vehicles at the intersection. Thereby, there should be a minimum and maximum green time

The C for four-legged intersections usually does not exceed 120s. Therefore, the cycle length change from 1.5 to 2 minutes will only increase the capacity by 2 (Kettlson & Associates 2008).

2.2.9 Automatic Traffic Counters

The DfT has two sources of vehicle counting data, manual and automatic. The DfT carries out 8000 manual counts of AADF traffic counts every year for statistics, and trained enumerators conduct the counts for twelve hours (7 am to 7 pm) on weekdays. The AADF data consists of the categorisation of vehicle types, including the number of axles of HGVs.

The DfT also have over 300 ATC all over GB. However, the HE runs over 10000 ATC on some motorways and 'A' roads in England (DfT-Traffic Counting, 2020). The ATC uses the inductive loop technique with a secondary technique of either piezo-electric sensor or infra-red technique that measures the length and speed of vehicles and categorises the vehicles according to their length by splitting vehicle counts over four categories of lengths of ≤ 5.2 m, 5.21-6.6 m, 6.61-11.6 m, and ≥ 11.6 m, as in Table 3-1. The ATC reports the traffic count every 15 minutes for the average working day of road link A5038-A5207 of DBR in Liverpool, UK, will be denoted by DBR in this research (HE-ATC, 2017); the average working day data are an average of working days for the period of three years from April-2015 to April 2018 for 24 hours a day in weekdays.

The ATCs are used by the DfT to monitor road traffic and congestion and collect statistics the facilitate future development, road design, and traffic control. The ATC differ in their methodology, accuracy, and reliability. Therefore, transport authorities usually install double or triple technology to maintain accuracy and reliability at the same time. ATCs accuracy depends on the time of the day, weather, traffic density, and collection intervals.

There are two groups of ATCs, intrusive and non-intrusive technologies.

2.2.9.1 Intrusive ATC Technologies

The intrusive technologies are usually installed on the road's pavement, such as the Pneumatic road tube sensors, inductive loop sensors, and weight in motion piezoelectric sensors (Bellucci 2010).

- 1- **Pneumatic tube sensor:** It works when a vehicle passes over the tube. The tube sends a blast of air pressure that closes an air switch that transmits an electric signal to a counter. It classifies the vehicle according to its number of axles and wheelbase (Traffic Technology Ltd 2021). It is effective for short term count and low traffic density and unsuitable for high traffic volumes, permanent, and long periods. The counting error is 10% (Windmill Software Ltd 2019).
- 2- **Inductive loop sensor:** The loop is embedded in the road pavement underneath the road surface, and it applies an electric signal to the loop, and the signal shape and frequency will change due to the metal body of the moving vehicle (Bellucci 2010). A two-loop sensor can detect the traffic flow count and occupancy, classify vehicles according to length, and measure the ATS (Windmill Software Ltd 2019).

The inductive loop accuracy is higher in medium traffic density than in low and high density, and 11% higher accuracy when collecting data every 15min than every 20s, and the average error is up to 9.4% (Bellucci 2010). The inductive loop method is widely utilised in traffic management because it is very cheap and reliable. The reliability of the inductive loop is measured by Bellucci (2010) to have the highest Mean Time Between Failure (MTBF) of 5064h.

- 3- **Weight in motion piezoelectric sensors:** It works by measuring the voltage caused by the moving car and allows the sensor to measure the axle's weight. It measures the vehicle's weight, length, the gap between axles, and speed and its accuracy is higher when combined with an inductive loop sensor, and the average error is 5.72%. However, the piezoelectric sensor is significantly less reliable than the inductive loop sensor with an MTBF of 531h (Bellucci 2010).

2.2.9.2 Non-intrusive ATC Technologies

Non-intrusive methods are installed on top of the road (on a gantry, bridge or a pole)), such as video imaging, laser scanner, and passive infrared sensors.

- 1- **Video Imaging Detector:** The camera detects vehicles, and the detected video images are collected by frame-by-frame analysis, and the average error is up to 34%, and it may get a higher error of up to 51% at night. However, it is more reliable than weight in motion sensors with an MTBF of 1026h (Bellucci 2010).
- 2- **Passive infrared sensor:** It works by comparing the reflected wave from the vehicle with the reflected wave from the road surface, and it measures traffic flow volume, occupancy, and speed. The sensors could detect vehicles with an accuracy of up to 99% (Oudat 2015). However, it could be affected by high temperature and weather conditions (Bellucci 2010).
- 3- **Laser scanner sensor:** this sensor usually mounted on a bridge above the centre of the road's lane. It works by sending a continuous beam to the road surface. The average error may get up to 19.8% when the collection period is 15min.

According to Bellucci (2010), the definition of the low, medium, and high traffic density is $TF < 600$ vehicle/ln/h, $TF \geq 600$ vehicle/ln/h, and $TF \geq 1400$ vehicle/ln/h (Bellucci 2010). Therefore, according to the ATC counts of vehicles during an average working day of DBR, there only low and medium TF and the medium TF is at the hours

8 am, 9 am, and 1 pm-7 pm (9 hours), and when converting the TF to PCE, the medium TF will be at the hours 8 am-7 pm (12 hours). Therefore, for combining inductive loop and piezoelectric sensors, the average error could be 5.72%. However, due to the piezoelectric sensor's lower reliability, the most dominant average error could get up to 9.4%.

2.2.10 System Dynamics

Forrester (1961) introduced the dynamic system approach to assess management systems, and later researchers utilised it in other fields such as transportation. The design of the SDM involves two parts, a qualitative assessment and a quantitative assessment. The qualitative assessment describes the causal relationships between the systems' variables through a causal loop model, and the quantitative assessment presents the mathematical relationship between systems' variables in a stock and flow model (Forrester 1961).

Qualitative models are useful in describing the system structure for decision-makers to form the primary strategy to improve system behaviour (Wortman 1983; Sterman 2000). However, qualitative assessment alone is not enough to obtain all the essential facts to design a new strategy. Usually, decision-makers require quantitative results to support qualitative assessment (Shepherd 2012).

Qiu (2015) assessed the impact of manufacturing and population growth in China (Qiu 2015). Aschauer (2015) demonstrated the effect of logistics and supply chain policies and strategy on truck utilisation and order flexibility (Aschauer 2015). The two SDMs were developed by Qiu (2015) and Aschauer (2015) to connect the supply chain with transportation. Qiu (2015) assessed the impact of manufacturing and population growth in China, and his research findings show that the CO₂ emission and congestion decrease if the average shipping capacity for freight trucks increases and/or the average fuel consumption per truck decreases. In addition, the CLD show the causal links between vehicle amount and pollution, congestion, and freight volume (Qiu 2015).

Aschauer (2015) went further into designing an SDM for the interdependencies between logistics strategy and freight transport that demonstrates the effect of logistics and supply chain policies and strategy of the truck's utilisation level and the order's flexibility. Aschauer (2015) designed the model to show how freight transport is affected by different logistics strategy parameters (Aschauer 2015).

Most of the researchers in the transportation problems analysis field utilised Discrete Event Simulation (DES) to assess queuing problems where the DES modelling requires high-frequency data (For example, count reports for every minute or less). Few other researchers have utilised SDM to perform qualitative and quantitative assessments to identify the variables responsible for unwanted behaviour and improve the system. The SDM does not require high-frequency data.

2.3 SUMMARY OF LITERATURE REVIEW

The above literature has highlighted the following gaps in the estimation of the PCE value. Therefore, the author broke down the literature review summary into six points:

- 1- The utilisation of vehicle proportion in PCE estimation does not reflect the vehicle's actual effect on the road unless the traffic flow is at its full capacity.
- 2- The utilisation of speed, delay, travel time, and queue discharge delay in PCE estimation requires the manufacturing details and speed for various vehicle types in the traffic flow composition.
- 3- The method that utilises the vehicle's headway has not considered acceleration delay for non-PC vehicles.
- 4- All the existing PCE methods have not addressed the driver's RT and BCL, affecting the vehicle SD and the PCE value. In addition, none of the PCE estimation methods utilised drivers' competency level and RT.
- 5- None of the researchers in the transportation system field utilised system dynamics assessment in estimating the PCE to estimate the impact of container carrier HGVs on the traffic flow operation.
- 6- The estimation of the capacity does not consider the average flow speed, and the traffic-light sequence estimation methods utilise the number of traffic flow vehicles without any consideration of their PCE.

CHAPTER THREE: PASSENGER CAR EQUIVALENT AND ROAD CAPACITY ESTIMATION

3.1 INTRODUCTION

The traffic flow proportions of various vehicle types have an adverse effect on the capacity and LOS of roads, especially for roads near container ports or industrial areas, due to the relatively high volume and percentage of HGVs in traffic flow.

The expansion of the Liverpool container terminal increases the demand for road freight, and roads that connect the terminal with the city and the nearby cities will suffer from congestion. Therefore, local authorities either try to overcome this problem by building new roads, tunnels, adding extra lanes to existing roads, establishing UCCs or utilising other modes of transport for freight transportation. To reach a feasible solution, the planners would require an accurate and efficient method of estimating HGVs' effect on road traffic flow, the environment, and the economy.

The determination of HGVs' effect requires estimating the PCE of the various vehicle types that make the traffic flow composition at different hours of the day. In addition, to obtain a correct estimation of the road traffic capacity and the LoS, it is essential to determine an accurate and realistic PCE of HGVs. The PCE value represents the equivalent effect of an LGV, HGVr or HGVa on traffic flow compared to PC vehicles.

Researchers who developed PCE estimation methodologies over the last 80 years rely on either vehicle's proportion, volume, length, speed, delay, travel time, EP or a combination of two to three of these variables. This research will propose two novel methods for estimating the PCE value and road capacity. The proposed methods should determine HGVs' actual effect, estimate the maximum available capacity to accommodate the increasing demand, and provide options for port managers and local authorities to develop the most feasible, economical, practical, logistical, and environmental solution.

The author has chosen the road under investigation due to the ongoing demand expansion of the container terminal of Liverpool. The author has obtained the data from HE by ATCs. The utilised data contains the traffic flow of

vehicle types according to their lengths and supplies their average speed every 15 minutes. The categorisation of vehicle types throughout this thesis is according to the vehicle's length, weight, and structure, as shown in. The author has determined the vehicle's categorisation according to the data collected by DfT and HE.

The inward and outward Liverpool port data for 2017 and 2018 is not available and required revision by DfT. Therefore, the author has only considered the data for 2016. The percentage of processed containers ≥ 40 ft is 70%, and every 40ft container is equivalent to 2 TEUs, and the percentage of processed containers ≥ 20 ft and < 40 ft is 30%, and every 20ft container is equivalent to 1 TEUs. The percentage of empty and loaded containers is 28% and 72%, respectively, with an average weight of 7.28 tonnes per container (DfT 2018).

3.2 METHODOLOGY

In this research, the author aims to estimate HGVs' impact on traffic flow and estimate HGVs' available capacity on the road to accommodate the demand increase due to the container terminal expansion. Expressing the effect of HGVs on traffic flow should be in PCE value. It is vital to accurately estimate PCE and determine the impact of HGVs on the road compared to PCs to assess the congestion level and the effect of congestion on travel time delay. Therefore, accurate and realistic values of PCE are crucial in estimating the road capacity.

The author aims to estimate the PCE by calculating the total length occupied by all traffic and the required travel time to have all vehicles clear the road within one hour. If the time required to drive throughout the entire length of the vehicles occupied by the vehicles exceeds one hour, the vehicles in the traffic flow are not in line with the safe spacing standard.

Typically, the average headway between following and leading vehicles decreases when traffic flow increases. However, with high volume levels, the average speed will drop, leading to a reduction in safe headways and a reduction in the required acceleration distance. Therefore, the road capacity calculation is on the basis of either uninterrupted flow or interrupted flow. The continuous or uninterrupted flow is when there is no construction work, accidents, broken vehicles, traffic lights, roundabouts, and intersections, with a specified FFS by the transport authority. The author based the calculation of road capacity on interrupted traffic flow.

The Average Traffic Speed (ATS) is directly proportional to road's capacity and inversely proportional to traffic density, as in $\{q=k*v\}$, where q is the traffic flow volume in the vehicle per hour (veh/h), and k is the traffic flow density in the veh/km/ln, and v is the traffic speed flow in kilometre per hour (km/h).

Therefore, the new out of the box approach depends on the ATS and PCE to determine the available capacity. In an out of the box approach, the author defines the ATS flow (in km/h) as the displacement of vehicles within one hour, e.g., if a vehicle moves with an average speed of 60km/h for one hour, then the vehicle has moved by 60km. Therefore, the road's availability will depend on the average speed and not on the FFS because the FFS applies when zero vehicles are on the road. Therefore, the average speed of traffic is a valid measure of the available capacity.

For example, if a road's FFS is 64.37km/h and the actual average speed of traffic is 30km/h, the vehicles only move 30km per hour. Thereby, 30km is the only available distance, and according to that distance, the author has calculated the available space for vehicles.

The author has considered aligning the vehicles according to their headways for every lane and calculates the availability or deficit of headway distance to insert or remove vehicles from traffic, considering the required SD for safety.

Out of the box Approach: Practical example

A Road Link Length (R_{LL}) with a length of 2km and an ATC installed at the R_{LL} 's entrance. The ATC measured the average speed for one hour ($15min \times 4$), and the speed is 64.4km/h; and the ATC also counted the vehicles entering the R_{LL} the same hour. The average headway length for PC (private cars) is 61m. Therefore, the number of PCs that can occupy a single lane of the R_{LL} at any given time is the ratio of the R_{LL} 's length to the PC headway, and it is equal to $2000/61=33$ PCs.

Let us first assume that the traffic flow is uninterrupted (with no traffic light). A vehicle with a speed of 64.4km/h will exit the end of the R_{LL} in 1.86min. More vehicles will keep entering the R_{LL} during the hour at a speed of 64.4km/h. A PC with the latter speed can drive uninterrupted for an hour and travel 64.4km, equal to 32 times that R_{LL} 's length (2km). The author can get the same result when using the measure of time by dividing 60min by the

time it takes to travel 2km (1.86min), and the result is 32. The result will be 1056 veh/h/ln (vehicles/hour/lane) by multiplying the Q value in the equation above.

From this perspective, it does not matter what the R_{LL} length can be 500m, 2km, or tens of kilometres long, but what matters is the traffic speed flow during the hour that provides space for vehicle displacement. If the model user wants to utilize the speed for every 15min, then when applying the vehicle displacement approach to calculate the capacity, he/she should divide the capacity formula by four.

If the ATC has reported a heterogeneous traffic flow volume of 1000 veh/h and 50 of the vehicles are HGVs with a PCE equals 3, then the 50 HGVs are equivalent to 150 PCs the PCE traffic flow volume is 1050 PC/h. The author has estimated the HGVs' actual impact on the traffic by converting the heterogeneous traffic flow volume to a PCE traffic flow. The author has calculated the headway for every vehicle type by estimating the SD by integrating the RT and the driver's professionalism.

Integrating the driver's professionalism to the headway, PCE, capacity, and rescheduling is vital for planning and development purposes. Professional drivers apply brakes to the maximum force of 20kg, while non-professional drivers apply only 50% of the brake pedal's maximum pressure (10kg). Therefore, in this paper, the author has considered professional drivers as 100% competent in braking, while non-professional drivers are 50% competent.

The authors will add 0.83s to the RT for 50% BCL drivers and 0.1s for 100% BCL drivers when assuming that professional drivers will only require another 0.05s to increase the pressure on the pedal to 20kg and that the non-professional drivers will only apply pressure up to 10kg (50% of the required pressure). Also, the authors will utilize the BCL in the braking force calculation, and a professional driver with a BCL equals to one will apply twice the pressure that non-professional drivers apply, which would significantly impact the deceleration level.

Definition 1: Braking Competency Level (BCL) measures the amount of pressure applied by the driver to the brake pedal and the time taken to achieve that. The BCL value is the driver's pedal pressure ratio during braking to the required maximum pedal pressure. The BCL contributes to the vehicle's deceleration rate and the RT of the driver. The higher the BCL, the shorter the required braking time.

The proposed PCE estimation depends on the deceleration and acceleration performances of vehicles. The PCE formula includes the vehicular length, acceleration performance, and SD. Therefore, the proposed PCE directly

relates to the deceleration distance, acceleration distance, speed, and length of various non-PC vehicles. The author has developed an algorithm to estimate the RT by utilising TABLE 2-4 and (3-1).

$$RT_i = EM + 0.5 \times ENE + 0.4 \times F + 0.4 \times AI + 0.45 \times M + 0.075 \times \text{Age} - 1.46 \times BCL + 1.56 \quad (3-1)$$

where,

BCL_i is the BCL for the driver of vehicle type (i), and it is 50-100%

EM is the basic eye movement time necessary to react, and it is 0.63s as in TABLE 2-4

ENE is the expected or not expected situation, and it is 0.5s for expected situations and 1s for the unexpected situation as in TABLE 2-4

AI is the delay due to the impact of alcohol intake, and it is 0s for no alcohol, 0.4s for alcohol intake of 0.05g/100ml, or 0.8s for alcohol intake of BAC of 0.1g/100ml as in TABLE 2-4

F is the fatigue effect, and it is 0 for not tired, 0.4s for no sleep for 17 hours as low fatigue, or 0.8s for no sleep for 24 hours as high fatigue as in TABLE 2-4

M is the manoeuvring effect, and it is 0 or 0.45s as in TABLE 2-4

Age is the age factor, and it is either 0 for young or 0.075s for elderly, as in TABLE 2-4

The proposed method measures the PCE value at all hours of the day and calculates the headway not according to availability and traffic flow volumes but according to the required safety gap that provides sufficient time and space for the driver to bring the vehicle to a standstill and prevent an accident. The calculated headway will ensure a safe traffic operation and a rescheduling plan.

Typically, when the ATS increase, the required SD will increase and when the traffic flow increases, the average speed will decrease, and the gap between the following and leading vehicles decreases, and the required acceleration performance to meet average speed will also decrease. The newly proposed PCE estimation method depends on the deceleration and acceleration performances of vehicles. The PCE formula includes the vehicular length, acceleration performance, and SD. Therefore, the proposed PCE directly relates to the deceleration distance, acceleration distance, speed, and length of various non-PC vehicles.

3.2.1 Deceleration Component

The deceleration capability of vehicles decreases with the increase in the vehicle's size and weight (Kutz 2004). Therefore, an HGV driver requires a longer distance to brake and bring the vehicle to a stand-still than PC drivers, and the stopping time for HGVs should be higher than the PCs stopping time. The braking force is the force caused

by the applied pressure by the braking pad/shoe on the surface area of the braking disc or drum, creating braking friction force, and it is by far higher than the rest of the braking forces

TABLE 3-1: Categorisation of the vehicle types

Index i	Vehicle type	Categorisation	Length
1	PC	PC saloon, taxi, small van, and minibus, up to eight seaters with two axles and four wheels	3-5.2 m
2	LGV	Medium and large transit vans and tractors. Small two trucks with two axles, four wheels, and MAM* of 3.5 tonnes	5.21-6.6 m
3	HGV _r	Heavy goods vehicles with 3-5 axles and of net weight of greater than 3.5 tonnes and MAM of 32 tonnes	6.61-11.6 m
4	HGV _a	Heavy vehicles consist of a combination of a tractor and a trailer with 3-8 axles and MAM of 44 tonnes	11.61-18.75 m

*MAM is the Maximum Authorised Mass

Using SD will ensure that any capacity assessment will be within the standard safety spacing requirement for drivers to react safely, stop, and manoeuvre (Katrakazas 2021). Thereby, the PCE estimation would be the ratio of the vehicle length and safe SD to the length of a PC and safe SD for PCs, and the deceleration component is the ratio of the vehicle's headway to the headway of a PC, as in (3-2) – (3-4). The author has utilised the subscript (i) in most of the equations in this chapter to differentiate between vehicle types. Therefore, please refer to the categorisation in TABLE 3-1.

$$H_i = SD_i + L_i \quad (3-2)$$

$$PCE_i = \frac{H_i}{H_1} \quad (3-3)$$

$$PCE_i = \frac{L_i + SD_i}{L_1 + SD_1} \quad (3-4)$$

where,

H_i is the headway distance of vehicle type i in m

L_i is the length of vehicle type i

SD_i is the required SD for the safety of vehicle type i in m

PCE_i is the PCE value of vehicle type i before including the acceleration component

The author has decided to apply an additional space behind HGVA in particular, and the extra space is equivalent to the BD of a PC, and it is equal to 0.91s at an ATS of 64.37km/h (16.30m), as in (3-5).

$$H_4 = SD_4 + L_4 + BD_1 \quad (3-5)$$

where,

H_4 is the headway distance of an HGVA in m

L_4 is the length of HGVA in m

SD_4 is the required SD for the safety of an HGVA in m

BD₁ is the required braking distance for the safety of a PC in m

The required extra space is to provide enough space behind long vehicles to enable the HGVa to establish a clear vision of following vehicles, provide flexibility in manoeuvring for the following vehicles, and provide sufficient space ahead of the following vehicles to enable the drivers to see further ahead traffic and pedestrians that could cross in front of the HGVa.

The decision to consider an extra space behind HGVa is due to the high probability of having a PC following an HGVa, and it is the highest after the probability of a PC following an LGV and for the HGVa having the most extended vehicle in the traffic flow. The parameters' values that the users require are available in TABLE 3- 2 and TABLE 3- 3 (Ando, 2002; Heisler, 2002; Rakha, 2001; Gillespie, 1992; DfT-Vehicle's Length, 2017; Volvo, 2017; Cummins, 2017; Ishak, 2016; Belhocine, 2013; Luhua, 2011; Talati, 2009; ICCT, 2019; Tata Steel, 2013; Peugeot, 2019; DfT-Vehicle's Length, 2017; HGV Direct, 2017; DfT-Maximum Length, 2017).

TABLE 3- 2: Composite vehicles' weights and dimensions

Vehicle Type	Weight (Tonne)		Vehicle Dimensions (m)		Brake Pad Details Dimensions (mm) (Front, Rear)	
PC	Tare	1.433	L	3-5.2	L	119, 87
	MAM	1.924	W	1.798	W	69,53
	Payload	0.491	H	1.536	Thickness	20
LGV	Tare	1.971	L	5.21-6.6	L	119,87
	MAM	3.5	W	1.935	W	69,53
	Payload	1.529	H	2-2.5	Thickness	20
HGVr and HGVa	Tare	12 and 15.9	L	6.61-11.6 and 11.61-18.75	L	249.5
	MAM	32 and 44	W	2.55	W	106.8
	Payload	20 and 28.1	H	3.5-4	Thickness	29

TABLE 3- 3: Composite vehicles and weather parameters

Vehicle type	EP in HP (kW)	Cd	T (°C)	Air Pressure (Pa)
PC	131 HP* (97.726kW)	0.29	-15 To 38.5°C average of 15°C	100485 Pa at 70.1m above sea level
LGV	122HP (91kW)	0.4		
HGVr or HGVa	400-600HP (300-522.2kW)	0.8 for HGVr and 0.9 for HGVa	(38.5°C is the maximum reported temperature in the UK)	

* HP stands for Horsepower, and it is equivalent to 745.7W

The calculation of SD and PCE values requires determining the braking forces' effect on the vehicle's SD. To estimate the braking forces, the author must utilise the dimensions, weight, air pressure, air temperature, and aerodynamics drag factors for the four types of vehicles' as in TABLE 3- 2 and TABLE 3- 3 (ICCT, 2019).

The focus of this research is on the container carriers' HGVs. A TEU is equivalent to a 20' International Organisation of Standardisation (ISO) dry container (20ft ISO container: Length=6.096m, W=2.44m, H=2.59m, a maximum weight of 24 tonnes), and a 40' ISO dry container (40ft ISO container: Length=12.192m, W=2.44m, H=2.59m, a maximum weight of 28.5 tonnes) and it is equivalent to two TEUs, as it has twice the volume of a 20' container, even though it can only carry 16-25% more weight. Therefore, the focus is on trucks with greater than four axles, i.e., HGVs that can transport 20ft and 40ft containers.

The braking time calculation is based on the longest and heaviest HGV, at its top speed with a maximum allowed speed for the road (A5036) of 64.37km/h (40mi/h). To estimate the PCE values for various non-PC vehicles, the author needed to calculate the SDs by applying the formula (3-6).

The kinetic energy formula is the main formula that calculates the distance required to decelerate or accelerate to the target speed, and it is also utilised to obtain the deceleration and acceleration rates with consideration to the starting speed, the weight of the vehicle, braking force, and engine power. Thus, the author has utilised the kinetic energy formula to obtain the deceleration rate, BD, SD, acceleration rate, and acceleration distance.

By substituting RT with Time elapse in (3-9) and substituting RD with BD_i in (3-8), and by combining (3-8) and (3-9). The author has obtained the RD from (3-11).

$$SD_i = BD_i + RD_i \quad (3-6)$$

$$KE_i = GM_i \times d_i \times LD = \frac{GM_i \times S^2}{2} \quad (3-7)$$

where,

SD_i is the SD of vehicle type i in m

BD_i is the braking distance of vehicle type i in m

RD_i is the distance equivalent to the RT for the driver of vehicle type i in m

KE_i is the kinetic energy of vehicle type i in J

d_i is the deceleration rate of vehicle type i in m/s^2

LD is the length of vehicle displacement in m

S is the vehicle's speed in m/s

By eliminating the GM_i from both sides of (3-7) and replacing the length of the BD_i with Length of Vehicle's Displacement (LD), it resulted in (3-8).

$$BD_i = \frac{S^2}{2 \times d_i} \quad (3-8)$$

$$d_i = \frac{S}{t} \quad (3-9)$$

$$BT_i = \frac{S}{d_i} \quad (3-10)$$

where,

BD_i is the braking distance of vehicle type i in m

d_i is the deceleration rate of vehicle type i in m/s^2

t is the elapsed time in s

S is the average flow speed in m/s

BT_i is the braking time of vehicle type i in s

The vehicle displacement length calculation before applying the brake does not fall under the dynamic kinetic energy rule. Therefore, the author has calculated the RD using (3-11).

$$RD = S \times RT \quad (3-11)$$

where,

RD is the distance equivalent to the RT in m

S is the average flow speed in m/s

RT is the driver's reaction time in s

The KE_i in (3-7) is equivalent to that in (3-12), and by eliminating LD from both equations, it resulted in (3-13)

$$KE_i = BF_i \times LD \quad (3-12)$$

$$d_{bi} = \frac{BF}{GM_i} \quad (3-13)$$

where,

d_{bi} is the deceleration due to braking of vehicle type i in m/s^2

KE_i is the kinetic energy of vehicle type i

BF is the vehicle braking force in N

LD is the length of vehicle displacement in m

GM_i is the GM of vehicle type i in kg

The deceleration force calculation due to rolling friction requires the Cr_i and the GM_i (3-14).

$$FR_i = Cr_i \times g \times GM_i \quad (3-14)$$

where,

FR_i is the deceleration force due to rolling resistance of vehicle type i in N

Cr_i is the rolling friction coefficient of vehicle type i

g is the acceleration due to gravity constant, and it is equal to $9.8066 m/s^2$

GM_i is the gross mass of vehicle type i in kg

The calculation of the Deceleration or Acceleration Force due to Wind (FW_i) requires ρ , Area of the Front Surface of the vehicle (AF_i), Wind Speed (WS), ATS in m/s (S), the Drag Coefficient (Cd) of the vehicle (Gillespie, 1992), and Acceleration due to Gravity (g) as in (3-15). When the wind is running in the opposite direction of the traffic flow, it will cause a deceleration effect (3-15).

$$FW_i = \frac{1}{2} \times Cd_i \times AD \times AF_i \times (WS + S)^2 \times g \quad (3-15)$$

where,

FW_i is the deceleration or acceleration force due to wind

AD is the air density in kg/m^3

AF is the area of the front surface of the vehicle in m^2

WS is the wind speed in m/s

S is the average traffic speed in m/s

Cd_i is the drag coefficient of the vehicle type i

g is the acceleration due to gravity constant, and it is equal to $9.8066 m/s^2$

The author calculated the braking force due to applying Braking Pressure (BP) to the braking pad, as in (3-16) – (3-18), and by including the BCL_i in (3-18) to reflect the actual pressure applied to the brakes.

$$FB_i = BP \times DPA_i \quad (3-16)$$

$$DPA_i = BPL_i \times BPW_i \quad (3-17)$$

$$FB_i = BP \times DPA_i \times BCL_i \quad (3-18)$$

where,

FB_i is the deceleration force due to applying brakes of vehicle type i in N

BP is the braking pressure in Pa

DPA_i is the braking disk pad area of vehicle type i in m^2

BPL_i is the braking pad's length in m

BPW_i is the braking pad's width in m

BCL is the braking competency level

The deceleration or acceleration force calculation due to road grade requires grade angle value, as in (3-19) - (3-20). The determination of whether the force is going to cause a deceleration or acceleration effect depends on whether the value of grade is positive or negative, as in (3-20), where θ is the road surface slope angle (upgrade or downgrade) in degrees ($^\circ$).

$$FG_i = \text{Grade} \times g \times GM_i \quad (3-19)$$

$$\text{Grade} = \sin(\theta) \quad (3-20)$$

The author included the Weather Factor (WF), representing rain, snow, and frost on the deceleration rate and influences deceleration and acceleration forces (3-21).

$$FD_i = WF \times (FR_i + FW_i + FB_i + FG_i) \quad (3-21)$$

where,

FD_i is the deceleration force for vehicle type i in N

FR_i is the deceleration force due to rolling resistance of vehicle type i in N

FW_i is the deceleration force due to wind resistance of vehicle type i in N

FB_i is the deceleration force due to applying brakes of vehicle type i in N

FG_i is the deceleration or acceleration force due to road upgrade or downgrades of vehicle type i in N

WF is the weather factor representing the effect of rain, snow, and frost on the deceleration rate that affects all aerodynamics forces ($WF=0.1, 0.25,$ and 0.5 when there is ice, snow, or rain, respectively) (GmbH, 2011)

Now, by combining (3-6), (3-7), (3-11), (3-13), and (3-21).

$$SD_i = S \times RT + \frac{S^2 \times GM_i}{2 \times FD_i} \quad (3-22)$$

where,

FD_i is the deceleration force of vehicle type i in N

FR_i is the deceleration force due to rolling resistance of vehicle type i in N

FW_i is the deceleration force due to wind resistance of vehicle type i in N

FB_i is the deceleration force due to applying brakes of vehicle type i in N

FG_i is the deceleration or acceleration force due to road upgrade or downgrades of vehicle type i in N

WF is the weather factor representing the effect of rain, snow, and frost on the deceleration rate that affects all aerodynamics forces ($WF=0.1, 0.25,$ and 0.5 when there is ice, snow, or rain respectively) (GmbH, 2011).

According to the (TRB 2000; TRB 2010; Mannering 2013), the Saturation Flow of the DAS method (SF_{DAS}) is the maximum volume through PC flow with consideration to the minimum required headway. However, in this research, the proposed SF_{DAS} is on the basis of the minimum required headway distance of a PC, as in (3-23).

$$SF_{DAS} = \frac{ATS \times 1000}{H_1} \quad (3-23)$$

where,

H_1 is the headway distance for PCs in m

ATS is the average traffic speed in km/h

SF_{PCE} is the saturated flow of the road before the integration of the effect of the traffic light, number of lanes, road width, and HGV delay effect in $Z \geq h$

3.2.2 Acceleration Component

The calculation of SF_{PCE} in (3-24) only considers the vehicle's length and deceleration effect on the road and does not include its acceleration performance effect. The determination of the acceleration performance effect is by considering the acceleration delay effect on the non-PC vehicles. The estimation of the acceleration delay is by calculating the acceleration rate required by the non-PC vehicle to meet the ATS compared to the acceleration rate of a PC. HGVs have lower acceleration performance than PCs, especially at intersections.

By integrating the acceleration delay in the PCE value, the author can estimate non-PC vehicles' effect on the traffic flow by determining the extra space required for the non-PC vehicles to accelerate the average traffic flow speed. Thereby, to estimate the capacity of the road, the HGV's acceleration delay must be estimated. It is necessary to set up the relationship between EP, GM_i , and the Acceleration Rate (a_i). By substituting the a_i with d_i in (3-8) as in (3-24) and converting Kinetic Energy (KE) to power, as in (3-25).

$$a_i = \frac{S^2}{2 \times LD} \quad (3-24)$$

$$P_i = \frac{KE}{dt} \quad (3-25)$$

where,

KE_i is the kinetic energy of vehicle type i in J

GM_i is the gross mass of vehicle type i in kg

S is the ATS in m/s

P_i is the EP of vehicle type i in w

LD is the length of the vehicle's displacement in m

By substituting (3-25) for S in (3-26), it will result in (3-28) and (3-29), and by substituting (3-31) for one LD in (3-30) and substituting (3-33) for the other LD in (3-30), they will result in (3-33)

$$S = \frac{LD}{t} \quad (3-26)$$

$$\frac{P_i \times dt}{GM_i} = \frac{S^2}{2} \quad (3-27)$$

$$\frac{P_i \times dt}{GM_i} = \frac{LD^2}{2 \times t^2} \quad (3-28)$$

$$\frac{P_i}{GM_i} = \frac{LD \times LD}{2 \times t \times t \times dt} \quad (3-29)$$

$$a_i = \frac{LD}{t \times dt} \quad (3-30)$$

$$LD=a_i \times t \times dt \quad (3-31)$$

$$LD=S \times t \quad (3-32)$$

$$\frac{P_i}{GM_i} = \frac{S \times a_i}{2} \quad (3-33)$$

From (3-33), the author calculated the acceleration rate with no losses, as in (3-35)

$$a_{nli} = \frac{P_i \times 2}{GM_i \times S} \quad (3-34)$$

where,

GM_i is the gross mass of vehicle type i in kg

a_{nli} is the acceleration rate of vehicle type i without losses in m/s^2

S is the ATS in m/s

P_i is the EP of vehicle type i in w

LD is the length of the vehicle's displacement in m

t is the elapsed time in s

dt is the change in time starting the acceleration to the end of it in s

The author estimated the acceleration rate losses by deducting or adding the deceleration or acceleration forces due to the vehicle's aerodynamics forces and excluding the braking force. The calculation of the acceleration rate with losses is by using (3-13), (3-14), (3-15), and (3-19) as in (3-33) – (3-36).

$$d_{ri} = \frac{FR_i}{GM_i} \quad (3-35)$$

$$d_{wi} = \frac{FW_i}{GM_i} \quad (3-36)$$

$$d_{gi} = \frac{FG_i}{GM_i} \quad (3-37)$$

where,

dr_i is the deceleration rate due to rolling friction of vehicle type i

d_{gi} is the deceleration or acceleration rate due to road grade of vehicle type i

d_{wi} is the deceleration rate due to wind of vehicle type i

GM_i is the gross mass of vehicle type i in kg

FR_i is the deceleration force due to rolling resistance of vehicle type i in N

FW_i is the deceleration or acceleration force due to aerodynamic drag resistance of vehicle type i in N

FG_i is the deceleration or acceleration force due to road upgrade or downgrades of vehicle type i in N

The author must include acceleration rate losses regarding vehicle design, consisting of the Traction Factor (Tf_i), and the range of k is from 0.3636 to 0.6 (GmbH, 2011). The Tf_i is the ratio between the load on driven or braked wheels and the total gross weight. The Tf_i ratio values in (3-38) for various types of vehicles are in TABLE 3-4 (GmbH 2011).

$$a_{i_i} = \frac{P \times 2}{GM_i \times S \times Tf_i} - \frac{FR_i}{GM_i} - \frac{FW_i}{GM_i} - \frac{FG_i}{GM_i} \quad (3-38)$$

TABLE 3-4: Tfi ratio values for various types of vehicles

PC (private cars, minibus, pickup, taxis up to 8 seaters, and small vans)	LGV (medium and transit Vans, Two axles Truck) <3.5 tonnes	HGVr of four to six axles and small school buses of 2 axels) 3.5 tonnes<HGVr <32 tonnes	HGVa of four to eight axles Semitrailers, transit buses and coaches of 2-3 axels) 15.6 tonne<HGVa<44 tonnes)
0.6	0.5	0.334	0.3636

Definition 2: Acceleration Space (AS) is the vehicle's space to accelerate up to the average traffic flow speed.

The calculation of the AS is by utilising (3-8) and substituting the acceleration rate of (3-38) with deceleration rate as in (3-39)

$$AS_i = \frac{s^2}{2 \times a_{i_i}} \quad (3-39)$$

where,

GM_i is the gross mass of vehicle type i in kg

a_{i_i} is the acceleration rate of vehicle type i with losses in m/s^2

S is the average flow speed in m/s

P_i is the EP of vehicle type i in w

FR_i is the deceleration force due to rolling resistance of vehicle type i in N

FW_i is the deceleration or acceleration force due to aerodynamic drag resistance of vehicle type i in N

FG_i is the deceleration or acceleration force due to road upgrade or downgrades of vehicle type i in N

Tf_i is the traction force ratio of vehicle type i in kg/kg

dr_i is the deceleration rate due to rolling friction of vehicle type i

d_{gi} is the deceleration or acceleration rate due to road grade of vehicle type i

d_{wi} is the deceleration rate due to wind of vehicle type i

The values of MAM for PC, LGV, HGVr, and HGVa are 1.87, 3.5, 32, and 44 tonnes, respectively, and their loading factor is equal to an average of 100%, 95%, 91%, and 80%, respectively as stated in (DfT-Lorries Types and Weights Guide, 2003; Butcher, 2009; Road Safety Authority, 2015; Tata Steel, 2013; DfT-Journey Time and Traffic Flow Data, 2015).

Developing the HGV factor is necessary to estimate the delay due to HGVs' low acceleration performance compared to PC acceleration performance. The HGV delay factor estimation starts by calculating the additional acceleration distance required for non-PC vehicles (compared with PC vehicles), allowing drivers to accelerate to

average flow speed. By utilising this value, the author can estimate the extra occupied space by the non-PCs due to their lower acceleration performance and convert the results to a ratio of the remaining space (3-39) - (3-43).

Definition 3: Space Available (SA) is the space available in the road from all of its lanes during an hour of driving.

As mentioned in section 2.7 in chapter two, the factors that affect space availability on the road for interrupting traffic flow are the NL, F_{hv} , f_w , f_p , and EGR. However, the method of obtaining space availability only considers the time elapsed, and in this case, it is one hour, and it is equal to 3600s. Therefore, in the new capacity estimation methodology, the author considers the ATS rather than time elapsed because the time elapsed approach assumes the road's maximum allowed speed, while the average speed of traffic represents the available distance of vehicles.

The author assumed an equal distribution of vehicles on all lanes and considered the ATS in the SA calculation. The speed rate is the displacement space of traffic in km/h. Therefore, when estimating the SA, the author utilised the speed as a measure of the space available per hour, and by multiplying the Speed by 1000, the author converted the speed to a displacement length of vehicles in m/h, as in (3-40).

The purpose of estimating the SA is to determine non-PC vehicles' impact on the road's capacity due to their low acceleration performance. Therefore, the author did not include the F_{hv} in the calculation of the SA, as in (3-40):

$$SA=ATS \times 1000 \times NL \times f_w \times EGR \quad (3-40)$$

where,

ATS is the average speed of the traffic flow for every hour in km/h

SA is the space (distance) available on the road in m/h

EGR is the effective green ratio

f_w is the lane width adjustment factor

f_p is the population factor; if the driver is a daily commuter, then f_p equals 1

Definition 4: Acceleration Space Occupied (ASO_i) is the extra space required for non-PC vehicles to accelerate to meet the average traffic flow speed compared to a PC.

The calculation of ASO_i is by utilising AS_i in (3-41).

$$AASO_i = AS_i - AS_1 \quad (3-41)$$

The author multiplied (3-41) by the Vehicle's Flow Volume (FV_i) to determine the total effect of that vehicle type, as in (3-42).

$$TAASO_i = AASO_i \times FV_i \quad (3-42)$$

where,

- AS_i is the acceleration space of vehicle type i in m
- $AASO_i$ is the additional acceleration space occupied of vehicle type i in m
- $TAASO_i$ is the total acceleration space occupied of vehicle type i in m
- FV_i is the flow volume of vehicle type i in veh/h
- AS_1 is the acceleration space of a PC in m

Definition 5: HGV Acceleration Performance Delay (HGV_{di}) is the proportion of the extra acceleration space required of vehicle type (i) in proportion to the required PC acceleration space for the vehicle to reach the average flow speed of the road traffic. The $THGV_d$ is the total HGV acceleration performance delay for all the non-PC vehicles available in traffic.

Now, the author has calculated the ratio of acceleration space occupied effect on the SA. The HGV Acceleration Delay (HGV_{di}) shows the proportion of space occupied by a vehicle type i due to the required acceleration space (3-43). The Total HGV Acceleration Delay ($THGV_d$) is the acceleration space effect of all vehicle types on the road, as in (3-44).

$$HGV_{di} = \frac{TASO_i}{SA} \quad (3-43)$$

$$THGV_d = \frac{\sum_{i=2}^{i-4} TASO_i}{SA} \quad (3-44)$$

where,

- SA is the space available before deducting the non-PC distance delay in m/h
- $TASO_i$ is the total effect of acceleration space occupied of vehicle type i in m
- HGV_{di} is the total HGV acceleration performance delay of vehicle type i in m/m
- $THGV_d$ is the total HGV acceleration performance delay of all non-PC in m/m

Definition 6: Total HGV Acceleration Performance Factor ($THGV_f$) is the proportion of the available space on the road after deducting the total extra acceleration space required by non-PC vehicles ($THGV_d$) as in (3-44).

The author has now calculated the $THGV_f$ representing the proportion of available space after deducting the percentage of total extra occupied space by non-PC vehicles due to their acceleration performance (3-44), as in (3-45).

$$THGV_f = 1 - THGV_d \quad (3-45)$$

where,

$THGV_d$ is the total HGV acceleration performance delay of all non-PC

$THGV_f$ is the total HGV acceleration performance factor for all non-PC vehicles

The HGV factor reflects the effect of the acceleration performance for larger vehicles than a PC on the space available in traffic flow. The estimation of acceleration delay in length enables us to estimate non-PC vehicles' effect on the PCE and the capacity estimation.

The lower the value of the HGV factor, the higher the effect of HGV delay on congestion. The HGV factor is not similar to the F_{hv} (TRB, 2000; TRB, 2010) because the F_{hv} aims to estimate the PCE capacity according to the given PCE values and vehicle type's percentage of the traffic flow. The proposed method estimates the HGV effect concerning the vehicles' acceleration performance compared to the PC acceleration performance.

Definition 7: Deceleration and Acceleration Space PCE value (PCE_{DASi}) is the PCE of vehicle type (i) on-the-basis deceleration and acceleration performance. The PCE_{DASi} reflects the effect of the deceleration and acceleration performances of non-PC vehicles in equivalent to PCs, and it includes the impact of vehicle's length, driver's competency level, reaction time, and gross weight of the vehicle.

The combination of the HGV_{di} in (3-45) and the PCE_i in (3-4) will result in the PCE_{DASi} , which includes both effects of deceleration and acceleration, as in (3-46).

$$PCE_{DASi} = PCE_i + HGV_{di} \quad (3-46)$$

where,

PCE_i is the PCE value of vehicle type i before including the HGV acceleration performance effect in m/m

HGV_{di} is the HGV acceleration performance delay of vehicle type i in m/m

PCE_{DASi} is the deceleration and acceleration space PCE value of vehicle type i in m/m

3.2.3 Effective Green Ratio

The EGR is the effective green time divided by the C. As discussed in section 2.2.8. To determine the required EGR, the author required to estimate the required green time and the effective green time. The purpose of (2-33) in subsection 2.2.8 is to estimate the minimum required green for N number of vehicles by utilising the distance between the detector and the stopping line ($\lceil d/x \rceil$). However, as discussed in section 2.8 in chapter two, this equation will only consider up to 5 vehicles for every lane. The author aimed to estimate the minimum required green time for all vehicles during hour per lane per cycle. Therefore, the author has replaced the number of PC/lane/hour with the d/x , as in (3-47) (Chang, 1985; Kettlson & Associates, 2008; U.S. Department of Transportation, 2017).

$$N = \frac{TF_{PCE} \times C}{NL \times 3600} \quad (3-47)$$

where,

- N is the number of vehicles per hour per lane in PC/h/lane
- TF_{PCE} is the hourly traffic flow per hour in PC/h
- NL is the number of lanes in lane
- C is the length of the traffic light cycle in s

The author has assumed the maximum C of 120s, replace the saturation headway with the minimum safe headway of PCs that includes the RT, and convert the headway length to its equivalent time. Thus, the EGR algorithm will be as in (3-48):

$$EGR = \frac{\left(\frac{3.6 \times H_1}{ATS}\right) \times (\text{INTEGER}(N)) + t_L}{C} \quad (3-48)$$

where,

- H_1 is the headway of PCs in m
- N is the number of vehicles per hour per lane in PC/h/lane
- t_L is the total start-up lost time in s
- C is the cycle length in s
- ATS is the average traffic speed in km/h
- EGR is the effective green ratio

The final EGR algorithm includes a minimum and maximum EGR limit of 0.5 and 0.66 and a start-up lost time of 2.95s, respectively, as in (3-49):

$$EGR = \begin{cases} EGR_{max}, & \frac{\left(\frac{3.6 \times H_1}{ATS}\right) \times (\text{INTEGER}(N)) + t_L}{C} > EGR_{max} \\ EGR_{min}, & \frac{\left(\frac{3.6 \times H_1}{ATS}\right) \times (\text{INTEGER}(N)) + t_L}{C} < EGR_{min} \\ \frac{\left(\frac{3.6 \times H_1}{ATS}\right) \times (\text{INTEGER}(N)) + t_L}{C}, & \text{else} \end{cases} \quad (3-49)$$

where,

EGR_{max} is the maximum limit of EGR

EGR_{min} is the minimum limit of EGR

EGR is the effective green ratio

ATS is the average flow speed in km/h

N is the number of vehicles in PC/h/ln

t_L is the start-up lost time in s

H_1 is the PC headway in m

3.2.4 Deceleration and Acceleration Space Capacity Method

This research utilises the $THGV_f$ in developing the C_{DAS} to reflect the actual effect of HGVs on traffic flow at heterogeneous vehicular and traffic volumes at different hours of the day. The proposed method will determine the hours of the day that the traffic volume exceeds the estimated capacity and the available capacity in other hours.

Definition 8: Deceleration and Acceleration Space Capacity (C_{DAS}) is the road's capacity in PCE value on the basis of the deceleration and acceleration performance of composite vehicle flow. The C_{DAS} dynamically changes in response to ATS, PC headway length, the volume of the non-PC vehicles, NL , and the total traffic volume.

The method will provide the tool to reschedule the excess HGVs carrying an International Organization for Standardization (ISO) containers in proportion to their effect on the LoS. Hence, by examining the LoS at different hours of the day and rescheduling the HGVs to off-peak hours, the traffic operators can improve the LoS of the road and meet the demand that has been increasing due to the expansion of the container terminal.

The author determined the C_{DAS} rate by considering the required safe gap between vehicles that would facilitate enough space to stop the vehicle safely and for manoeuvring, including the delay caused by non-PC vehicles (mainly HGVs) deceleration and acceleration performances of HGVs. The author multiplied the $THGV_f$ by the SA and divided it by the H_1 as in (3-51), and this would determine the exact effect of HGVs on the space available and traffic volume and average flow speed. The author has replaced the h_s with the minimum required H_1 (3-50).

$$C_{DAS} = \frac{SA \times THGV_f}{H_1} \quad (3-50)$$

The author estimated the TF_{PCE} by calculating the sum of all vehicle types' volumes multiplied by their PCE value (3-47), as in (3-51).

$$TF_{PCE} = \sum_{i=1}^{i=4} (FV_i \times PCE_{DASi}) \quad (3-51)$$

where,

C_{DAS} is the dynamic space capacity before in Z^2/h

SA is the space available before rescheduling

$THGV_f$ is the total HGV acceleration performance factor of all non-PCs

PCE_{DASi} is the deceleration and acceleration space PCE value of vehicle type i

FV_i is the volume of vehicle type i in $|Z|/h$

TF_{PCE} is the traffic volume in PCE value in $|Z|/h$

After calculating the C_{DAS} and the TF_{PCE} , The author determined the Available Capacity in PCE (AC_{PCE}) by deducting the TF_{PCE} in (3-51) from the C_{DAS} in (3-50), as in (3-52).

$$AC_{PCE} = C_{DAS} - TF_{PCE} \quad (Z^2/h) \quad (3-52)$$

where,

AC_{PCE} is the excess capacity in PC

C_{DAS} is the deceleration and acceleration space capacity in Z^2/h

TF_{PCE} is the PCE converted traffic flow volume value in $|Z|/h$

If the traffic volume exceeds the C_{DAS} value, the port managers and logistic companies can estimate the excess flow is equivalent to TEUs and reschedule or change the routes of these HGVA. By doing so, the companies can improve the LoS and make it possible to determine the number of TEUs that the road can accommodate. In addition, the method would achieve rescheduling calculation with consideration to the D-LoS. In this research, the D-LoS is when the average spacing between vehicles is higher than the SD required to stop the vehicles without crashing the leading vehicle, as designed in the author's methodology.

3.2.5 Rescheduling HGVA

The author has developed formulas to reschedule HGVA to mitigate congestion or/and increase road traffic capacity.

The reason behind rescheduling only HGVA is that the HGVA vehicles are the only type of vehicles that carry dry

and cryogenic intermodal containers. It has been substantiated through field observation and manual counting the author has conducted to investigate road A5036.

In this research, the author has proposed two approaches to reschedule HGVa. The first approach is to reschedule traffic flow to meet the existing total daily sum of HGVa, as in (3-52)-(3-56). The second approach is to reschedule traffic up to 85% of traffic flow capacity. For both approaches, the author required the rescheduling factor (RF) to control the total daily number of HGVa and, therefore, TEUs.

Definition 9: Rescheduling Factor (RF) is a factor that allows the user to control the total number of HGVa for every day by utilising the required average HGVa traffic volume for every hour and deducting the HGVa volume before rescheduling the current total traffic volume.

The RF value represents the required ratio to accomplish the first approach is equal to one, while the RF value to achieve the second approach varies according to the ABCL value that impacts many variables in the system.

The dynamic rescheduling considers the effect of increasing or decreasing the number of HGVa for every hour of the day on the total traffic volume, capacity, ATS After Rescheduling (ATSa) PCE_{DASia} . The rescheduling of HGVa works by deducting the existing HGVa in PCE value from the current total traffic volume and adding the new distribution of HGVa in their PCE_{DASia} values to the traffic volume that excludes the existing HGVa. The objective is to reduce the total traffic volume at peak hours, reduce the $VtCR$, improve the LoS, and increase the throughput of the road to increase the delivered TEUs towards meeting the demand targets set by the Mersey ports.

If the aim is to achieve the first approach, improve the traffic flow operation and reduce the congestion by rescheduling the dispatch of HGVa vehicles with keeping the same daily amount of HGVa vehicles. Therefore, the target of the daily number of HGVa After Rescheduling (AR) should be equal to the daily number of HGVa Before Rescheduling (BR). If the aim is to achieve the second approach, utilise the road up to its maximum capacity of HGVa vehicles where the $VtCR$ is equal to one and increases the TEUs. Therefore, the daily amount of HGVa vehicles will not be equal to its current amount, and it will vary according to the drivers' ABCL.

Also, to improve the ATS, the $VtCR$ value has to be enforced at ≤ 0.85 to avoid a steep reduction in the ATS, and in this case, the RF value should be multiplied by 0.85 in both approaches. However, the feasibility of enforcing a

VtCR of 0.85 depends on having a sufficient number of HGVa vehicles to remove from peak hours and sufficient space at off-peak hours to insert the HGVa vehicles in.

For every removed or inserted HGVa, there will be changes in hourly HGVa that will result in dynamic changes in the EGR, ATS, ASO_i, HGV_{di}, THGV_d, THGV_f, TF_{PCEa}, PCE_{DASi} and C_{DAS} due to changes in the HGVa traffic volume. These changes will lead to dynamic loops that will force a recalculation for every single move. The algorithms in (3-53) and (3-54) reflect the relationship between variables BR and AR when considering the first approach. For example, if the user removes or inserts an HGVa to an hour slot during rescheduling, then the PCE_{DAS4b} for the current schedule will change to PCE_{DAS4a} for the new schedule for that hour.

The determination of PCE_{DAS4a} and PCE_{DASa} values depend on the number of HGVa After Rescheduling (FV_{4a}), and the determination of the allowable change in HGVa traffic volume (FV₄) is dynamically affected by the values of PCE_{DAS4a} and PCE_{DASa} for every insertion or removal. Therefore, these dynamic relationships will create simultaneous equations such as (3-56), where variables are dependent on each other on both sides of the equations. The author utilised a system dynamics software called Vensim, which solves the model's simultaneous equations. The results showed the calculations of the variables FV_{4a}, PCE_{DAS4a}, TF_{PCEa}, ASO_{4a}, HGV_{d4a}, THGV_{fa}, ATSa, and EGRa and PCE_{DAS4a} are involved in many dynamic loops that will be discussed in chapter six.

$$AFV_{4b} = \frac{\int_{k=1}^{k=24} FV_{4b} \times dk}{24} \quad (3-53)$$

$$AFV_{4a} = AFV_{4b} \quad (3-54)$$

where,

- AFV_{4b} is the daily average volume of HGVa per hour before rescheduling in Z²/h
- FV_{4b} is the volume of HGVa before rescheduling in HGVa/h
- AFV_{4a} is the required daily average volume of HGVa per hour after rescheduling in Z²/h
- k is the time in hours

$$RF = \int_{h=1}^{h=24} \left(\frac{AFV_{4a} \times PCE_{DAS4a} + TF_{PCEb} \cdot FV_{4b} \times PCE_{DAS4b}}{24 \times C_{DASa}} \right) \times dh \quad (3-55)$$

$$FV_{4a} = \frac{RF \times C_{DASa} \times (TF_{PCEb} \cdot FV_{4b} \times PCE_{DAS4b})}{PCE_{DAS4a}} \quad (3-56)$$

where,

- AFV_{4a} is the required daily average volume of HGVa per hour after rescheduling
- C_{DASa} is the deceleration and acceleration space capacity after rescheduling
- PCE_{DAS4b} is the deceleration and acceleration space PCE value of vehicle type (4) before rescheduling

PCE_{DAS4a}	is the deceleration and acceleration space PCE value of vehicle type (4) after rescheduling
FV_{4a}	is the volume of HGVa after rescheduling in Z^2/h
FV_{4b}	is the volume of HGVa before rescheduling in $HGVa/h$
RF	is the rescheduling factor that allows control over the total daily HGVa and TEUs (Definition 8)
h	is the time in hours

3.3 FINDINGS AND ANALYSIS

In this section, the author has applied the formulas in the literature review chapter and this chapter to determine the headway, PCE, capacity, and $VtCR$, and the rescheduling effect on all the latter variables.

3.3.1 Vehicle's Headway

The results in FIGURE 3-1 and FIGURE 3-2 show that the vehicles' headways are directly proportional to the ATS. The results in FIGURE 3-3 show the required HGVa headway before and after adding an extra space, and the results in FIGURE 3-4 show that the HGVs' required headway is inversely proportional to the GM, and by every increase of 20% of MAM the headway of HGVR and HGVa vehicles increase by 10m and 11m, respectively.

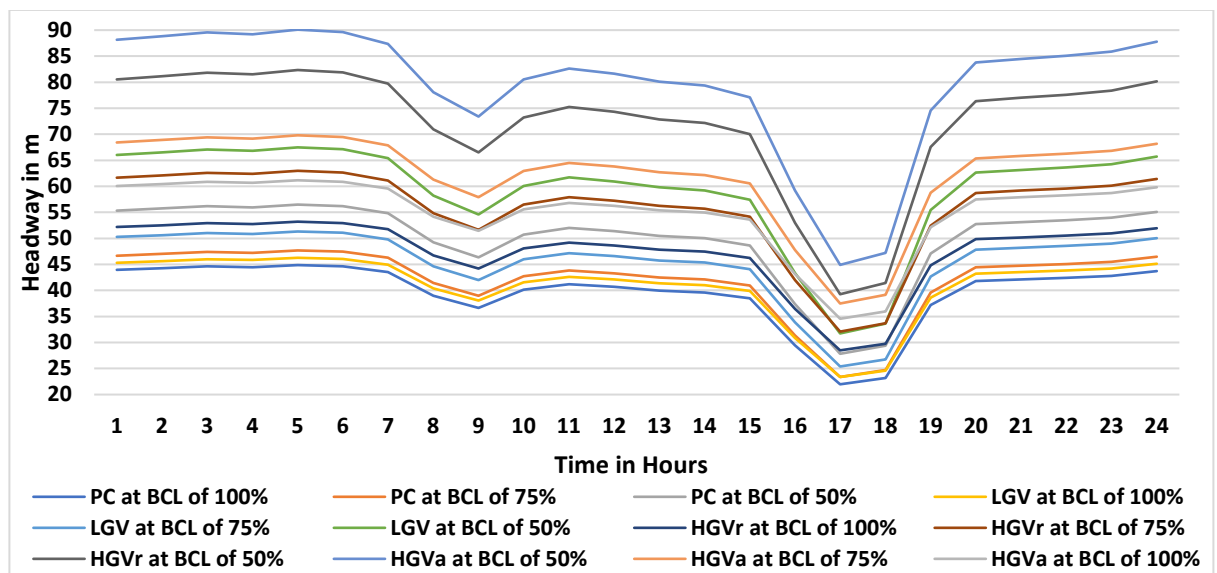


FIGURE 3-1: Vehicles' headways at ABCL of 50%, 75%, and 100% and ATS of DBR

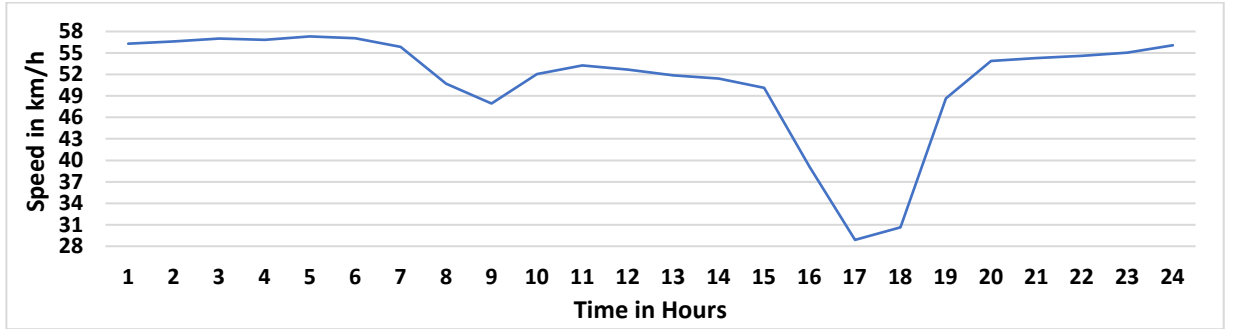


FIGURE 3-2: The ATS obtained from ATCs at ATS of DBR

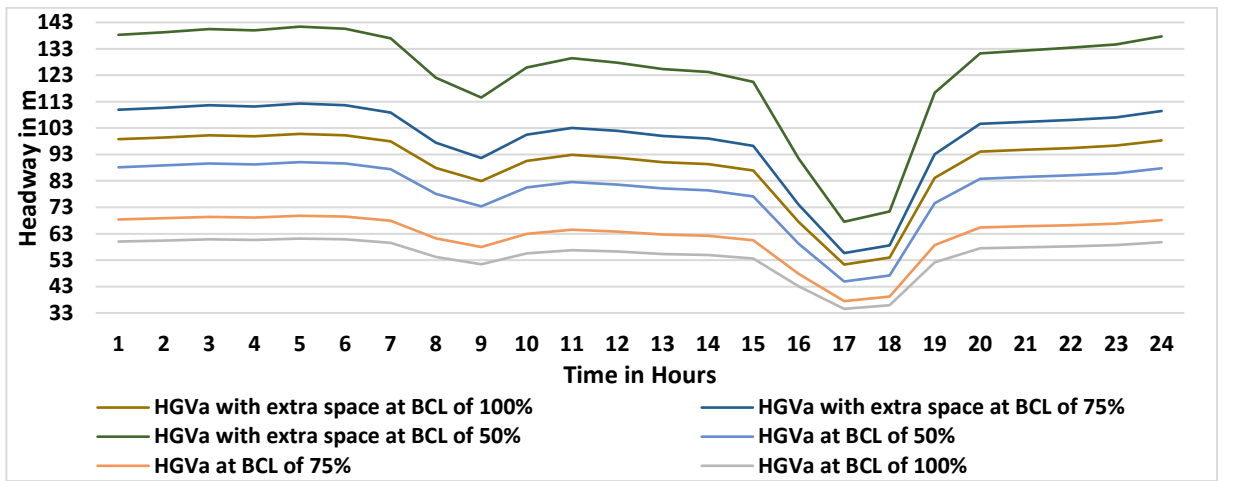


FIGURE 3-3: HGVa headway before and after adding an extra space at ABCL of 50%, 75%, and 100% and ATS of DBR

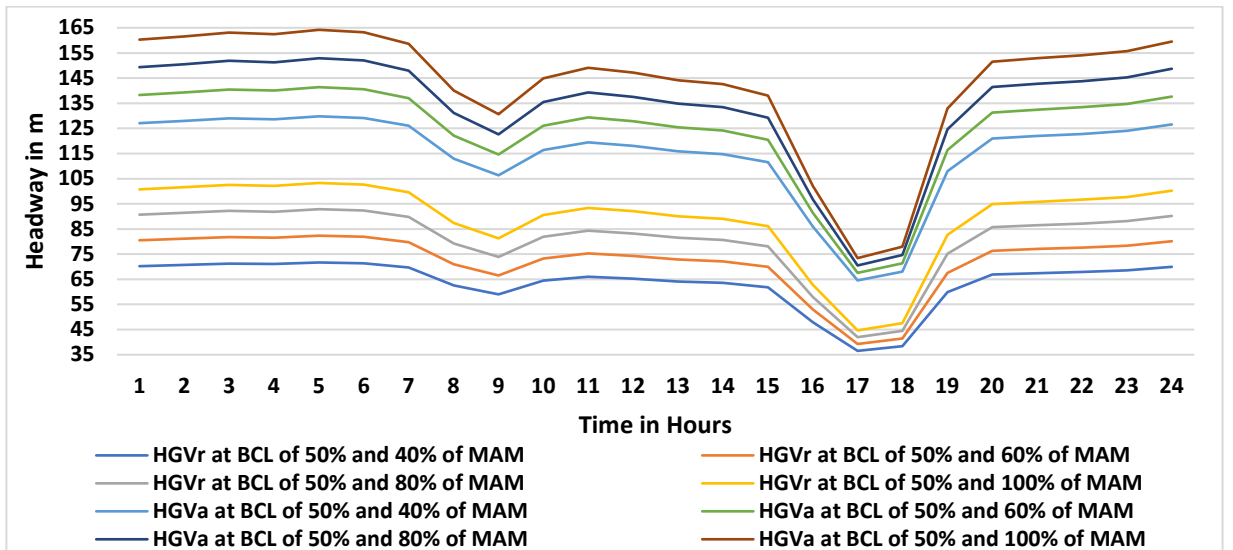


FIGURE 3-4: Impact of changing the HGVs' GM on their safe headways at ABCL of 50%, 75%, and 100% and ATS of DBR

The results in TABLE 3-5 present the components of headway of SD, BD, and RD in distance measurement for PC, LGV, HGVr, and HGVA vehicles (HGVA without adding an extra space), and TABLE 3-6 present the later variables in time measurement. The SD, BD, and RD increase with the decrease of BCL, and the SD value represents the minimum required gap between the vehicle and the leading vehicle. Therefore, the PCE_{DAS} , H, SD, BD, and RD are inversely proportional to the BCL of the vehicle's driver.

TABLE 3-5: SD, BD, and RD for PC, LGV, HGVr, and HGVA at a BCL of 50%-100% when utilising an ATS of 64.37km/h

Speed in km/h	BCL	PC			LGV			HGVr			HGVA		
		SD	BD	RD	SD	BD	RD	SD	BD	RD	SD	BD	RD
64.37	100%	29.4	16.3	13.1	29.35	16.3	13.1	33.8	20.7	13.1	35.6	22.6	13.1
	75%	32.5	16.3	16.2	35.28	19.07	16.2	43.7	27.5	16.2	46.1	29.9	16.2
	50%	42.4	16.3	26.1	54.37	28.3	26.1	66.8	40.7	26.1	70.4	44.2	26.1

TABLE 3-6: ST, BT, and RT for PC, LGV, HGVr, and HGVA at a BCL of 50%-100% when utilising an ATS of 64.37km/h

Speed in km/h	BCL	PC			LGV			HGVr			HGVA		
		ST	BT	RT	ST	BT	RT	ST	BT	RT	ST	BT	RT
64.37	100%	1.64	0.91	0.73	1.64	0.91	0.73	1.89	1.16	0.73	1.99	1.26	0.73
	75%	1.82	0.91	0.91	1.97	1.07	0.91	2.44	1.54	0.91	2.58	1.67	0.91
	50%	2.37	0.91	1.46	3.04	1.58	1.46	3.74	2.28	1.46	3.94	2.47	1.46

The author considered the RT where the driver is highly alert and aware and has only time for eye movement and pressing the brakes and did not include the RT required for manoeuvring and unexpected situations. Therefore, the drivers on the road should require an extra 0.95s to the results of ST and RT in TABLE 3-6 as in TABLE 3-7.

TABLE 3-7: ST and RT values for PC, LGV, HGVr, and HGVA at ABCL of 50%-100% when utilising an ATS 64.37km/h after adding the RT required for manoeuvring and unexpected situations

Speed in km/h	BCL	PC			LGV			HGVr			HGVA		
		ST	BT	RT	ST	BT	RT	ST	BT	RT	ST	BT	RT
64.37	100%	2.59	0.91	1.68	2.59	0.91	1.68	3.4	1.16	1.68	2.94	1.26	1.68
	75%	2.77	0.91	1.86	2.93	1.07	1.86	3.57	1.54	1.86	3.53	1.67	1.86
	50%	3.32	0.91	2.41	3.99	1.58	2.41	4.69	2.28	2.41	4.89	2.47	2.41

3.3.2 Passenger Car Equivalent

The results in TABLE 3-8 present the values of PCE_{DASi} and the required headway for HGVs before and after adding extra space to the HGVA vehicles' headway. The results show that the PCE_{DASi} and headway values increase with the decrease of BCL and increase when adding extra space to the headway's HGVA vehicles' headway. The results in FIGURE 3-5 present the PCE_{DASi} values of LGV, HGVr, and HGVA vehicles at variable ATS for an average working day. FIGURE 3-5 shows the PCE_{DAS} of HGVA vehicles before adding an extra space behind the HGVA, and the results in FIGURE 3-6 show the PCE_{DAS} of an HGVA after adding the extra space.

TABLE 3-8: PCE_{DAS} and H values for HGVR, and HGVA at BCL of 50%-100% when utilising an ATS of 64.37km/h

Speed in km/h	BCL	HGVR		HGVA			
		PCE in PC/veh	H in metre	PCE with extra space in PC/veh	PCE without extra space in PC/veh	H with extra space in metre	H without extra space in metre
64.37	100%	1.32	45.4	2.41	1.56	81.5	52.1
	75%	1.47	55.3	2.57	1.71	95.1	62.6
	50%	1.65	78.6	2.77	1.88	129.3	86.9

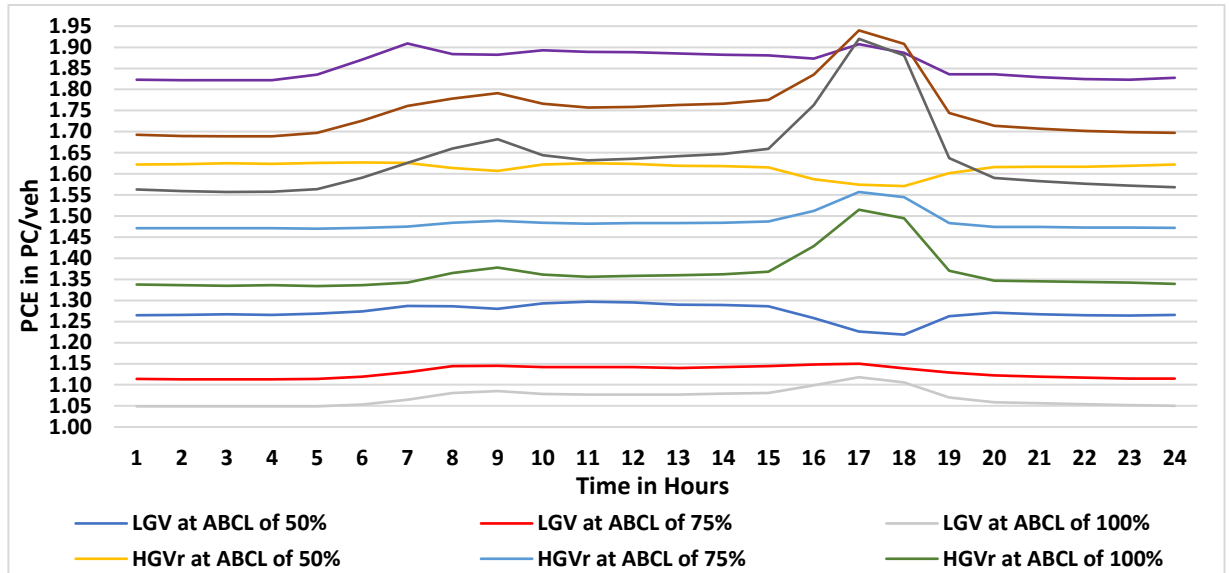


FIGURE 3-5: PCE_{DASi} values for LGV, HGVR, and HGVA (no extra space) vehicles at an ABCL of 50%, 75%, and 100% and ATS of DBR

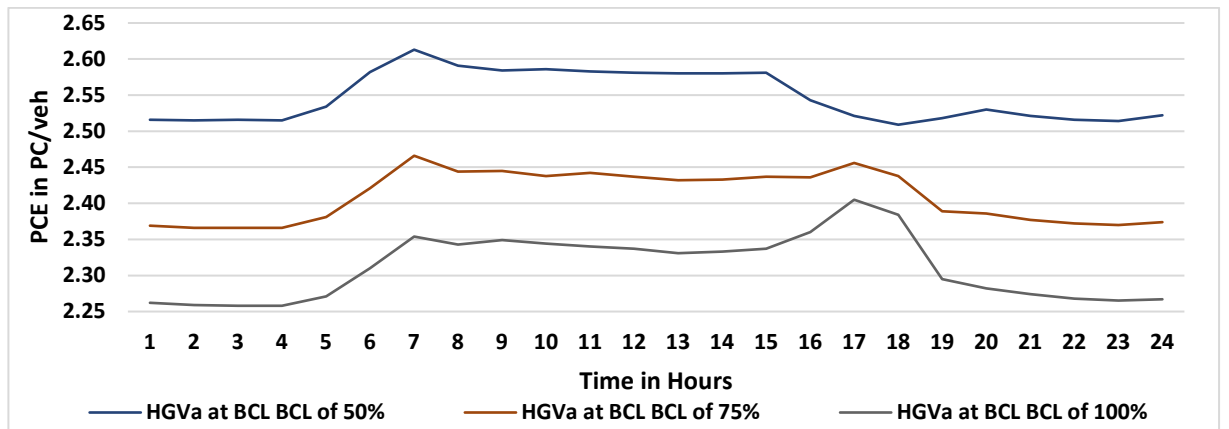


FIGURE 3-6: PCE_{DAS} values for HGVA after adding an extra space at an ABCL of 50%, 75%, and 100% and ATS of DBR

The LGV and HGVA vehicles reach their morning peak volume at hour 9.00 while the HGVR vehicles reach their morning peak volume at hour 10.00, and at the evening peak, the LGV and HGVR vehicles reach their peak volume at hour 16 while the HGVA vehicles reach their evening peak volume at hour 17.00. Also, the Average Available Gap (AAG) at ABCL of 50% is slightly higher than at ABCL of 75% and 100%, and the difference in AAG is up

to 6.22m/veh at the morning peak hours while it is only up to 1.32m/veh at evening peak hours due to sharp decrease in the ATS, as shown in FIGURE 3-2.

Therefore, the PCE_{DAS} for LGV and HGVr vehicles have decreased in the morning peak at hours 8.00-9.00 and evening peak at hours 17.00-18.00 at an ABCL of 50%, as shown in. On the other hand, the PCE_{DAS} of HGVa vehicles did not experience any decreases during these hours because the LGV and HGVr vehicles require shorted SDs in comparison to HGVa vehicles and also because the LGV and HGVr vehicles peak volumes are at hour 16.00, and due to low ATS, as shown in FIGURE 3-2.

The road under investigation connects to the Liverpool container terminal, and its HGV percentage is over five times the percentage of HGVs for UK major roads that do not connect to ports. The results in FIGURE 3-5 and FIGURE 3-6 show how the PCE_{DASi} is proportional to the vehicle type and average flow speed, and total traffic volume in PCE exhibits the same pattern the peak and off-peak hours of the initial TF.

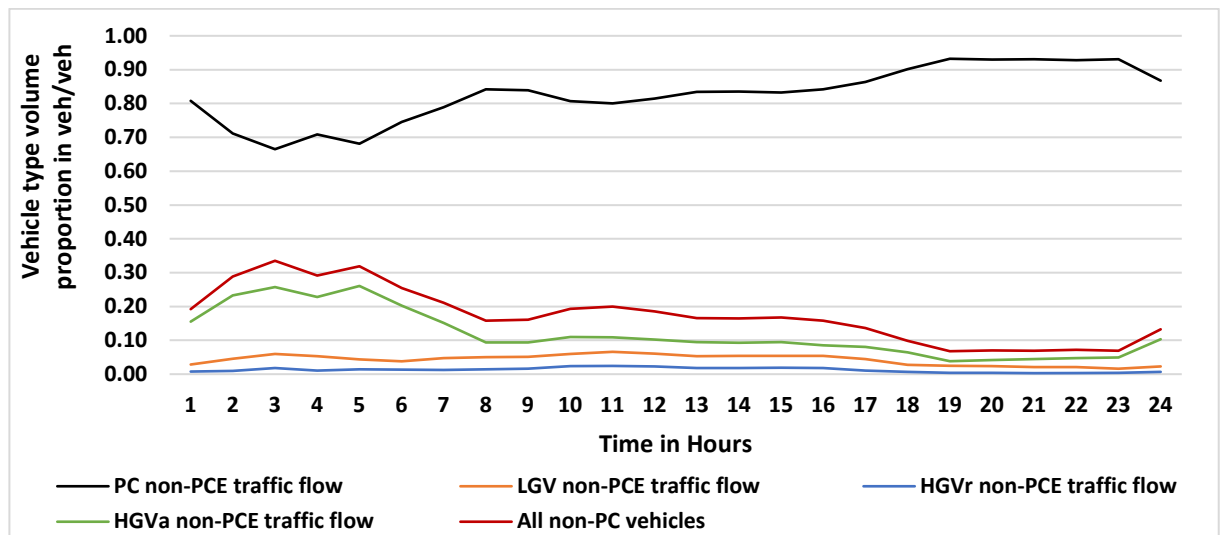


FIGURE 3-7: Composite proportions of non-PCE traffic flow volumes and ATS of DBR

FIGURE 3-7 shows the proportions of PC, LGV, HGVr, HGVa, and all non-PC vehicles using a non-PCE traffic flow volume. The results show that during the hours 2.00-6.00am, the HGVs' proportion in the TF is equal to or greater than 0.20, but the TF during these hours is low (up to 7% of capacity) while the PC vehicles were up to 26% of capacity. The PCs dominate the flow volume, especially during the evening peak hours of 17.00-19.00, where the PC proportion exceeds 0.90. Therefore, it seems at first that the HGVs are not responsible for traffic

congestion. However, the author has converted the traffic flow volumes to their PCE value to determine the full extent of the HGV impact on the traffic flow.

Researchers have concluded that when the VtCR exceeds 0.85, the ATS starts to decrease steeply, and the VtCR has exceeded 0.85 at the hours 8.00-19.00 (TRB, 2000; Rogers, 2016), and the ATS will have a further decrease when the traffic density reaches its maximum value. Therefore, HGVs' existence on the road at peak hours may cause a higher impact than at off-peak hours. However, the author has converted the traffic flow volumes to their PCE value to determine the full extent of the HGV impact on the traffic flow. The results in FIGURE 3-8, FIGURE 3-9, and FIGURE 3-10 present the vehicles' proportions in PCE at ABCL of 50%, 75%, and 100%. The results show that the proportion of non-PC vehicles has increased at morning peak hours by 51%, 43%, and 36% at an ABCL of 50%, 75%, and 100%, respectively.

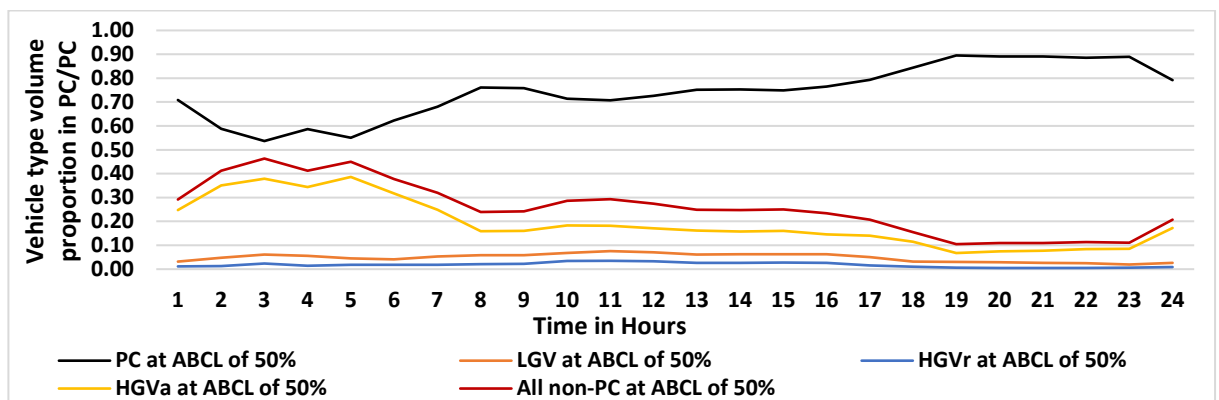


FIGURE 3-8: Vehicles' proportions of traffic flow using PCE converted traffic flow volumes at ABCL of 50% and ATS of DBR

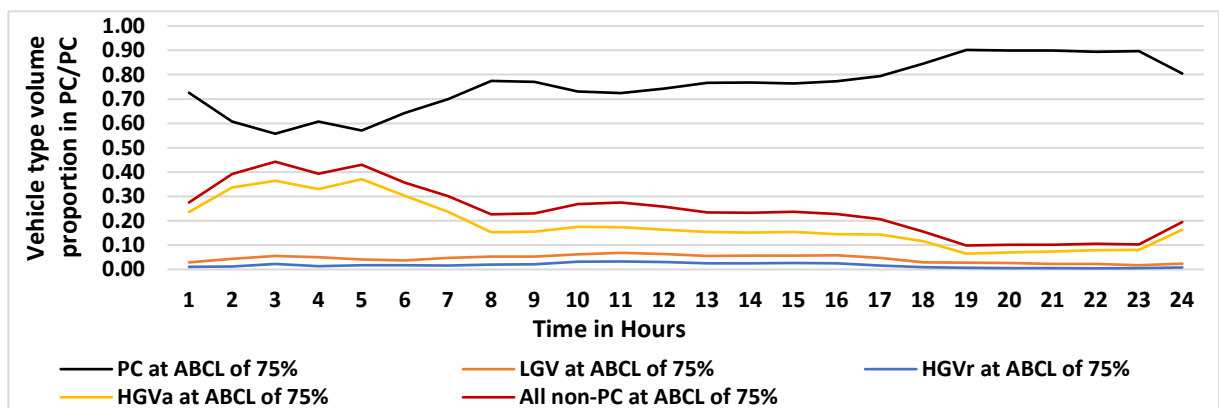


FIGURE 3-9: Vehicles' proportions of traffic flow using PCE converted traffic flow volumes at ABCL of 75% and ATS of DBR

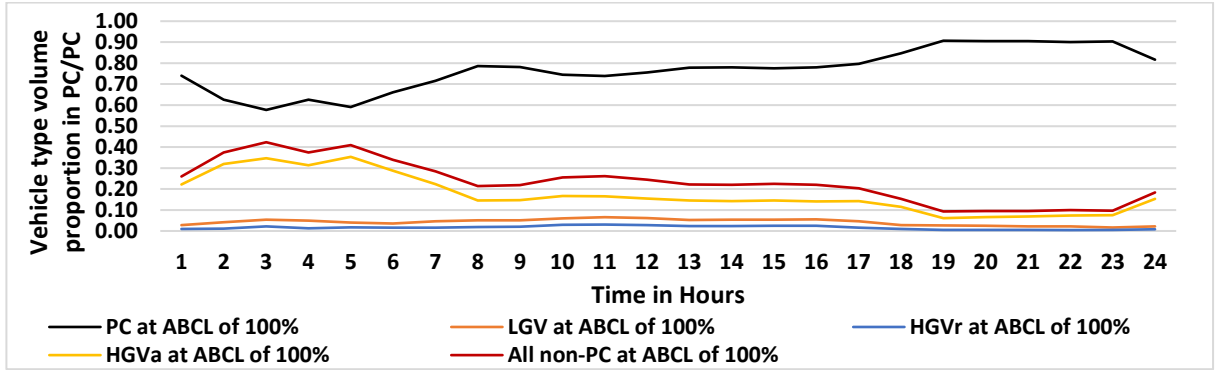


FIGURE 3-10: Vehicles' proportions of traffic flow using PCE converted traffic flow volumes at ABCL of 100% and ATS of DBR

The results also show an increase at evening peak hours by up to 57%, 57%, and 54% at an ABCL of 50%, 75%, and 100%, respectively. Therefore, the non-PC vehicles' proportion before the PCE conversion of up to 16% does not reflect the actual impact on traffic flow operation, and the HGVs may have a significant impact on the traffic flow during peak hours.

The average, minimum, and maximum proportions of all HGVs before converting the HGVs vehicles to their PCE_{DASi} values are 13%, 4%, and 28%, respectively, and the average, minimum, and maximum proportions of all HGVs after PCE conversion at an ABCL of 50%, 75%, and 100% are 21%, 7%, and 41%; 20%, 7%, and 39%; 19%, 7%, and 37%, respectively. The percentage of increase of the average, minimum, and maximum proportions after PCE conversion at an ABCL of 50%, 75%, and 100% are 64%, 46%, and 74%; 57%, 40%, and 76%; 49%, 34%, and 73%, respectively.

However, the PC flow volume remains the main contributor to traffic flow. FIGURE 3-11 shows the ATC data set of traffic flow volumes for four types of vehicles, and the TF volume before and after PCE conversion, FIGURE 3-11 also shows the morning and evening peak hours 8.00-9.00 and 17.00-18.00, respectively. At the evening peak from 4 pm-7 pm, the VtCR exceeds 85%, which forces the traffic speed flow to fall sharply, as shown in FIGURE 3-2. The speed does not have a clear relationship with the HGV_d, because on the one hand, when the speed decreases, the headway and ASO decrease. On the other hand, when the speed decreases, the SA decreases.

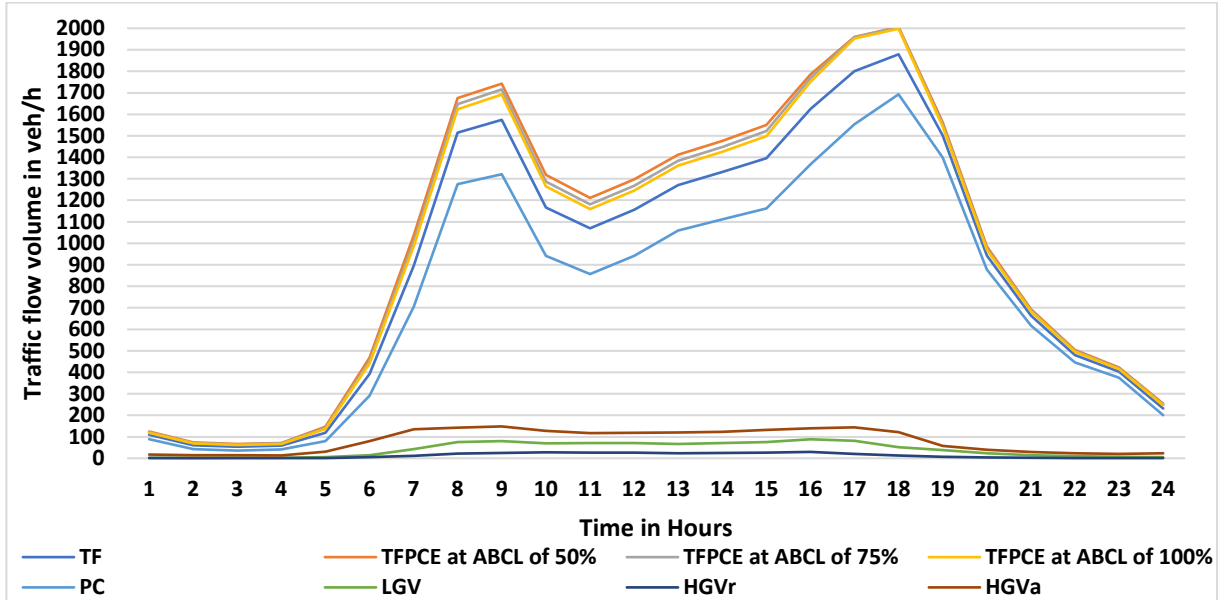


FIGURE 3-11: PC, LGV, HGVR, HGVA, TF, and TFPCE flow volumes at ABCL of 50%, 75%, and 100% and ATS of DBR

The results show that the PCE_{DAS4} is inversely proportional to the BCL. The results show that the increase of BCL from 50% to 100% will reduce the PCE_{DAS4} by an average of 23.53%, and it is equivalent to a reduction of 0.79 of PCE_{DAS4} . However, this relationship gets more dominant among other variables, such as GM. Therefore, the PCE_{DAS4} (for HGVA) is directly proportional to GM, as shown in FIGURE 3-12, the PCE_{DAS4} decreases by an average of 0.11 for every reduction of 20% of MAM.

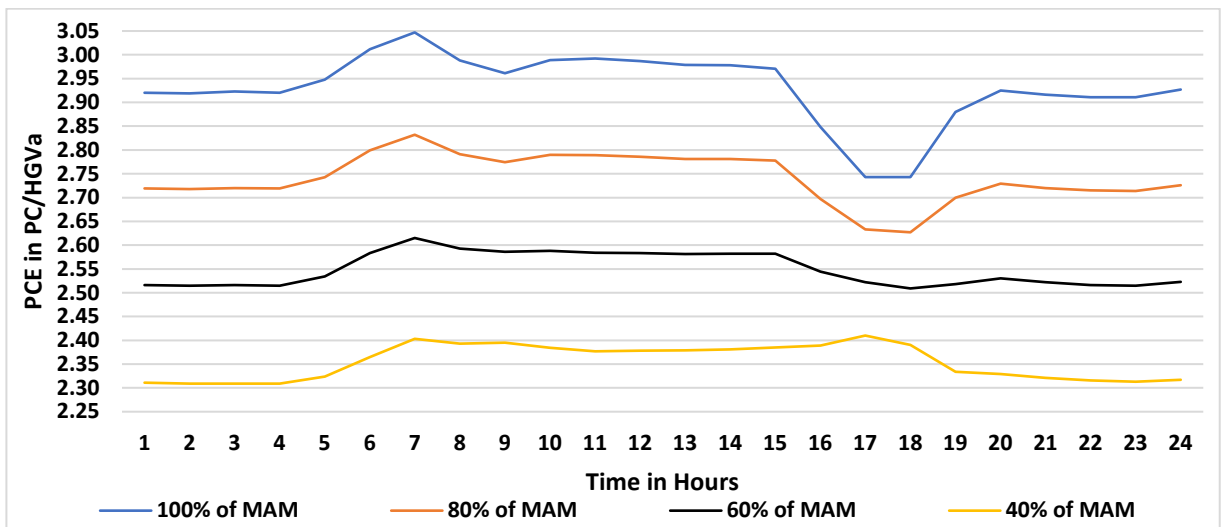


FIGURE 3-12: Impact of GM (as a percentage of MAM) level on the PCE_{DAS4} and ATS of DBR

The results in FIGURE 3-13 show that the PCE_{DAS4} is also directly proportional to the ATS, and for every decrease of ATS by 16.093km/h (10mi/h), there will be a decrease of an average of 7%. However, when the speed is lower than the optimum speed of DBR (36.34km/h (22.6mi/h)), the PCE_{DAS} changes to be inversely proportional to ATS.

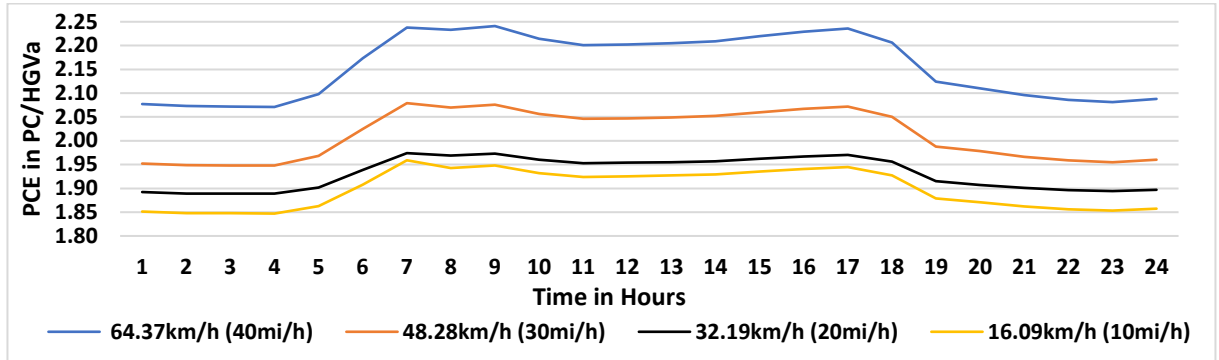


FIGURE 3-13: Impact of ATS level on the PCE_{DAS} and TF of DBR

3.3.3 Volume to Capacity Ratio and Capacity

The author has applied changes to the ABCL of all vehicles, ATS, and the GM of HGVs to determine their impact on the $VtCR$ and capacity based on the Saturation Flow Method (SF) and Deceleration and Acceleration Space Method (DAS). FIGURE 3-14, FIGURE 3-15, and FIGURE 3-16 show that the $VtCR_{SF}$ and CSF are slightly affected by the change of ABCL and ATS due to the lack of representation of the ATS in the calculation of the capacity.

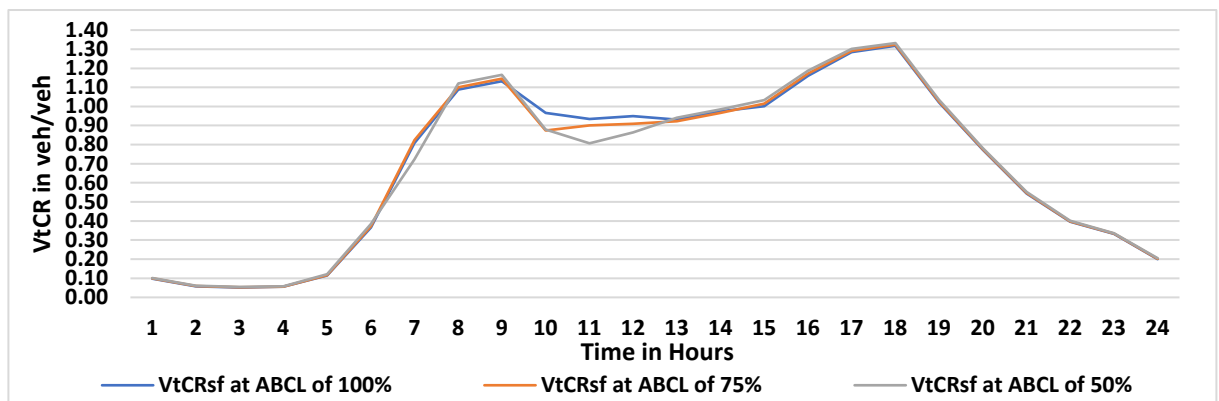


FIGURE 3-14: Impact of changes in ABCL on the $VtCR_{SF}$ of DBR

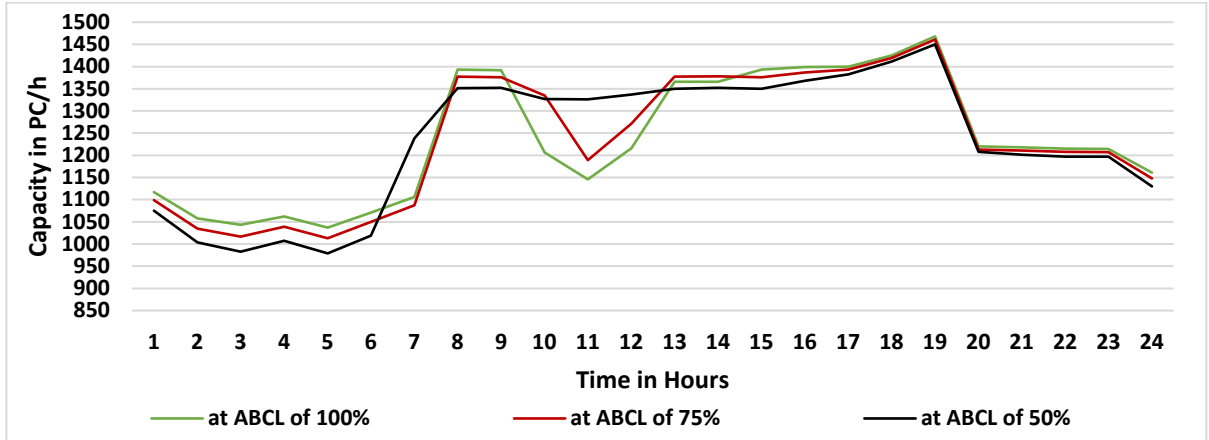


FIGURE 3-15: Impact of changes in ABCL on the C_{SF} of DBR

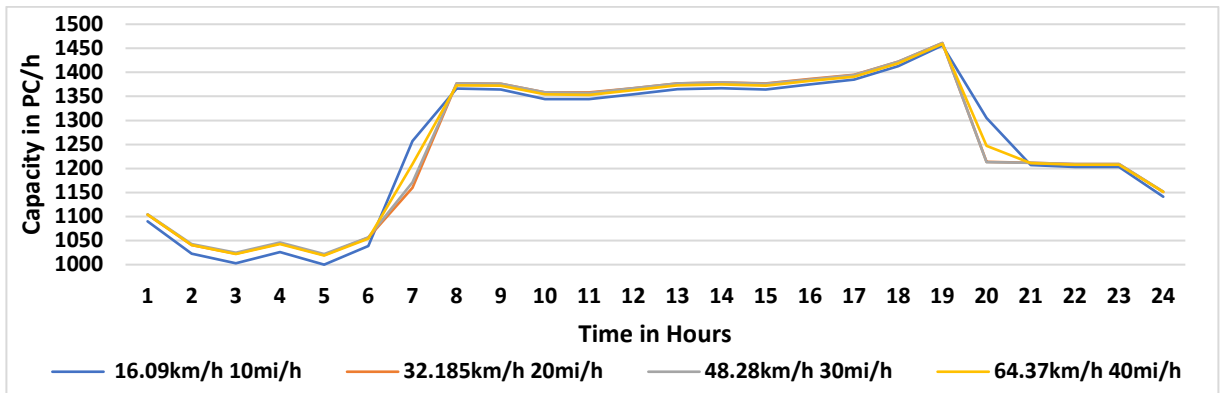


FIGURE 3-16: Impact of changes in ATS on the C_{SF} of DBR

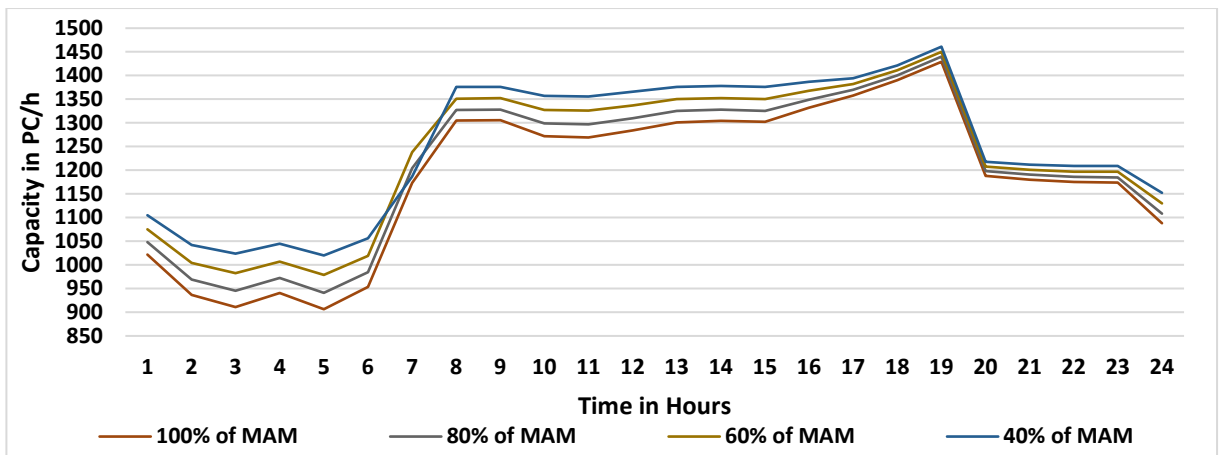


FIGURE 3-17: Impact of changes in GM on the C_{SF} of DBR

However, FIGURE 3-17 show that the C_{SF} is more affected by the change in the HGVs' GM, and the C_{SF} is inversely proportional to the GM.

In contrast to the SF method, the DAS method shows the high impact of ABCL, GM, and ATS of $VtCR_{DAS}$ and C_{DAS} . The results in FIGURE 3-18 and FIGURE 3-19 show that the $VtCR_{DAS}$ is inversely proportional to the ABCL and the C_{DAS} is directly proportional to the ABCL. The C_{DAS} increases by 26.09% at off-peak hours and 29.1% at peak hours when the ABCL increases from 50% to 100%.

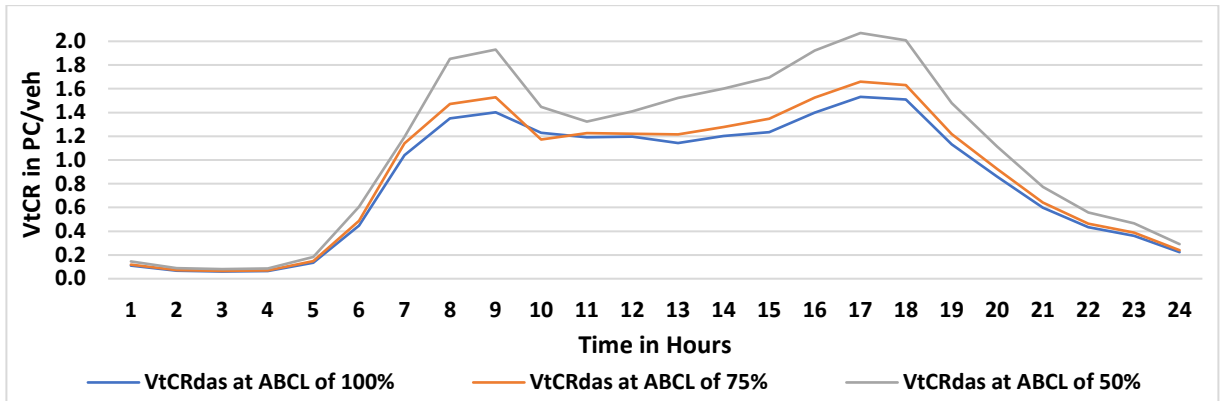


FIGURE 3-18: Impact of changes in ABCL on the $VtCR_{DAS}$ of DBR

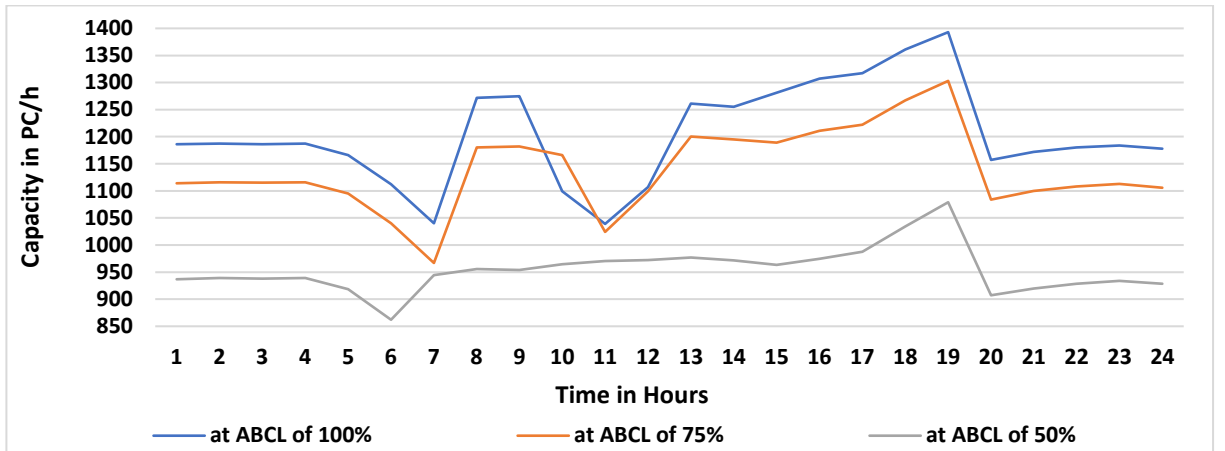


FIGURE 3-19: Impact of changes in ABCL on the C_{DAS} of DBR

FIGURE 3-20 and FIGURE 3-21 show that the $VtCR_{DAS}$ is directly proportional to the GM and the C_{DAS} is inversely proportional to the GM. However, the impact of the GM on the $VtCR_{DAS}$ and C_{DAS} reduce with the reduction of ATS. Therefore, the HGVs' GM's impact is minimal during the evening peak hours due to the sharp decrease in ATS, especially at the hours of 17.00 and 18.00.

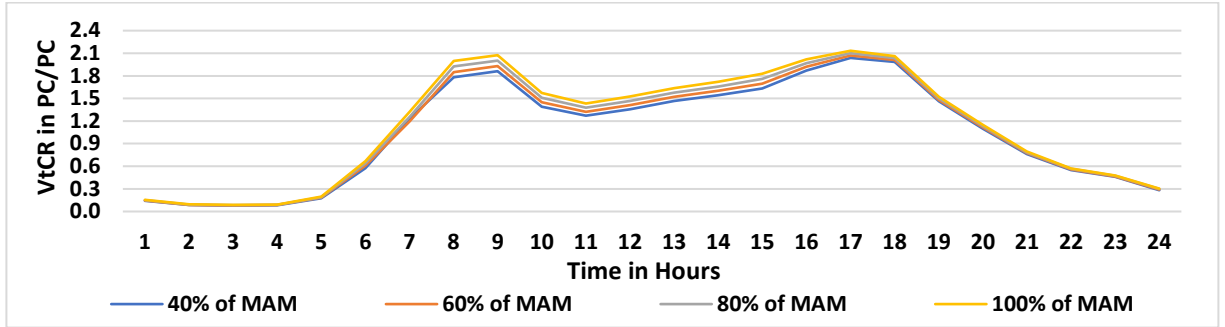


FIGURE 3-20: Impact of changes in GM on the $VtCR_{DAS}$ of DBR

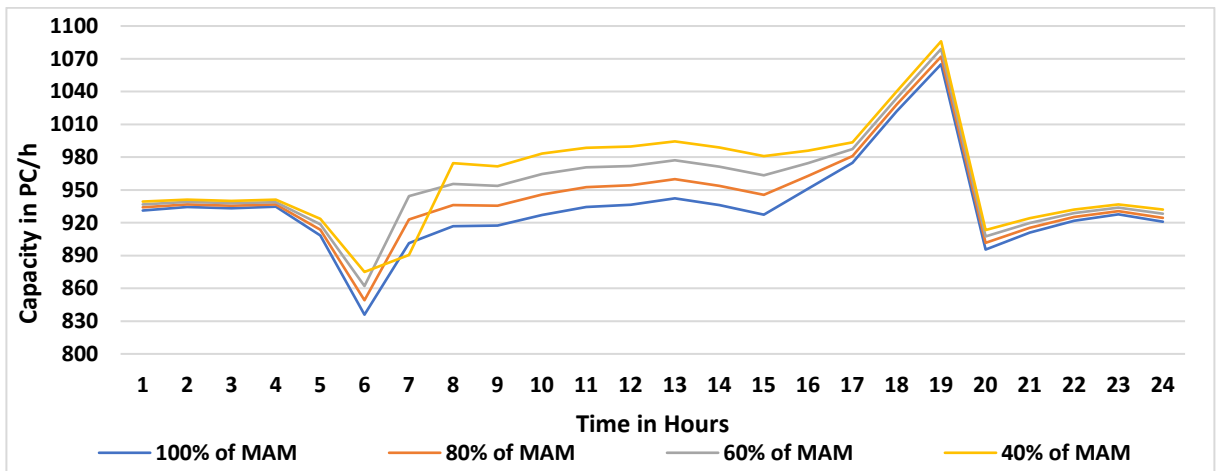


FIGURE 3-21: Impact of changes in GM on the C_{DAS} at an ABCL of 50% of DBR

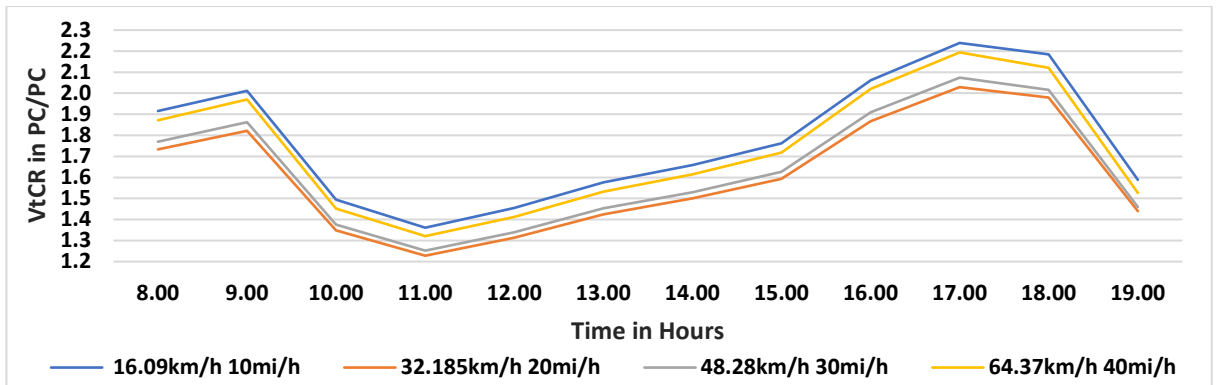


FIGURE 3-22: Impact of changes in ATS on the $VtCR_{DAS}$ at an ABCL of 50% of DBR

According to the results in FIGURE 3-22, the $VtCR_{DAS}$ decreases when the ATS decrease until the ATS reduces to a value lower than optimum speed, then the $VtCR_{DAS}$ will rapidly increase until it exceeds the $VtCR_{DAS}$ at ATS of 48.28 km/h. The results in FIGURE 3-23 show the same impact, but in an inverse proportion, as the ATS

decreases, the C_{DAS} increases until the ATS is lower than the optimum speed, then the C_{DAS} will sharply decrease and get lower than its value at ATS of 48.28 km/h.

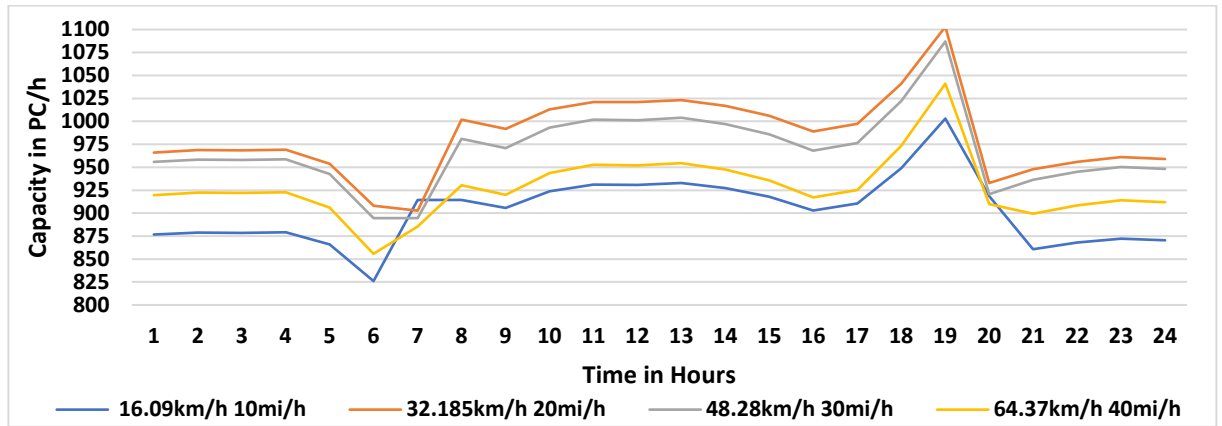


FIGURE 3-23: Impact of changes in ATS on the C_{DAS} at an ABCL of 50% of DBR

In contrast to the C_{SF} estimation method, the C_{DAS} estimation method shows a correlation between TF and HGV traffic volume as it shows that the SF method has overestimated and underestimated the HGV effect on the capacity in peak and off-peak hours, respectively. This is because the capacity estimation methods dependent on vehicle proportion assume that the traffic flow is at the capacity level.

3.3.4 Passenger Car Equivalent Methods

The author has applied the formulas of the PCE estimation methods discussed in the literature review chapter two to the BDR's road link under investigation. The results for the SF, St John, and Gwyn in FIGURE 3-24 and FIGURE 3-25, respectively, show that the PCE increases when the proportion increase even though the TF and the non-PC vehicle's flow volume are low levels,

According to FIGURE 3-7 to FIGURE 3-10, FIGURE 3-24, and FIGURE 3-25 at the hours of 1.00-8.00am, the PCE increases with the increase of non-PC proportion until the proportion reaches its peak, then the PCE starts to decline with the decline of the proportion until the V_tCR exceeds one. The downside of the proportion methods that the high proportion increase PCE even though the TF is far from reaching capacity

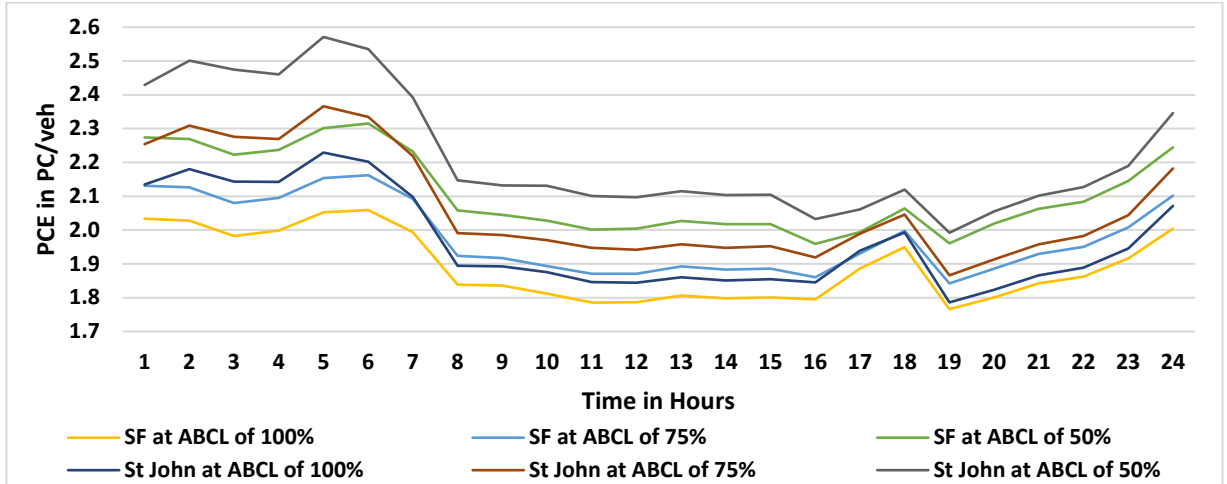


FIGURE 3-24: The results of the SF and St Johns methods of estimating the PCE at ABCL of 50%, 75%, and 100% by utilising vehicle's traffic flow proportion

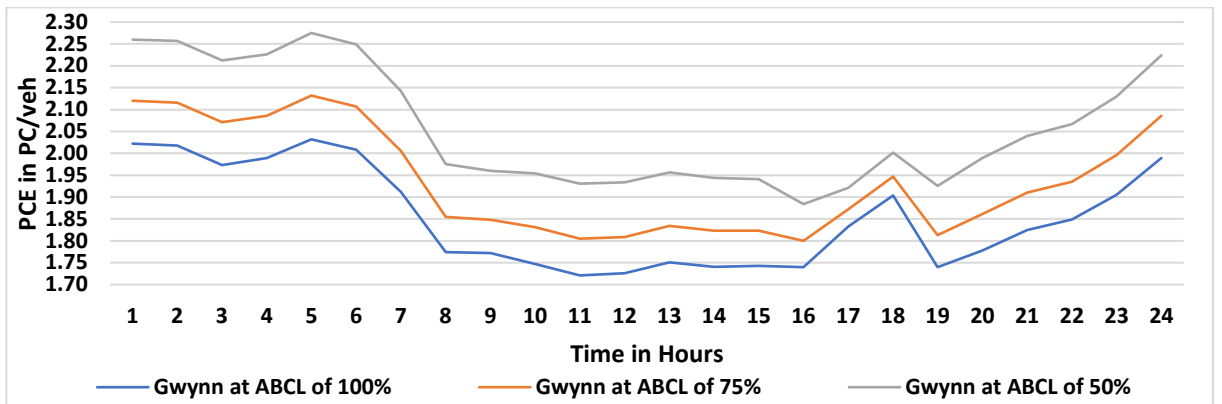


FIGURE 3-25: The results of the Gwynn (1968) method of estimating the PCE at ABCL of 50%, 75%, and 100% by utilising vehicle's traffic flow proportion and vehicles' headways

The Sumner (1984) and Benekohal (2000) methods were also based on the vehicle's proportion and showed extremely high PCE values at the evening off-peak times, as shown in FIGURE 3-26. However, the Benekohal (2000) method utilised the delay of non-PC vehicles and the delay of PCs, while Sumner (1984) utilised only the PC's proportion and the non-PC vehicle's proportion. Therefore, the proportion based PCE estimation methods work only when the TF is at the capacity level (Sumner, 1984; Benekohal, 2000).

The Huber (1982) and Chandra (2000) methods shown the PCE is proportional to the TF and the non-PC vehicles' traffic flow volumes due to their utilisation of speed of individual vehicles' types and dimensions, as shown in FIGURE 3-27 and FIGURE 3-28. The Chandra (2000) method provided higher values than the Huber (1982) method because it considered the width of the vehicles and the length.

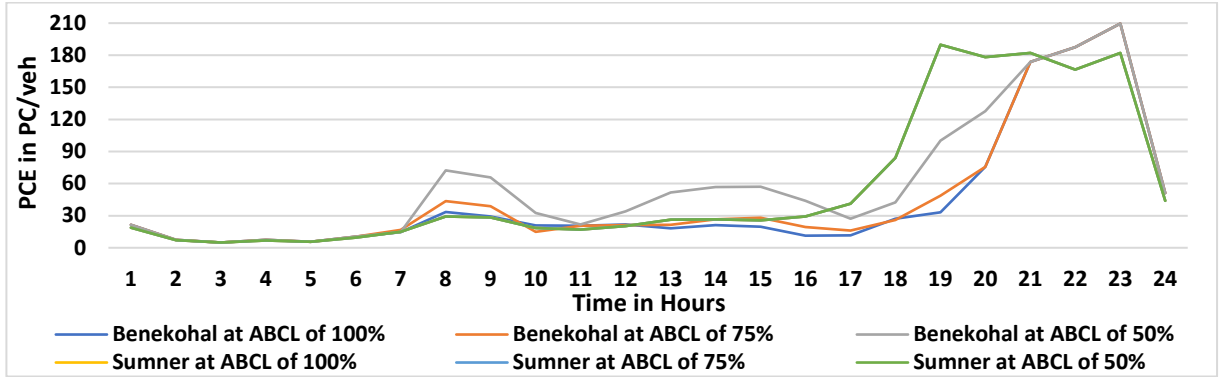


FIGURE 3-26: The results of the Benekohal (2000) and Sumner (1984) methods of estimating the PCE at ABCL of 50%, 75%, and 100%

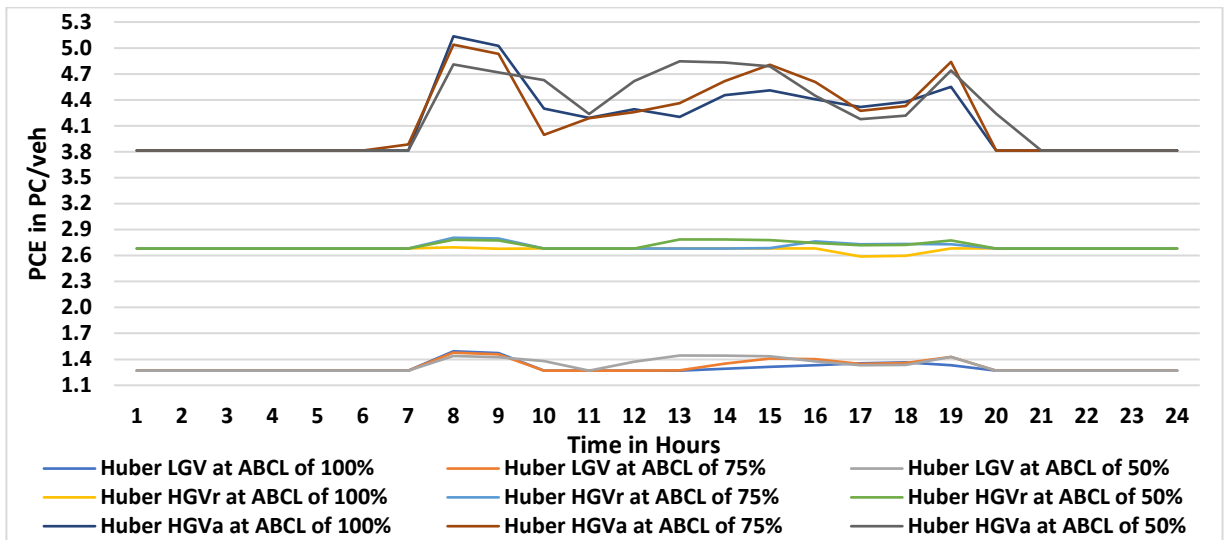


FIGURE 3-27: Huber (1982) PCE estimation method at ABCL of 50%, 75%, and 100%

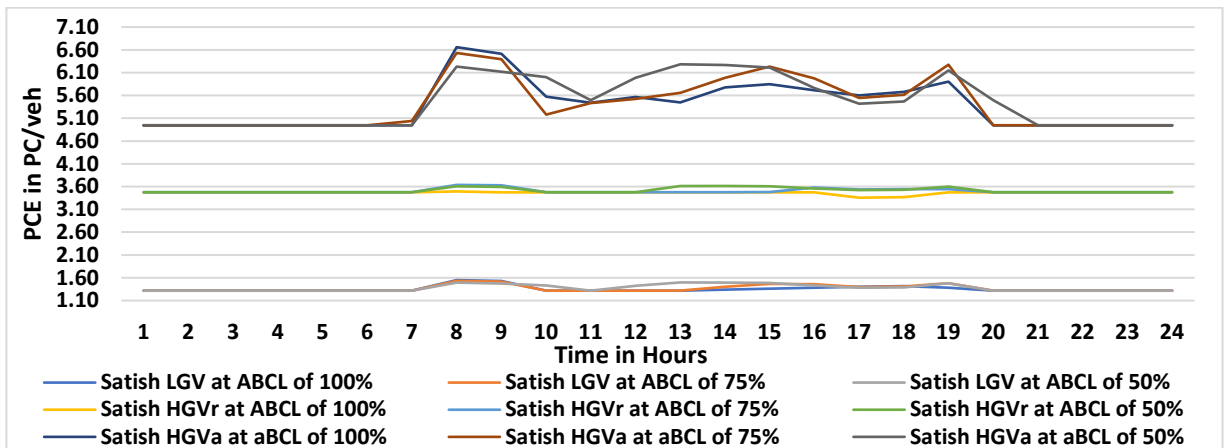


FIGURE 3-28: Chandra (2000) PCE estimation method at ABCL of 50%, 75%, and 100%

The PCE methods the mainly use vehicle's headway such as the Greenshields (1935), Seguin (1982), Cunagin (1982), Fan (1990), Molina (1987), and Krammes (1986) methods are directly proportional to the speed at peak hours at an ABCL of 50% and directly proportional to TF at ABCL of 75% and 100%, as shown in FIGURE 3-29, FIGURE 3-30, and FIGURE 3-31, the DAS method has similar performance at peak hours. However, the DAS method is directly proportional to the TF during off-peak hours, as shown in FIGURE 3-5.

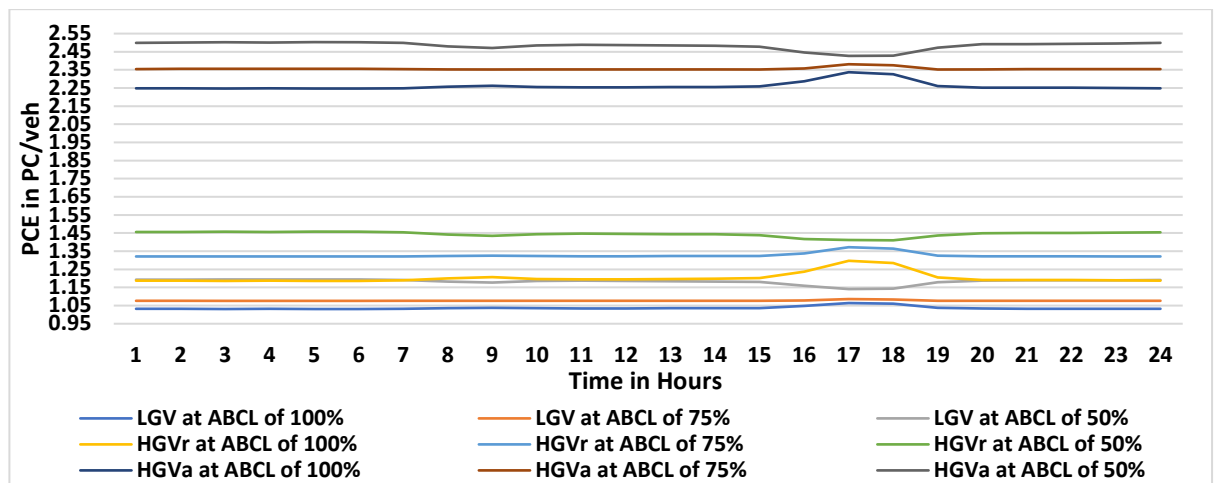


FIGURE 3-29: Greenshields (1935), Seguin (1982), Cunagin (1982), and Fan (1990) PCE estimation methods at ABCL of 50%, 75%, and 100%

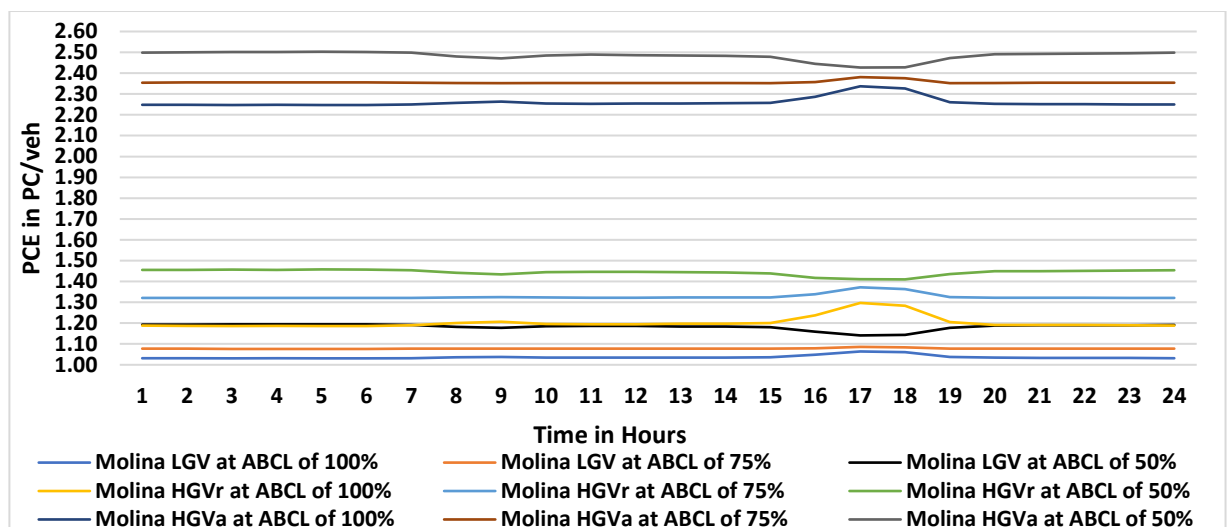


FIGURE 3-30: Molina (1987) PCE estimation method at ABCL of 50%, 75%, and 100%

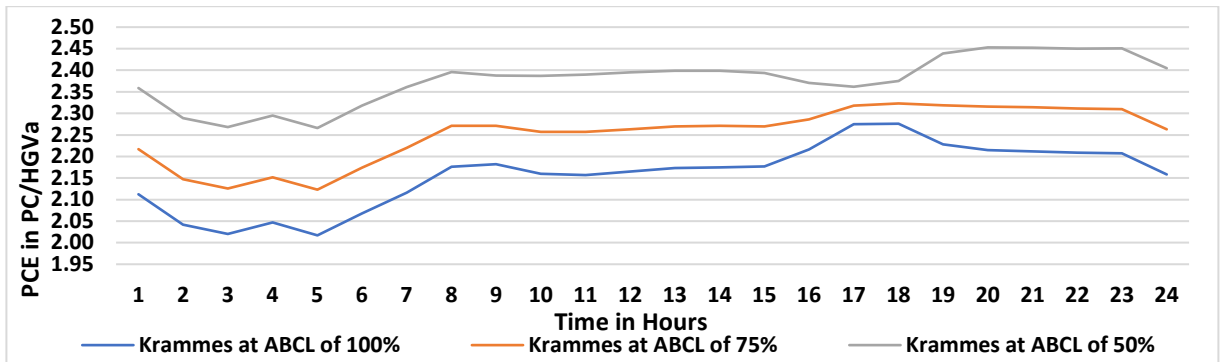


FIGURE 3-31: Krammes (1986) PCE estimation method at ABCL of 50%, 75%, and 100%

The reason for this behaviour is that the ATS is at its lowest level at evening peak hours, as shown in FIGURE 3-32, and HGvA's headway reduction is at its highest due to the reduction of the required SD. The reduction of the SD of the HGvA is significantly higher at ABCL of 50% than at ABCL of 75% and 100%. The Lu (2020) method utilise the queue length and the headway, but the TF is dominant. FIGURE 3-33 show that the Lu (2020) method is inversely proportional to TF and directly proportional to the ATS.

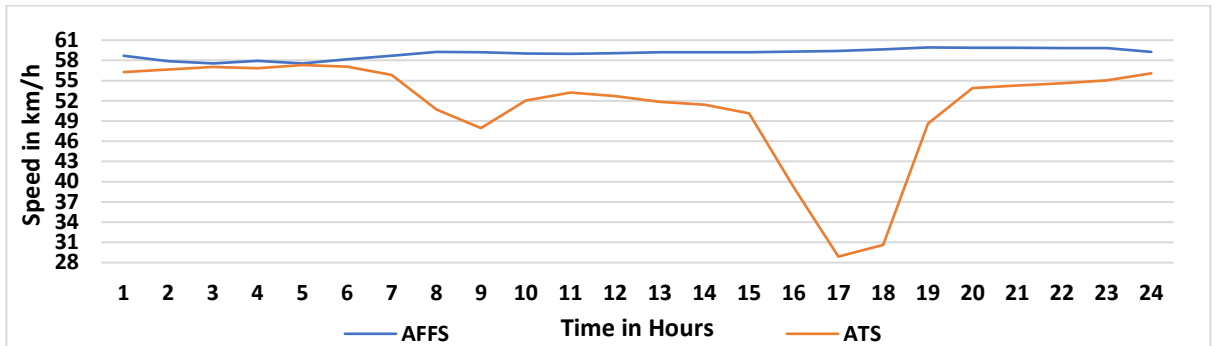


FIGURE 3-32: ATS and average FFS

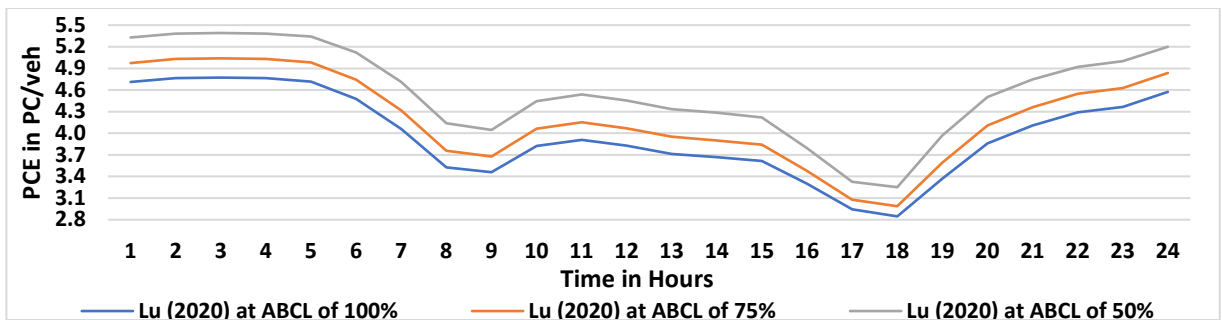


FIGURE 3-33: Lu (2020) PCE estimation method at ABCL of 50%, 75%, and 100%

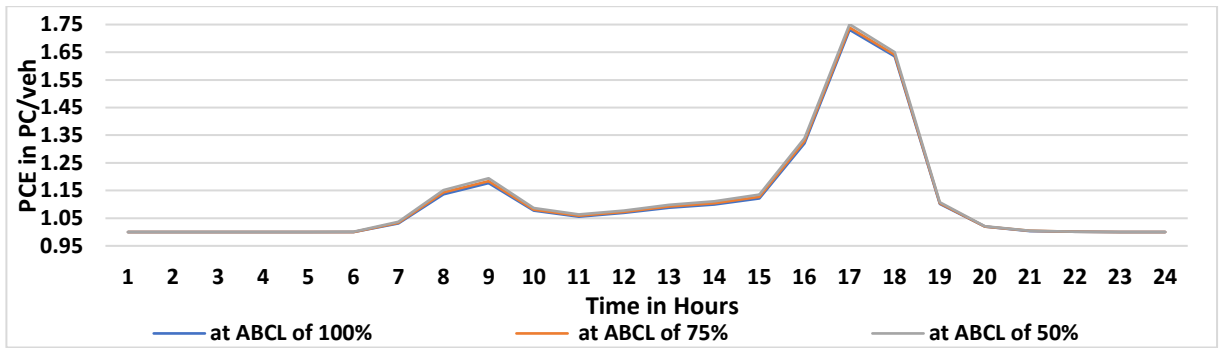


FIGURE 3-34: Keller (1984) PCE estimation method at ABCL of 50%, 75%, and 100%

The Keller (1984) and Rahman (2005) methods are based on delay, although they used different approaches. Nevertheless, they show a similar pattern, and both of them are inversely proportional to the ATS, as shown in FIGURE 3-2, FIGURE 3-34, and FIGURE 3-35 (Keller, 1984).

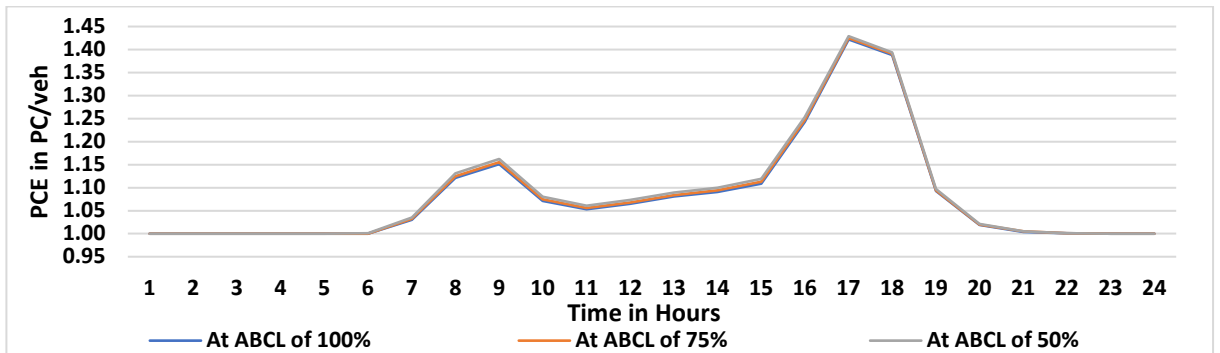


FIGURE 3-35: Rahman (2005) PCE estimation method at ABCL of 50%, 75%, and 100%

3.3.5 Rescheduling HGVa

The two rescheduling approaches are to either reschedule the HGVa vehicles to their current daily volume or reschedule them to their maximum capacity. The results of the two approaches in FIGURE 3-36 and FIGURE 3-37 in comparison to FIGURE 3-18 show that the VtCR has been reduced at the hours of 8.00-19.00 at ABCL of 50%, 75%, and 100% by an average of 30%, 20%, and 20%, respectively, equally at both approaches.

As mentioned before, rescheduling effectiveness to reduce congestion and improve the ATS depends on the available HGVa vehicles at every peak hour. Therefore, the rescheduling reduced the VtCR to lower than 1 only at

the hours 10.00-12.00 of the peak hours at the first approach while the VtCR at the remaining peak hours is still over one.

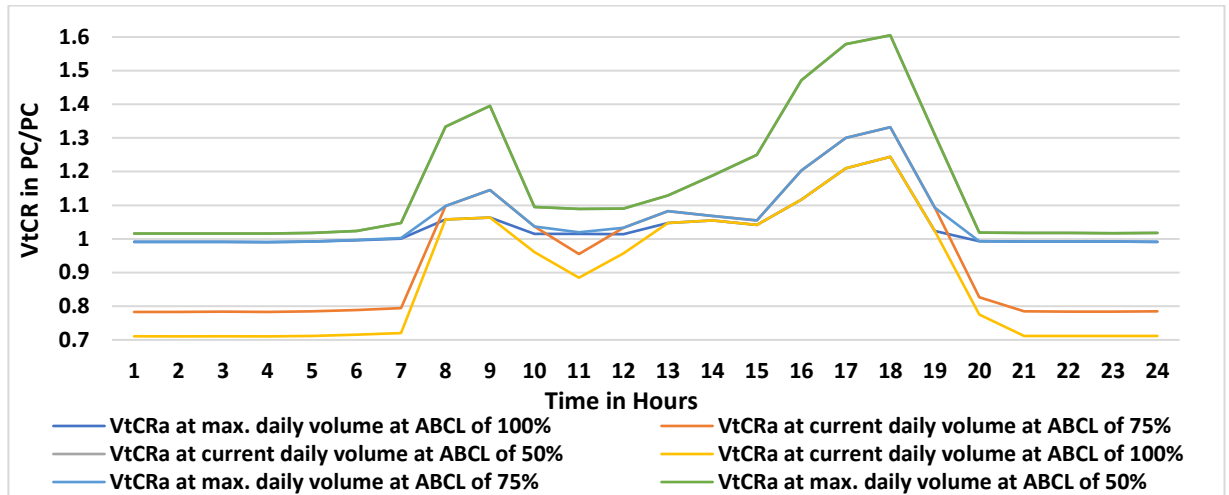


FIGURE 3-36: Impact of the two rescheduling approaches on the VtCR at ABCL of 50%, 75%, and 100%

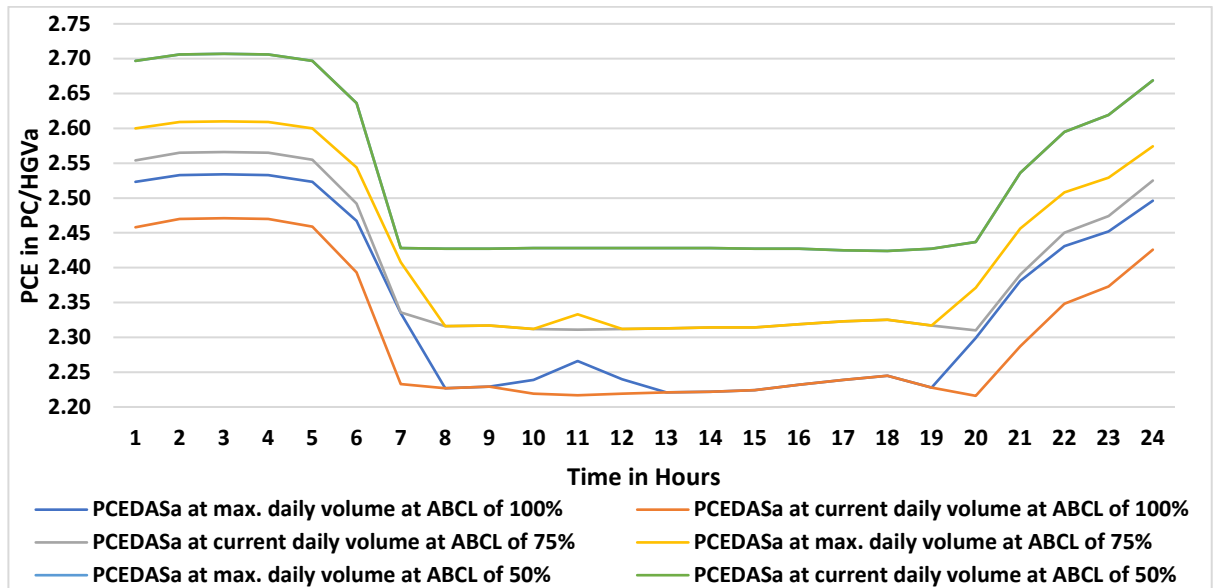


FIGURE 3-37: Impact of the two approaches of rescheduling on the HGVA PCE_{DAS} at ABCL of 50%, 75%, and 100%

3.3.5 Annual TEU

As mentioned in section 3.1, the annual TEU target for the dual carriageway road of DBR 1326kTEU by 2020 and 1989kTEU by 2030, respectively.

The results in TABLE 3-9 show that if the EP of HGVa increased to 700HP, it improved the output from 58.31% of the year 2020 target while increasing the HGVa drivers' BCL to 100% will improve the result to 65.9% by the year 2020 target. However, if both the EP and the driver's BCL of an HGVa increased to the maximum, it will meet 71.72% of the 2020 target. The author has obtained the results in TABLE 3-9 by assuming that the average RT includes manoeuvring and recognising unexpected situations that add 0.95s for every driver. Therefore, when the author excluded these RT components, the results were much higher by 29.17%, 36.86%, and 47.1%, respectively, and it will meet the target of the year 2020. However, it will put the drivers, pedestrians, and traffic flow operation at risk of injury, death, and major disruption.

TABLE 3-9: Annual TEU Capacity for 35% of HGVa that are Container Carriers originated from the container terminal variable Speed, RT, and EGR dual carriageway data of DBR

Drivers' BCL	HGVa EP in HP	Maximum capacity of TEUs of DBR BR HGVa in kTEU	Maximum capacity of all TEUs for the container terminal AR of HGVa in kTEU
All vehicles drivers have 50% BCL	500	721.7	1088.53
	600	750.6	1132.127
	700	773.2	1166.214
HGVa drivers have 100% BCL	500	873.9	1318.099
	600	916.7	1382.655
	700	951	1434.339

The results in TABLE 3-9 also show that the port management requires to increase the NL or to build a new two-lane road to meet 100% of the years 2020 and 2030 targets. The DfT may require increasing the utilisation of freight rail from 1.64% to 8.79% of the 2030 target or improve it to only 6.18% if the utilisation of inland waterway freight has met the 5% target.

3.4 SUMMARY, CONTRIBUTION AND NOVELTY

The contribution of the PCE and capacity estimation methods is as follows:

- 1- Measuring the headway based on the required safe gap and not according to the available gap and utilise the ATS of the road and not the FFS. The required gap for safety changes with change in the ATS and depends on the vehicle's type, size, weight, deceleration performance, and road conditions. For example, considering the driver's BCL and RT in the calculation of the deceleration performance.

- 2- Determining the deceleration performance of the vehicle according to the driver's ability to bring the vehicle's speed down to a standstill without crashing the leading vehicle, and that is when considering that the leading vehicle is at a standstill at the time the following vehicle starts to decelerate
- 3- Determining the vehicle's acceleration performance by considering the required time and distance for the vehicle to accelerate up to the average flow speed of the traffic.
- 4- Estimating the PCE based on the vehicle's size, deceleration performance, and acceleration performance
- 5- The author has integrated the impact of acceleration performance in the road capacity estimation because the low HGV's acceleration performance affects the road's space.
- 6- The current capacity estimation method defines saturation headway as the time headway between two vehicles departing from the same lane under continuous queuing conditions. The author has replaced the saturation headway with the minimum required headway for a PC in this research. This change is essential to ensure that the estimation method works in both congestion and non-congestion.
- 7- In the current capacity estimation method, the developers dealt with the driver's BCL and RT by proposing the f_p . In this research, the author has integrated the BCL and RT into the headway
- 8- The integration of the deceleration performance and the driver's BCL and RT will allow planning and rescheduling with consideration to safety and road service

CHAPTER FOUR: TRAFFIC SPEED FLOW PREDICTION

4.1 INTRODUCTION

The expansion of the Liverpool container terminal increases the demand for road freight, and roads that connect the terminal with the city and the nearby cities will suffer from congestion. Therefore, local authorities either try to overcome this problem by building new roads, tunnels, adding extra lanes to existing roads, UCC or utilising other modes of transport for freight transportation. However, to reach a feasible solution, the planners would require an accurate and efficient method of estimating HGVs' effect on road traffic flow.

Any change in various vehicles' traffic volumes will lead to a change in traffic-flow speed. Therefore, to determine the impact of HGVs on traffic congestion AR or change in the NL or the HGV access rates, the author must estimate the traffic flow speed after making the changes.

Since the year 1935, researchers have been researching the traffic flow speed and the relationship between the flow speed and the traffic flow density. Predicting the traffic flow speed is necessary for traffic operation monitoring and road planners, especially in supply chain operations, where managers require seamless materials and products flow. In this research, the focus will be on the effect of HGV on traffic flow.

As explained in previous chapters, the way to determine HGVs' effect is by measuring the PCE of the HGV. Therefore, the utilisation of PCE traffic volumes in predicting the traffic flow speed could provide values useful in determining increasing the HGV traffic volume on traffic congestion.

Many speed flow prediction methods use the traffic flow density to estimate the flow speed. The author has discussed these methodologies, determine which method is the most accurate, and estimate the effect of increasing HGV traffic volume on traffic congestion and delay.

4.2 FLOW SPEED ESTIMATION METHODS

4.2.1 Greenshields Method

The development of the speed-density relationship started by Greenshields (1935). Greenshields concluded that (Greenshields 1935) that the relationship between speed and density is linear (Greenshields 1935; Rogers 2016), and the relationship between maximum flow and jam density is as in (4-1) to (4-7). Therefore, Greenshields suggest that the traffic jam density is twice the maximum flow density (4-7).

$$TF = k \times ATS \quad (4-1)$$

$$ATS = FFS \times \left(1 - \frac{k}{k_j}\right) \quad (4-2)$$

$$TF = FFS \times \left(1 - \frac{k}{k_j}\right) \times k \quad (4-3)$$

$$TF = FFS \times \left(k - \frac{k^2}{k_j}\right) \quad (4-4)$$

$$\frac{dTF}{dk} = FFS \times \left(1 - \frac{2 \times k}{k_j}\right) = 0 \quad (4-5)$$

$$1 - \frac{2 \times k_m}{k_j} = 0 \quad (4-6)$$

$$k_m = \frac{k_j}{2} \quad (4-7)$$

where,

TF is the total mixed traffic flow of all vehicle types in veh/h

dTF is the change difference in traffic volume in veh/h

k is the traffic flow density in veh/km

dk is the change difference in traffic density in veh/km

ATS is the average traffic speed in km/h

FFS is the free flow speed in km/h

k_j is the traffic jam density in veh/km

k_m is the traffic maximum flow density in veh/km

However, the speed-density relationship's problem is that to predict the speed, the author must determine the traffic flow density, and the calculation of the density, as in (4-1), requires the flow speed. Therefore, the speed-density relationship is not useful because if the flow speed is unknown. Therefore, the author was not able to calculate the flow density. However, it is possible to obtain traffic jam density by calculating the maximum capacity of the traffic flow, as in (4-8) to (4-16) (Rogers 2016). By utilising (4-2), the author can determine the traffic jam density.

$$k=k_j \times \left(1 - \frac{ATS}{FFS}\right) \quad , \quad (4-8)$$

$$TF=k_j \times \left(ATS - \frac{ATS^2}{FFS}\right) \quad (4-9)$$

By differentiation of (4-9) with respect of ATS, $k_j \neq 0$, to determine the maximum flow speed as follows:

$$\frac{dTF}{dATS} = k_j \times \left(1 - \frac{2 \times ATS}{FFS}\right) = 0 \quad (4-10)$$

$$1 - \frac{2 \times ATS}{FFS} = 0 \quad (4-11)$$

$$ATSo = \frac{FFS}{2} \quad (4-12)$$

where,

TF is the total mixed traffic flow of all vehicle types in veh/h

q_m is the maximum traffic volume in veh/h

k is the traffic flow density in veh/km

ATS is the average traffic speed in km/h

ATSo is the optimum average traffic speed in km/h

FFS is the free flow speed in km/h

k_j is the traffic jam density in veh/km

k_m is the traffic maximum flow density in veh/km

Now, by combining (4-1) with (4-7) and (4-12), The author can estimate the traffic jam density, as in (4-13), (4-14), and (4-15), where q_m is the traffic maximum traffic volume in veh/h

$$q_m = ATSo \times k_m = \frac{FFS}{2} \times \frac{k_j}{2} \quad (4-13)$$

$$q_m = \frac{FFS \times k_j}{4} \quad (4-14)$$

Therefore,

$$k_j = (q_m \times 4) / FFS \quad (4-15)$$

4.2.2 Greenberg Method

Greenberg (1959) assumed that the traffic flow behaved like a continuous fluid and stated that the fluid dynamic analogy applies to traffic flow when there are continuous interactions between vehicles. Such interactions on the road affect the vehicle's speed and headway (Greenberg, 1959). Therefore, Greenberg (1959) developed a speed-density formula, as in (4-16). Greenberg stated that at optimum traffic speed, the jam density is 2.718 times the maximum flow density, and when the flow density reaches an optimum level, the speed will be equal to the flow speed at an optimum level.

$$ATS = ATSo \times \ln\left(\frac{k_j}{k}\right) \quad (4-16)$$

Greenberg also determined the relationship between the vehicle's headway and the flow speed density, as in (4-17)

$$h = h_j \times e^{\frac{ATS}{ATSo}} \quad (4-17)$$

where,

h is the vehicle headway in m

h_j is the vehicle headway at a traffic jam in m

ATS is the average traffic speed in km/h

k_j is the traffic jam density in veh/km

$ATSo$ is the optimum average traffic speed volume in km/h

According to (4-17), by assuming that the vehicle h_j is 7.173 m, the headway at $ATSo$ is 2.718 times the h_j , equal to 19.5 m.

4.2.3 Underwood Method

Underwood (1961) developed a speed-density formula with an exponential function to improve the Greenberg method (Greenberg, 1959). Underwood used an FFS of 76.8 km/h in (4-18) (Underwood 1961).

$$ATS = FFS \times e^{-\frac{k}{k_m}} \quad (4-18)$$

where,

k is the traffic flow density in veh/km

ATS is the predicted average traffic speed in km/h

FFS is the free flow speed in km/h

k_m is the traffic maximum flow density in veh/km

According to (4-18), when the flow density is zero, the flow speed will be equal to FFS, and when the flow density is at maximum flow, the optimum speed will be 28.25 km/h. For example, if the author assumed that the jam density is 2.718 times the optimum density, like in section 4.2.2 with an FFS of 76.8 km/h, then the jam speed will be equal to 5.07 km/h. On the one hand, the underwood formula has a drawback that the speed flow will not reach zero unless the traffic density reaches a significantly high level up to infinity. On the other hand, the method will be suitable for roads with controlled intersections where the traffic is on/off flow.

Assuming that the vehicle will only move forward for a distance equal to its jam headway, then the jam density will be 9.27 times the maximum flow density. Therefore, in contrast to the Greenberg formula, where the flow

speed reaches zero when the flow density reaches jam level, the underwood formula will not be useful in estimating the jam density.

4.2.4 Two Regime Method

Eddie (1961) developed a formula to obtain flow speed and proposed a two-regime formula, where the first regime was for non-congested traffic and the second regime was for congested traffic as in (4-18) and (4-16), respectively, as in (4-19) (Eddie 1961). Eddie concluded that jam densities in tunnels are higher than in freeways due to their lower FFS. Eddie also suggested that the FFS is equal to 74 km/h when the traffic flow is zero, according to (4-18), the $ATS_o = 27.23$ km/h when the flow density is at the optimum value of 56 veh/km, and the flow speed will be zero at jam density of 155 veh/km as in (4-19).

$$ATS = \begin{cases} FFS \times e^{-\frac{k}{k_m}} & \text{Non-Congested Traffic} \\ ATS_o \times \ln\left(\frac{k_j}{k}\right) & \text{Congested Traffic} \end{cases} \quad (4-19)$$

where,

- k is the traffic flow density in veh/km
- ATS is the average traffic speed in km/h
- FFS is the free flow speed in km/h
- k_m is the traffic maximum flow density in veh/km

Easa (1982) developed two regimes formula for non-congested traffic as in (4-20) and congested traffic as in (4-21) and stated that the two-regime formula provides flexibility to fit the prediction curve (Easa, 1982).

$$u_1 = \frac{1}{0.02 + 2.15 \times 10^{-8} \times k^{3.3}} \quad \text{non-congested} \quad (4-20)$$

$$u_2 = \frac{438.4}{k^{0.5}} - 31 \quad \text{Congested} \quad (4-21)$$

where,

- u_1 is the predicted speed at non-congested traffic where $k < 50$ veh/km
- u_2 is the predicted speed at congested traffic where $k \geq 50$ and < 200 veh/km

4.2.5 Pipes's Method

Pipe (1967) developed a method based on (4-2), as in (4-22), where the value of n changes according to the traffic flow density and the time of the day (Pipes 1967). Pipe (1967) proposed to have $n > 1$ to represent driving at night

in low traffic density, $n=0$ to represent driving in an open highway (at FFS), and $n<1$ to represent driving in roads with high traffic density. Pipes (1967) proved that the value of n equals one concerning the Greenshields (1935) and equals 1.718 concerning Greenberg (1959).

$$ATS=FFS \times \left(1 - \frac{k}{k_j}\right)^n \quad (4-22)$$

where,

ATS is the traffic flow speed in km/h

FFS is the free flow speed in km/h

k is the traffic flow density in veh/km

k_j is the traffic jam density

4.2.6 Drew's Method

Drew (1965) derived a formula where he utilised the variable m , as in (4-23) and (4-24) (Drew 1965).

$$ATS=FFS \times \left(1 - \left(\frac{k}{k_j}\right)^{\frac{m+1}{2}}\right) \quad (4-23)$$

$$m = \frac{3 \times ATS_o - FFS}{FFS - ATS_o} \quad (4-24)$$

where,

k is the traffic flow density in veh/km

ATS is the average traffic speed in km/h

FFS is the free flow speed in km/h

k_j is the traffic jam density in veh/km

ATS_o is the optimum average traffic speed in km/h

4.2.7 Drake's Method

Drake (1967) proposed a formula based on a speed-density relationship where he used the maximum traffic flow density (4-26). However, Drake stated that the (4-25) formula had no theoretical foundation (Drake 1967).

$$ATS=FFS \times e^{-0.5 \times \frac{k}{k_m}} \quad (4-25)$$

where,

k is the traffic flow density in veh/km

ATS is the predicted average traffic speed in km/h

FFS is the FFS in km/h

k_m is the maximum traffic flow density in veh/km

4.2.8 Kinetic wave speed Method

Del Castillo (1995) developed a formula based on Kinetic Wave Speed (C_j), as in (4-26), where the C_j , as in (4-27) (Del Castillo 1995). Del Castillo (1995) derived his formula from the Newell (1961) (Newell 1961) formula (Chen 2016).

$$ATS = FFS \times \left(1 - e^{-\left(\frac{C_j}{FFS} \left(1 - \frac{k_j}{k} \right) \right)} \right) \quad (4-26)$$

$$C_j = \frac{H_c}{t_s} \times 3.6 \quad (4-27)$$

where,

- k is the traffic flow density in veh/km
- ATS is the predicted average traffic speed in km/h
- FFS is the FFS in km/h
- k_j is the maximum traffic flow density in veh/km
- C_j is the kinetic wave speed in km/h
- H_c is the headway of a PC at 10 km/h on/off traffic condition in m
- t_s is the time required to start the vehicle in s

Fosu (2020) proposed a modified linear formula based on Del Castillo (2012) (Del Castillo 2012) and stated that it is suitable for macroscopic flow (Fosu 2020), as in (4-28).

$$ATS = FFS \times \left(1 - e^{-\left(\frac{C_j \times (1 - \sigma)}{\sigma \times FFS} \right)} \right) \quad (4-28)$$

where,

- ATS is the predicted average traffic speed in km/h
- FFS is the free flow speed in km/h
- σ is the ratio of traffic flow density to the jam traffic density
- C_j is the kinetic wave speed in km/h

4.2.9 Logistic curve method

Wang (2011) developed a logistic speed-density relationship, as (4-29), and based it on the MacNicholas (2008) five requirements to identify a suitable function for a speed–density relationship (MacNicholas, 2008; Wang, 2011).

Wang (2011) determined the values of the parameters, as in (4-30) and (4-31), where $u_b = 9$ km/h while K_t varies depending on the road.

$$ATS = u_b + \frac{FFS - u_b}{\left(1 + e^{\frac{(k - K_t)^2}{\theta_1}}\right)^{0.2}} \quad (4-29)$$

$$\theta_1 = 0.1612 \times K_t + 0.0337 \quad (4-30)$$

$$\theta_2 = 0.0093 \times K_t - 0.0507 \quad (4-31)$$

where,

ATS is the predicted average traffic speed in km/h

FFS is the free flow speed in km/h

u_b is the speed during on/off traffic flow at F-LoS in km/h

K_t is the traffic density where the speed-density curve changes from FFS in veh/h

4.2.10 Gaddam's method

Gaddam (2019) modified Lee (1998) formula, as in (4-32) (Lee, 1998), where a, b, θ , and E are shape parameters and estimated them as 4, 1, 2.14, and 10.3, respectively. Gaddam (2019) also developed another formula, as in (4-33), where a=0.6 (Gaddam, 2019).

$$ATS = FFS \times \frac{\left(1 - \left(\frac{k}{k_j}\right)^a\right)^b}{1 + E \times \left(\frac{k}{k_j}\right)^\theta} \quad (4-32)$$

$$ATS = FFS \times \left(\frac{e^{-\left(\frac{k}{k_m}\right)^{1+a}} - e^{-\left(\frac{k_j}{k_m}\right)^{1+a}}}{1 - e^{-\left(\frac{k_j}{k_m}\right)^{1+a}}} \right) \quad (4-33)$$

where,

a, b, θ , and E are shape parameters

k is the traffic flow density in veh/km

k_j is the traffic jam density in veh/km

k_m is the maximum traffic density in veh/km

ATS is the predicted average traffic speed in km/h

FFS is the free flow speed in km/h

4.3 SPEED PREDICTION PARAMETERS

The method of calculating the capacity depends on the saturated capacity, the NL, PC headway in seconds (PC Headway), F_{nv} , f_w , and f_p as in (4-34) and (4-35) (TRB 2010; Rogers 2016). The author has utilised the PC's

headway calculated value in chapter three that is equal to 4.94s and 3.46s at BCL of 50% and 100%, respectively, at a flow speed of 64.37 km/h.

$$\text{Capacity} = \left(\frac{3600}{H_1} \right) \times \text{NL} \times F_{\text{hv}} \times f_w \times f_p \quad (\text{PC/h}) \quad (4-34)$$

where f_p is equal to 1 (weekday), f_w is equal to 0.94 (obstruction on both sides of the roadway), and the calculation of F_{hv} is in (4-35) (Rogers 2016; TRB 2010). The author has utilized a different expression of F_{hv} because there is more than one vehicle type of non-PC vehicles. Therefore, the formula (4-36) represents the effect of all non-PC vehicles

$$F_{\text{hv}} = \frac{1}{1 + \sum_{i=2}^4 P_i \times (\text{PCE}_i - 1)} \quad (4-35)$$

where,

P_i is the traffic volume proportion of vehicle type i

PCE_i is the PCE of vehicle type i

The author has estimated the average of FFS according to the proportions of vehicle types in the traffic flow, as in (4-36) and (4-37). The method of calculating the FFS is by deducting the Lane Width Adjustment Factor (f_{LW}) (it is an adjustment factor similar to the f_w , but for measuring the FFS), and the Access Point Adjustment Factor (f_A) (it is the adjustment factor for roads that have one access side road or more), as in (4-36) (Rogers 2016).

$$\text{FFS}_i = \text{BFFS} - f_{\text{LW}} - f_A \quad (\text{km/h}) \quad (4-36)$$

$$\text{AFFS} = \frac{\left(\sum_{i=1}^4 \text{FFS}_i \times V_i \right)}{\text{TF}} \quad (\text{km/h}) \quad (4-37)$$

where,

FFS_i is the free flow speed of vehicle type i in km/h

AFFS is the average FFS in km/h

BFFS is the base free flow speed in km/h, and it is equal to the road's speed limit of 64.37km/h

f_{LW} is the lane width adjustment factor in km/h, and it is equal to 2.737-7.567 km/h depends on vehicle type

f_A is the access point adjustment factor in km/h, and it is equal to is 0-4.025 km/h

FV_i is the traffic volume of vehicle type i in veh/h

TF is the total mixed traffic flow of all vehicle types in veh/h

However, the Average FFS (AFFS) values will not reflect the impact of traffic composition and traffic volumes on the traffic flow speed. Therefore, to determine the required flow speed that will help maintain enough space between following and leading vehicles, the author must utilise the traffic flow in PCE value and the PCE safe

headway. Although this method will not provide the actual flow speed of traffic, it can predict the speed required to maintain a minimum of D-LoS.

4.3 FLOW SPEED ANALYSIS

The author has applied the formulas of the methods described in 4.2 on the road described in chapter 1 to determine which of the flow speed prediction methods is the most accurate compared to the speed provided by the ATC. The described model in chapter 3 has provided the tool to determine the maximum flow density and the optimum flow speed.

4.3.1 Flow Speed Parameters

The author assumed that vehicles' total flow only contains PCs with a variable BCL and utilised the BCL values of 50%, 75%, and 100% for a single lane with uninterrupted traffic flow. Therefore, the optimum density will change with the change of the Average BCL (ABCL). The results showed that the maximum flow density varies according to the ABCL from 27 to 34 PC/km, as shown in FIGURE 4-1, and the optimum speed is 36.34 km/h, as shown in FIGURE 4-2.

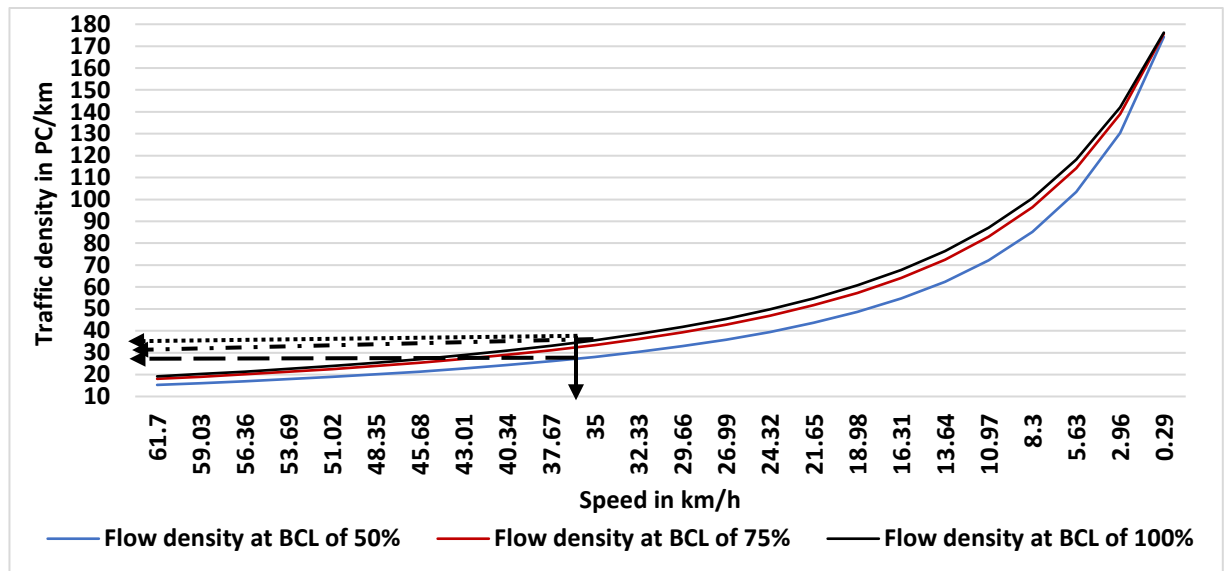


FIGURE 4-1: Speed-Density curve for a single lane and interrupted traffic flow

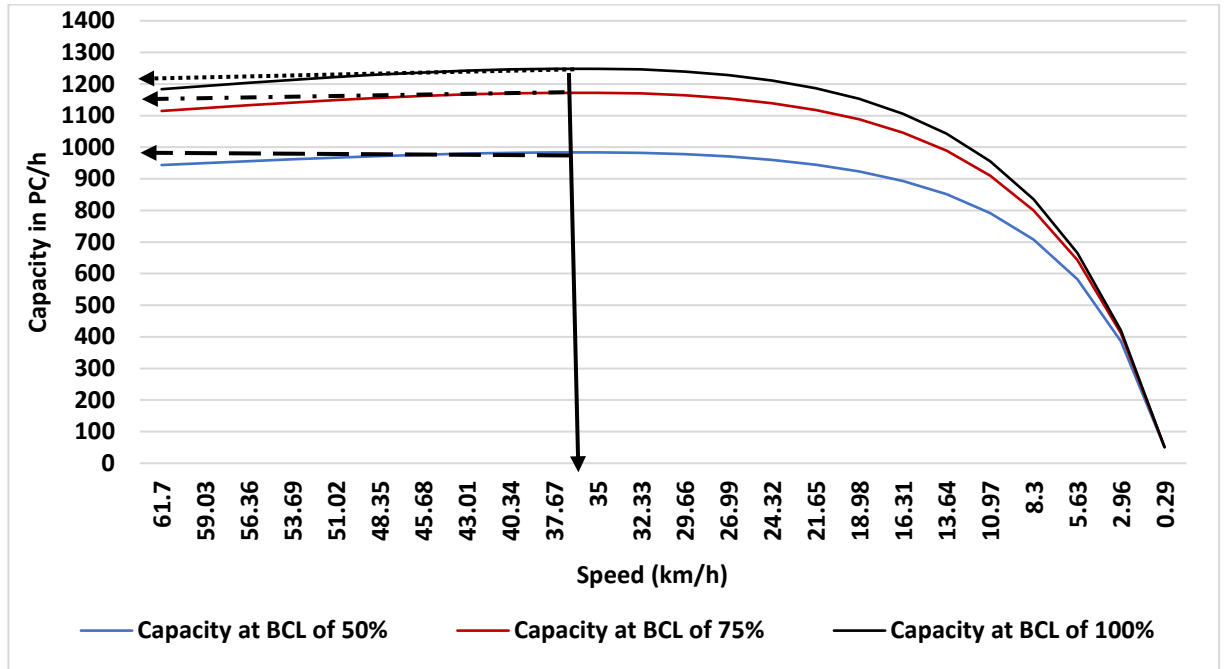


FIGURE 4-2: Speed-Capacity curve for uninterrupted traffic flow

Therefore, by estimating the k_m , k_j , FFS, and u_m , the author can test the literature review methodologies and determine the most accurate. Estimating the traffic jam rate utilises the average PC headway at optimum capacity and divided by the jam headway. The jam headway consists of maximum PC length and the gap distance between the following and leading vehicles at a standstill. The author has based the calculation on the notion that the driver of the following vehicle should see the rear tyres of the leading vehicle and objects of a minimum height of 25.4 cm (10 inches), as shown in FIGURE 4-3.

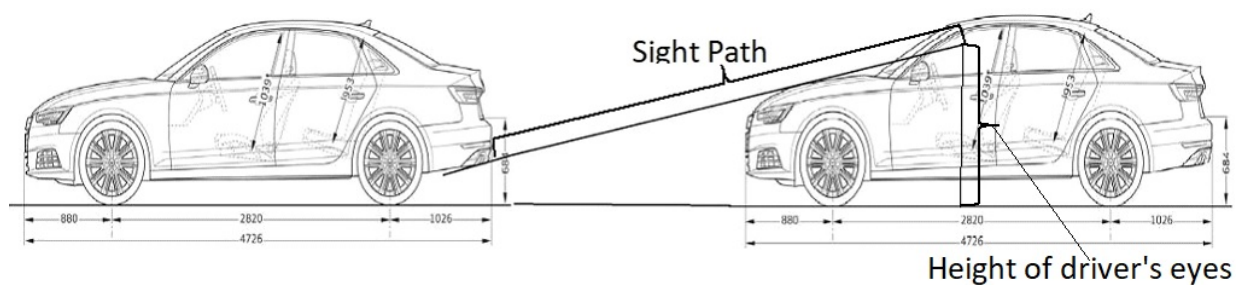


FIGURE 4-3: Traffic jam gap at standstill vehicle (Carwow Ltd 2020)

FIGURE 4-4 shows the mathematical method of estimating the jam gap between PCs. Therefore, the gap can be obtained by utilizing (4-38). The author has estimated the optimum speed, maximum density, jam density, and

headways in maximum flow, jam traffic, and by considering a PC flow only and an ABCL of 50-100% by utilising FIGURE 4-1, FIGURE 4-2, FIGURE 4-3, FIGURE 4-4, (4-38), and (4-39)

$$\text{Gap}_j = \frac{0.451}{\tan(\theta)} \quad (4-38)$$

$$k_j = \frac{R_{LL} \times 1000 \times \text{EGR}}{L_1 + \text{Gap}_j} \quad (4-39)$$

where,

Gap_j is the gap between every two PC waiting in a queue during a traffic jam in m

θ is the angle between the driver's eye and the front edge of the PC in Degree

K_j is the jam traffic density in PC/km

R_{LL} is the road link length in km

L_1 is the maximum length of a PC in m

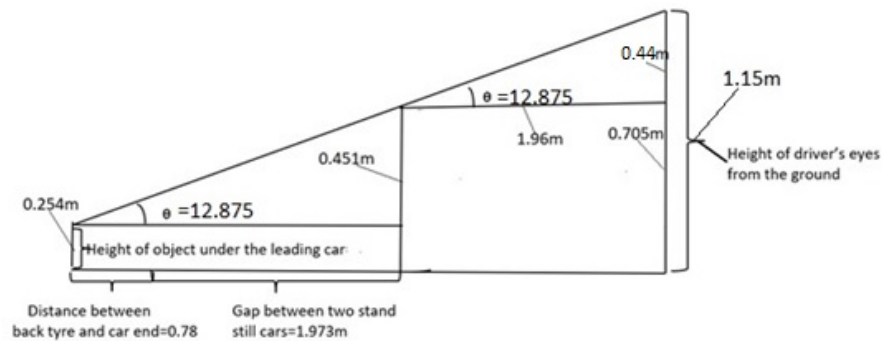


FIGURE 4-4: Jam gap calculation method (the author has created this figure)

4.3.2 Flow Speed Methods' Analysis

The author has applied the described methods in section 4.2 by utilising the parameters in TABLE 4-1 and TABLE 4-2, where the author has determined the Optimum ATS (ATSo) and the k_m and k_j . The testing method is by utilising the traffic flow before and after conversion to PCE value and considered three levels of drivers' ABCL (50%, 75%, and 100%). The analysis's objective is to identify the method that provides the closest match to the ATC data of speed and utilise its formula to predict the change in flow speed due to the change of the HGV traffic flow volumes due to rescheduling or road planning.

TABLE 4-1: Flow speed prediction parameters for microscopic modelling

ABCL	Maximum traffic flow density in PC/km/NL	Maximum traffic flow volume in PC/h	Headway at maximum traffic flow volume in metre	ATSo in km/h
50%	27	984	34.73	36.34
75%	32	1172	29.14	
100%	34	1248	27.36	

TABLE 4-2: Flow speed prediction parameters for macroscopic modelling

ABCL	kj in PC/km/NL	kj/km ratio	Hj at 0 km/h in metre	k at 10 km/h and EGR=0.6 in PC/R _{LL}	Kj/ ratio at 10 km/h and EGR=0.6	H at 10 km/h in metre
50%	139	5.15	L ₁ +1.973=	91.78	3.39	12.29
75%		4.34	7.173	104.93	3.28	10.75
100%		4.09		109.94	3.23	10.26

The author has presented the results starting with non-PCE converted traffic flow followed by PCE converted traffic flow. The focus is the predictor's performance at peak hours. The two peak periods that the author has determined are the morning peak hours between 6.00-10.00 and the evening peak hours between 15.00-19.00 on normal working days of the week. The author has based his choice of the best prediction method on the RMSE, as in (4-40), the Root Mean Square Percent Error (RMSPE), as in (4-41), the Mean Error (ME), as in (4-42), the Mean Percent Error (MPE), as in (4-43), the Sum of Square Error (SSE), as in (4-44). Theil's inequality coefficient, as in (4-45), (4-46), (4-47), (4-48), and (4-49), and Chi-Square Goodness of Fit (Chi-Sq-GF) method, as in (4-50) (Toledo 2004; Wasserman 2005; Wetherill 1981; Dalglish 2008; Cady 2017).

$$RMSE = \sqrt{\frac{1}{N} \sum_{h=1}^{h=24} (ATS_{Ph} - ATS_h)^2} \quad (4-40)$$

$$RMSPE = \sqrt{\frac{1}{N} \sum_{h=1}^{h=24} \left(\frac{ATS_{Ph} - ATS_h}{ATS_h} \right)^2} \quad (4-41)$$

$$ME = \frac{1}{N} \sum_{h=1}^{h=24} (ATS_{Ph} - ATS_h) \quad (4-42)$$

$$MPE = \frac{1}{N} \sum_{h=1}^{h=24} \left(\frac{ATS_{Ph} - ATS_h}{ATS_h} \right) \quad (4-43)$$

$$SSE = \sum_{h=1}^{h=24} (ATS_{Ph} - ATS_h)^2 \quad (4-44)$$

where,

N is the total number of intervals

ATS_{Ph} is the value of the estimated ATS per hour

ATS_h is the value of the collected ATS from the ATC per hour

h is the time in hours

$$U_1 = \frac{RMSE}{\sqrt{\left(\frac{1}{N} \sum_{h=1}^{h=24} V_{Ph}^2 \right) + \left(\frac{1}{N} \sum_{h=1}^{h=24} V_h^2 \right)}} \quad (4-45)$$

$$U_M = \frac{(AV_{Ph} - AV_h)^2}{RMSE^2} \quad (4-46)$$

$$U_S = \frac{(STD_p - STD)^2}{RMSE^2} \quad (4-47)$$

$$U_C = \frac{2 \times (1 - \rho) \times STD_p \times STD}{RMSE^2} \quad (4-48)$$

$$U_2 = \sqrt{\frac{\frac{1}{N} \sum_{h=1}^{h=24} (ATS_{Ph} - ATS_h) / ATS_{h-1}}{\frac{1}{N} \sum_{h=1}^{h=24} (ATS_h - ATS_{h-1}) / ATS_{h-1}}} \quad (4-49)$$

where,

- U_1 is Theil's inequality coefficient
- U_M is Theil's inequality coefficient for bias
- U_S is Theil's inequality coefficient for variance
- U_C is Theil's inequality coefficient for convergence
- U_2 is Theil's suitability test
- STD_p is the standard deviation of the estimated values
- STD is the standard deviation of the collected values
- AV_p is the average value of samples of the variable estimated method
- AV is the average value of samples of the variable collected
- ρ is the correlation coefficient between the collected ATS and the predicted ATS

The purpose of (4-50) is to determine whether Theil's method is effective in validating the goodness of fit of the model or not. If the result of (4-50) is less than 1, then Theil's method is suitable, and if the result is higher than 1, then it is not suitable. It is because the Chi-Sq-GF depends on the X^2 value in (4-51), and the higher the value is, the lower the p-value, and if the p-value is less than α ($\alpha = 0.05$), then the null hypothesis will be rejected, and when it is higher than α the null hypothesis will be accepted (good fit) and the higher the p-value (up to 1) the better the fit.

$$X^2 = \sum_{h=1}^{h=24} \frac{(ATS_{Ph} - ATS_h)^2}{ATS_h} \quad (4-50)$$

where,

- ATS_{Ph} is the value of the estimated values per hour
- ATS is the value of the collected values per hour
- h is the time in hours

The third point is due to the sharp decrease in speed at the evening peak, and the difference between the lowest speed during the morning peak and the evening peak is 20 km/h. Therefore, predicting the accurate speed for the evening peak is necessary to assess HGVs' rescheduling, traffic operation, and road planning. The results for all the thirteen speed prediction methods for non-PCE converted traffic flow and PCE converted traffic flow at ABCL of 50%-100% are in FIGURE 4-5 to FIGURE 4-17.

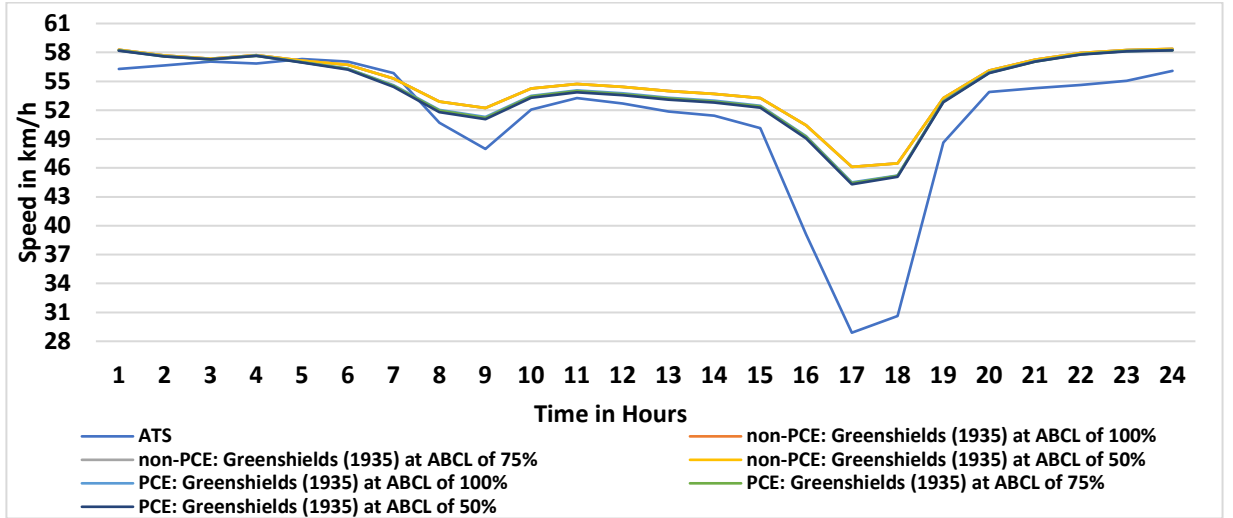


FIGURE 4-5: Results of the Greenshields (1935) speed prediction method for non-PCE and PCE converted flow

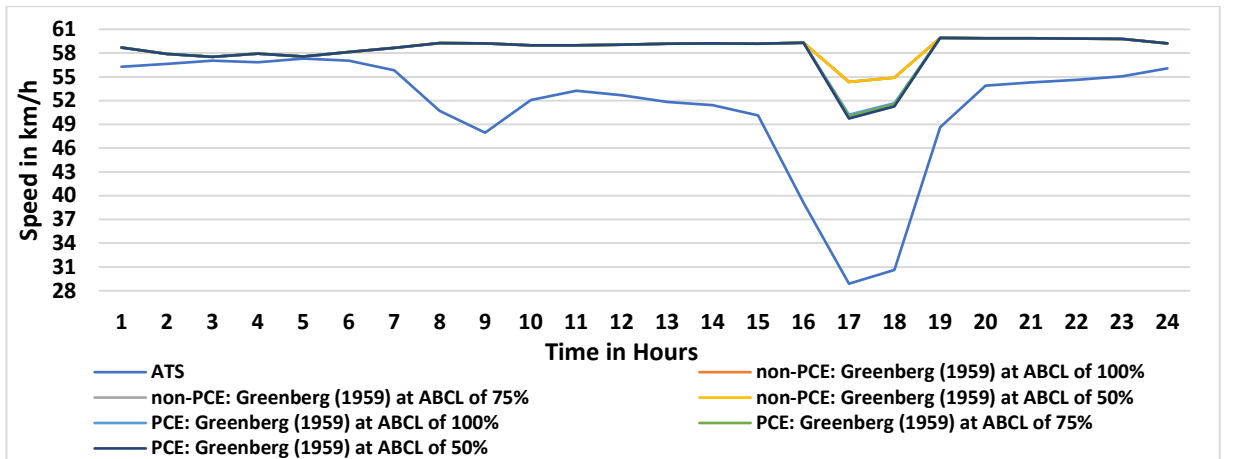


FIGURE 4-6: Results of the Greenberg (1959) speed prediction method for non-PCE and PCE converted flow

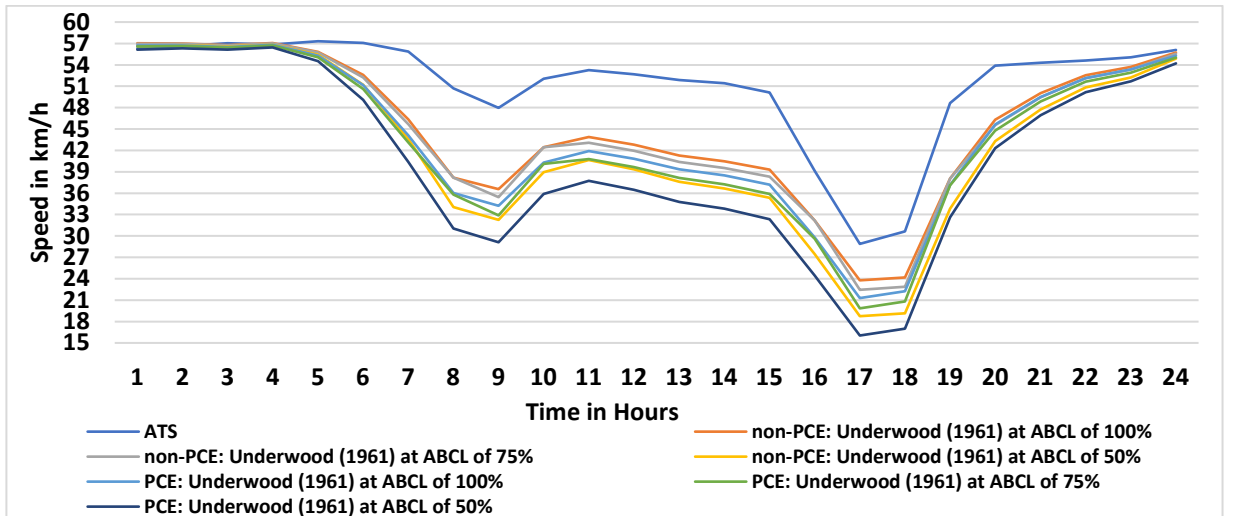


FIGURE 4-7: Results of the Underwood (1961) speed prediction method for non-PCE and PCE converted flow

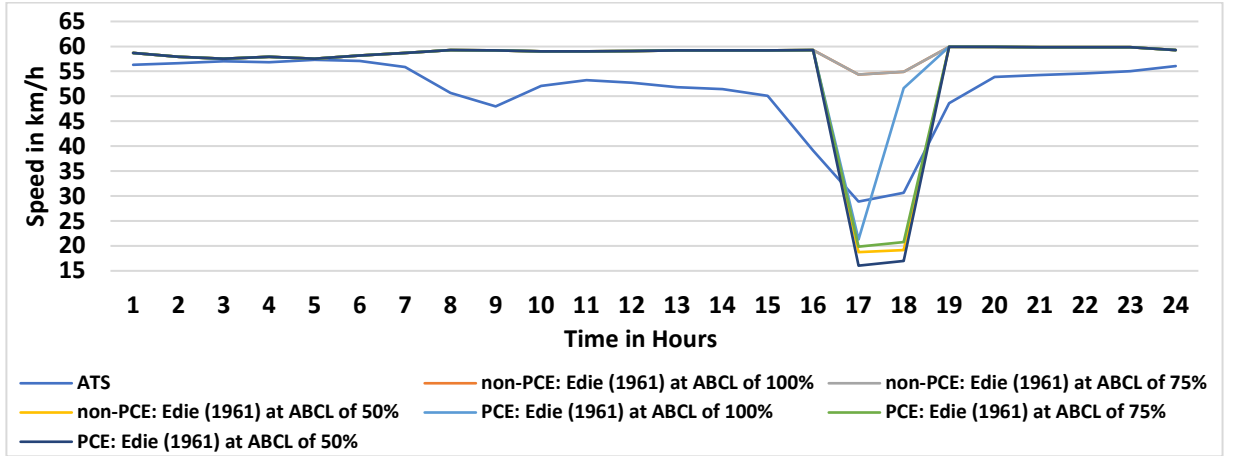


FIGURE 4-8: Results of the Edie (1961) speed prediction method for non-PCE and PCE converted flow

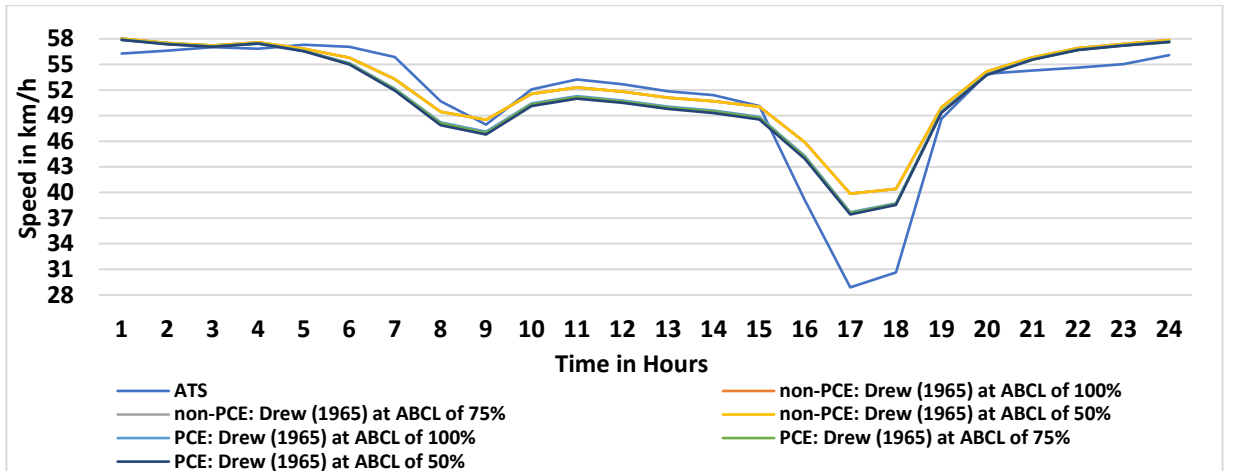


FIGURE 4-9: Results of the Drew (1965) speed prediction method for non-PCE and PCE converted flow

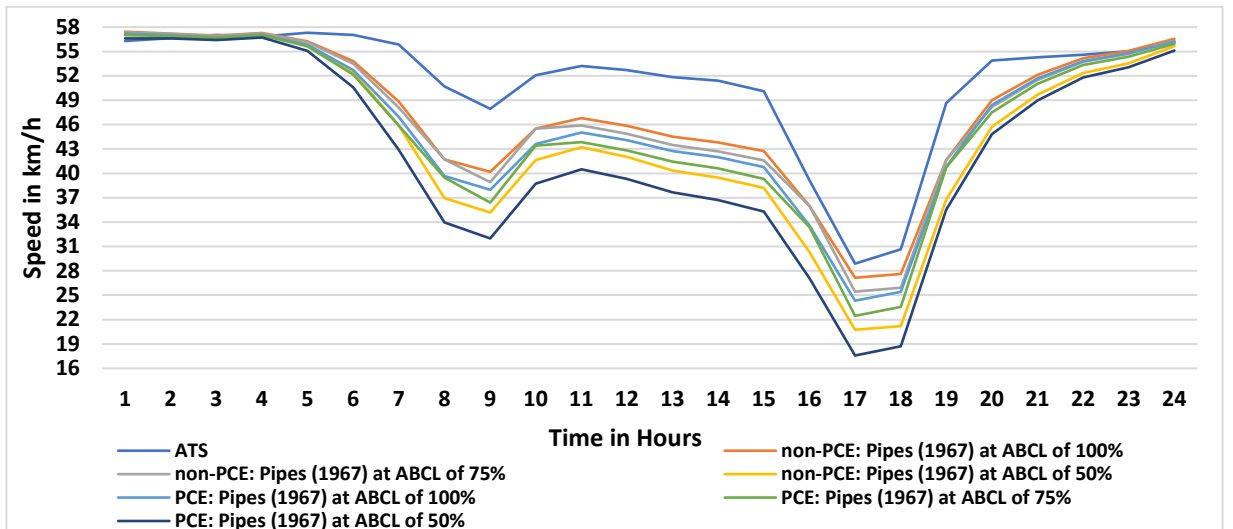


FIGURE 4-10: Results of the Pipes (1967) speed prediction method for non-PCE and PCE converted flow

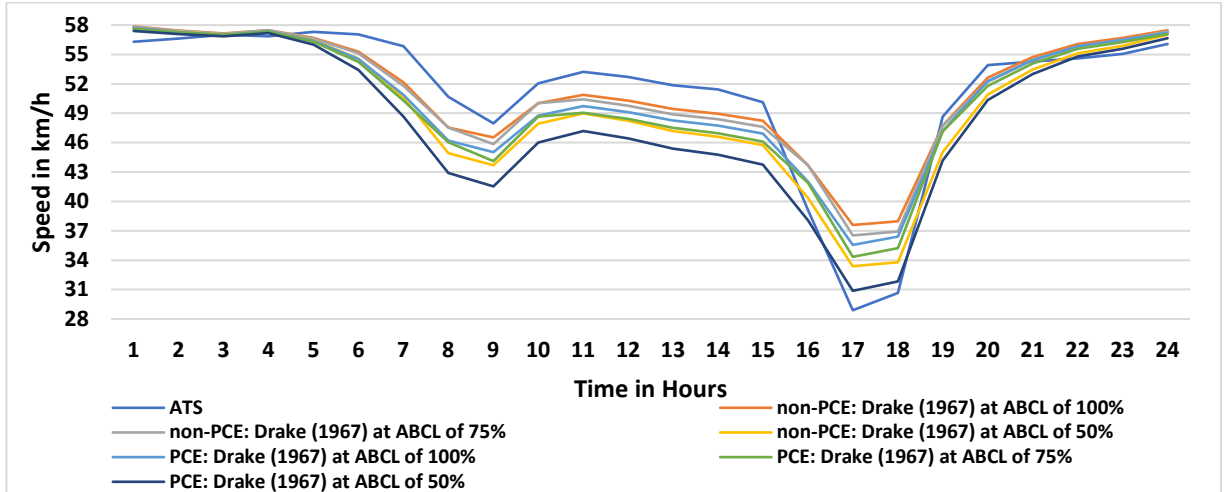


FIGURE 4-11: Results of the Drake (1967) speed prediction method for non-PCE and PCE converted flow

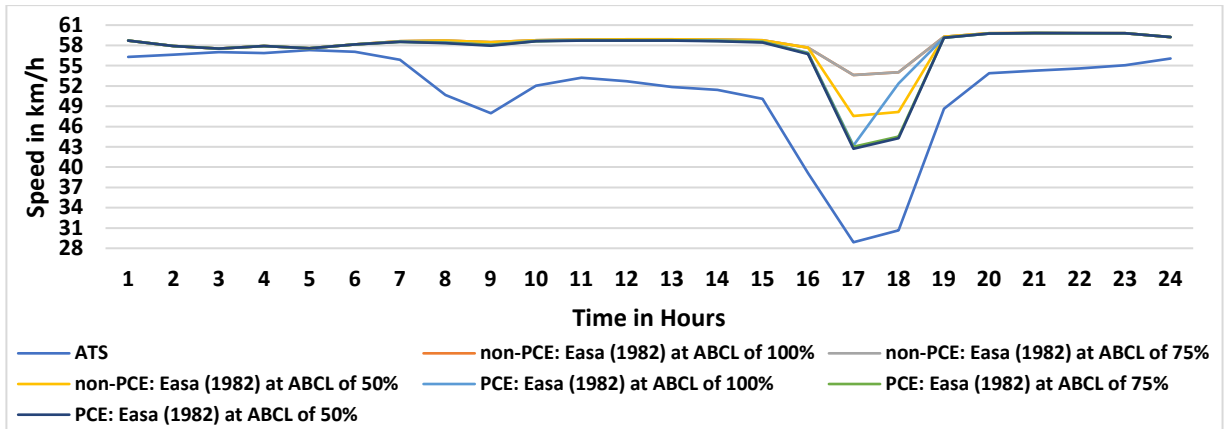


FIGURE 4-12: Results of the Easa (1982) speed prediction method for non-PCE and PCE converted flow

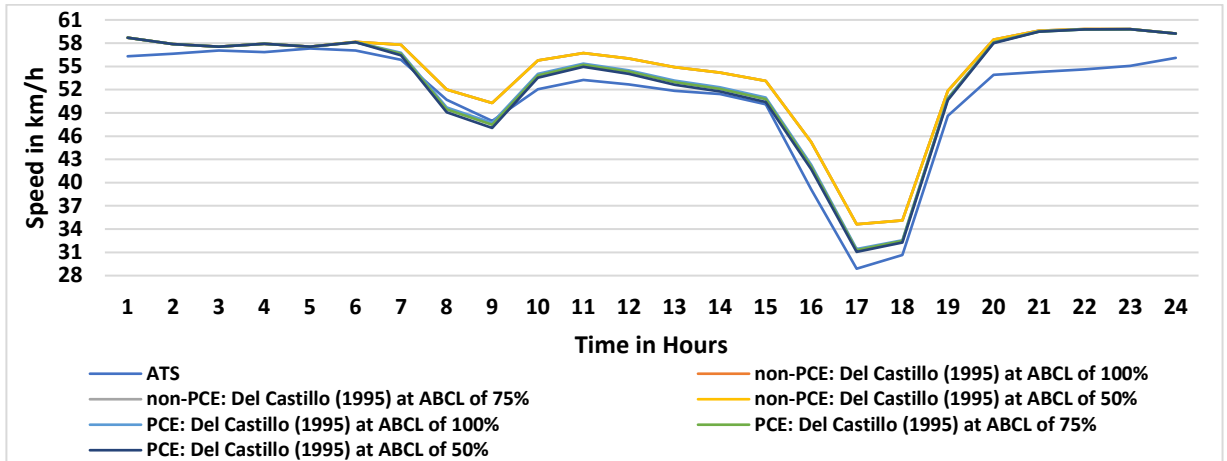


FIGURE 4-13: Results of the Del Castillo (1995) speed prediction method for non-PCE and PCE converted flow

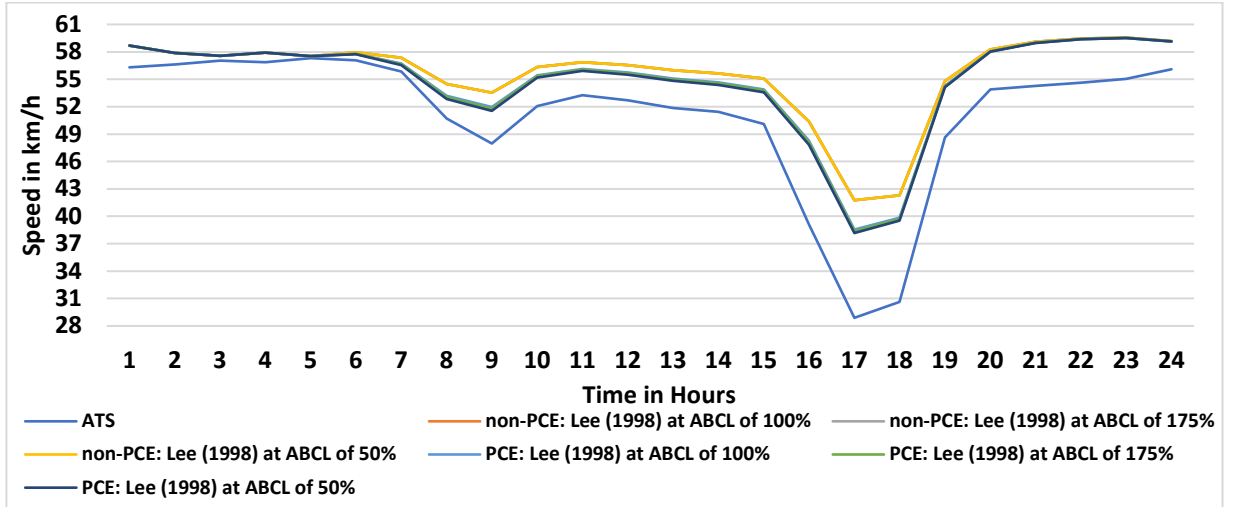


FIGURE 4-14: Results of the Lee (1998) speed prediction method for non-PCE and PCE converted flow

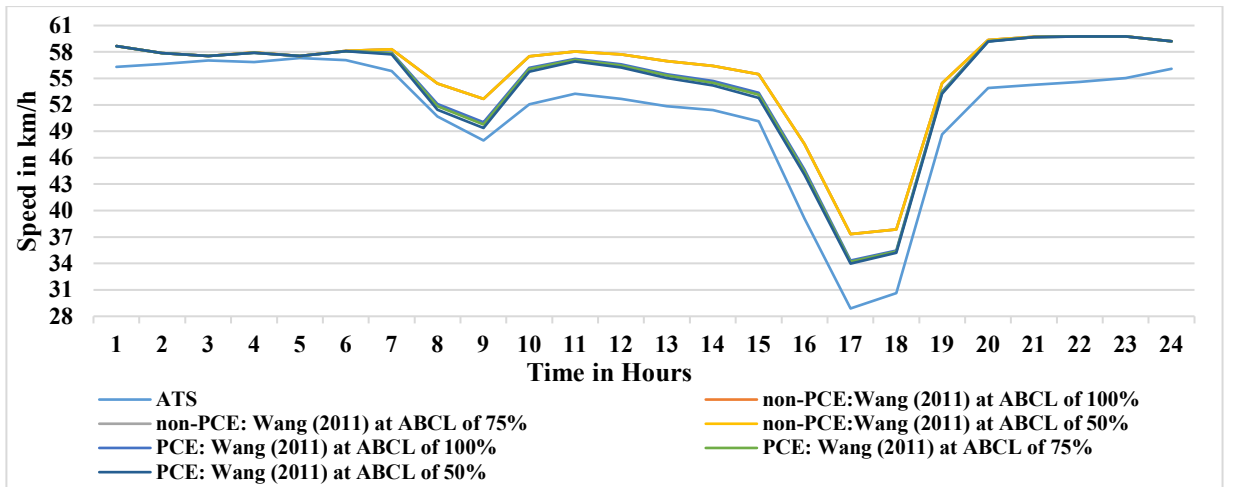


FIGURE 4-15: Results of the Wang (2011) speed prediction method for non-PCE and PCE converted flow

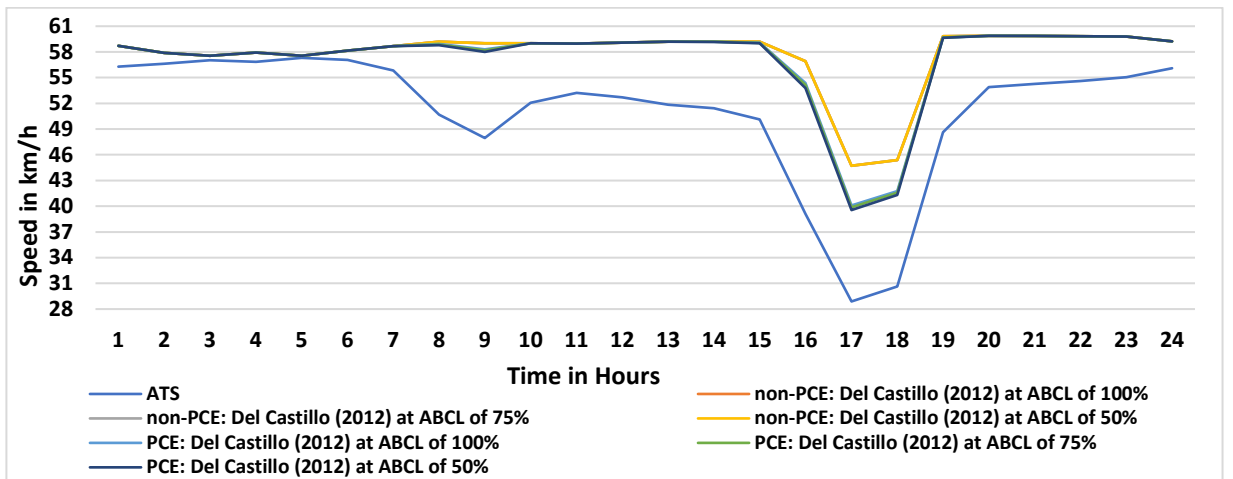


FIGURE 4-16: Results of the Del Castillo (2012) speed prediction method for non-PCE and PCE converted flow

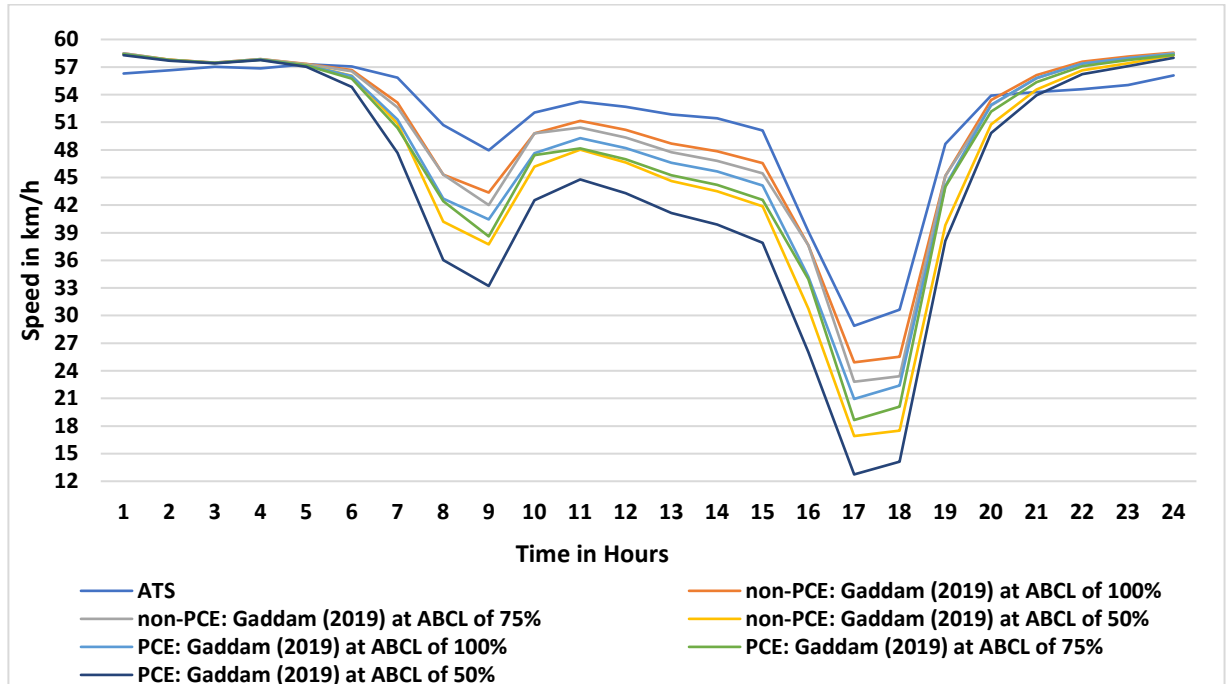


FIGURE 4-17: Results of the Gaddam (2018) speed prediction method for non-PCE and PCE converted flow

According to the ATC sensor's lowest and highest error, the highest expected average error of 9.4% for inductive loop sensors and 5.72% for piezoelectric sensors. The method of calculating the error is as in (4-51). In the first stage, if the prediction method's result provided an RMSE higher than 4.81 (9.4%), it will be excluded from further analysis. In the second stage, if the prediction method result showed an RMSE higher than 2.927 (5.72%), then it will be excluded from further analysis, as shown in TABLE 4-3.

$$\text{Error} = 100\% \times \left(\frac{\text{ATS}_p - \text{ATS}}{\text{ATS}} \right) \quad (4-51)$$

where Error is the percentage of error in speed prediction, ATS is the collected average traffic speed from the ATC, and ATS_p is the predicted average traffic speed

TABLE 4-3: The average maximum error of the ATCs utilised to obtain the ATS data

Status	Average ATC Error	Morning Peak speed in km/h	Evening Peak speed in km/h
Desirable error $\leq 5.72\% $	Piezoelectric (+5.72%)	50.70	27.28
	Piezoelectric (-5.72%)	45.22	28.89
Acceptable error $\leq 9.4\% $	Inductive Loop (+9.4%)	52.47	31.60
	Inductive Loop (-9.4%)	43.45	26.17

According to the results of the goodness of fit test in TABLE 4-4 for non-PCE traffic flow density, the Greenshields (1935), Greenberg (1959), Underwood (1961), Edie (1961), and Easa (1982) have exceeded the maximum

acceptable error set in TABLE 4-3 by far at all ABCL levels. Greenberg (1959), Easa (1982), and Edie failed the Chi-Sq-GF test apart from at an ABCL of 50% where Edie (1961) provided a better fit, and the Pipes (1967), Underwood (1961), and Gaddam (2019) had their worst performance at an ABCL of 50%.

TABLE 4-4: Results of the goodness of fit for all thirteen methods using non-PCE traffic flow density for 24 hours period

Estimation Method	ABCL	RMSE	RMSPE	ME	MPE	SSE	U ₁	U _M	U _s	U _c	U ₂	Chi-Sq-GF
Greenshields (1935)	100%	5.76	0.18	3.56	0.09	796	0.05	0.38	0.54	0.08	0.21	0.40
	75%	5.76	0.18	3.56	0.09	796	0.05	0.38	0.54	0.08	0.21	0.40
	50%	5.76	0.18	3.56	0.09	796	0.05	0.38	0.54	0.08	0.21	0.40
Greenberg (1959)	100%	10.08	0.29	7.44	0.18	2437	0.09	0.54	0.38	0.01	0.31	0.00
	75%	10.08	0.29	7.44	0.18	2437	0.09	0.54	0.38	0.01	0.31	0.00
	50%	10.08	0.29	7.44	0.18	2437	0.09	0.54	0.38	0.01	0.31	0.00
Underwood (1961)	100%	7.46	0.15	-6.01	-0.12	1336	0.08	0.65	0.09	0.07	0.19	0.25
	75%	7.99	0.17	-6.51	-0.14	1531	0.08	0.66	0.10	0.06	0.20	0.11
	50%	10.46	0.22	-8.68	-0.18	2626	0.11	0.69	0.13	0.04	0.25	0.00
Edie (1961)	100%	10.08	0.29	7.44	0.18	2437	0.09	0.54	0.38	0.01	0.31	0.00
	75%	10.08	0.29	7.44	0.18	2437	0.09	0.54	0.38	0.01	0.31	0.00
	50%	7.73	0.19	4.46	0.08	1434	0.07	0.33	0.21	0.16	0.26	0.07
Drew (1965)	100%	3.52	0.11	1.33	0.04	298	0.03	0.14	0.51	0.35	0.16	1.00
	75%	3.52	0.11	1.33	0.04	298	0.03	0.14	0.51	0.35	0.16	1.00
	50%	3.52	0.11	1.33	0.04	298	0.03	0.14	0.51	0.35	0.16	1.00
Pipes (1967)	100%	5.01	0.10	-3.76	-0.08	602	0.05	0.56	0.05	0.27	0.15	0.97
	75%	5.59	0.11	-4.32	-0.09	749	0.06	0.60	0.07	0.22	0.17	0.89
	50%	8.38	0.18	-6.81	-0.14	1685	0.09	0.66	0.13	0.12	0.21	0.05
Drake (1967)	100%	3.05	0.09	0.10	0.01	223	0.03	0.00	0.35	0.65	0.15	1.00
	75%	2.96	0.08	-0.22	0.01	211	0.03	0.01	0.29	0.71	0.14	1.00
	50%	3.32	0.07	-1.62	-0.03	264	0.03	0.24	0.03	0.73	0.14	1.00
Easa (1982)	100%	9.64	0.28	7.14	0.17	2228	0.09	0.55	0.39	0.02	0.30	0.00
	75%	9.64	0.28	7.14	0.17	2228	0.09	0.55	0.39	0.02	0.30	0.00
	50%	8.48	0.23	6.64	0.15	1725	0.08	0.61	0.28	0.05	0.27	0.00
Del Castillo (1995)	100%	3.49	0.08	3.08	0.07	293	0.03	0.78	0.05	0.17	0.17	1.00
	75%	3.49	0.08	3.08	0.07	293	0.03	0.78	0.05	0.17	0.17	1.00
	50%	3.49	0.08	3.08	0.07	293	0.03	0.78	0.05	0.17	0.17	1.00
Lee (1998)	100%	5.50	0.15	4.41	0.10	726	0.05	0.64	0.29	0.06	0.21	0.69
	75%	5.50	0.15	4.41	0.10	726	0.05	0.64	0.29	0.06	0.21	0.69
	50%	5.50	0.15	4.41	0.10	726	0.05	0.64	0.29	0.06	0.21	0.69
Wang (2011)	100%	4.81	0.12	4.25	0.09	556	0.04	0.78	0.11	0.11	0.20	0.95
	75%	4.81	0.12	4.25	0.09	556	0.04	0.78	0.11	0.11	0.20	0.95
	50%	4.81	0.12	4.25	0.09	556	0.04	0.78	0.11	0.11	0.20	0.95
Del Castillo (2012)	100%	6.07	0.13	5.25	0.11	885	0.06	0.75	0.03	0.05	0.22	0.70
	75%	5.86	0.12	5.03	0.10	825	0.05	0.73	0.01	0.06	0.22	0.79
	50%	4.53	0.09	3.72	0.07	494	0.04	0.67	0.06	0.13	0.20	0.99
Gaddam (2019)	100%	2.89	0.07	-1.22	-0.03	201	0.03	0.18	0.38	0.44	0.15	1.00
	75%	3.51	0.09	-1.74	-0.04	296	0.03	0.25	0.42	0.34	0.17	1.00
	50%	6.51	0.16	-4.22	-0.10	1018	0.07	0.42	0.42	0.16	0.21	0.36

TABLE 4-5: Results of the goodness of fit for all thirteen methods using PCE converted traffic flow density for 24 hours period

Estimation Method	ABCL	RMSE	RMSPE	ME	MPE	SSE	U ₁	U _M	U _S	U _C	U ₂	Chi-Sq-GF
Greenshields (1935)	100%	5.14	0.16	2.98	0.08	633	0.05	0.34	0.54	0.12	0.20	0.69
	75%	5.10	0.16	2.92	0.08	623	0.05	0.33	0.54	0.13	0.20	0.70
	50%	5.05	0.16	2.84	0.07	611	0.05	0.32	0.54	0.14	0.20	0.72
Greenberg (1959)	100%	9.26	0.25	7.09	0.17	2058	0.08	0.59	0.30	0.02	0.29	0.00
	75%	9.23	0.25	7.08	0.17	2043	0.08	0.59	0.30	0.02	0.29	0.00
	50%	9.19	0.25	7.06	0.17	2026	0.08	0.59	0.30	0.03	0.28	0.00
Underwood (1961)	100%	9.12	0.19	-7.49	-0.16	1996	0.09	0.67	0.11	0.04	0.22	0.01
	75%	9.88	0.21	-8.19	-0.17	2343	0.10	0.69	0.12	0.04	0.24	0.00
	50%	12.80	0.28	-10.75	-0.23	3933	0.14	0.70	0.14	0.03	0.29	0.00
Edie (1961)	100%	8.38	0.21	5.89	0.13	1687	0.08	0.49	0.00	0.11	0.30	0.01
	75%	7.60	0.18	4.56	0.08	1388	0.07	0.36	0.18	0.19	0.26	0.09
	50%	8.07	0.20	4.24	0.07	1563	0.07	0.28	0.28	0.20	0.28	0.02
Drew (1965)	100%	3.06	0.09	0.47	0.02	224	0.03	0.02	0.38	0.60	0.16	1.00
	75%	3.06	0.09	0.38	0.02	225	0.03	0.02	0.36	0.62	0.16	1.00
	50%	3.08	0.09	0.26	0.02	228	0.03	0.01	0.34	0.65	0.16	1.00
Pipes (1967)	100%	6.51	0.13	-5.13	-0.11	1018	0.07	0.62	0.09	0.19	0.18	0.60
	75%	7.35	0.15	-5.90	-0.12	1297	0.07	0.64	0.11	0.17	0.20	0.26
	50%	10.69	0.23	-8.82	-0.19	2743	0.11	0.68	0.15	0.10	0.26	0.00
Drake (1967)	100%	3.13	0.08	-0.83	-0.01	235	0.03	0.07	0.15	0.78	0.15	1.00
	75%	3.28	0.07	-1.28	-0.02	258	0.03	0.15	0.08	0.77	0.15	1.00
	50%	4.48	0.09	-2.99	-0.06	481	0.04	0.45	0.00	0.55	0.15	0.99
Easa (1982)	100%	8.31	0.22	6.49	0.15	1658	0.08	0.61	0.24	0.06	0.28	0.01
	75%	7.54	0.19	6.13	0.14	1365	0.07	0.66	0.19	0.09	0.25	0.07
	50%	7.48	0.19	6.09	0.14	1344	0.07	0.66	0.18	0.11	0.25	0.08
Del Castillo (1995)	100%	2.48	0.05	1.86	0.04	148	0.02	0.56	0.01	0.44	0.17	1.00
	75%	2.43	0.05	1.73	0.03	142	0.02	0.51	0.01	0.48	0.16	1.00
	50%	2.38	0.05	1.56	0.03	136	0.02	0.43	0.02	0.55	0.16	1.00
Lee (1998)	100%	4.36	0.11	3.58	0.08	456	0.04	0.67	0.23	0.10	0.19	0.98
	75%	4.27	0.11	3.49	0.08	438	0.04	0.67	0.22	0.11	0.19	0.98
	50%	4.16	0.11	3.38	0.08	416	0.04	0.66	0.22	0.12	0.19	0.99
Wang (2011)	100%	3.57	0.08	3.16	0.07	305	0.03	0.78	0.03	0.18	0.18	1.00
	75%	3.46	0.08	3.04	0.06	287	0.03	0.77	0.03	0.20	0.18	1.00
	50%	3.32	0.07	2.88	0.06	265	0.03	0.75	0.02	0.22	0.18	1.00
Del Castillo (2012)	100%	4.99	0.10	4.28	0.09	598	0.05	0.74	0.00	0.11	0.21	0.97
	75%	4.71	0.09	3.89	0.07	533	0.04	0.68	0.04	0.14	0.21	0.99
	50%	3.73	0.09	1.90	0.03	333	0.04	0.26	0.49	0.29	0.20	1.00
Gaddam (2019)	100%	4.77	0.12	-2.80	-0.07	546	0.05	0.34	0.40	0.25	0.18	0.95
	75%	5.70	0.14	-3.56	-0.08	780	0.06	0.39	0.40	0.21	0.20	0.72
	50%	9.45	0.23	-6.62	-0.15	2141	0.10	0.49	0.37	0.14	0.26	0.00

According to the PCE converted results in TABLE 4-5, all the methods showed improvements when utilising the PCE converted traffic density, as in TABLE 4-5, apart from the Gaddam (2019), Pipes (1967), and Underwood (1961) that showed an increase in error. Greenberg (1959) failed the Chi-Sq-GF in the non-PCE and PCE tests. Therefore, the author has excluded the Greenberg (1959) method from further analysis.

The author has excluded the methods that fail the RMSE and RMSPE test for acceptable fit and fail the ME and MPE test for desirable fit for PCE converted traffic flow density. The remaining methods are Drew (1965), Drake (1967), Del Castillo (1995), Wang (2011), and Del Castillo (2012), and they all passed the Chi-Sq-GF test, as in TABLE 4-5. Predicting the ATS by utilising the PCE converted traffic flow density is necessary to show the impact of HGVs during rescheduling or increase of HGV flow volumes. Therefore, the focus must be on predicting the ATS based on PCE traffic density.

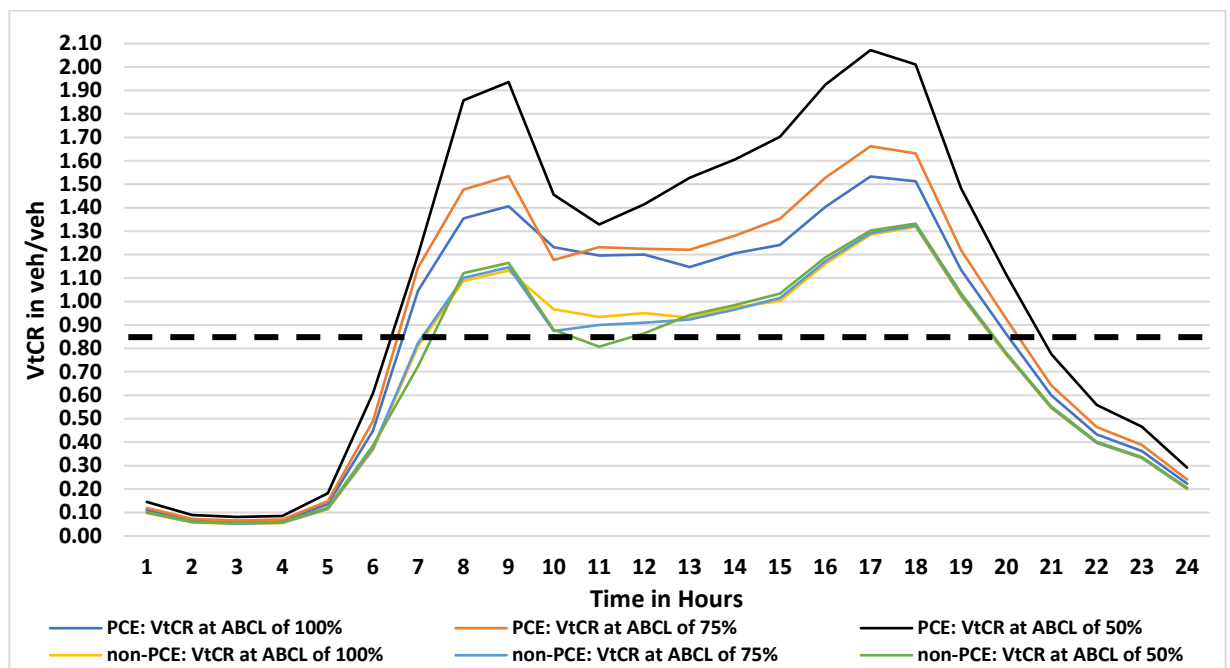


FIGURE 4-18: VtCR values of non-PCE and PCE converted traffic flow volume

The author has tested the latter five methods for only 12 hours of 8.00-19.00 to assess the accuracy of these methods during peak times where the VtCR has exceeded 0.85, as shown in FIGURE 4-18, and found that Del Castillo (1995) method has provided the best fit so far where it achieved a desirable fit at RMSE, RMSPE, ME, MPE, highest Chi-Sq-GF, lowest U_1 , and highest U_c , as in TABLE 4-6. In addition, the Del Castillo (1995) method provided the desirable fit for 12 hour period and 24 hour period, as in TABLE 4-5.

TABLE 4-6: Results of only five-speed estimation methods test using PCE traffic flow density at peak hours of 8.00-19.00

Estimation Method	ABCL	RMSE	RMSPE	ME	MPE	SSE	U ₁	U _M	U _s	U _c	U ₂	Chi-Sq-GF
Drew (1965)	100%	3.97	0.12	0.63	0.03	377	0.04	0.03	0.92	0.05	0.22	0.89
	75%	3.96	0.12	0.49	0.03	377	0.04	0.02	0.93	0.05	0.22	0.89
	50%	3.98	0.12	0.31	0.03	380	0.04	0.01	0.94	0.06	0.22	0.90
Drake (1967)	100%	3.99	0.10	-1.35	-0.01	382	0.04	0.11	0.83	0.05	0.20	0.94
	75%	4.14	0.10	-2.01	-0.03	412	0.05	0.23	0.69	0.07	0.20	0.94
	50%	5.73	0.11	-4.77	-0.09	787	0.06	0.69	0.27	0.03	0.20	0.73
Del Castillo (1995)	100%	1.67	0.04	1.23	0.03	33	0.02	0.54	0.04	0.42	0.22	1.00
	75%	1.53	0.04	0.99	0.02	28	0.02	0.42	0.06	0.50	0.22	1.00
	50%	1.40	0.03	0.67	0.02	23	0.01	0.23	0.10	0.66	0.22	1.00
Wang (2011)	100%	3.83	0.10	3.64	0.09	352	0.04	0.90	0.02	0.08	0.25	0.96
	75%	3.63	0.09	3.41	0.08	316	0.04	0.88	0.03	0.09	0.25	0.97
	50%	3.38	0.09	3.11	0.07	274	0.03	0.85	0.04	0.12	0.24	0.98
Del Castillo (2012)	100%	6.14	0.13	5.72	0.12	906	0.06	0.87	0.09	0.04	0.30	0.60
	75%	5.69	0.12	4.94	0.10	777	0.06	0.75	0.18	0.07	0.30	0.72
	50%	3.97	0.10	0.97	0.00	378	0.04	0.06	0.83	0.10	0.28	0.94

4.3.3 New Flow Speed Methodology

The author aims to improve the prediction methods at hours where the traffic density exceeds the road's maximum traffic density. Therefore, the author has proposed modifying the Del Castillo (1995) method by considering the non-PC vehicles impact of lower acceleration performance on the traffic flow. Furthermore, the author has proposed to multiply the $THGV_f$ by the Del Castillo (1995) formula when the k_{pce} is greater than k_m , as in (4-52) (Makki 2019a).

$$ATS_{SDE} = \begin{cases} THGV_f \times ATS_p & \text{if } k_{pce} > k_m \\ ATS_p & \text{if } k_{pce} \leq k_m \end{cases} \quad (4-52)$$

where,

ATS_{SDE} is the average traffic speed prediction method based on speed-density-acceleration performance in km/h

ATS_p is the predicted average traffic speed before modification

k_{pce} is the total traffic volume of the street in PC/km/NL

k_m is the maximum traffic density in PC/km/NL

$THGV_f$ is the total HGV factor for PCE converted traffic flow in m/m

According to TABLE 4-7, the modification method reduced the error of prediction of 24 hours period and 12 hours period at all ABCL levels and reduced the error at peak hours two 50% of the desired error level, as shown in FIGURE 4-19.

TABLE 4-7: Results of analysis of the improvement provided by the new method

Estimation Method	ABCL	RMSE	RMSPE	ME	MPE	SSE
Del Castillo (1995) 24 Hour period	100%	2.48	0.049	1.86	0.037	148
	75%	2.43	0.048	1.73	0.035	142
	50%	2.38	0.047	1.56	0.031	136
Del Castillo (1995) 12 Hour period	100%	1.67	0.041	1.23	0.030	33
	75%	1.53	0.038	0.99	0.025	28
	50%	1.40	0.035	0.67	0.018	24
Modified Del Castillo (1995) 24 Hour period	100%	2.44	0.047	1.77	0.035	143
	75%	2.38	0.045	1.57	0.029	136
	50%	2.36	0.045	1.32	0.023	134
Modified Del Castillo (1995) 12 Hour period	100%	1.55	0.035	1.06	0.024	29
	75%	1.35	0.029	0.67	0.014	22
	50%	1.33	0.031	0.21	0.002	21

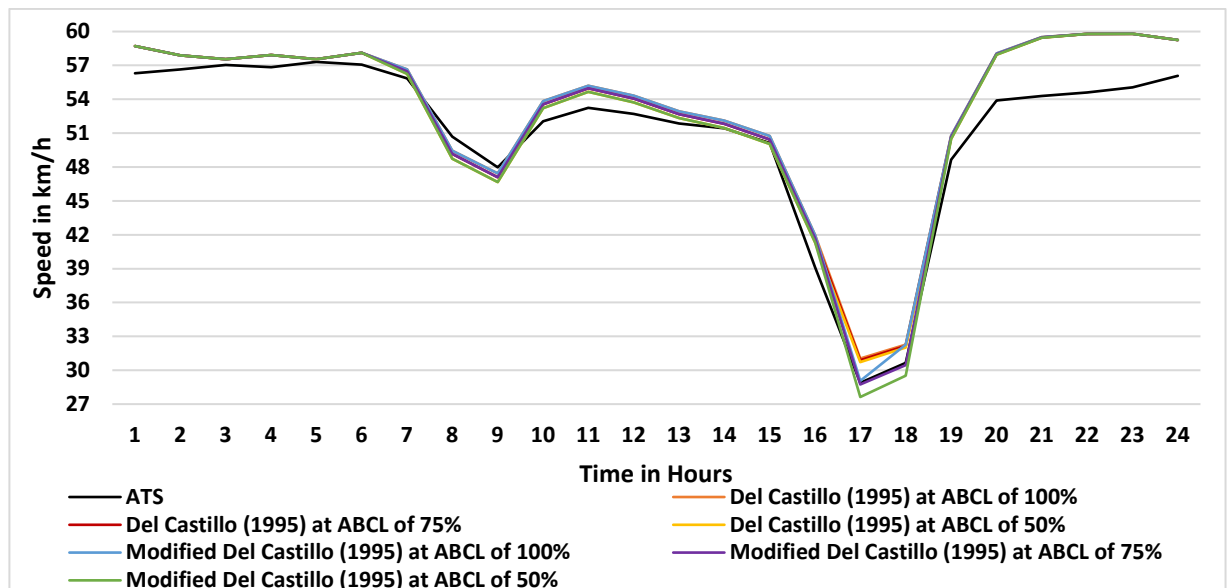


FIGURE 4-19: The modified Del Castillo prediction method for PCE converted traffic flow

4.4 ESTIMATING INDIVIDUAL VEHICLE'S SPEEDS

It is possible to estimate the speed of every vehicle type on the road by calculating the available average gap between following and leading vehicles on the road as in (4-53) and utilizing (4-54) to determine the maximum

ability of drivers to accelerate towards the vehicle's FFS, as in (4-55). However, the drivers do not necessarily accelerate up to their maximum abilities. Therefore, there is a margin of error caused by drivers' behaviours.

$$AAG = ATS_{SDE} \times 1000 \times EGR \times NL \times f_w - \sum (FV_i \times L_i) \quad (4-53)$$

where,

AAG is the available average gap between following and leading vehicles in m/h

ATS_{SDE} is the modified Del Castillo (1995) method for PCE converted traffic flow in km/h

EGR is the effective green ratio

NL is the number of lanes

f_w is the width correction factor

L_i is the average length of vehicle type i in m

$$AS_i = \left(\frac{0.5 \times \left(\frac{MPS_{pce}}{3.6} \right)^2}{\frac{EP_i \times 746 \times 2}{\left(\frac{MPS_{pce}}{3.6} \right) \times T_i \times GM_i} \cdot \frac{FR_i + FG_i + FW_i}{GM_i}} \right) + \left(\frac{MPS_{pce}}{3.6} \right) \times RT_i \quad (4-54)$$

$$ES_i = \frac{FFS_i \times AAG}{AS_i} \quad (4-55)$$

where,

AS_i is the average acceleration space of vehicle type i in m/h

EP_i is the average engine power of vehicle type i in HP

GM_i is the average gross mass of vehicle type i in kg

FR_i is the rolling force of vehicle type i in N

FG_i is the road's grade force of vehicle type i in N

FW_i is the wind's force resistance of vehicle type i in N

RT_i is the average reaction time of the driver of vehicle type i in s

FFS is the FFS of vehicle type i in km/h

ES_i is the estimated speed of vehicle type i in km/h

The author has presented the prediction results for PC, LGV, HGVr, and HGVa vehicles at three different ABCL level, as shown in FIGURE 4-20, FIGURE 4-21, FIGURE 4-22, and FIGURE 4-23, respectively.

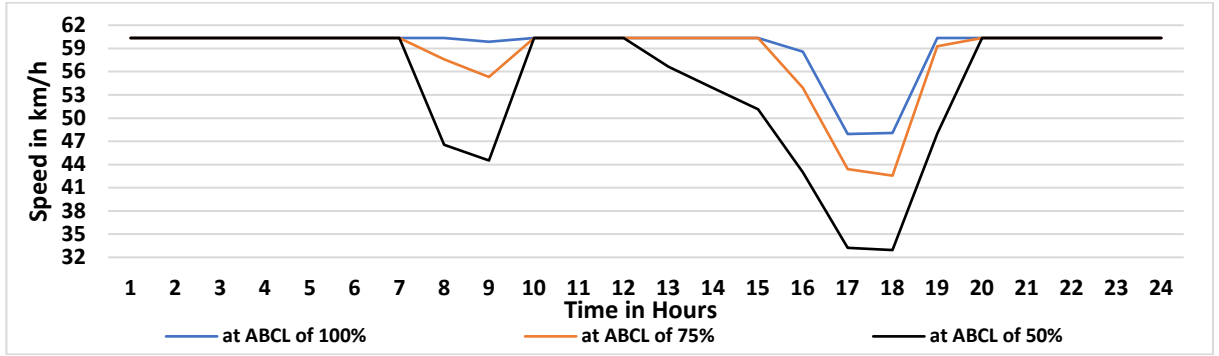


FIGURE 4-20: Estimated speed of PC (ES₁) at ABCL of 50%, 75%, and 100%

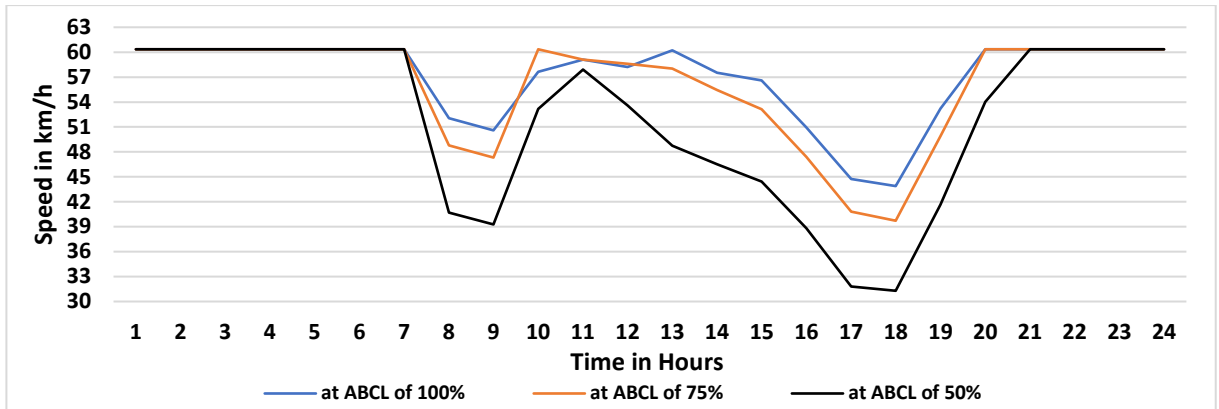


FIGURE 4-21: Estimated speed of LGV (ES₂) at ABCL of 50%, 75%, and 100%

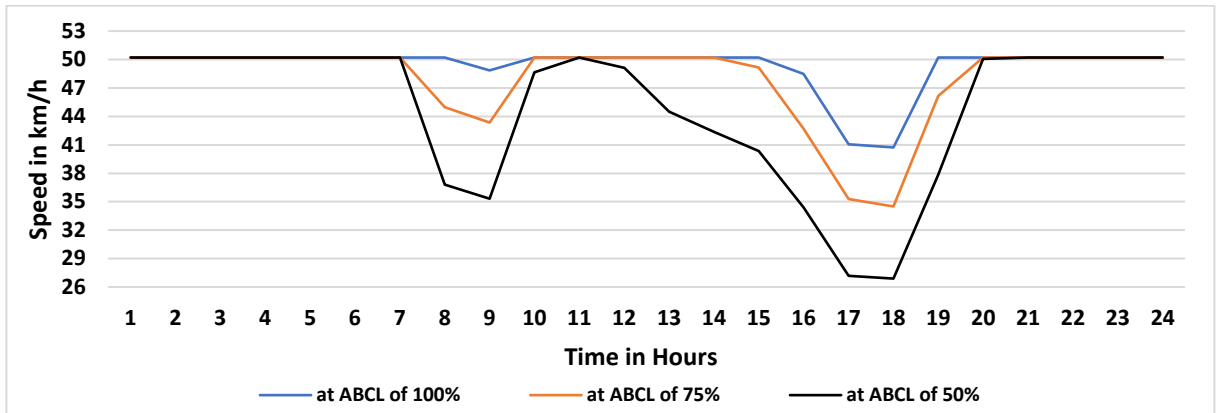


FIGURE 4-22: Estimated speed of HGVr (ES₃) at ABCL of 50%, 75%, and 100%

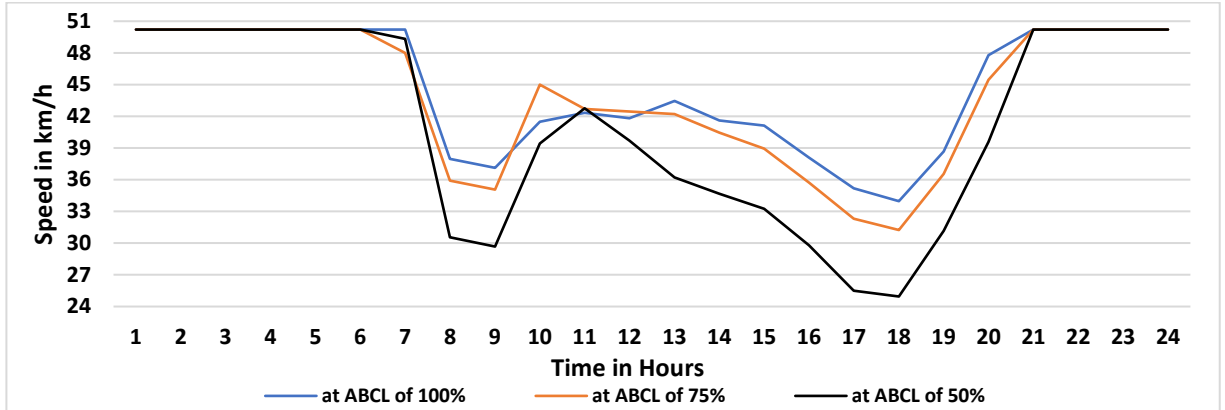


FIGURE 4-23: Estimated speed of HGVa (ES4) at ABCL of 50%, 75%, and 100%

Thereby, the author has estimated the average traffic flow speed by utilizing (4-53), (4-54), and (4-55) for all four categories of vehicles and by considering the traffic flow proportions of these vehicle types, as in (4-56). Applying equation (4-56) has resulted in an error for an average of 24 hours of $\pm 5.84\%$ and an RMSE and SSE of 3.015 km/h and 307, respectively, and for an average of 12 hours (hours 8 am-7 pm) of $\pm 6.98\%$ and an RMSE and SSE of 3.25 km/h and 169, respectively.

$$ATS_{APE} = \frac{\sum(FV_i \times ES_i)}{TF} \quad (4-56)$$

where,

ATS_{AP} is the average traffic speed estimated by acceleration performance in km/h

FV_i is the traffic flow volume of vehicle type i in veh/h

TF is the total non-PCE traffic flow in veh/h

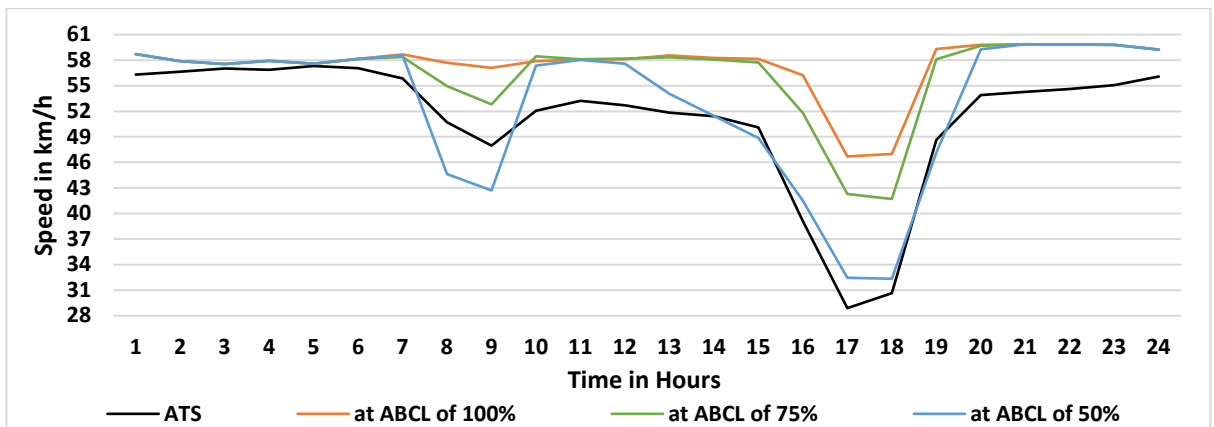


FIGURE 4-24: Average Estimated Speed (AES) for a composite of all four types of vehicles at ABCL of 50%, 75%, and 100% with comparison to ATS

The prediction results for the average traffic flow speed that the author has obtained from (4-57) show that the best prediction fit has been provided at ABCL of 50%, as shown in FIGURE 4-24. The results of this method show higher error than the error provided by the modified Del Castillo method. Due to the proposed average values of EP, GM, L, The prediction results change when the author changes these values. Therefore, by obtaining the vehicles' specifications using the road and the drivers' behaviour, the user can determine speed prediction with lower error rates.

4.5 RESCHEDULING ARTICULATED HGVA

After developing an efficient ATS prediction formula, the rescheduling of HGVA vehicles became possible because the ATS changes with the change of traffic density, and the ATS change will impact the capacity and PCE estimation. As in chapter three, the author has proposed two approaches to rescheduling. The first approach is to reschedule the HGVA vehicles by removing them from time slots that traffic flow has exceeded the C_{DAS} and inserting them to time slots that traffic flow has sufficient free spaces. The second approach is to reschedule the HGVA vehicles up to the C_{DAS} all day long where and it will lead to a $VtCR_{DAS}$ equal to one, as shown in FIGURE 4-25, FIGURE 3-36 and FIGURE 3-37.

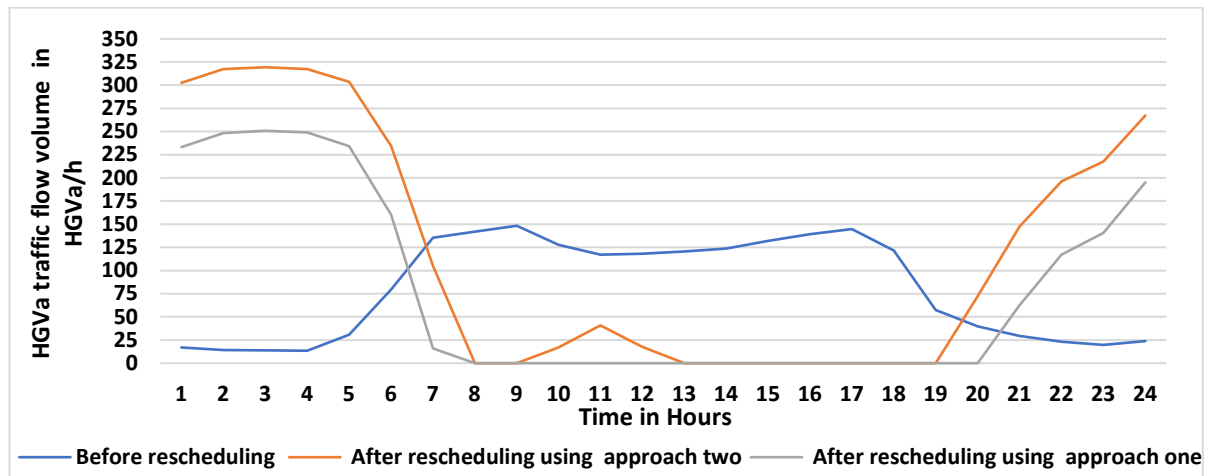


FIGURE 4-25: The change HGVA vehicle's flow volume AR at an ABCL of 100%

Therefore, due to the decrease of HGVA vehicles during the hours of 06.30-19.30 and the increase of HGVA vehicles during the hours of 19.30-06.30, as shown in FIGURE 4-25, the ATS will increase during the hours of 06.30-19.30 and decrease during the hours of 19.30-06.30, as shown in FIGURE 4-26. The ATS with rescheduling approach

two suffers more decrease during off-peak hours because, in approach one, the total number of HGVA vehicles a day is 1944 HGVA/h, while in approach two, the number increases by 50%, as shown in FIGURE 4-25.

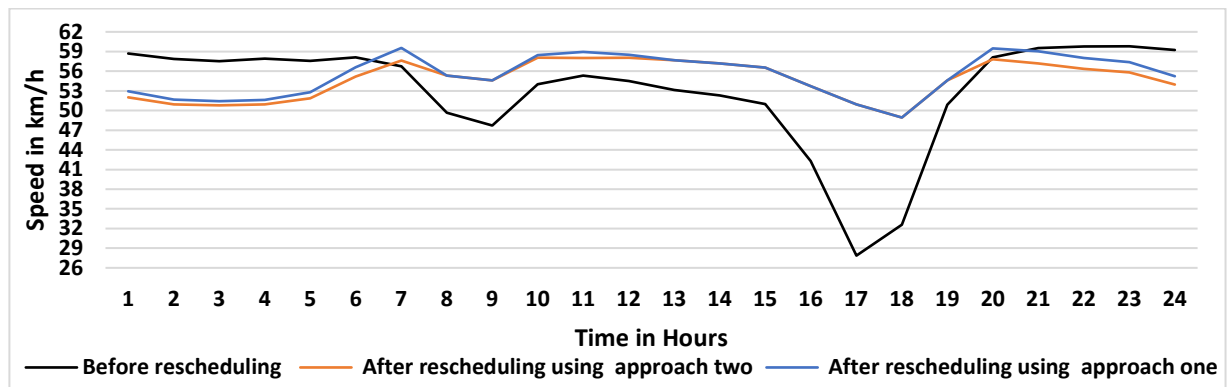


FIGURE 4-26: The predicted ATS before and AR at an ABCL of 100%

4.6 LOGISTICS AND ROAD PLANNING OPTIONS

The expansion of the Liverpool container terminal increases the demand for road freight, and roads that connect the terminal with the city and the nearby cities will suffer from congestion. Therefore, local authorities either try to overcome this problem by building new roads, tunnels, adding extra lanes to existing roads, or utilising other transport modes for freight transportation. To reach a feasible solution, the planners would require an accurate and efficient method of estimating HGVs' effect on road traffic flow, safety, and logistics.

The author has explored thirteen scenarios where the road freight meets the targets for 2020 and 2030. In all of these scenarios, the author has considered HGVs with MAM, variable speed, several scenarios of the number of lanes, width of lanes, separate roads, and accessibility (Makki 2019b)

- Scenario 1: Utilising the current two-lane road
- Scenario 2: Building an HGV-access two-lane road in parallel to the current two-lane road
- Scenario 3: Building an all-access two-lane road in parallel to the current two-lane road
- Scenario 4: Building an additional lane to the current two-lane road where the added lane is HGV-access
- Scenario 5: Building an additional lane to the current two-lane road where the added lane is all-access
- Scenario 6: Repeating scenarios 4 with a lane width of 3.3m, and 3m
- Scenario 7: Repeating scenarios 5 with a lane width of 3.3m, and 3m

The purpose of scenarios 1-5 is to assess the feasibility of meeting the targets of the years 2020 and 2030 by utilising the existing two-lane in comparison to creating a new two-lane road with all access or HGV access only and explore adding third and fourth lanes to the existing two-lane road and make for all access in comparison to HGV access only. Scenarios 6-7 aim to assess the reduction of lane width from 3.65m to 3m. The objective is to ensure that ATS should always be equal or greater than the optimum ATS of 36.34 km/h.

The current HGVa access to the road allows transporting 1.101MTEUs annually. Therefore, to meet the years 2020 and 2030 targets, the HGVa vehicles have to be increased by 182% and 272%, respectively. Therefore, scenario 1 is the worst-case scenario where all the targets must be met by utilising only the current two-lane road without adding a third lane or a new two-lane road.

The results of scenario one in FIGURE 4-27 and TABLE 4-8 show that increasing the number of HGVa vehicles to meet the target for the year 2020 will significantly reduce the ATS by an average of 6.03% and reduce the ATS to lower than the ATSo by three hours (an increase by an hour), and by increasing the HGVa vehicles' flow to meet the target of the year 2030, the ATS will decrease by an average of 12.5% (twice the impact of meeting the year 2020 target) and increase the number of hours that the ATS becomes lower than the ATSo to four hours.

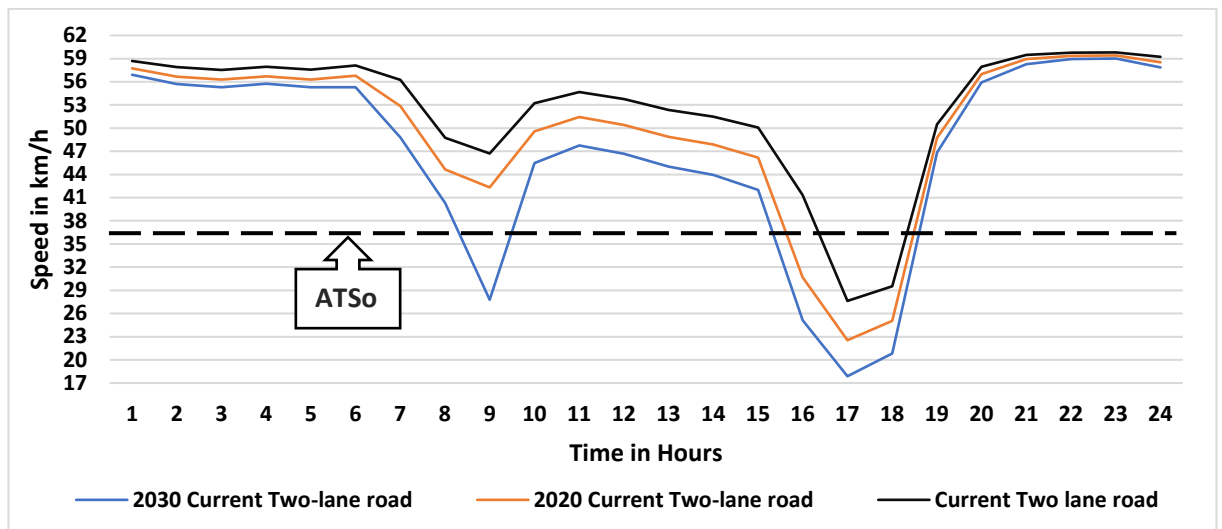


FIGURE 4-27: ATS for Scenario one in comparison to the current ATS

TABLE 4-8: Reduction of ATS due to the increase of HGVa vehicles in scenario one

Time	7.00	8.00	9.00	10.00	11.00	12.00	13.00	14.00	15.00	16.00	17.00	18.00
2020's Target	-6.1%	-8.5%	-9.3%	-6.9%	-5.9%	-6.2%	-6.7%	-7.0%	-7.8%	-25.7%	-18.4%	-15.1%
2030's Target	-13.2%	-17.4%	-40.5%	-14.6%	-12.6%	-13.2%	-14.0%	-14.6%	-16.1%	-39.2%	-35.3%	-29.5%

Scenarios two and three provide the best solution for meeting the targets where the author proposed a new two-lane road and the current road. In scenario two, the author has proposed to make the new road an HGV access the only road and proposed in scenario three to make it an all-access road, and the all-access means in this thesis that the new road will have the new road same traffic flow volumes for non-HGVa vehicles.

The results of scenarios two and three in FIGURE 4-28 and TABLE 4-9 shows that building a new all-access two-lane road and increasing the HGVa vehicles to meet the target for the years 2020 and 2030 will slightly increase the current ATS by 0.6% slightly decrease it -2.4%, respectively. However, the results also showed how making the new two-lane road an HGV-access only significantly increases the current ATS by 10.1% and 7% when meeting the years 2020 and 2030 targets, respectively. Scenario two also increases the ATS to higher than the ATSo at all hours.

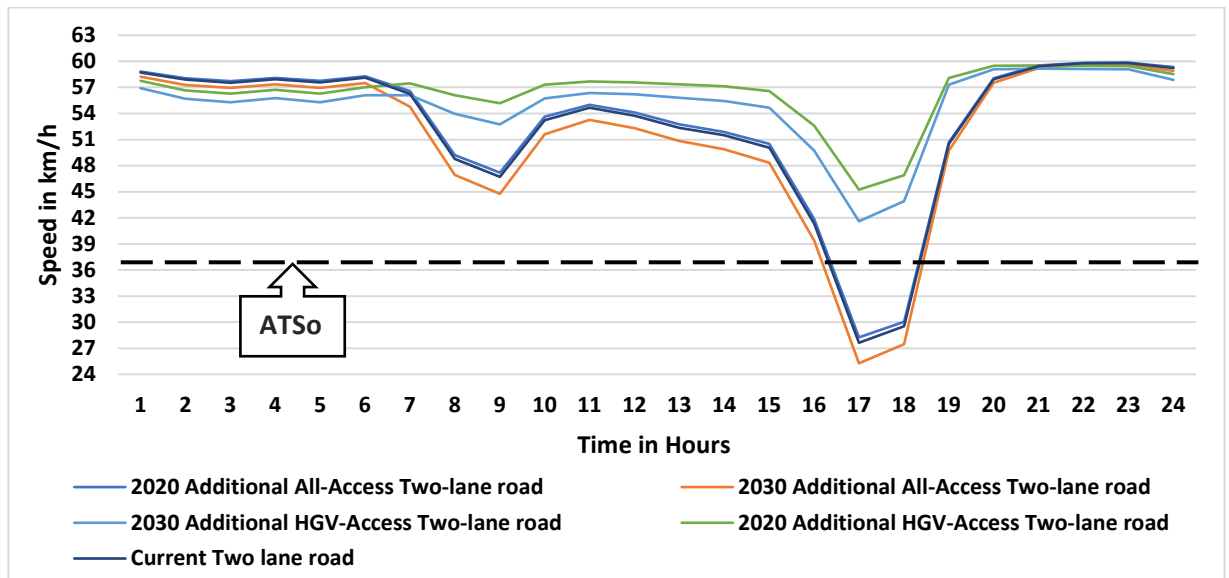


FIGURE 4-28: ATS for Scenarios two and three in comparison to the current ATS

TABLE 4-9: Change in ATS due to building an extra two-lane road in scenarios two and three

Time	8.00	9.00	10.00	11.00	12.00	13.00	14.00	15.00	16.00	17.00	18.00	19.00
2020 Additional All-Access Two-lane road	0.9%	1.0%	0.8%	0.6%	0.7%	0.7%	0.8%	0.9%	1.2%	2.2%	1.8%	0.4%
2030 Additional All-Access Two-lane road	-3.8%	-4.2%	-3%	-2.6%	-2.7%	-2.9%	-3.1%	-3.5%	-4.7%	-8.5%	-7%	-1.5%
2020 Additional HGV-Access Two-lane road	15%	18.2%	7.7%	5.5%	7.1%	9.5%	10.9%	13%	27.2%	63.7%	58.9%	15%
2030 Additional HGV-Access Two-lane road	10.7%	13%	4.7%	3.1%	4.5%	6.6%	7.7%	9.2%	20.3%	50.6%	48.7%	13.5%

The author proposed adding an extra lane to the current two-lane road and chose it to be an HGV-access only in scenario four and an all-access in scenario five. The results in FIGURE 4-29 and TABLE 4-10 show that building an extra lane to the current two-lane road and make it all-access will increase the ATS by an average of 3.2% and reduce it by an average of -1% for the years 2020 and 2030 targets, respectively, and if the extra lane becomes HGV-access only it will increase the ATS by an average of 4.8% and 0.1% for the years 2020 and 2030 targets, respectively.

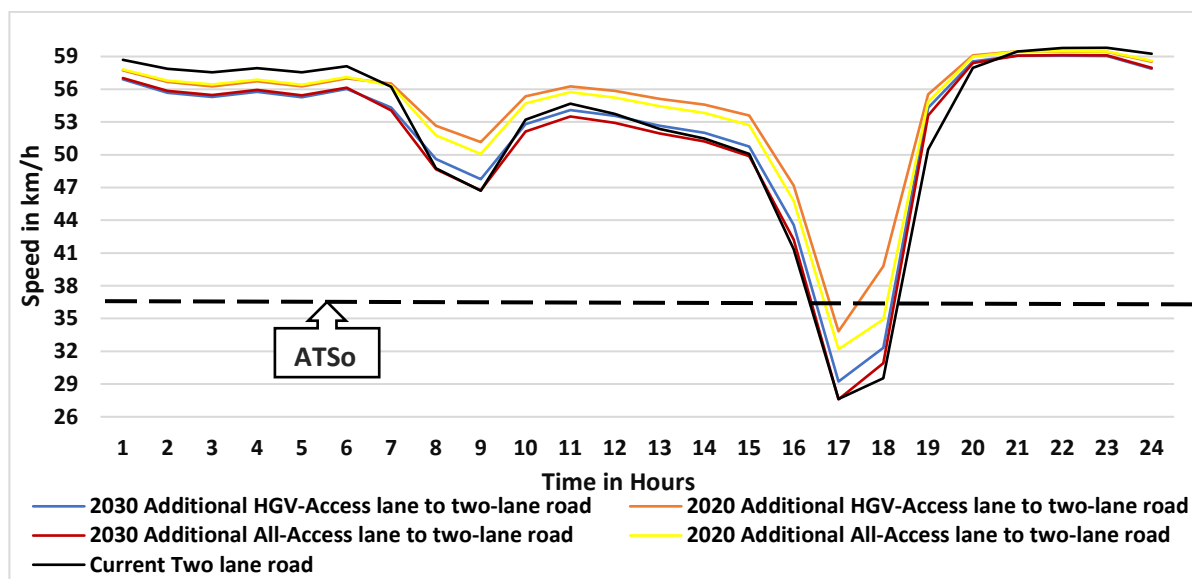


FIGURE 4-29: ATS for Scenarios four and five in comparison to the current ATS

TABLE 4-10: Change in ATS due to building a third lane in scenarios four and five

Time	8.00	9.00	10.00	11.00	12.00	13.00	14.00	15.00	16.00	17.00	18.00	19.00
2030 Additional HGV-Access lane to two-lane road	1.7%	2.3%	-0.8%	-1%	-0.4%	0.6%	1%	1.3%	5.3%	5.8%	9.5%	7.5%
2020 Additional HGV-Access Lane to two-lane road	8%	9.5%	4%	2.9%	3.9%	5.3%	6%	7.0%	14.1%	22.4%	34.8%	10%
2030 Additional All-Access Lane to two-lane road	-0.2%	0.1%	-2%	2.1%	1.6%	0.8%	0.5%	0.4%	2.1%	-0.1%	4.7%	6.1%
2020 Additional All-Access Lane to two-lane road	6.2%	7.3%	2.8%	2%	2.8%	4%	4.6%	5.3%	10.7%	16.5%	18.3%	8.6%

The choice of an all-access third lane will maintain the current ATS at peak hours and thereby maintain the same number of hours with an ATS of less than the ATSo, while the choice of making the third lane as an HGV-access only will reduce these hours by one hour when meeting the year 2020 target.

Developers may reduce the road's lanes when building an extra lane due to limited available space. Therefore, following up on the previous scenarios of four and five, the author must investigate the probability of lane's width

reduction from the standard width of 3.65m to 3.3m and 3m in scenarios six and seven compared to scenarios four and five.

The results of scenario six in FIGURE 4-30 and TABLE 4-11 show that when reducing the lane’s width for the year 2020 target from 3.65m to 3.3m and 3m, the ATS will be reduced by an average of 0.2% and 0.3%, respectively, and for the year 2030 target, the ATS will decrease by an average of 0.4% and 0.7%, respectively. Scenario six has maintained the same performance as scenario four in the number of hours where the ATS is lower than ATSo.

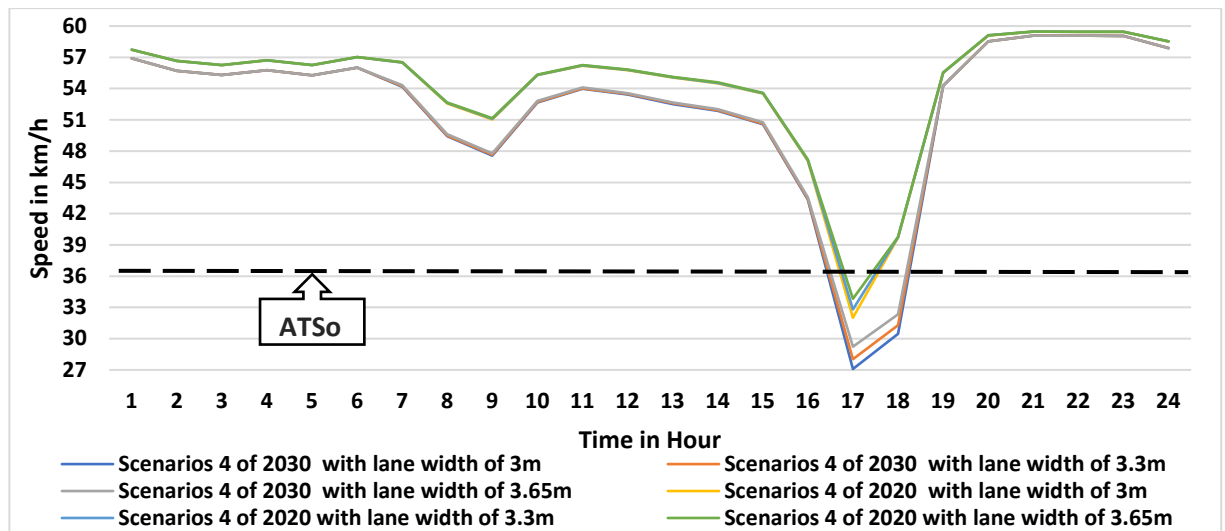


FIGURE 4-30: ATS for Scenario six in comparison to the ATS of Scenario four

TABLE 4-11: Change in ATS due to reducing lanes’ width in scenario six in comparison to scenario four

Time	8.00	9.00	10.00	11.00	12.00	13.00	14.00	15.00	16.00	17.00	18.00	19.00
Scenarios 4 of 2030 with lane width of 3m	-0.4%	-0.4%	-0.3%	-0.2%	-0.2%	-0.3%	-0.3%	-0.3%	-0.4%	-7.3%	-5.7%	-0.1%
Scenarios 4 of 2030 with lane width of 3.3m	-0.2%	-0.2%	-0.2%	-0.1%	-0.1%	-0.2%	-0.2%	-0.2%	-0.3%	-4.1%	-3.2%	0.0%
Scenarios 4 of 2020 with lane width of 3 m	-0.2%	-0.2%	-0.1%	-0.1%	-0.1%	-0.1%	-0.1%	-0.1%	-0.2%	-5.4%	-0.2%	0.0%
Scenarios 4 of 2020 with lane width of 3.3 m	-0.1%	-0.1%	-0.1%	-0.1%	-0.1%	-0.1%	-0.1%	-0.1%	-0.1%	-3.0%	-0.1%	0.0%

TABLE 4-12: Change in ATS due to reducing lanes' width in scenario seven in comparison to scenario five

Time	8.00	9.00	10.00	11.00	12.00	13.00	14.00	15.00	16.00	17.00	18.00	19.00
Scenarios 5 of 2030 with lane width of 3m	-	-	-	-	-	-	-	-	-	-	-	-
Scenarios 5 of 2030 with lane width of 3.3m	8.6%	9.8%	5.2%	4.1%	4.9%	6.2%	6.8%	7.7%	33.9%	24.9%	23.9%	9.1%
Scenarios 5 of 2030 with lane width of 3.3m	-	-	-	-	-	-	-	-	-	-22%	-	-
Scenarios 5 of 2030 with lane width of 3.3m	8.5%	9.6%	5.1%	4.0%	4.8%	6.1%	6.7%	7.6%	30.9%	-	21.7%	9.1%
Scenarios 5 of 2020 with lane width of 3m	-	-	-	-	-	-	-	-	-	-	-	-
Scenarios 5 of 2020 with lane width of 3m	8.1%	9.3%	4.6%	3.5%	4.4%	5.6%	6.2%	7.1%	12.4%	23.2%	22.5%	8.8%
Scenarios 5 of 2020 with lane width of 3.3m	-	-	-	-	-	-	-	-	-	-	-	-
Scenarios 5 of 2020 with lane width of 3.3m	8.0%	9.2%	4.6%	3.5%	4.3%	5.6%	6.2%	7.0%	12.3%	21.2%	20.9%	8.8%

Unlike scenario six, scenario seven considers all-access lanes. Therefore, the impact of scenario seven on the ATS will be higher. The results in FIGURE 4-31 and TABLE 4-12 show that for the year 2020 target, the ATS has been reduced by an average of 4.5% and 4.6% for a lane width of 3.3m and 3m, respectively, and for the year 2030 target an average reduction of 5.5% and 5.8%, respectively.

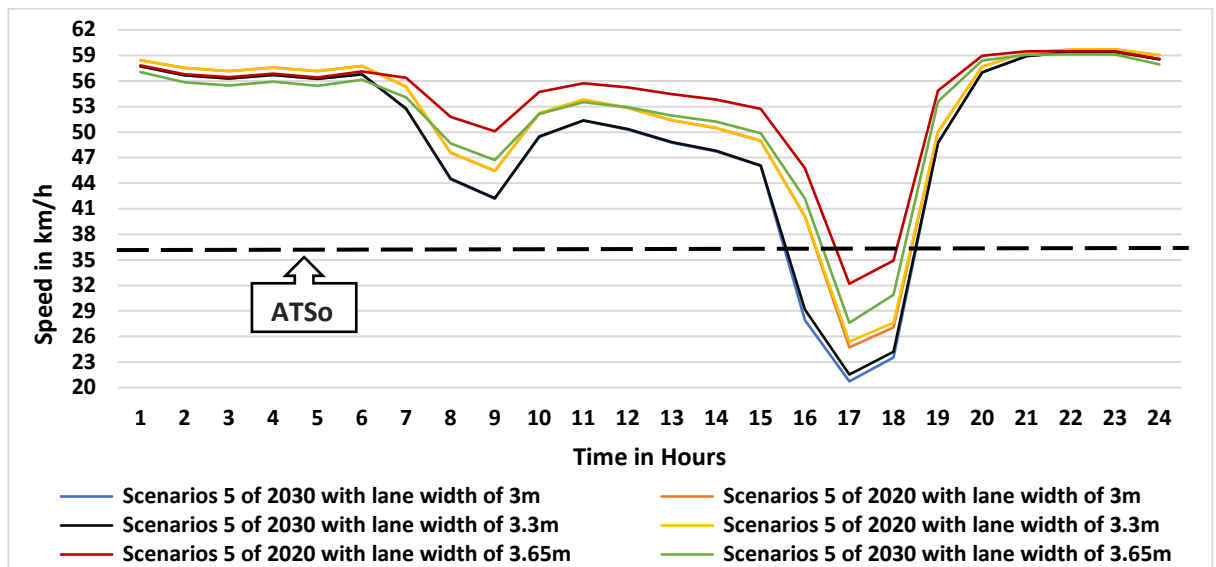


FIGURE 4-31: ATS for Scenario 7 in comparison to the ATS of Scenario 5

The author has concluded that the best solution to meet the targets and improve the traffic operation and safety is scenario two, where the new two-lane road is an HGV-access only, and it significantly improves the ATS and prevents congestion. In the second place comes scenario four, which suggests building a third lane with HGV access only. Finally, scenario four increases the ATS, reduces congestion and improves traffic operation and safety. However, if the developers decided to reduce the road lanes' width, they should not be less than 3.3m wide.

4.7 SUMMARY AND CONTRIBUTION AND NOVELTY

To facilitate rescheduling to reduce congestion and increase the throughput of the road, the author required to predict the ATS by utilising the traffic density because the speed-density method will allow estimating the effect of changing the traffic density on the ATS of the traffic. Among the thirteen current methodologies that the author has reviewed, the Del Castillo (1995) method provided the closest fit to the average flow speed collected from the ATC. Besides, the closest match occurred at an average drivers' competency level of 75%.

The author has proposed modifying the Del Castillo (1995) formula by applying the $THGV_f$ to the flow speed when the k_{pcc} exceeds k_m because the PCE for HGVs is at its highest at peak times. The integration of the $THGV_f$ significantly reduces the prediction error and reflect the impact of non-PC vehicles on traffic at peak hours.

Utilising the traffic volume in PCE makes predicting the ATS is useful in rescheduling, road planning, and predicting future reductions in ATS due to further increases in traffic flow volumes. Also, it allows traffic controllers and local authority to explore all possible changes in road conditions that would provide better road service and fewer congestion periods.

The author also developed an ATS prediction method that considers the vehicle's acceleration performance and the AAG. This method has many benefits, such as predicting an individual vehicle's speed, and it facilitates planning by utilising the vehicle registration data and the port's registration and shipments data.

The author has conducted an assessment to determine the best solution to meet the 2020 and 2030 targets and improve the traffic and logistics operations and safety. The author has concluded the scenario two provides excellent performance, and scenario four provides an acceptable performance wherein both scenarios, the lanes are HGV-access only.

CHAPTER FIVE: LEVEL OF SERVICE

5.1 INTRODUCTION

There is a difference in approach between the HCM approach of the LoS (TRB 2000) and the British approach of LoS. Britain does not adopt the HCM method to estimate and present the LoS (O'Flaherty 2006). The HCM LoS describes the road traffic conditions from level A (as the best) to level F (the worst). The focus is on the traffic condition at level C-F, and the focus of the HCM LoS is travel time, delay, traffic density, the gap between vehicles, and VtCR. The British LoS approach does not use the A-F scale; instead, it utilises four performance measures to evaluate the LoS, which are Poor, Fair, Good, and Excellent (Ireland, 2008), and it focuses on safety, availability (accessibility), and environment.

In this research, the author develops an LoS method that measures safety by utilising the HCM measure of LoS. The method will determine the LoS for each type of vehicle to facilitate a planning and development tool to improve the accessibility of the road and reduce accidents and brings about transportation performance.

The author has utilised the deceleration and acceleration performance in the development of PCE in chapter three and measured the deceleration performance on the basis of the ability to bring the vehicle to a standstill in case of an emergency and keeping a safe distance between the following and leading vehicles to avoid hitting the leading vehicle. Therefore, the author can determine the risk of hitting a pedestrian, sustaining a severe injury, and death.

In this chapter, the author has presented four new LoS methods for roads dependent on available RT and accident impact on pedestrians. The objective is to create a tool to measure the LoS according to the risk of an accident to pave the way for traffic operators and local authorities to plan to reduce accidents and economic losses. The cost effect of road accidents reached £36 billion in 2016 in the UK for accident types, as shown in TABLE 5-1 (DfT Accidents, 2018), averaging over £2 million for every fatality accident, up to £238,000 for every severe injury accident, and up to £25,000 for slight injury accident (DfT Accidents 2018), as shown in TABLE 5-2.

TABLE 5-1: Total Annual Cost In million £ (DfT Accidents 2018)

Accident/casualty type	Fatal	Serious	Slight	All injury accidents	Damage only accidents	Non-fatal accidents not reported to the police	All accidents
lost output	1,150	592	381	2,123	0	2,483	4,606
Medical and Ambulance	11	355	162	528	0	1,301	1,829
Human costs	2,265	4,034	1,817	8,116	0	14,713	22,829
Police costs	34	51	69	154	82	0	236
Insurance and admin	1	5	14	20	126	51	197
Damage to property	21	123	377	521	4,401	1,339	6,260
Total	3,479	5,160	2,819	11,458	4,609	19,887	35,953
Built-up roads	1,509	3,439	2,050	6,998	3,817	-	-
Non-Built-up roads	1,790	1,540	610	3,939	672	-	-
Motorways	181	181	159	521	121	-	-
All Roads	3,479	5,160	2,819	11,458	4,609	19,887	35,953

TABLE 5-2: Average Cost in £ (DfT Accidents 2018)

Accident/casualty type	Fatal	Serious	Slight	Average for all severities	Damage only accidents	All injury accidents	All accidents
Cost per casualty	1841315	206912	15951	59358	-		
Cost per accident	2053814	237527	24911	83893	2211		
Built-up roads	1,971,998	228,149	23,514	-	2,093	67,924	5,613
Non-Built-up roads	2,125,862	258,046	28,576	-	3,060	139,961	18,617
Motorways	2,075,937	265,305	34,322	-	2,940	96,330	13,799
All Roads	2,053,814	237,527	24,911	-	2,211	83,893	7,235

Road accidents also lead to the long-term recovery of up to two years after the accident (Tournier, 2014). To reduce severe and fatal injuries' accidents by road traffic planning, the author must address the cause of death or severe injuries. Apart from the driver's behaviour, the leading cause of accidents is the lack of an available gap between two vehicles or between vehicles and pedestrians. The required SD to bring a vehicle to a stand-still depends on speed, vehicle type, and driver's alertness. The SD is a combination of BD and the braking RT distance, and the required braking RT depends on the driver's alertness level. The deceleration capability of vehicles decreases with an increase in size and weight.

Thus, an HGV require a longer distance to brake to stand still, and the stopping time for HGVs should be higher than for PC. When drivers do not leave enough gap between their vehicles and the leading vehicles or the pedestrians, the risk of having a severe injury or fatal accident will be higher. The increasing number of vehicles on the road would increase accidents due to congestion and a higher proportion of HGVs (Lloyd, 2015).

The type of the vehicle and its speed would determine the minimum force applied to the pedestrian that may cause bone fractures. For example, Tefft (2013) assessed the average risk for a pedestrian struck by a car or a light truck and found that the average risk of sustaining an injury would range from 10 to 90% for a speed range from 17.1 to 48.1mi/h and that the average risk of death ranges from 10 to 90% for a speed range from 24.1 to 48mi/h.

Even though the driver would not bring the vehicle to a standstill, the driver would reduce the vehicle's speed to an acceptable level that would not cause death or a severe injury. For example, Kroyer (2015) assessed the safety level in driving at a speed of 18.63mi/h by determining whether an accident with this speed would cause severe injury to a pedestrian or not and found that 18.63mi/h may not be as safe as previously believed.

According to the DfT (2015), from the 1st of November 2015, most newly registered HGVs in the UK must have AEB fitted as standard. The problem with the AEB is that it is limited in response concerning speed range. The AEB sensor is set based on the notion that three-quarters of all collisions occur at speeds less than 20mi/h (DfT-Working Together to Build a Safer Road System, 2015; Thatcham Research, 2015).

Hence, the AEB would help avoid crashes at speeds up to 15mi/h and mitigate those up to 25mi/h. The AEB intervenes a second before impact to reduce the effect of a collision, and according to DfT (2015) and AASHTO (2011), when excluding RT, one second is sufficient to stop a PC with a speed of up to 15mi/h. However, it is not enough to prevent an accident at a vehicle speed higher than 15mi/h (DfT-Working Together to Build a Safer Road System, 2015; AASHTO, 2011).

The AEB only reduces a vehicle's speed if the vehicle's speed is equal to 25mi/h or less, e.g. the AEB can reduce the vehicle's speed from 11.18 m/s to 4.472 m/s (10mi/h) at the time of the crash. However, the vehicle would still be 3m short of the required SD (Tefft, 2013). Furthermore, HGVs usually require a longer time to make an emergency stop. Therefore, the AEB does not help vehicles with a higher speed than 25mi/h for PC, let alone for HGVs.

In this research, the author assessed the LoS depending on the risk of pedestrian death or sustained injury concerning speed and vehicle type. So far, existing LoS methods have not addressed the Available Reaction Time (ART), the risk of sustaining a severe injury, and the risk of death (TRB, 2010). Thereby, developing an LoS that addresses these issues will help road and traffic control planners understand road transport challenges.

5.2 LEVEL OF SERVICE

The LoS is a measure of the quality of traffic operation from the user's point of view (TRB, 2010; Mannering, 2013; Rogers, 2016). One of this research's main objectives is to improve the operational quality of road traffic,

reduce congestion, and improve traffic safety by maintaining the safe gap between following and leading vehicles. One of the main existing LoS methods is the VtCR LoS method.

The LoS purpose is to measure the quality of operational traffic conditions from the road user's perspective (TRB, 2010; Mannering, 2013; Rogers, 2016). At C-level, the increasing traffic density could cause a reduction in the flow speed. It shows stable traffic flow at LoS-D with high flow density, but if a small increase in traffic volume occurs, it could cause significant operational difficulties and accidents. Finally, at levels E and F, the traffic flow reaches and exceeds capacity level and shows unstable operational conditions. There are four main performance parameters to measure the LoS:

- Travel delay in (s/km) and is linked to travel time and flow speed
- The gap between following and leading vehicles in m
- Traffic flow density in PC/ km/lane
- VtCR in veh/veh

TABLE 5-3: Current main LoS methods' criteria

LoS	Travel Delay (s/km)	Traffic flow density (veh/km/ln)	Gap (m)	VtCR (veh/veh)
A	≤10	>10 & ≤6.8	≥167	≤0.26
B	>10 & ≤20	>6.8 & ≤11.2	<167 & ≥100	>0.26 & ≤0.43
C	>20 & ≤35	>11.2 & ≤16.2	<100 & ≥50	>0.43 & ≤0.62
D	>35 & ≤55	>16.2 & ≤21.7	<50 & ≥37	>0.62 & ≤0.82
E	>55 & ≤80	>21.7 & ≤28	<37 & ≥20	>0.82 & ≤1
F	>80	>28	<20	>1

The thresholds for these parameters are in TABLE 5-3 (Rogers, 2016; TRB, 2000). The flow density, gap, and VTCR methods describe the high traffic volumes, distances between vehicles, and capacity levels, while the travel delay method only considers the flow speed.

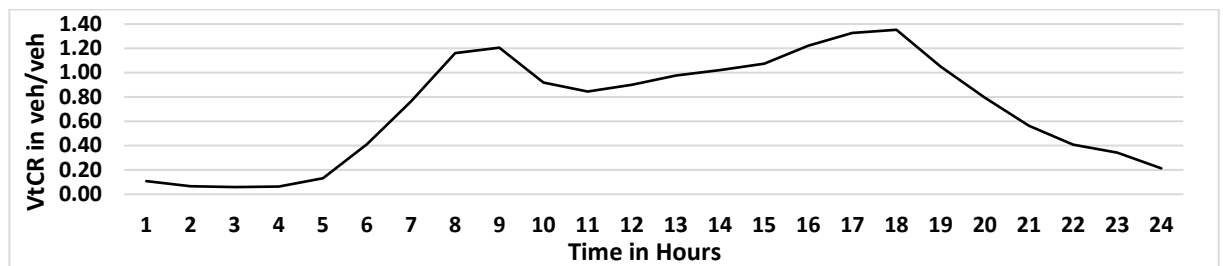


FIGURE 5-1: VtCR for non-PCE traffic flow

The author has presented the VtCR and the LoS in this section by utilising non-PCE traffic flow, and according to FIGURE 5-1, FIGURE 5-2, FIGURE 5-3, FIGURE 5-4, and TABLE 5-3, the LoS of the road base on delay, gap, k, and VtCR is as shown in FIGURE 5-3.

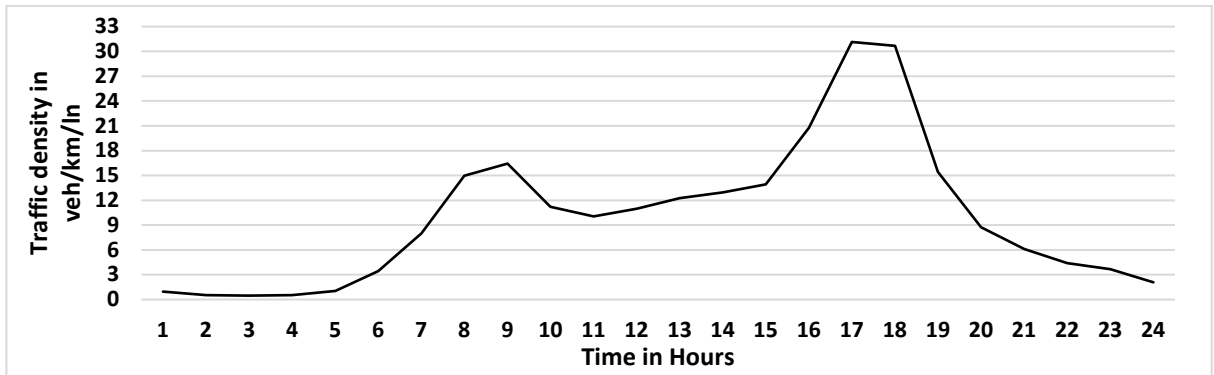


FIGURE 5-2: Traffic flow density of non-PCE traffic flow

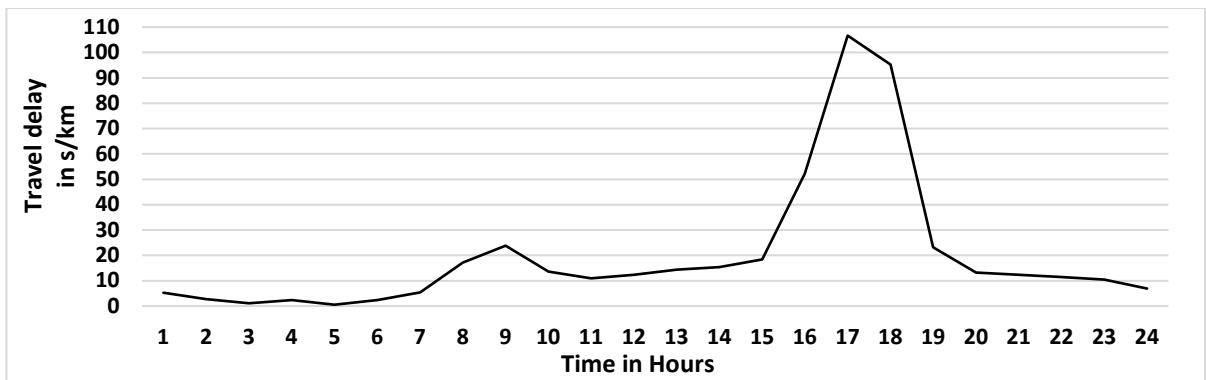


FIGURE 5-3: Travel delay for controlled intersections

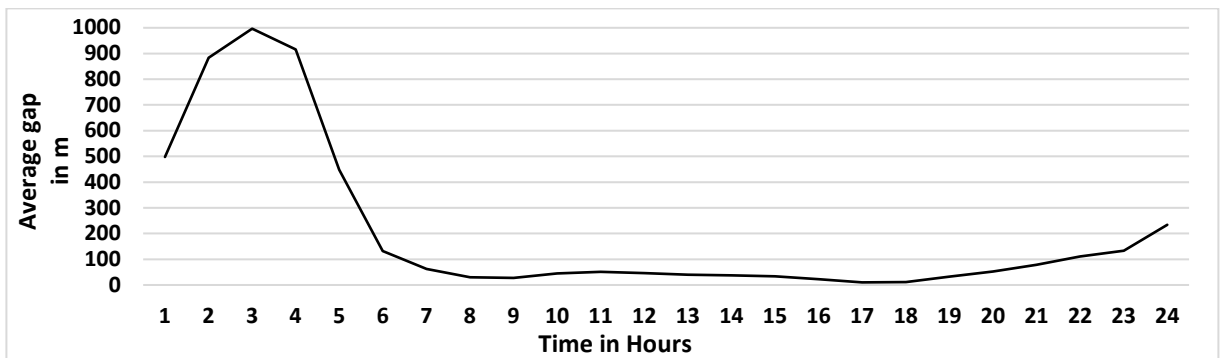


FIGURE 5-4: The average gap between following and leading vehicles

The results in FIGURE 5-5 show that the LoS based on VtCR defines the congestion hours in their widest range compared to the LoS based on the gap that narrows down the evening congestion hours from 4 to 2 hours. The LoS

based k and delay give a more realistic estimation of congestion during evening peak hours at 17.00 and 18.00. However, these four methods do not express the dynamic relationship between traffic flow density and traffic flow speed, and the LoS settings in TABLE 5-3 do not work with all road types and speed limits. Besides, they do not consider traffic safety, driver's behaviour, RT, and the road's risk. For example, when the traffic flow speed increases, the following and leading vehicles' safe gap dynamically increases and vice versa.

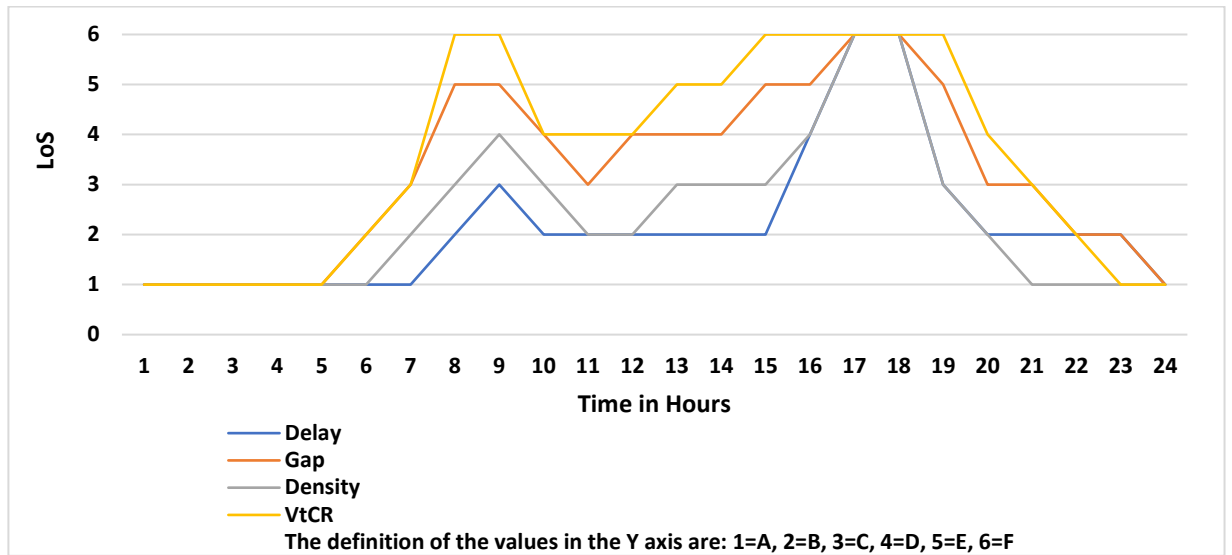


FIGURE 5-5: LoS based on travel delay, traffic density, VtCR, and gap BR

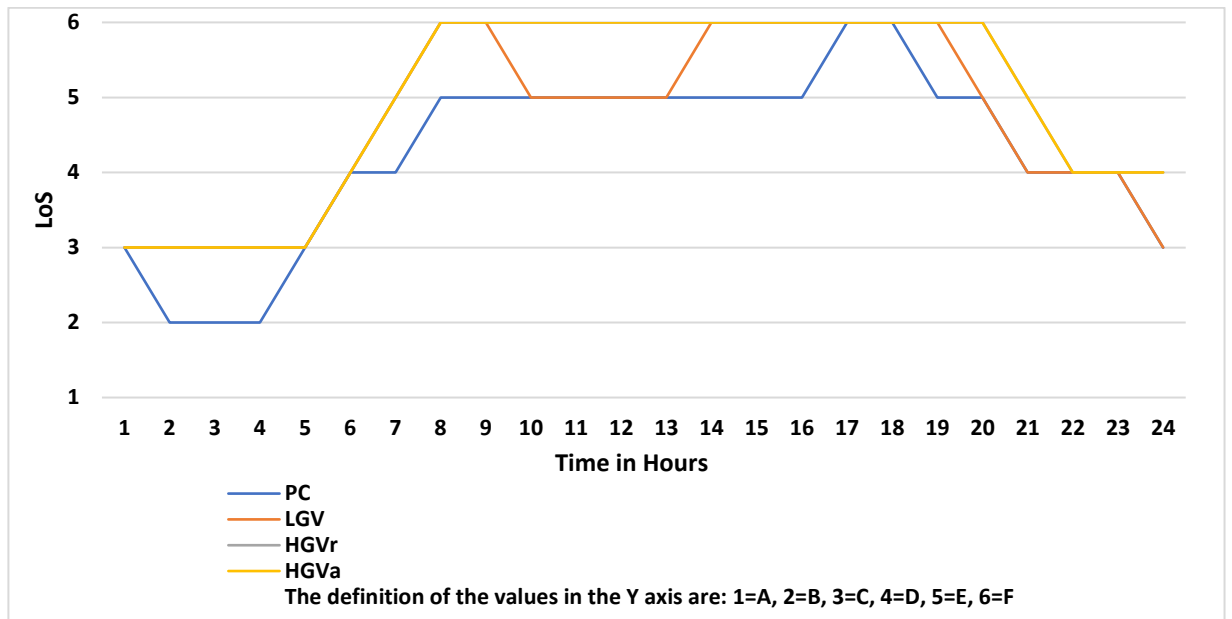


FIGURE 5-6: LoS based on travel delay, traffic density, VtCR, and gap AR

Rescheduling container carriers' HGVA and move them from peak hours to off-peak hours, the LoS of the four methods has shown better road service and shows the benefit of rescheduling on easing congestion, as shown in FIGURE 5-5, FIGURE 5-6, and TABLE 5-4.

TABLE 5-4: The change in LoS due to rescheduling, LoS levels of A-F refer to section 5.1

Type of LoS	Status	LoS-A	LoS-B	LoS-C	LoS-D	LoS-E	LoS-F
VtCR	BR	7 hours	2 hour	2 hour	4 hours	2 hours	7 hours
	AR	0 hour	6 hours	10 hours	3 hours	3 hours	2 hours
Gap	BR	6 hours	3 hours	4 hours	4 hours	5 hours	2 hours
	AR	0 hours	6 hours	7 hours	5 hours	6 hours	0 hours
Density	BR	10 hours	4 hours	6 hours	2 hours	0 hours	2 hours
	AR	10 hours	6 hours	6 hours	2 hours	0 hours	0 hours
Delay	BR	8 hours	11 hours	2 hours	1 hour	0 hours	2 hours
	AR	0 hours	22 hours	2 hours	0 hours	0 hours	0 hours

5.3 METHODOLOGY

This research aims to develop LoS methods to describe the risk of having an accident and causing severe injuries or death to pedestrians. To achieve this, the author must estimate the average available gap for every PC after converting the composite traffic flow volume to all PCs by utilising PCE. The author takes into consideration the PCE, road capacity, and the required average headway for a PC to determine the average available gap between the following and leading vehicles,

In this research, the author has utilised the automatic traffic count data for road link A5038-A5207 of road A5036 in Sefton, Liverpool, UK. The author has chosen this road because it is highly congested, and the average daily traffic volume of HGVs is four times the average UK major roads' traffic volume for HGVs. In addition, the chosen road links the Liverpool container terminal with the NorthWest of England and the rest of the UK.

In this method, the author has decided that the headway for HGVA would require an additional gap, and the location of the extra gap is behind the HGVA. The reason for the extra space is to allow the driver of the following vehicle to have plenty of eyesight distance to see the traffic ahead and determine whether pedestrians are crossing the road and passing in front of the leading vehicle.

5.3.1 Available reaction time and available stopping distance

The aim is to determine if there will be a sufficient AAG to stop the vehicle and avoid hitting a vehicle or a pedestrian. The first contribution is the development of LoS based on Available RT (LoS_{arti}) and the Available SD (LoS_{asdi}). The RT is the time required for the driver to react to incidents on the road, and the SD is the required distance that allows the driver to decelerate the vehicle to a stand-still safely. As stated by AASHTO (2011), the RT should be 2.5s, while other researchers suggested that the RT is in the range from 0.67 to 2.5s, which depends on the driver's competency and the situation on the road. Therefore, the author has chosen the LoS_{arti} threshold values to represent the RT range from 0.67 to 2.5 s (5-1).

$$LoS_{arti} = \begin{cases} A & \text{if } ART_i > 2.5 \\ B & \text{if } 2.5 \geq ART_i > 2 \\ C & \text{if } 2 \geq ART_i > 1.5 \\ D & \text{if } 1.5 \geq ART_i > 1 \\ E & \text{if } 1 \geq ART_i > 0.67 \\ F & \text{else} \end{cases} \quad (5-1)$$

where,

ART_i is the available reaction time in s/veh

LoS_{arti} is the road LoS based on ART

The calculation of the ART is by utilising the BD and the AAG as in (4-50) and (5-2) - (5-8).

$$BD_i = \frac{S^2}{2 \cdot d_i} \quad (5-2)$$

$$d_i = \frac{S^2}{2 \cdot BD_i} \quad (5-3)$$

$$BT_i = \frac{S}{d_i} \quad (5-4)$$

where,

BD_i is the required braking distance to bring the vehicle to a standstill in m

BT_i is the required braking time to bring the vehicle to a standstill in s

d_i is the deceleration rate in m/s^2

S is the average traffic-flow speed in m/s

Now, by substituting (5-3) for d_i in (5-4), it resulted in (5-5)

$$BT_i = \frac{S}{\frac{S^2}{2 \cdot BD_i}} \quad (5-5)$$

where,

BD_i is the required braking distance to bring the vehicle to a standstill in m

BT_i is the required braking time to bring the vehicle to a standstill in s
 S is the average traffic-flow speed in m/s

Therefore, by eliminating the vehicles' speed from the nominator and the denominator, equation (5-5) leads to (5-6).

$$BT_i = \frac{2*BD_i}{S} \quad (5-6)$$

Now, after calculating the required BT_i , the author required to calculate the ART_1 by calculating the ART Distance (ARD_1), and the ARD_1 is equal to the remaining average available PC gap after deducing the required BD_1 from AAG (4-50), as in (5-7). Therefore, the author has calculated the ART_i by utilizing (5-7) (5-8).

$$ARD_1 = AAG - BD_1 \quad (5-7)$$

$$ART_1 = \frac{ARD}{S} \quad (5-8)$$

where,

ARD_i is the remaining average available PC gap after deducing the required BD_i in s

ART_i is the available reaction time in s

BD_i is the required braking distance to bring the vehicle to a standstill in m

AAG is the average available gap between the following and the leading vehicle in traffic flow in m

S is the average traffic-flow speed in m/s

According to (5-5) - (5-8), the ART and Available Braking Distance (ABD) are inversely proportional to BD and RT, respectively. Therefore, the results from (5-8) could also reflect the limited ABD effect. For example, if the driver spent the maximum RT of 2.5s, then the ABD will not be sufficient at LoS_{arti} of B and lower and in case of an accident, the driver would not have enough time and space to slow down to bring the vehicle to a stand-still.

The LoS_{asdi} method requires utilising the BD_i and the distance equivalent to the driver's RD_i , as in (5-2) and (5-9).

The measure of the LoS_{asdi} is according to the ratio of the AAG to the SD_i as in (5-7) - (5-8). When the SD ratio equals one, the AAG is sufficient for the driver to slow down the vehicle safely to a stand-still and avoid crashing the leading vehicle, which satisfies the LoS-D as in (5-9).

The author has chosen the LoS_{asdi} threshold values in (5-9) to represent the available SD_i of equal or greater than the minimum SD_i necessary to avoid crashing the leading vehicle at D- LoS_{asdi} . Therefore, the RT_i for the LoS_{asdi} assessment is at 1.86 s, where the driver has average competency and considers the reaction to an expected situation on the road.

$$d_i = \frac{S}{t} \quad (5-9)$$

where,

d_i is the deceleration rate for a vehicle of type i in m/s^2

S is the flow speed of vehicle type i in m/s

t is the time elapsed in s

Now, by substituting (5-9) for d_i in (5-2) and substitute RD_i for BD_i , the author obtained the RD_i , as in (3-11). The more accurate approach is to calculate the ABD_i , by deducting the RD_i from the AAG, as in (5-10)

$$ABD_i = AAG - RD_i \quad (5-10)$$

where,

RD_i is the reaction distance in m/veh

ABD_i is the average available braking distance in m/veh

AAG is the average available gap between the following and the leading vehicle in traffic flow in m/veh

The LoS method in (5-13) depends on the required SD_i in (5-11), and by calculating the ratio of AAG to the SD_i as in (5-12), the author can calculate the LoS_{asdi} as in (5-13).

$$SD_i = RD_i + BD_i \quad (5-11)$$

$$SDR_i = \frac{AAG}{SD_i} \quad (5-12)$$

where,

RD_i is the reaction distance in m/veh ,

BD_i is the required braking distance to bring the vehicle to a standstill in m ,

SD_i is the safe SD in m ,

SDR_i is the ratio of AAG to the required SD in m/m ,

AAG is the average available gap between the following and the leading vehicle in traffic flow in m/veh

$$LoS_{asdi} = \begin{cases} A, & SDR_i \geq 4 \\ B, & 4 > SDR_i \geq 3 \\ C, & 3 > SDR_i \geq 2 \\ D, & 2 > SDR_i \geq 1 \\ E, & 1 > SDR_i \geq 0.75 \\ F, & \text{else} \end{cases} \quad (5-13)$$

where,

SDR_i is the ratio of AAG to the required SD in m/m

LoS_{asdi} is the LoS based on available SD

5.3.2 Risk of sustaining severe injuries or death

The second contribution is the development of road LoS based on the risk of severe injury (LoS_{rsii}) and the risk of death (LoS_{rdi}). To estimate the difference of impact between a PC and a non-PC, the author calculated the impact factor (IF) that represents the effect of heavier vehicles on the level of impact pressure, as in (5-14) – (5-16). Equations (5-14) – (5-16) allow the author to determine the speed of the vehicle at the moment of the impact as in (5-17). By utilising the assessment results from (Lloyd 2015) and the Impact Speed (IS_i) from (5-17), the author has determined the road's LoS_{rsii} and LoS_{rdi} as in (5-18)-(5-19). The estimation of IS_i considers the distance of the pedestrian from the approaching vehicle. Thereby, the author utilises the Passenger Distance Ratio (PDR) (It is the ratio of the distance of the pedestrian from the approaching vehicle to the AAG) that ranges from 0.25 to 1 as in (5-19)-(5-20).

$$F_i = P_i \times A_i \quad (5-14)$$

$$P_i = \frac{F_i}{A_i} \quad (5-15)$$

$$IF_i = \frac{P_i}{P_1} \quad (5-16)$$

$$IS_i = \begin{cases} 0, & (AAG \times PDR - BD_i + L_i) \geq 0 \\ ATs - \sqrt{(AAG \times PDR \times 2 \times d_i)} \times 3.6, & (AAG \times PDR - BD_i + L_i) < 0 \\ 0, & ATs - \sqrt{(AAG \times PDR \times 2 \times d_i)} \times 3.6 < 0 \\ ATs - \sqrt{(AAG \times PDR \times 2 \times d_i)} \times 3.6, & \text{else} \end{cases} \quad (5-17)$$

where,

F_i is the force of impact of vehicle type i in N

P_i is the impact pressure of the crash of vehicle type i in Pa

A_i is the area of the surface of the impact of vehicle type i in m^2

IF_i is the ratio of the impact pressure of vehicle type i to the impact pressure of a PC in Pa/Pa

PDR is the ratio of the distance of the pedestrian from the vehicle to the AAG

IS_i is the impact speed of vehicle type i in km/h

The author has utilised the threshold values that were concluded by Tefft (2013) for LoS_{sii} and LoS_{di} , as in (5-18) and (5-19), Tefft (2013) obtained these thresholds by empirical assessment. The threshold values represent the vehicle impact speed when hitting a pedestrian according to the probability of causing a severe injury or death (Tefft 2013).

Tefft (2013) concluded that the average risk of severe injury for a pedestrian struck by a PC reaches 10%, 25%, 50%, 75%, and 90% at an IS of 25.8km/h, 37km/h, 49.9km/h, 62.8km/h, and 74km/h, respectively, and the average risk of death for a pedestrian reaches 10%, 25%, 50%, 75%, and 90% at an IS of 37km/h, 51.5km/h, 67.6km/h, 80.5km/h, and 93.3km/h, respectively.


$$LoS_{sii} = \begin{cases} A, & IS_i * IF_i \leq 25.8 \\ B, & IS_i * IF_i \leq 37 \\ C, & IS_i * IF_i \leq 49.9 \\ D, & IS_i * IF_i \leq 62.8 \\ E, & IS_i * IF_i \leq 74 \\ F, & IS_i * IF_i > 74 \end{cases} \quad (5-18)$$

$$LoS_{di} = \begin{cases} A, & IS_i * IF_i \leq 37 \\ B, & IS_i * IF_i \leq 51.5 \\ C, & IS_i * IF_i \leq 67.6 \\ D, & IS_i * IF_i \leq 80.5 \\ E, & IS_i * IF_i \leq 93.3 \\ F, & \text{else} \end{cases} \quad (5-19)$$

where,

- F_i is the force of impact of vehicle type i in N
- IF_i is the ratio of the impact pressure of vehicle type i to the impact pressure of a PC in Pa/Pa
- IS_i is the impact speed of vehicle type i in km/h
- LoS_{di} is the road LoS for the risk of death of vehicle type i
- LoS_{sii} is the road LoS for the risk of sustaining a severe injury of vehicle type i

FIGURE 5-7 shows three types of vehicles and their Safe Stopping Time (SST), RT, and Safe Braking Time (SBT) according to their drivers' level of BCL of 100% or 50%.



	PROFESSIONAL TO NON-PROFESSIONAL DRIVERS		
SAFETY STOPPING TIME	2.68-4.42 sec	2.81-4.6 sec	5.28-9.28 sec
REACTION TIME	1.13-1.86 sec	1.13-1.86 sec	1.13-1.86 sec
SAFETY BRAKING TIME	1.55-2.56 sec	1.68-2.74 sec	4.15-7.42 sec

FIGURE 5-7: Vehicles types and their stopping time, RT, and braking time according to the drivers' competency levels (Makki 2019c)

For example, if the pedestrian position is at a PDR equals to 1, the driver will have enough time to slow down the vehicle to a standstill if he/she has already kept the minimum safe SD with the leading vehicle. On the other hand, if the pedestrian position is at a PDR equal to 0.25, the driver will only have less than the required RT time for

professional drivers, and there will be no time for braking. Equation (2-28) shows the relationship between speed, deceleration, and time elapsed.

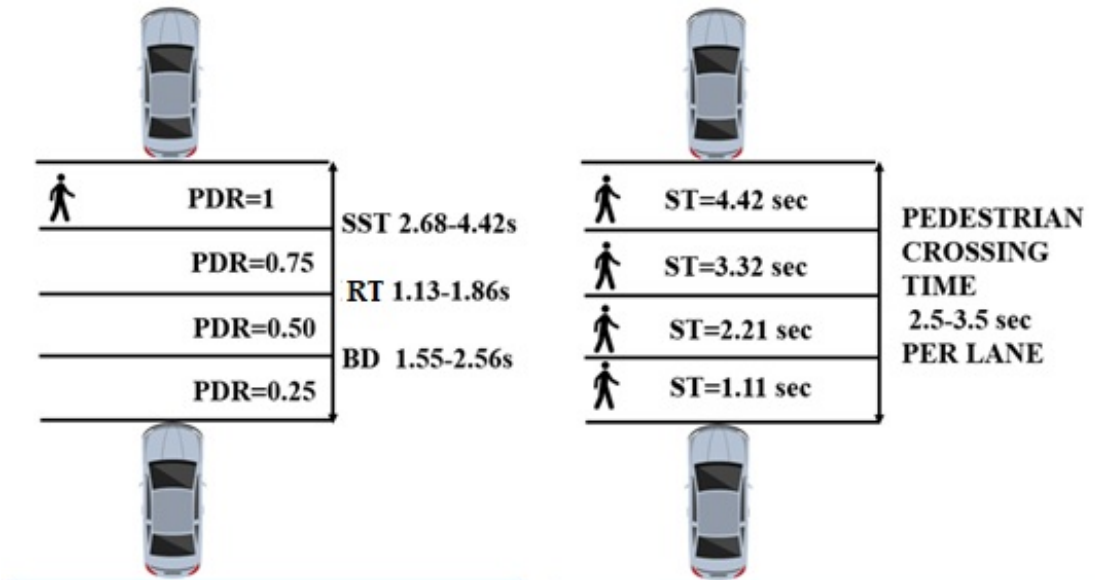


FIGURE 5-8: Diagram of the pedestrian position from the approaching vehicle and the available stopping time based on the pedestrian's position (Makki 2019c)

According to the BD required to slow down the vehicle to a standstill, the deceleration rate is 6.98 m/s^2 , and by assuming that the deceleration rate will be constant during the entire braking process, the author can estimate the vehicle speed at all four positions, as shown in FIGURE 5-8 and (5-17). For example, if the vehicle is travelling with a speed of 64.37 km/h and the driver starts braking after an RT of 1.86 s , the driver will be able to reduce the vehicle's speed to 55.57 km/h at a PDR of 0.5 and reduce the vehicle's speed to 27.81 km/h at a PDR of 0.75 and 0 km/h at a PDR of 1 . FIGURE 5-8 shows a diagram describing the pedestrian's position from the following car and SST available to slow down the vehicle.

The author has surveyed intersections zebra pedestrian crossings, and the purpose of the survey is to determine the time required for pedestrians of different ages and health to cross the road; and the author assessed several roads with two, three, four, and five lanes and with lane widths between $2.7\text{-}3.6 \text{ m}$ (Rogers 2016). In addition, the author has conducted a field survey to assess the time required to cross the road. There are more details on the survey in chapter six. The survey findings showed that the pedestrians require an average of $2.5\text{-}3.5 \text{ s}$ to cross the road lane according to its width, age, and pedestrian's health.

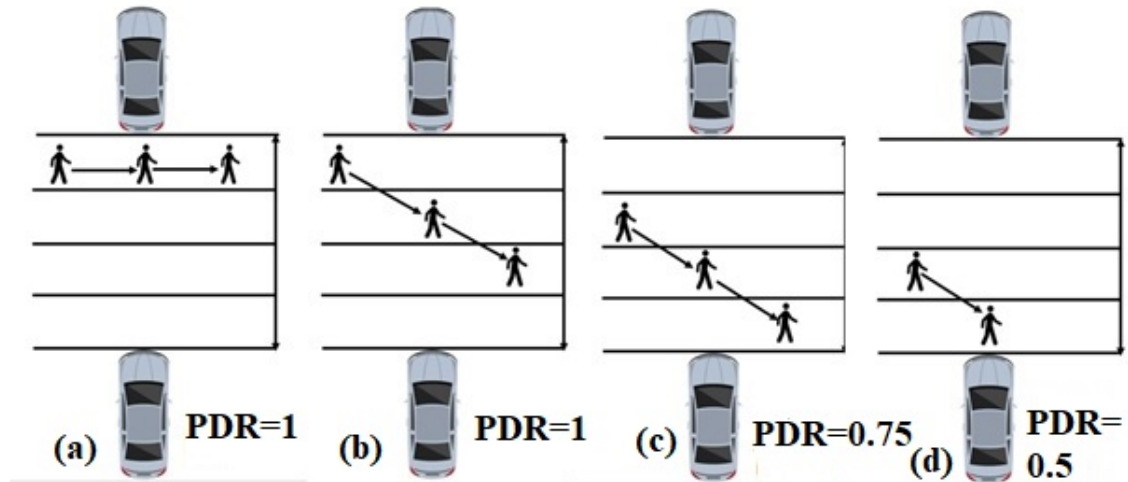


FIGURE 5-9: Four scenarios of pedestrians' crossing position based on the PDR value (the author has created this figure) (Makki 2019c)

Therefore, the pedestrian crossing scenario in FIGURE 5-9a would only work if the following and leading vehicles are in a standstill state. If the vehicles are moving with a speed of 64.37 km/h, then the pedestrian will move from PDR of 1 to PDR of 0.75 to PDR of 0.5 when crossing the road as shown in FIGURE 5-9b. Therefore, a driver with BCL=100% will stop the vehicle without crashing the leading vehicle or run over a pedestrian.

If the driver with BCL=50%, he/she will require higher RT and BT and would only be able to reduce the vehicle's speed to 27.81km/h. Thereby, the author can estimate the LoS for PCs moving at a road with an average speed of 64.37km/h for the pedestrian crossing positions in the scenarios shown in FIGURE 5-9b-d by utilising (5-18) –(5-19). The results in subsection 5.4 are for all four types of vehicles, and the LoS estimation will be different for every type of vehicle and every situation (severe injury or death). Due to the maximum speed limit of 64.37km/h and according to (5-18) and (5-19), the worse LoS_{sij} that can be is LoS-E and the worse LoS_{di} that can be is LoS-C, and the author will substantiate it in the results in subsection 5.4.

5.4 FINDINGS

The results in FIGURE 5-10 show that the LoS_{art} is at F-Level during the hours of 08.00-09.00 hours and the hours of 13.00-19.00 hours for HGVr and HGVa and during the hours of 08.00-9.00 and hours 17.00-18.00 for LGVs, and only during the hours of 17.00-18.00 for PC. The results for PCs and LGVs in FIGURE 5-10 reflect the same

pattern as in FIGURE 5-1 for peak times. The traffic volume at these hours has exceeded the capacity, as shown in FIGURE 5-1 and caused a reduction in the gap and the road's available capacity.

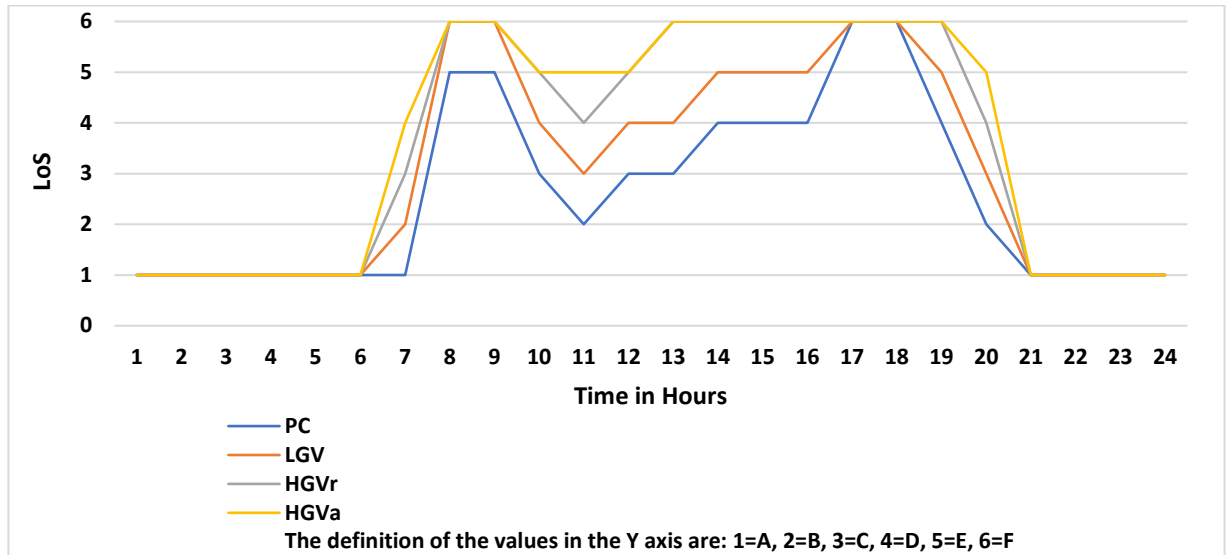


FIGURE 5-10: The LoS based on the ART at an average flow speed of BR

The reason for this prolonged period of F-Level is the short gap available between following and leading vehicles. The HGVR and HGVA are longer and heavier than the rest of the traffic vehicle composition. Thereby, they occupy a larger space than PCs and LGVs and require a longer gap to decelerate the HGV and bring it to a standstill. Therefore, there will be insufficient time to react to an incident on the road and avoid an accident.

The ART LoS method estimates the available average RT after deducting the required BT. Therefore, the higher the speed, the higher the BT and the lower is the ART. Therefore, on the one hand, the rescheduling of HGVA will reduce the traffic flow density at peak hours that increase the AAG at these hours, and on the other hand, it increases the speed of the traffic flow will, in turn, increase the required BT. Therefore, the rescheduling of HGVA will lead to conflicting results that may improve the LoS at some hours and worsen the LoS at other hours, as shown in FIGURE 5-10, FIGURE 5-11, and

TABLE 5-5.

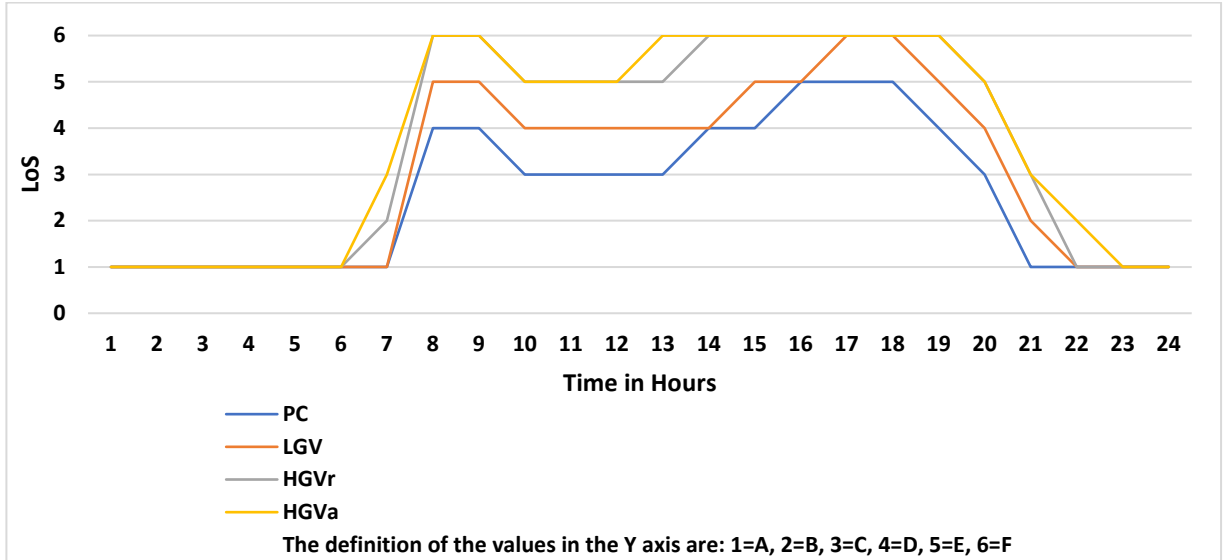


FIGURE 5-11: The LoS based on the ART at an average flow speed AR

TABLE 5-5: The change in LoS_{art} for four types of vehicles BR and AR

LoS _{art}	Status	LoS-A	LoS-B	LoS-C	LoS-D	LoS-E	LoS-F
PC	BR	11 hours	2 hours	3 hour	4 hours	2 hours	2 hours
	AR	11 hours	0 hours	5 hours	5 hours	3 hours	0 hours
LGV	BR	10 hours	1 hour	2 hours	3 hours	4 hours	4 hours
	AR	10 hours	1 hour	0 hours	6 hours	5 hours	2 hours
HGVR	BR	10 hours	0 hours	1 hour	2 hours	2 hours	9 hours
	AR	9 hours	1 hour	1 hour	0 hours	5 hours	8 hours
HGVA	BR	10 hours	0 hours	0 hours	1 hour	4 hours	9 hours
	AR	8 hours	1 hour	2 hours	0 hours	4 hours	9 hours

The author has set the required RT value to 2.41s at BCL of 50% and 1.68s at BCL of 100%, while all the results of ART for HGVs BR and AR at the hours of 8.00-19.00 are less than 2.41s apart from the ART for PCs BR at 11.00 hours that exceeded the required value by 0.3s and at the hours 10.00 and 12.00 where the ART reached 2.41s, as shown in FIGURE 5-12. Thus, the ART for HGVs has not even reached the RT at BCL of 100%. The rescheduling made a minor improvement to the ART, e.g., the ART for HGVA have increased AR at the hour 8.00 by 0.36s and at the hour of 18.00 by 0.21s, as shown in FIGURE 5-12. Therefore, the LoS_{art} that meets the required RT at a BCL of 100% lies between LoS_{art}-B and LoS_{art}-C, and the LoS_{art} that meets the required RT at BCL of 50% lies between LoS_{art}-A and LoS_{art}-B.

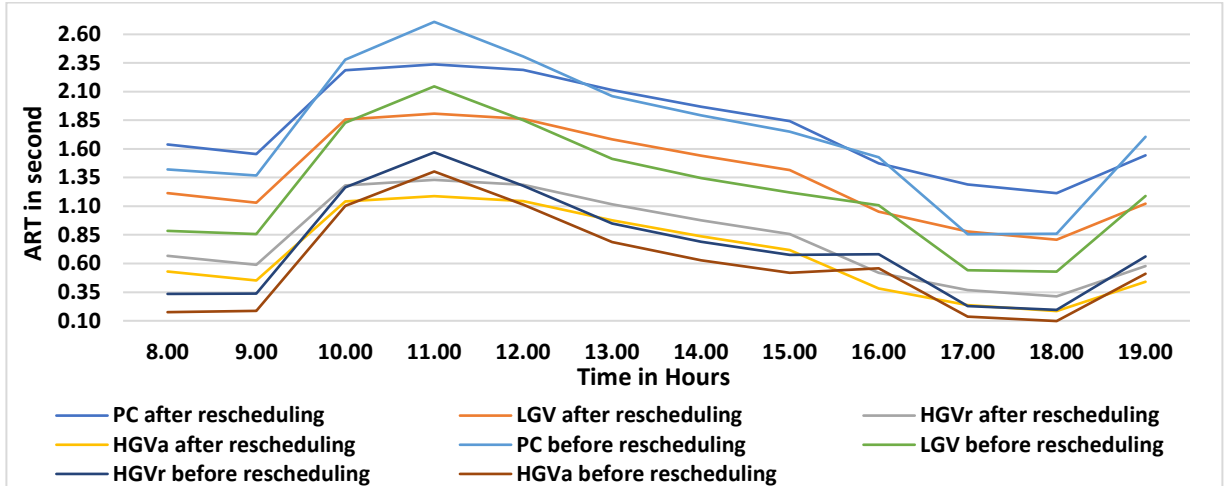


FIGURE 5-12: ART values BR and AR at the hours of 8.00-19.00

The ASD method results in FIGURE 5-13 show the same pattern as in FIGURE 5-13, and the only time that the traffic provides a sufficient gap for HGVs is at hours 00.00-06.00 hours and 21.00-24.00 hours. The lowest LoS provided by the ASD method at hours of 8.00-19.00 are LoS-D for PCs and LoS-E for LGVs and HGVs, and the lowest LoS provided by the ART method at hours of 8.00-19.00 are LoS-B for PCs, LoS-C for LGVs, LoS-D for HGVR, and LoS-E for HGVa.

The latter results show that the ASD method has higher sensitivity than the ART method. However, the ASD method is similar to the ART method regarding the rescheduling impact because it estimates the required SD compared to the AAG. Therefore, the rescheduling will not necessarily improve LoS, as shown in FIGURE 5-13, FIGURE 5-14, and TABLE 5-6.

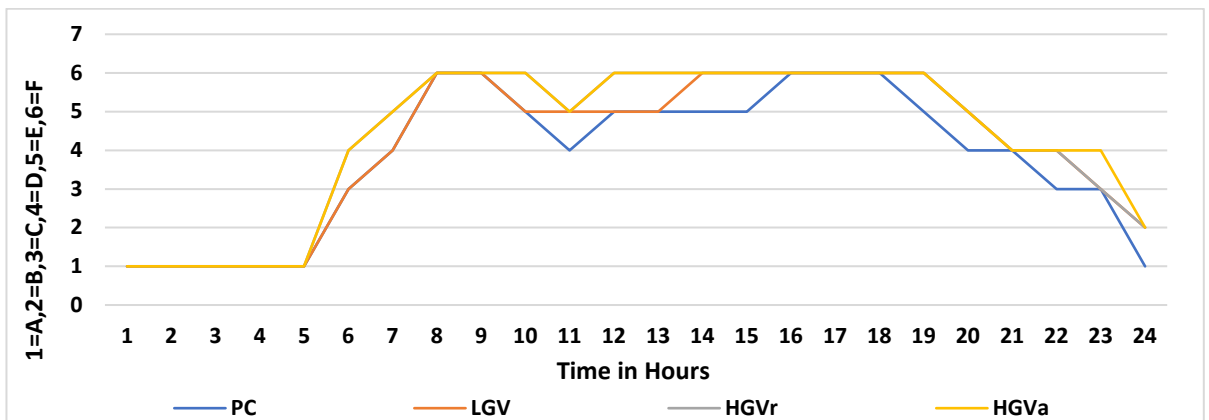


FIGURE 5-13: LoS based on the ASD at an ATS BR

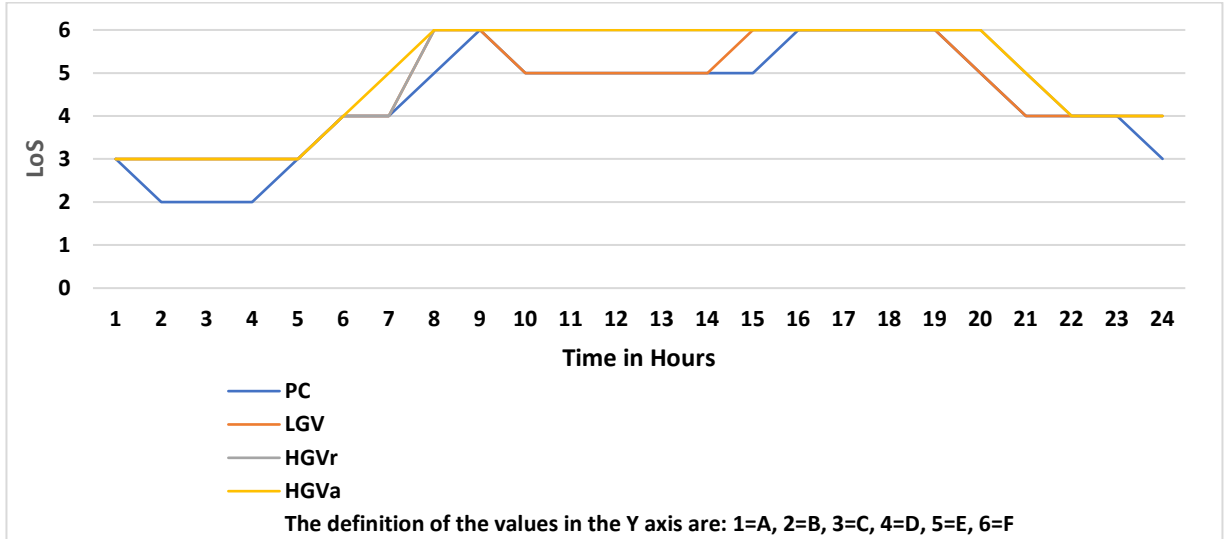


FIGURE 5-14: LoS based on the ASD at an average flow speed AR

TABLE 5-6: The change in LoS_{asd} for four types of vehicles BR and AR

LoS _{asd}	Status	LoS-A	LoS-B	LoS-C	LoS-D	LoS-E	LoS-F
PC	BR	7 hours	2 hours	2 hours	4 hours	2 hours	7 hours
	AR	0 hours	6 hours	10 hours	3 hours	3 hours	2 hours
LGV	BR	6 hours	3 hours	4 hours	4 hours	5 hours	2 hours
	AR	0 hours	6 hours	7 hours	5 hours	6 hours	0 hours
HGVR	BR	10 hours	4 hours	6 hours	2 hours	0 hours	2 hours
	AR	10 hours	6 hours	6 hours	2 hours	0 hours	0 hours
HGVA	BR	8 hours	11 hours	2 hours	1 hour	0 hours	2 hours
	AR	0 hours	22 hours	2 hours	0 hours	0 hours	0 hours

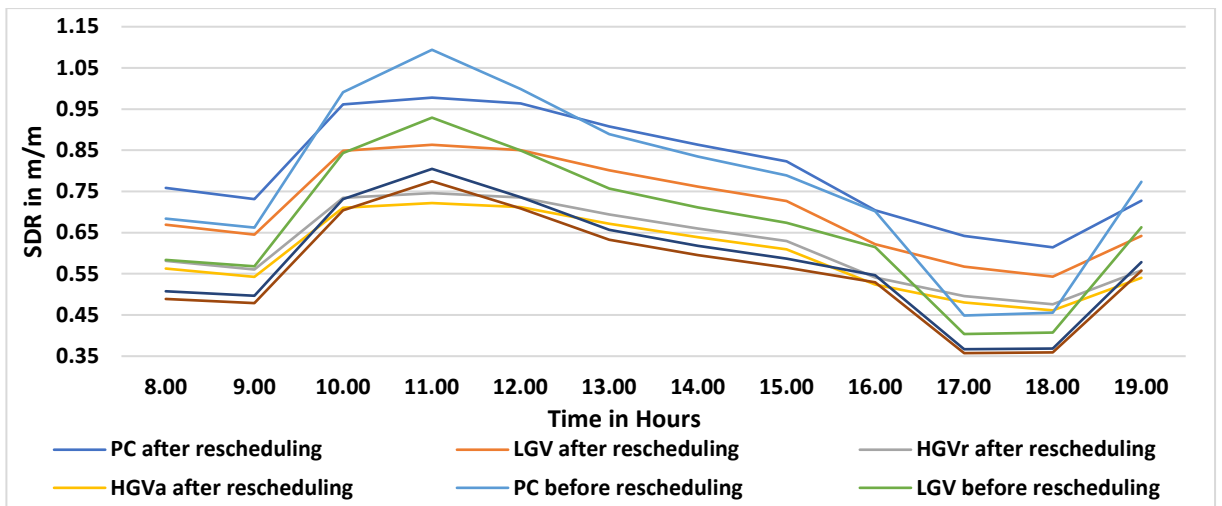


FIGURE 5-15: SDR values BR and AR HGVA

The minimum required SDR to secure enough space for the driver to bring the vehicle to a stand-still is 1, and the LoS_{asd} assessment by LoS_{asd}-D represents it, and it has not been reached by all the LoS_{asd} results apart from the hour 11.00 for PCs BR, as shown in FIGURE 5-15.

The ASD method considers sufficient RT and BD, while the ART method considers the RT after securing the required BD. Therefore, the ART method is more practical than the ASD because RT comes before braking. The results of LoS for the Risk of Sustaining a Severe Injury (LoS_{rsii}) show the common-sense relationship between the distance of the pedestrian from the vehicle and the risk of sustaining a severe injury. The closer the pedestrian is to the vehicle, the higher the risk that the driver will not be able to decelerate the vehicle to stand still or reduce the speed to a level that does not cause severe injuries. The results in FIGURE 5-16 show that due to the relatively high braking performance of PCs and LGVs considering their GM, the available gap is sufficient to avoid causing a pedestrian a sustained injury even at a PDR of 0.25.

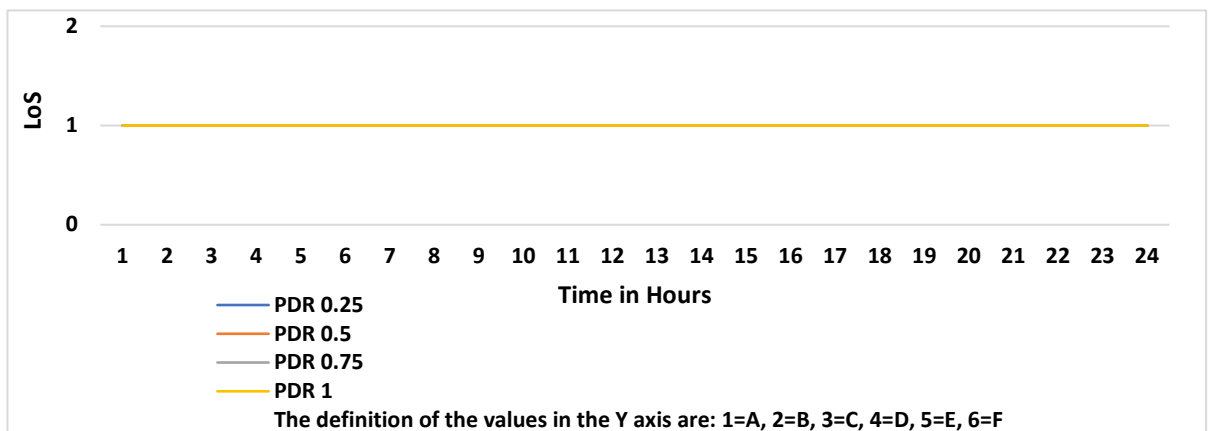


FIGURE 5-16: LoS based on the risk of a pedestrian sustaining a severe injury for PCs and LGVs at a variable PDR

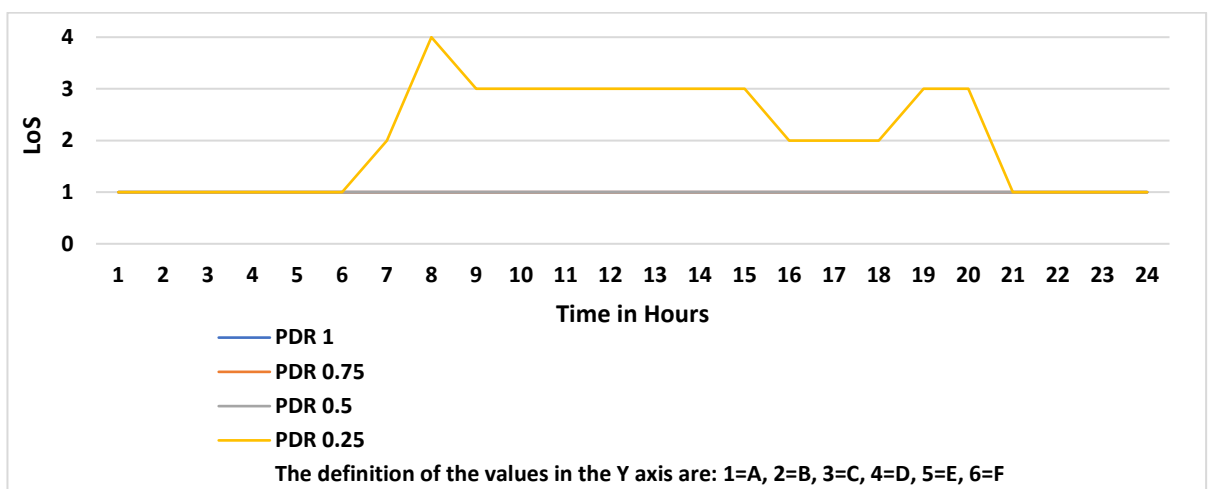


FIGURE 5-17: LoS based on the risk of a pedestrian sustaining a severe injury by an HGVR at a variable PDR BR

However, the results in FIGURE 5-17 and FIGURE 5-18 show that, unlike the PCs and LGVs, the HGVs will not have enough AAG to decelerate and avoid LoS_{arti} and LoS_{asdi} when the ATS increases, the LoS will deteriorate and when the ATS decreases the LoS improves.

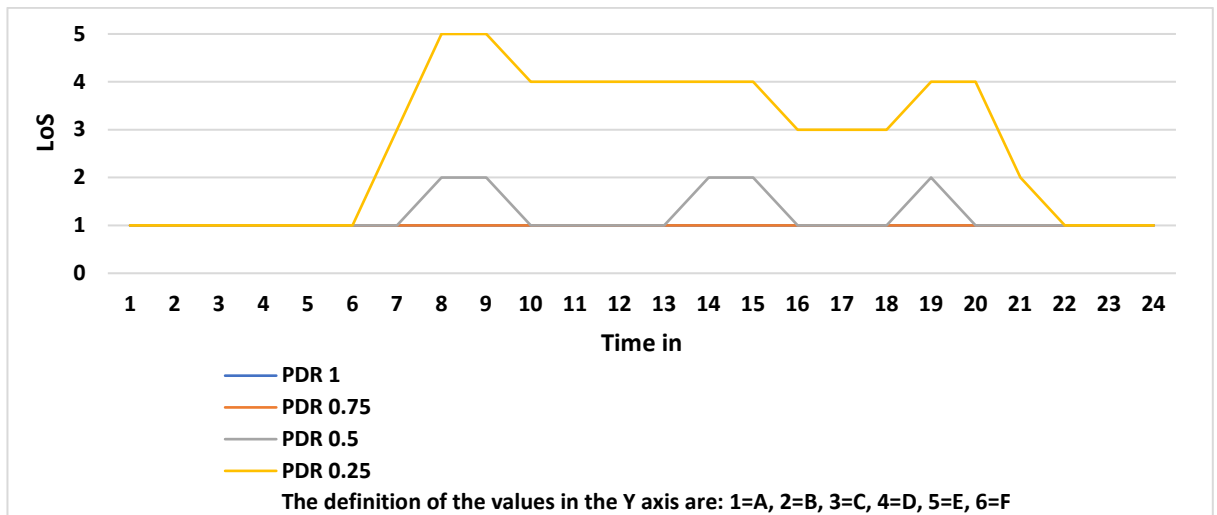


FIGURE 5-18: LoS based on the risk of a pedestrian sustaining a severe injury for HGVa at a variable PDR BR

The HGVr will the pedestrian's position is at a PDR of 0.25 end of the available gap (where the PDR=1), the risk of sustaining severe injuries would be still high for HGVs compared to PCs LGVs. The high risk is due to the insufficiently available gap at high traffic flow density, and the results confirm that the risk of having a severe injury gets higher when the vehicle is larger and heavier.

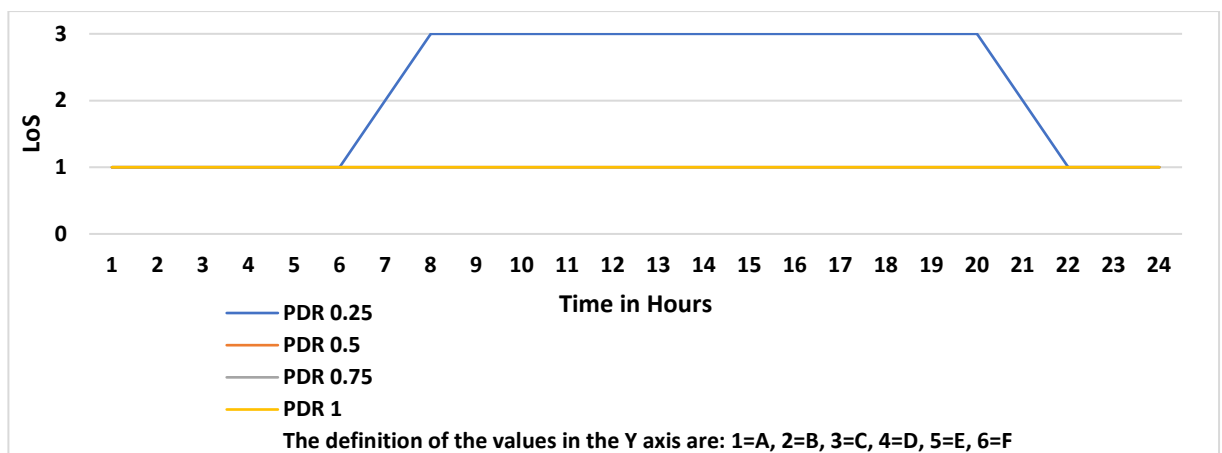


FIGURE 5-19: LoS based on the risk of a pedestrian sustaining a severe injury by an HGVr at a variable PDR AR

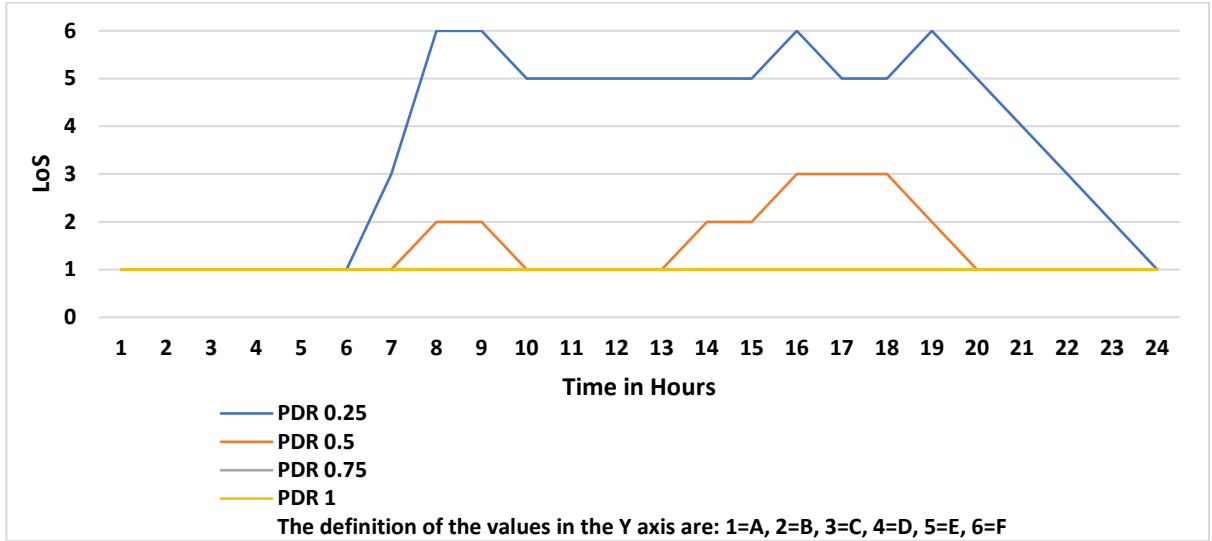


FIGURE 5-20: LoS based on the risk of a pedestrian sustaining a severe injury for HGVA at a variable PDR AR

Rescheduling the HGVA has the same impact on the risk of sustaining injury method as in the ART and ASD methods. The rescheduling will increase the average speed at peak hours due to the removal of HGVA vehicles, increasing the required deceleration time to reduce the vehicle's speed to a safe level. Therefore, rescheduling leads to a worsened LoS_{rsi} for HGVs, as shown in FIGURE 5-17, FIGURE 5-18, FIGURE 5-19, FIGURE 5-20, and TABLE 5-7.

TABLE 5-7: The number of hours that each LoS_{rsi} level for all-day, LoS levels of A-F refer to section 5.1

LoS_{rsi}	Status	LoS-A	LoS-B	LoS-C	LoS-D	LoS-E	LoS-F
HGVr at a PDR of 0.5	BR	24 hours	0 hours	0 hours	0 hours	0 hours	0 hours
	AR	22 hours	2 hours	0 hours	0 hours	0 hours	0 hours
HGVr at a PDR of 0.25	BR	10 hours	4 hours	9 hours	1 hour	0 hours	0 hours
	AR	8 hours	2 hour	1 hour	13 hours	0 hours	0 hours
HGVA at a PDR of 0.5	BR	19 hours	5 hours	0 hours	0 hours	0 hours	0 hours
	AR	16 hours	5 hours	3 hours	0 hours	0 hours	0 hours
HGVA at a PDR of 0.25	BR	9 hours	1 hour	4 hours	8 hours	1 hour	0 hours
	AR	7 hours	1 hour	2 hours	1 hour	9 hours	4 hours

The results of the risk of death LoS method for BR and AR, as shown in FIGURE 5-21, FIGURE 5-22, FIGURE 5-23, FIGURE 5-24, and TABLE 5-8, have shown the same pattern of effect as the risk of sustaining a severe injury.

The risk of death also depends on the speed, AAG, and deceleration performance of vehicles and affected by the required SD. According to FIGURE 5-15, the highest SDR for HGVR and HGVA have reached 0.8 and 0.77 BR at the hour 11.00, respectively, and AR 0.75 and 0.72, respectively.

Therefore, only the HGVs have a high risk of causing pedestrian death. It is due to their heavyweight, massive structure, and lower deceleration performance.

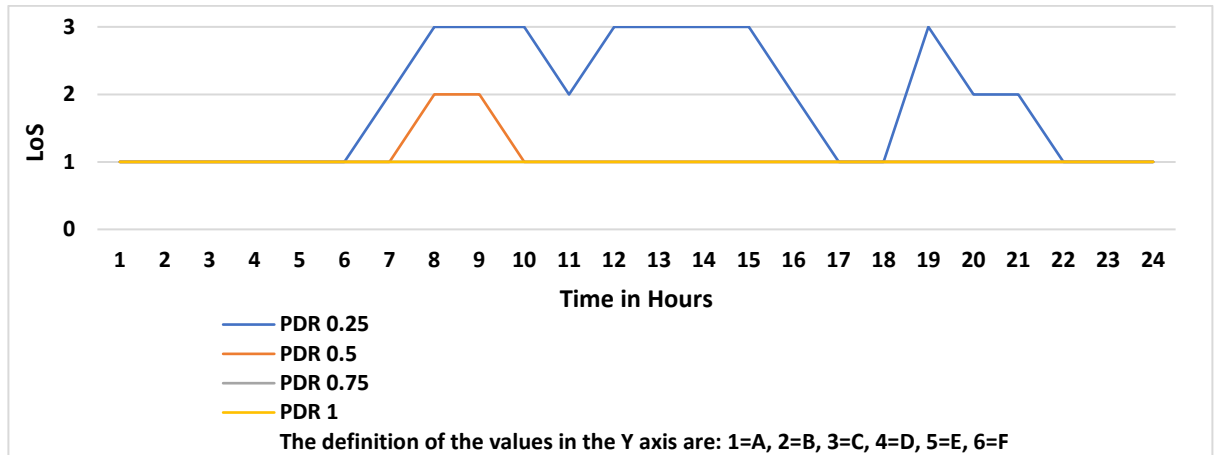


FIGURE 5-21: LoS based on the risk of a pedestrian death for HGVR at a variable PDR BR

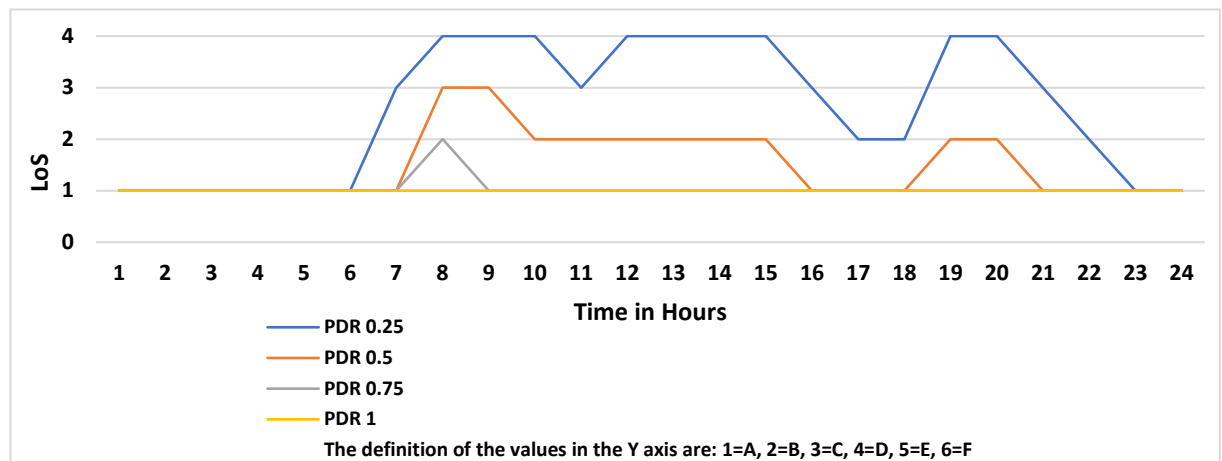


FIGURE 5-22: LoS based on the risk of a pedestrian death for HGVA at a variable PDR BR

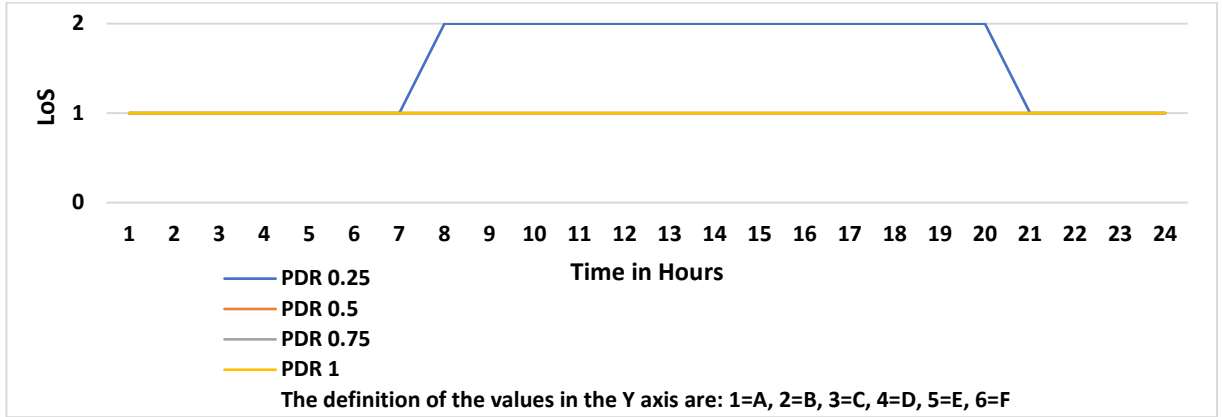


FIGURE 5-23: LoS based on the risk of a pedestrian death for HGVR at a variable PDR AR

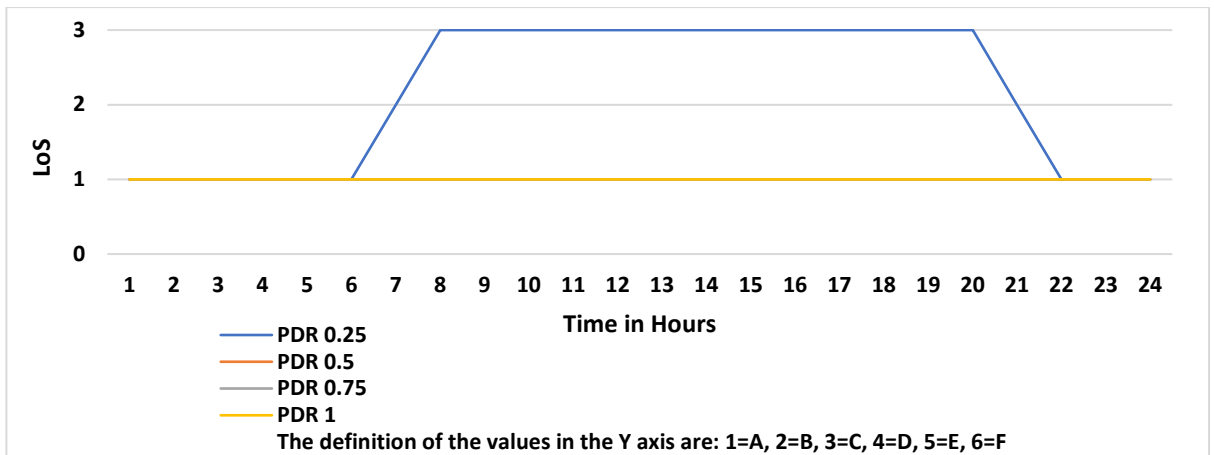


FIGURE 5-24: The LoS based on the risk of a pedestrian death for HGVA at a variable PDR AR

TABLE 5-8: The number of hours that each LoS_{rtdi} level for all-day, LoS levels of A-F refer to section 5.1

LoS _{rtdi}	Status	LoS-A	LoS-B	LoS-C	LoS-D	LoS-E	LoS-F
HGVR	BR	14 hours	10 hours	0 hours	0 hours	0 hours	0 hours
	AR	11 hours	13 hours	0 hour	0 hours	0 hours	0 hours
HGVA	BR	10 hours	4 hours	10 hours	0 hours	0 hours	0 hours
	AR	9 hours	2 hours	13 hours	0 hours	0 hours	0 hours

The results in TABLE 5-7 and TABLE 5-8 show that the risk of sustaining a severe injury or death for passengers that are hit by HGVA vehicles increases at high-density traffic because of a deficiency in available gaps, but at the same time, the risk increases AR because the ATS will increase and leads to an increase in the safe gap. However, the author has considered an average adult and not children or elderly pedestrians in measuring the risk of causing severe injuries or death. Therefore, there must be further future research on the effect of accidents on children and the elderly.

5.5 SUMMARY

The AEB sensor is set based on the notion that three-quarters of all collisions occur at speeds less than 20mi/h. The intervention of the AEB a second before impact to reduce the effect of a crash can be sufficient to stop a PC with a speed of up to 15mi/h. By including a sufficient BCL and RT of the driver, the chances to prevent an accident will increase. The time required for a pedestrian to pass cross the approaching vehicle ranges from 1.66 to 2s, and the required gap between the leading and following vehicles

Rescheduling the container carriers to off-peak periods will not significantly reduce the risk of accidents because it will increase the average flow speed and increase the required safe gap between vehicles. By considering the available average gap between vehicles, the only solution to reduce the risk of accidents is to reduce the number of vehicles on the road to increase the available gap. The more vehicles on the street, the higher is the risk of having an accident.

5.6 CONTRIBUTION AND NOVELTY

As mentioned in section 5.1, in this research, the author has developed an LoS method that measures safety by utilising the HCM measuring levels of LoS. The method combines the British approach's aims and requirements for LoS and the measuring levels of the HCM approach for LoS. The method will determine the LoS for each type of vehicle and each situation (ART, available SD, sustaining a severe injury, and death). According to the literature review, the LoS measurements' methodologies always considered the road's LoS in general. In this research, the author considers the estimation of the LoS for each vehicle type separate and each road situation separate for each vehicle type.

The new LoS methods are unique because they provide the LoS with consideration to TF and speed and the vehicle type, GM, braking system, driver's RT, and BCL. The author has designed LoS methods to evaluate the safety of traffic according to individual types of vehicles. The new methodology will provide a planning and development tool to improve the accessibility of the road and reduce accidents, and brings about transportation performance.

Determining HGVs' impact on traffic safety allows planners and developers to limit HGVs' access to the road of interest or build a new road with HGV access only or PCs limited access. The methods also reduce congestion, prevent traffic jams, and improve drivers and logistics' driving standards and safety awareness.

Also, safety levels of roads can become available on the map, and local and national authorities can utilise these methods in futuristic plans to restrict some drivers from utilising specific roads according to their licence penalty points and behaviour and inform drivers of the safest route for their journey according to the type of vehicle, payload, weight, number of passengers, and the purpose of the journey.

CHAPTER SIX: MODEL'S SYSTEM AND DATA VALIDATION

6.1 INTRODUCTION

The utilisation of SDM will allow us to determine the available capacity and the effect of rescheduling container carriers in a qualitative and quantitative assessment. Researchers have utilised SDM in transportation. However, researchers have not utilised SDM to assess PCE before, as in section 2.9 of chapter two.

The expansion of the Liverpool container terminal increases the demand for road freight, and roads that connect the terminal with the city and the nearby cities will suffer from congestion. Therefore, local authorities either try to overcome this problem by building new roads, tunnels, adding extra lanes to existing roads, establishing consolidation centres, or utilising other modes of transport for freight transportation. However, to reach a feasible solution, the planners would require an accurate and efficient method of estimating HGVs' effect on road traffic flow.

We have chosen the road under investigation because of the ongoing expansion of the Liverpool container terminal. The data collection is from the DfT in the UK, conducted by ATCs. The utilised data holds the traffic flow of four vehicle categories based on the vehicle's length and their average traffic flow speed for every hour.

6.2 THE BUILDING OF THE SYSTEM DYNAMICS MODEL

The development of the system dynamic model requires conceptualisation, purpose, formulation, testing, and implementation (Albin 1997; Forrester 1980; Forda 2005):

6.2.1 Conceptualization

The conceptualisation of the model requires defining the purpose, the boundary, behaviour, and fundamental mechanism of the system:

6.2.1.1 Purpose

The purpose is to determine HGVs' effect on traffic flow and congestion by estimating the HGV's PCE. The author must assess the impact of variables such as aerodynamic resistance, braking system, driver's competency, load factor, and weather conditions on acceleration and deceleration performance. Any change in these variables could affect the value of PCE and congestion.

The goal is to develop policies that will improve system behaviour and provide solutions for the congestion problem by proposing rescheduling scenarios to port management and traffic control. Hence, this would lead to a better LoS and smooth delivery operation, reduce accidents and fatalities, and improve traffic flow operation.

6.2.1.2 Variable's Relationship

The purpose of this section is to describe the relationship between the variables C_{DAS} , PCE_{DAS} , ATS, EGR, RT, H, BCL, EP, $THGV_f$, FV_2 , FV_3 , FV_4 , TF, TF_{PCE} , and GM based on the formulas of these variables as follows:

1. H is directly proportional to ATS, GM, and RT and inversely proportional to BCL and C_{DAS}
2. C_{DAS} is directly proportional with ATS, EGR, EP, and $THGV_f$
3. PCE_{DAS} is directly proportional to TF, TF_{PCE} , GM, ATS and RT, and inversely proportional to BCL
4. $THGV_f$ is inversely proportional to ATS, FV_2 , FV_3 , FV_4 , and GM, directly proportional to EP

6.2.1.3 Mechanism

If an HGVA were removed from or inserted into an hour slot, then the PCE_{DAS4} for the current schedule will change for that hour's new traffic volume. This is because the determination of PCE_{DAS4} depends on the number of HGVA, and determining the feasible change in HGVA volume is dynamically affected by values of PCE_{DAS4} for every insertion or removal. Therefore, these dynamic relationships will create simultaneous equations where variables are dependent on each other on both sides of the equations. The author has utilised a system dynamics software called Vensim, which solves the model's simultaneous equations.

The presented model is part of a more extended model that involves hundreds of loops because it includes rescheduling of vehicles, speed prediction, and exploring road planning scenarios, as shown in section 4.6. Therefore, the author has only presented the following three dynamic loops, as in FIGURE 6-1

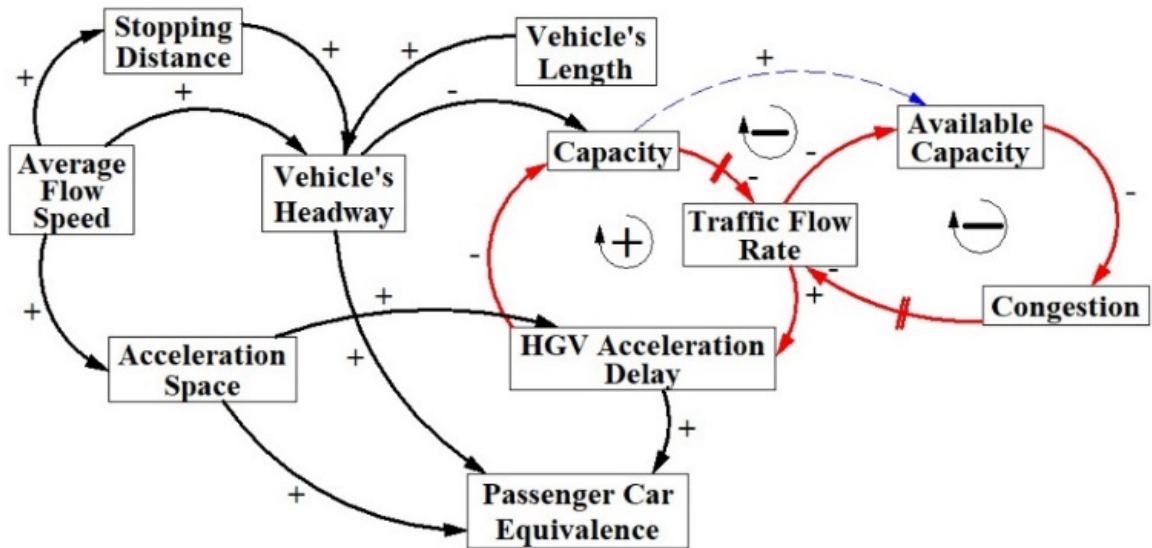


FIGURE 6-1: The developed system dynamics qualitative assessment's main causal loops due to HGVA rescheduling

This model's three balanced loops (negative loops) show the system's dynamic mechanism, and systems with balancing loops are controllable while supporting loops (positive loops) are uncontrollable. This model's users can use their PCE values, and they are not restricted by the deceleration and acceleration space PCE method. However, to maintain the system dynamics loops and mechanisms, they must update system variables when replacing the internally produced PCE with external PCE values.

The author has explored HGVs' rescheduling options that would accommodate the highest possible HGVs and meet the TEU capacity target while improving the traffic flow operation, LoS, ART, and PCE values and reducing or eliminating congestion peak hours. The dynamic rescheduling process would involve several variables and formulate four dynamic loops for rescheduling only HGVA. There are hundreds of causal loops in this model for rescheduling HGVA that will be available online. Therefore, the author has shown four main balance loops, as shown in FIGURE 6-1:

- Capacity → HGVA's Traffic volume → HGVA's Acceleration Delay Factor → Capacity
- HGVA's Traffic volume → Available road Capacity → Traffic congestion → HGVA's Traffic volume
- HGVA Acceleration Delay Factor → Capacity → Available Capacity → Congestion → HGVA's Traffic volume → HGVA's Acceleration Delay Factor
- Congestion → PCE Traffic Volume → Available Capacity → Congestion

TABLE 6-1 shows the variables that are part of dynamic loops and the number of loops in each variable. The results show that the number of loops for the variables AR is extremely higher than BR, and this is because the author utilized the ATS obtained from the ATC and did not estimate the ATS BR. FIGURE 6-2 shows the variables that contribute to the estimation of ATS AR, and FIGURE 6-3 shows the variables that the ATS contribute to AR. For example, FIGURE 6-2 shows that PCE_{DAS4a} , TFa , FV_{4a} , TF_{PCEa} , $THGV_{fa}$, $AFFSa$, and k_{pcea} contribute to the estimation of $ATSa$, and at the same time, the $ATSa$ contributes to the estimation of these variables, as shown in FIGURE 6-3.

TABLE 6-1: Model variables that are part of loops and the count of these loops BR and AR

Variables BR	Number of loops when utilising ATS_o	Number of loops when utilising ATS_{SDE}	Variables AR	Number of loops
EGR_b	3	126	EGR_a	626
HGV_{d2b}	1	66	HGV_{d2a}	251
HGV_{d3b}	1	66	HGV_{d3a}	251
HGV_{d4b}	1	66	HGV_{d4a}	394
$THGV_{fb}$	0	129	$THGV_{fa}$	552
PCE_{DAS2b}	1	47	PCE_{DAS2a}	167
PCE_{DAS3b}	1	47	PCE_{DAS3a}	167
PCE_{DAS4b}	1	59	PCE_{DAS4a}	370
C_{DASb}	0	0	C_{DASa}	487
$TFPCE_b$	3	153	$TFPCE_a$	662
$AFFS_b$	0	0	$AFFS_a$	438
FV_{4b}	0	0	FV_{4a}	642
ATS_b	0	180	ATS_a	813
H_{1b}	0	66	H_{1a}	315
H_{2b}	0	12	H_{2a}	45
H_{3b}	0	12	H_{3a}	45
H_{4b}	0	24	H_{4a}	120
FD_{1b}	0	44	FD_{1a}	210
FD_{2b}	0	8	FD_{2a}	30
FD_{3b}	0	8	FD_{3a}	30
FD_{4b}	0	8	FD_{4a}	40
k_{pceb}	0	52	k_{pcea}	137

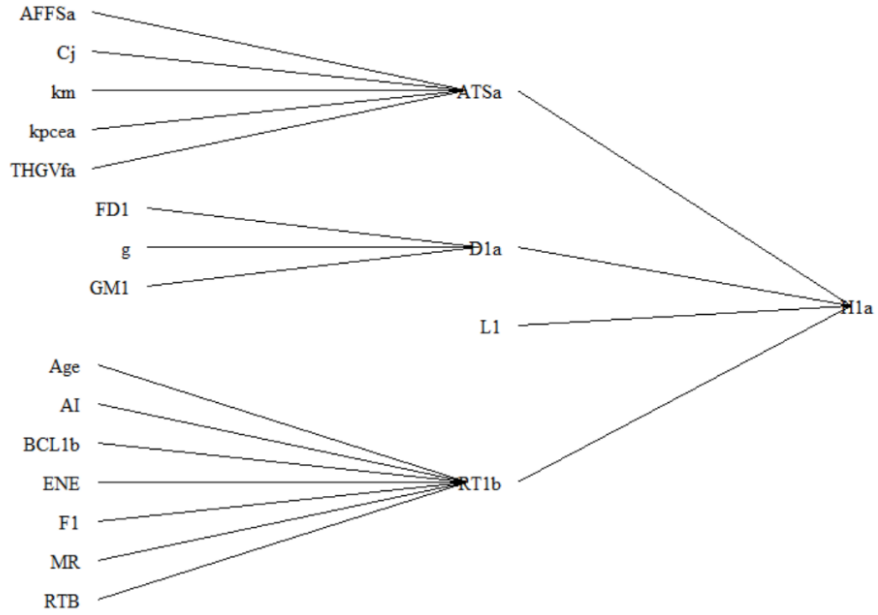


FIGURE 6-4: The variables that contribute to the calculation of the headway of a PC AR (The author has extracted this image from the SDM software, Vensim)

FIGURE 6-4 shows that $THGV_{fa}$, k_{pcea} , $AFFS_a$, and ATS_a contribute to the estimation of H_{1a} , and H_{1a} contributes to the estimation of HGV_{da} , and FV_{4a} , as shown in FIGURE 6-5. Therefore, H_{1a} contributes to the estimation of $THGV_{fa}$, k_{pcea} , $TFPCE_a$, $AFFS_a$, and ATS_a ,

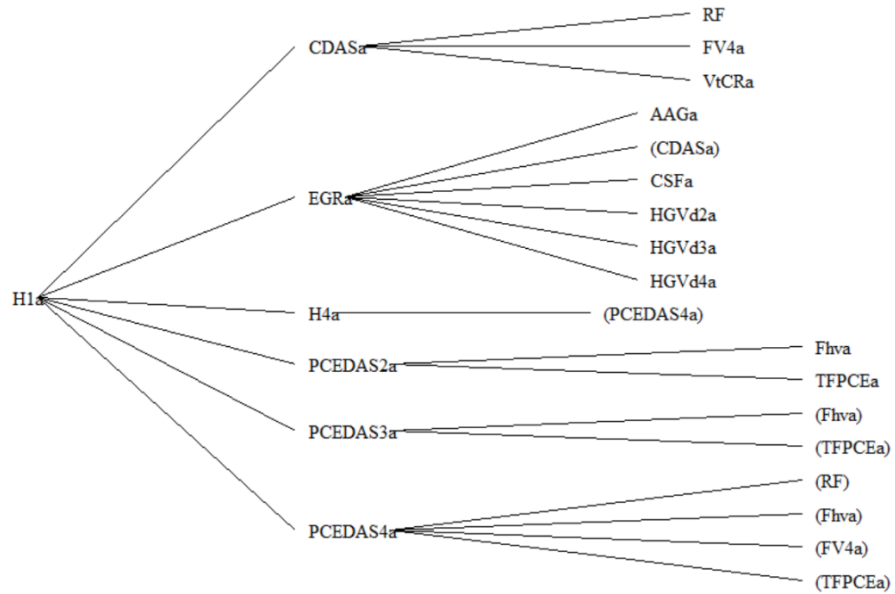


FIGURE 6-5: The variables that the headway of a PC contribute to AR (The author has extracted this image from the SDM software, Vensim)

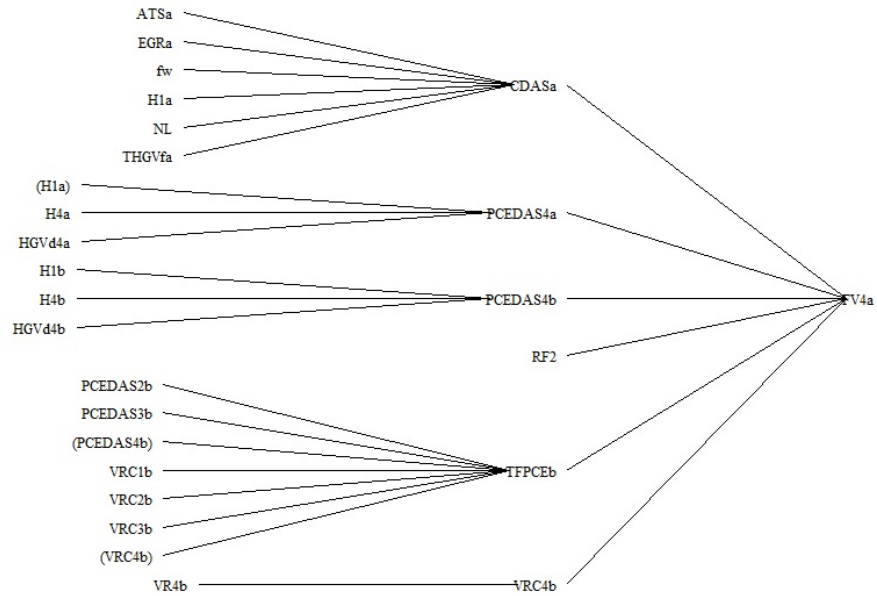


FIGURE 6-6: The variables the contribute to the rescheduling estimation of FV_{4a} (The author has extracted this image from the SDM software, Vensim)

This model can use their PCE values, and there is no restriction to the deceleration and acceleration space PCE method. However, to maintain the system dynamics loops and mechanisms, they must update system variables when replacing the internally produced PCE with external PCE values. The dynamic rescheduling considers the effect of increasing or decreasing the number of HGVa for every hour of the day on the total traffic volume, capacity, and generic PCE. The rescheduling of HGVa works by deducting the existing HGVa in PCE value from the current total traffic volume and adding the new distribution of HGVa in their generic PCE values to the traffic volume excludes the existing HGVa. The objective is to reduce the total traffic volume at peak hours, reduce the $VtCR$, and improve the LoS.

There are two approaches to rescheduling. If the aim is to achieve the first approach, then the HGVa AR target (FV_{4a}) should equal the average number of HGVa BR (FV_{4b}). Therefore, the author can determine the amount of shifted (removed from or inserted into the composite traffic flow) HGVa. If the aim is to achieve the second approach, the author can maintain the $VtCR$ value at ≤ 0.85 to ensure seamless flow, optimum flow speed, and avoid road congestion. For every removed or inserted HGVa, there will be changes in hourly HGVa that will result in dynamic changes in the EGR, average flow speed, ASO_i , HGV_{di} , $THGV_{di}$, $THGV_f$, $TFPCE_a$, PCE_{DAS_i} , and C_{DAS} due to changes in the HGVa traffic volume.

These changes will lead to dynamic loops that will force a recalculation for every single move. The rescheduling algorithms reflect the dynamic relationship between variables BR and AR. Therefore, if an HGVa was removed or added to an hour slot during rescheduling, then PCE_{DAS4b} for the current schedule will change to PCE_{DAS4a} for the new schedule for that hour. The determination of PCE_{DAS4a} depends on FV_{4a} , and the determination of feasible change in HGVa traffic volume is dynamically affected by values of PCE_{DAS4a} for every insertion or removal of an HGVa. Therefore, these dynamic relationships will create simultaneous equations where variables are dependent on each other on both sides of the equations.

6.2.2 Model Structure

The author designed the model's structure according to the system's nature and requirements. The system requires an estimation of the deceleration and acceleration performance impact on the road that the headway, HGV_d , and $THGV_f$ represent, as shown in FIGURE 6-7, FIGURE 6-8, and FIGURE 6-9. Rescheduling HGVa vehicles requires estimating the ATS BR and AR to utilise the PCE_{DAS4} BR and AR, as shown in FIGURE 6-10 and FIGURE 6-11, and also because the rescheduling formulas requires the value of C_{DAS} AR.

As mentioned before, in chapter three, the mathematical model contains simultaneous equations where two or more equations share dependent variables. A dependant variable can be a function of other dependent variables (Martin 2013); for example, the ATS obtained from ATC is an independent variable. Therefore, it is the function of a dependent variable, and the ATS becomes a dependent variable the moment the author estimate it. The same effect happens to the HGVa vehicles because they are independent variables the author obtained from the ATC, and the moment the author reschedule the HGVa vehicles, they become dependent variables. Thus, the simultaneous equations become simultaneous dynamic equations when utilising an exogenous variable, such as applying rescheduling (removing and inserting vehicles) (Hill 1984).

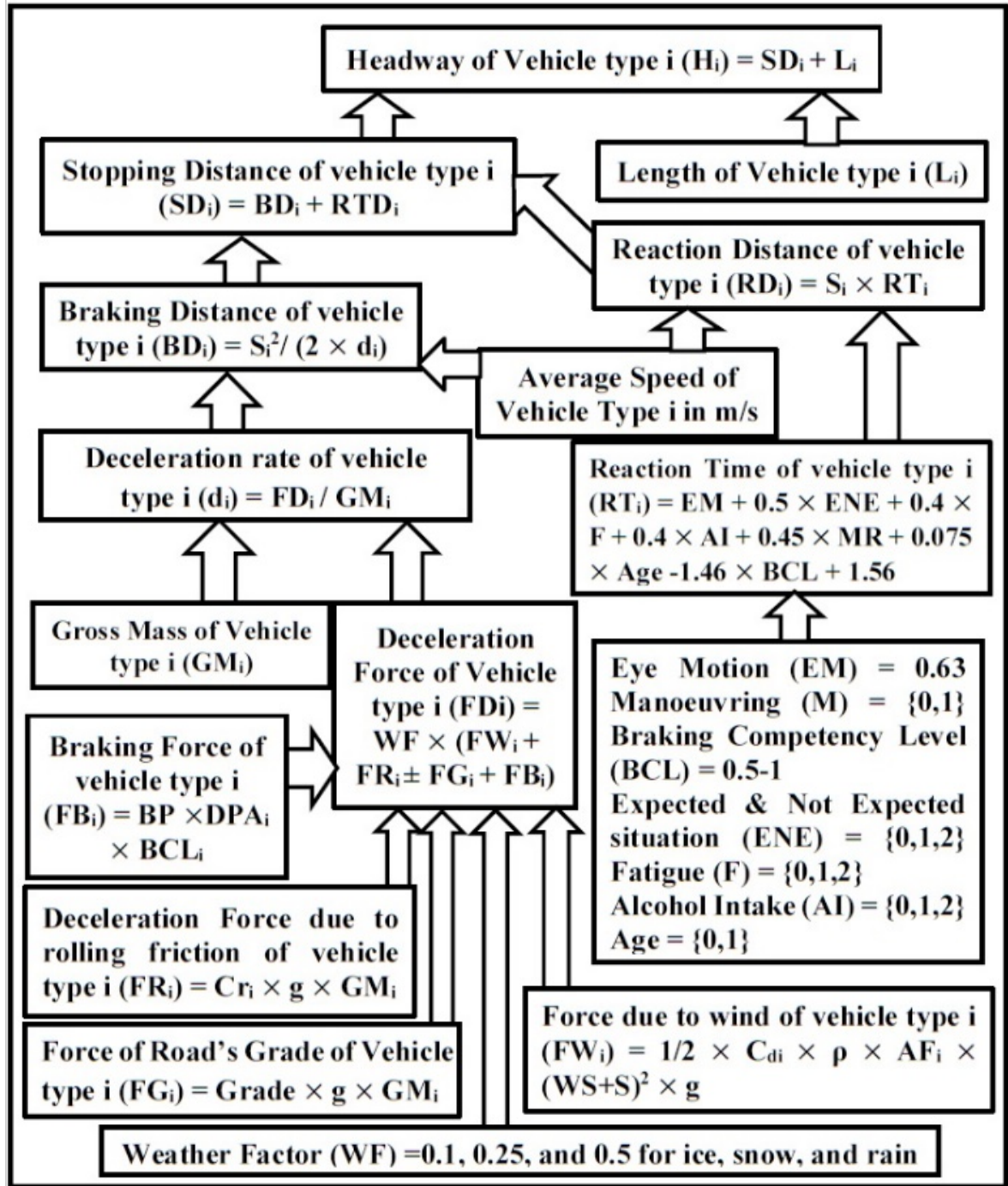


FIGURE 6-7: Estimating the vehicle's headway that represents the deceleration impact (The author has created this image)

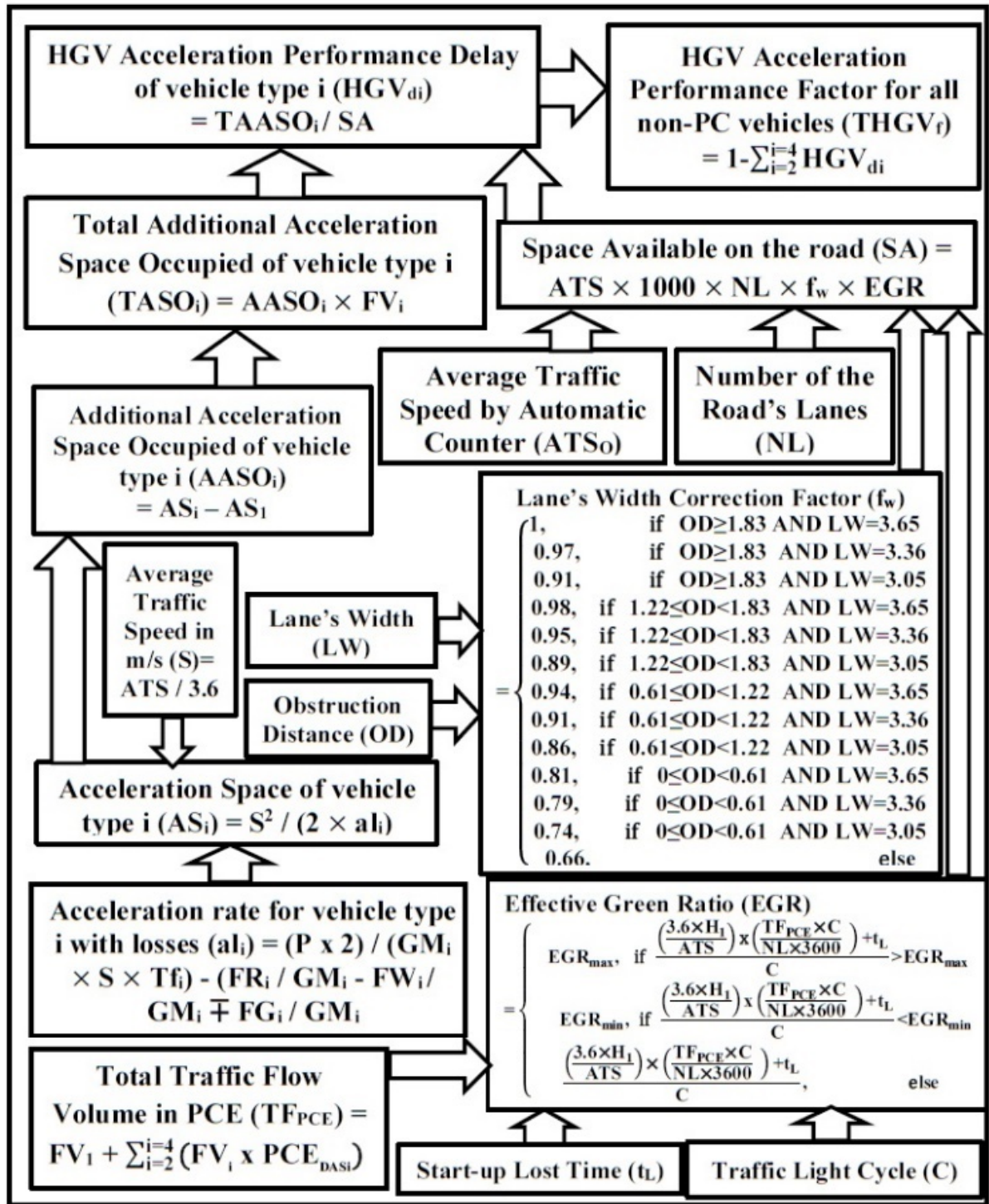


FIGURE 6-8: Estimating HGV_{di} and $THGV_f$ that represent the acceleration impact (The author has created this image)

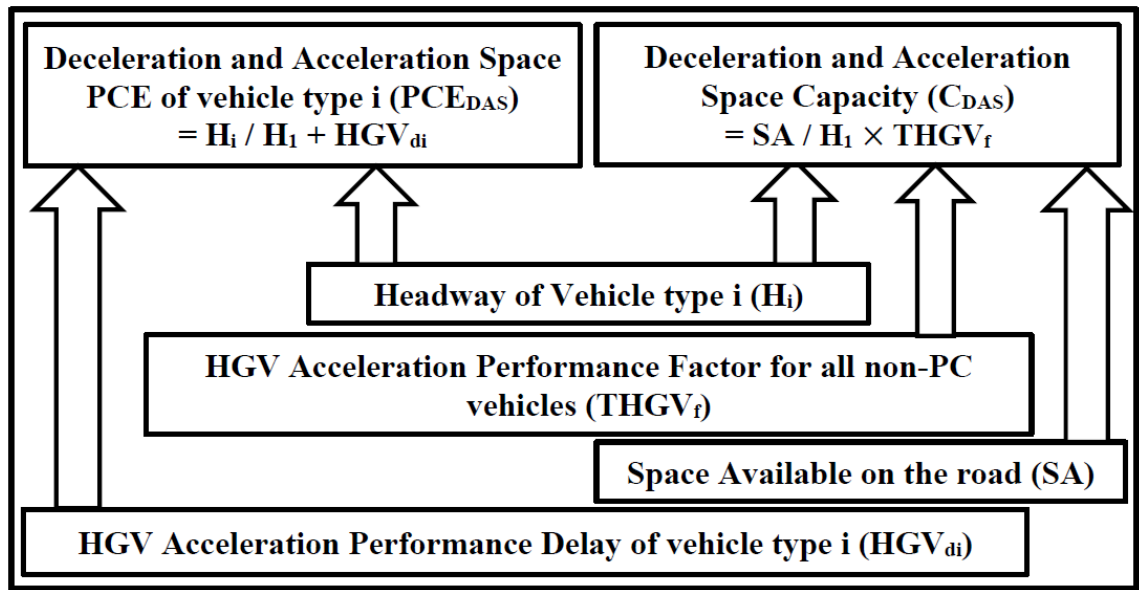


FIGURE 6-9: Deceleration and acceleration space PCE and capacity (The author has created this image)

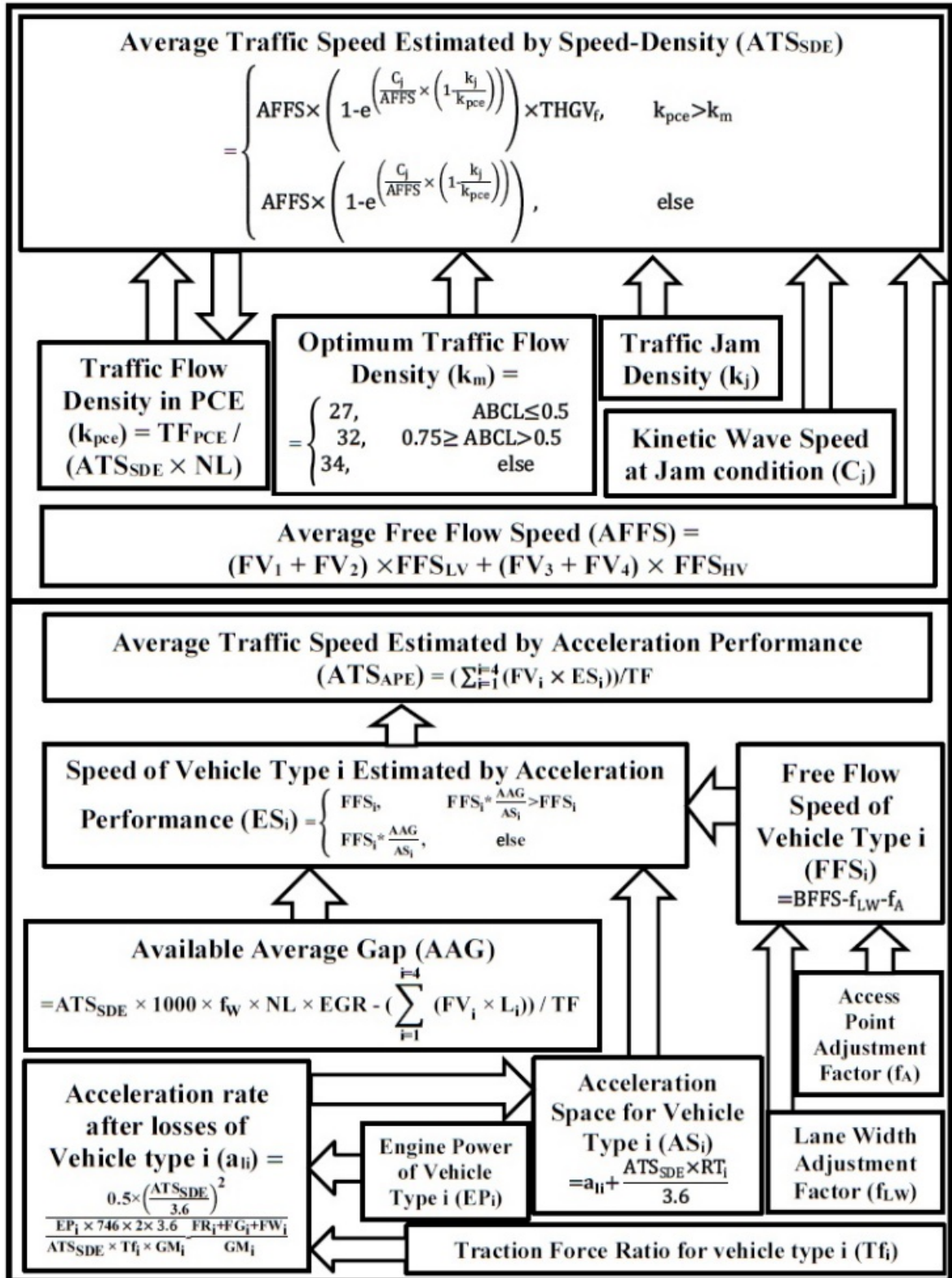


FIGURE 6-10: The two estimation methods of ATS using speed-density and acceleration performance

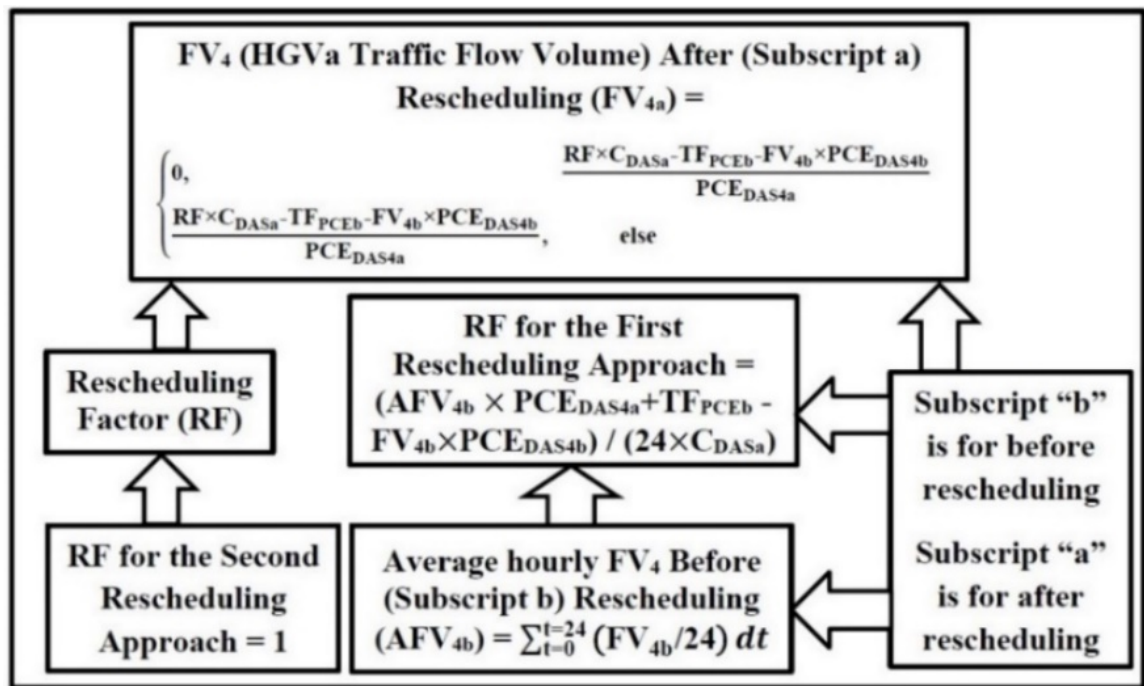


FIGURE 6-11: The rescheduling of HGVA vehicles (The author has created this image)

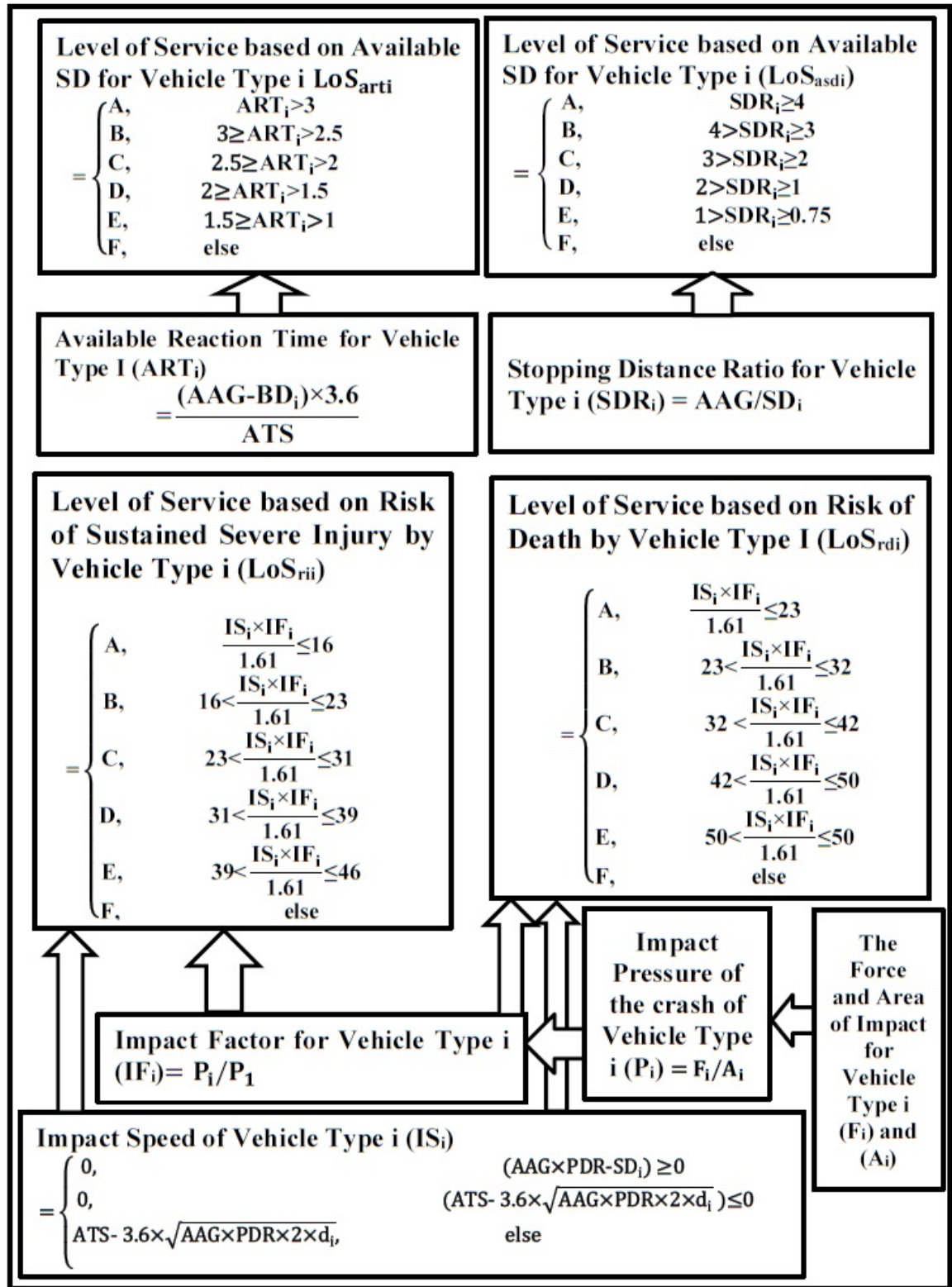


FIGURE 6-12: Estimation of all four LoS methods (The author has created this image)

6.3 DATA VALIDATION

6.3.1 Data Evaluation

The data by design should include local date (in year, month, and day), time (in hours and minutes), day type, road link name and id, average flow speed in km/h and mi/h, traffic flow, data quality, and vehicle speed counts, as in TABLE 6-2.

TABLE 6-2: Information on the fields of the ATC data table

Local Date	Local Time	Day Type ID	Total Carriageway Flow	Total Flow vehicles less than 5.2m	Total Flow vehicles 5.21m-6.6m	Total Flow vehicles 6.61m-11.6m	Total Flow vehicles Above 11.6m	ATS in km/h	Quality Index
22/08/20	07:15:00	1	888	701	110	22	55	55.23	15

These data segments are available every 15-minutes; however, even though these classification segments should be available by design, some are not available for every road link, such as average flow speed in m/h and vehicle speed counts. The classification of the day type is according to the typical working day, weekend days, bank holidays, and Christmas days, as in TABLE 6-3 (DfT-Journey Time and Traffic Flow Data 2015).

TABLE 6-3: The data file content' fields and description

Field Name	Field Description
Local Date	Date local to BST
Local Time Slot	15-minute time intervals local to BS
Day Type Id	The values are the following: 0 - First working day of the normal week 1 - Normal working Tuesday 2 - Normal working Wednesday 3 - Normal working Thursday 4 - Last working day of the normal week 5 - Saturday, but excluding days falling within type 14 6 - Sunday, but excluding days falling within type 14 7 - First day of school holidays 9 - Middle of week - school holidays, but excluding days falling within type 12, 13 or 14 11 - Last day of the week - school holidays, but excluding days falling within type 12,13 or 14 12 - Bank Holidays, including Good Friday, but excluding days falling within type 14 13 - Christmas period holidays between Christmas day and New Year's Day 14 - Christmas Day/New Year's Day.
Road	The name of the road.
Total Carriageway Flow	The number of vehicles detected on any lane within the 15-minute time slice.
Total Flow vehicles less than 5.2m	The number of vehicles less than 5.2m detected on any lane within the 15-minute time slice.
Total Flow vehicles 5.21m - 6.6m	The number of vehicles between 5.21m - 6.6m detected on any lane within the 15-minute time slice.
Total Flow vehicles 6.61m - 11.6m	The number of vehicles between 6.61m - 11.6m detected on any lane within the 15-minute time slice.
Total Flow vehicles above 11.6m	The Number of vehicles above 11.6m detected on any lane within the 15-minute time slice.
Speed Value	The average speed of all vehicles for all lanes measured by the site over the 15 minutes in km/h
Quality Index	The indication of the quality of the data provided. The number of valid one-minute records reported and used to generate the Total Traffic Flow and speed. A quality index of 0 indicates no valid records.
Average Speed in m/h	The average speed of vehicles per NTIS link for the 15-minute time slices.

The author has made assumptions according to the manufacturing ranges of length for four main types of vehicles and their maximum permissible lengths to identify the vehicle type, as shown in TABLE 6-4 (DfT-Maximum Length 2017).

TABLE 6-4: Maximum allowed vehicle' length (DfT-Maximum Length of Vehicles used in Great Britain, 2017)

Vehicle Type	Maximum allowed length
HGV _r	12m
Buses with two axles	13.5m
Buses with more than two axles	15m
HGV _a	16.5m
HGV _a carrying containers or swap bodies up to a maximum length of 45 feet as part of an intermodal transport operation	16.65m
HGV _a incorporating a low loader trailer	18m
Motor vehicle drawing one trailer which is not a semi-trailer	18.75m

Those vehicles are PC (includes private cars, commercial cars, taxis up to eight seaters), LGV (includes vans and two-axle trucks), HGV_r of 3-5 axles (includes school buses, public buses, and minibuses with two axles), and HGV_a of 3-8 axles (include long public buses, and transit buses with three axles). Another source of traffic data is available at the DfT traffic data (DfT-AADF 2017). The AADF data provide traffic counts according to the vehicle type, number of axles, and differentiates between HGV_r and HGV_a. For example, the data in (DfT-AADF 2017) of DBR for the year 2015 shows that vehicle types of PC, LGV, HGV_r, HGV_a account for 74.67%, 15.67%, 2.44%, and 6.15% of traffic, respectively, while the data in (HE-ATC Data 2017) shows that vehicles types of PC, LGV, HGV_r, and account for 61.78%, 23.89%, 5.17%, and 9.15% of traffic respectively.

The difference between the two indicates that either the ATC in (HE-ATC Data, 2017) is over/under-counting, or the inaccuracy is due to that the manual counters in (DfT-AADF, 2017) because they made their counts for only 2-3 hours at peak times and used a conversion factor to estimate the average of the day. Therefore, these assumptions are not entirely accurate due to the overlap of LGVs with PCs and HGV_rs, and the overlap of HGV_r with HGV_a. Due to some PCs that exceed 5.2m, some LGVs that exceed 6.6m, some HGV_rs that exceed 11.6m, and HGV_a vehicles could be shorter than 11.6m (Dalglish, 2008).

According to Liverpool container terminal data, the number of TEUs entering the port from the sea is 1400kTEUs annually with 66% of the containers are ≥ 40 ft that accounts for 80% of the TEUs, while containers of 20-30ft long are 34% of the containers and account for only 20% of the TEUs. Accordingly, the percentage of container carriers

from all HGVs are only 40-50%. Hence, any overlap between vehicle types volume will not affect the calculation of the number of TEUs.

For the road link in consideration, i.e., road A5036 of road link A5038-A5207, there is a lack of available data: AADF data for this road link is only available for 2000-2015 ATC data for the same road link is for 2015-2018. Thereby, the author must combine the two datasets to have the right prediction on the SDM. However, due to the overlap of vehicle categorisation of ATC data with the AADF data, the author must first validate the two sets of data.

6.3.2 ATC Data Imputation

ATC data goes through an imputation process before utilising the data in the SDM. The author has removed the hourly flows that failed the automatic and manual validation tests and replaced them with values from the previous year's flows on the same week, day, hour, site, and direction to give a typical flow for that site. If the week's flow is unsuitable, the author utilised the following week's flow (DfT-Data Imputation 2018). There are two reasons why the ATC data require imputation:

- The ATC data are faulty and producing no data or incorrect data
- The ATC is functioning correctly, but because of road works, or an event, there are extreme traffic levels on the road

The imputed ATC data are available in Appendix B as an average working day and an average day for 2015-2018.

6.3.3 Headway Measurement

Greenshields (1935), Cunagin (1982) and Seguin (1983) had different approaches in obtaining headway data, while all of the three utilized a type of photography system to determine the headway time. Greenshields (1935) obtained headway data by taking photos at a single site for every 5 seconds from the top of a nearby building, and Cunagin (1982) utilized Super-8 movie films by using a time-lapse projector, and Seguin (1983) obtained his data by installing a traffic evaluator system at the intersections of 11 sites (Makki 2020)

The author has considered in chapter three the required stopping distance for safety. However, most drivers do not follow the safety gap recommended by the HC. Therefore, rather than obtaining the headway data from field

measurements, the authors of this paper have determined the headway distance by utilizing the vehicle's length and calculating the safe stopping distance, considering the reaction time and braking competency level for drivers. Therefore, the authors have not measured vehicles' headway and speed on the survey site (Makki, 2020).

6.3.4 Manual Count and Observation

The author has made a field observation at several road links of A5036 in July 2018 and conducted a manual count at the peak period of 4-6 pm for road A5036 at road link of A5038-A5207 for several days in July 2018. The findings of the field observation are:

- the container carriers utilised to transport intermodal shipping containers are always HGVA with 5-7 axles, and even if the container is 20ft long or less
- the coaches with three axles are not longer than the coaches with two axles, and the third axle exists due to the luggage cabinet at the back of the bus
- the tanker trucks are all with 5-6 axles, and this is regardless of the length of the tank
- the difference between a five-axle truck and a six-axle truck is only when the six-axle truck raise one or two axles
- Unloaded HGVA with no trailer are short, and they could overlap with vehicles with a length $\leq 6.6\text{m}$.

The focus of the manual counting was on the CC-HGVA to determine the proportion of the five axles HGVA, the proportion of loaded CC-HGVA from all the 5-6 axles HGVs, the proportion of non-CC-HGVs with 5-6 axles, and the proportion of HGVA without a trailer. The results for the manual count show that the average of:

- loaded 5-6 axles CC-HGVA are 35% of all 5-6 axles HGVs
- loaded five axles, CC-HGVA are 41% of all loaded 5-6 CC-HGVA
- unloaded 2-4 axles HGVA without trailers are 11.4% of all 5-6 axles HGVs and are 24.52% of HGVA
- loaded non-CC curtain/box HGVA with 5-6 axles are 40.3% of all loaded 5-6 axles HGVs

As mentioned in chapter five, the author has surveyed several sites to measure pedestrians' time to cross the roads and every single lane of the road. The author has conducted the test using a stopwatch at the controlled intersections of two-lane, three-lane, four-lane, and five lanes' roads. Typically, the width of every lane in urban roads in the UK is 3.65m, and when the number of lanes of the road increases, the width of every lane decreases.

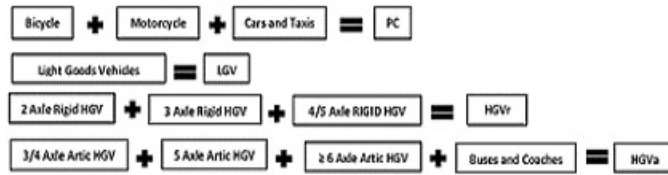
Roading engineers consider several factors when deciding the minimum road width, such as the road's type, vehicle's types using the road, traffic flow volumes, and the speed limit. For example, the lane's width is directly proportional to the vehicle's length, width, and speed, the vehicle has to complete any turn in the road, including roads (Right Driver, 2020). The road under investigation is a trunk road (A Road type) with a speed limit of 64.37 km/h (40 mi/h), the maximum HGV's width and length are 2.55m and 18.75m (the maximum observed HGV length on this road is 16.5m), and it is a highly congested road. Therefore, the lane should be a minimum of 3m, and it can be lower at lower speed limits.

The survey results showed that it took pedestrians to cross every road lane a range from 2.5 to 3.5s depending on the pedestrian's age and the lane's width. For example, the time to cross could be at its highest when crossing a two-lane road with a lane width of 3.65m, and at its lowest, they are crossing a five-lane road because the road's lane is at the lowest width.

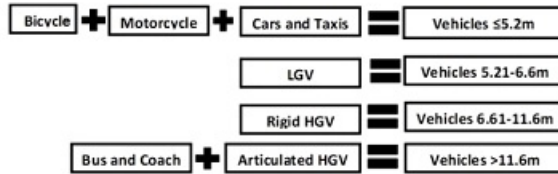
6.3.5 Traffic Flow Data Validation and Analysis

The author utilised both AADF and ATC data sets in the SDM and confirmed their interconnection. The data validation included the vehicles' registration data for GB and Northwest England (NW). The validation involves analysing the amount of overlap of the vehicles' classifications in the AADF data set as shown in FIGURE 6-13a, and the proposed vehicle classification in the ATC data set as shown in FIGURE 6-13b.

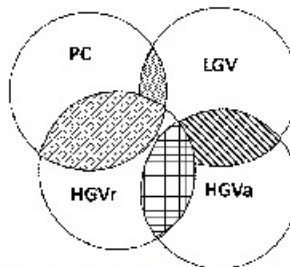
There is an overlap between the cars/taxis and the LGV categories and an overlap in length between the LGV and the HGVr categories, and that would lead to inconsistency between the two data sets, as shown in FIGURE 6-13c and FIGURE 6-13d. Besides, articulated tractors without trailers fall within the range from 6.61 to 11.6m at four axles and within the range from 5.21 to 6.6m at three axles. On the other hand, the HGVr can fall within the 5.21-6.6m category at two axles and fall within the >11.6m category at some of the HGVr of 4-5 axles as shown in FIGURE 6-13d.



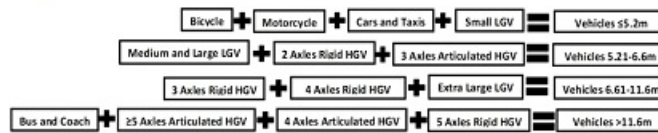
A. Vehicle's classification according to the AADF data set



B. The proposed classification according to the ATC data set



C. Overlap between vehicle categories in the AADF data and the ATC data



D. Overlap between vehicle categories in the AADF data when considering their lengths the ATC data

FIGURE 6-13: Vehicle classification in the AADF data set and overlap between the proposed vehicle categories in the ATC data set

After analysing the vehicles' registration data and various sources of vehicles' dimensions, the author found that the overlap in length between LGV and PC is an average of 24%, HGVr and LGV is an average 38.52%, between HGVr and HGVa is an average of 16.81%, and between HGVa and LGV is an average of 1.42% (Rushton, 2014; DfT-Vehicle's Length, 2017; DfT-Statistical data, 2018). These results will help estimate the overlaps between vehicles' categories at ATC and AADF, leading to a closer match between the two. However, to utilise these results, the author must evaluate the relationship between the vehicles' registration data and the AADF data.

6.3.5.1 Data validation process

To determine the effect of overlap on the proposed ATC classification, as shown in FIGURE 6-13b, the author has analysed the vehicles' registration data set and the AADF data set for road A5038 of link A566-A5036 by utilising regression analysis, as in TABLE 6-5 and TABLE 6-6:

- Analysed the vehicles' registration data set and the AADF data set for road A5038 of link A566-A5036 by utilising correlation analysis.
- Analysed the AADF data and the ATC data sets of road A5036 of link A5038-A5207 by utilising regression analysis.
- Compensating of vehicle type overlap by correcting the ATC data using the vehicle registration data

TABLE 6-5: Registration data of vehicle proportion of NW and GB

Year	PC NW	PC GB	HGV NW	HGV GB	Bus NW	Bus GB	MC NW	MC GB	LGV NW	LGV GB
2001	0.860	0.845	0.020	0.016	0.003	0.006	0.029	0.034	0.086	0.083
2002	0.870	0.844	0.019	0.016	0.003	0.006	0.030	0.035	0.085	0.083
2003	0.859	0.841	0.018	0.016	0.004	0.006	0.031	0.036	0.086	0.085
2004	0.858	0.838	0.018	0.016	0.004	0.006	0.031	0.037	0.089	0.087
2005	0.862	0.837	0.018	0.015	0.004	0.005	0.031	0.037	0.090	0.089
2006	0.852	0.835	0.018	0.015	0.004	0.005	0.030	0.037	0.091	0.091
2007	0.851	0.832	0.018	0.015	0.004	0.005	0.031	0.037	0.094	0.094
2008	0.849	0.831	0.018	0.015	0.004	0.005	0.031	0.038	0.094	0.094
2009	0.897	0.832	0.017	0.014	0.005	0.005	0.032	0.038	0.092	0.094
2010	0.882	0.833	0.017	0.014	0.004	0.005	0.032	0.036	0.086	0.094
2011	0.865	0.832	0.017	0.014	0.004	0.005	0.033	0.036	0.084	0.095
2012	0.891	0.832	0.018	0.013	0.004	0.005	0.033	0.035	0.084	0.095
2013	0.881	0.832	0.018	0.013	0.003	0.005	0.032	0.035	0.084	0.096
2014	0.886	0.831	0.018	0.013	0.002	0.005	0.033	0.034	0.085	0.097
2015	0.872	0.830	0.018	0.013	0.003	0.004	0.033	0.034	0.087	0.100
2016	0.868	0.828	0.018	0.013	0.003	0.004	0.033	0.033	0.089	0.102

TABLE 6-6: AADF data for road A5038

Year	PC	HGV	Bus	MC	LGV
2002	0.857	0.032	0.008	0.009	0.094
2003	0.861	0.027	0.011	0.006	0.095
2004	0.863	0.027	0.010	0.006	0.094
2005	0.872	0.021	0.012	0.008	0.087
2006	0.870	0.021	0.012	0.008	0.088
2007	0.859	0.019	0.012	0.005	0.104
2008	0.854	0.019	0.012	0.005	0.111
2009	0.845	0.018	0.012	0.005	0.120
2010	0.860	0.023	0.007	0.005	0.105
2011	0.856	0.023	0.007	0.005	0.109
2012	0.837	0.023	0.010	0.004	0.127
2013	0.835	0.023	0.009	0.004	0.129
2014	0.817	0.024	0.009	0.004	0.145
2015	0.808	0.024	0.009	0.004	0.154
2016	0.800	0.024	0.009	0.004	0.164
2017	0.842	0.022	0.005	0.005	0.126

6.3.5.2 Data validation step one: Regression Analysis of Registration vs AADF data

The author has analysed the AADF data by utilising the vehicle registration data if GB and NW and compared the proportions of PCs, LGVs, and HGVs with the same vehicle type's percentages average major roads in Liverpool. The author has chosen the major road A5038 because it does not lead to or from the Liverpool container terminal. The A5036 road has a high proportion of HGVs compared to other UK roads with the same characteristics. Therefore, the comparison with vehicle registration proportions with the A5038 road will be realistic. The best method of determining the closest match is calculating the SSE of the two data sets. The results in

For example, in TABLE 6-7, the prediction models for all vehicle types and locations show significantly better fit without an intercept constant ($B_0 = \text{zero}$) where the F value is significantly high in comparison to its value when utilising an intercept coefficient, and the R Square and Multiple R are also significantly higher without an intercept coefficient.

TABLE 6-8 and For example, in TABLE 6-7, the prediction models for all vehicle types and locations show significantly better fit without an intercept constant ($B_0 = \text{zero}$) where the F value is significantly high in comparison to its value when utilising an intercept coefficient, and the R Square and Multiple R are also significantly higher without an intercept coefficient.

TABLE 6-8 shows that the closest match with the A5038 data is the GB data for PC, LGV, Bus, and NW data for HGV and Motorcycles (MC).

The results of the regression analysis are in TABLE 6-7, and the definitions of all the coefficient in the table are as follows:

- 1- Multiple R: is a measure of how well a given variable can be predicted using a linear function of a set of other variables, and it serves as a measure of the correlation between the variable's values.
- 2- R Square: is a measure to determine the goodness of fit by how close the data are to the fitted regression line. If the R Square value is one, then the model explains all of the variability of the data around its mean.
- 3- Standard Error is the absolute measure of the distance that the data points fall from the regression line. The lower the standard error, the higher the R Square and the better the goodness of fit.

- 4- F is the test of the null hypothesis in the regression model, where it tests how the added B0 coefficient (the intercept of the regression line) suitability to improve the prediction model, and the higher the F value, the better the fit.
- 5- B1: is the slope coefficient of the regression line

TABLE 6-7: Regression Analysis for GB, NW, and A5038 data results

Vehicle type		Location	Multiple R: Correlation Factor	R Square: Goodness of Fit Factor	Standard Error	F	B0	B1
PC	No constant	GB-5038	0.999763	0.999525	0.019045	31581	0.000000	1.014050
		NW-5038	0.999405	0.998811	0.030140	12600	0.000000	0.973138
	constant	GB-5038	0.590660	0.348879	0.018029	7.501	-1.29201	2.562416
		NW-5038	0.385735	0.148791	0.020613	2.447	1.338679	-0.56681
HGV	No constant	GB-5038	0.988492	0.977116	0.003654	640.473	0.000000	1.590404
		NW-5038	0.993354	0.981845	0.003339	865.322	0.000000	1.287816
	constant	GB-5038	0.158961	0.025269	0.003576	0.36293	0.015789	0.507131
		NW-5038	0.778586	0.606196	0.002273	21.551	-0.03884	3.438594
LGV	No constant	GB-5038	0.988442	0.977017	0.018474	637.659	0.000000	1.259457
		NW-5038	0.978475	0.957414	0.025147	337.226	0.000000	1.312087
	constant	GB-5038	0.799737	0.639580	0.014640	24.844	-0.19873	3.401918
		NW-5038	0.260853	0.068044	0.023541	1.022	0.270609	-1.76112
MC	No constant	GB-5038	0.954084	0.910276	0.001740	152.180	0.000000	0.150047
		NW-5038	0.942506	0.888318	0.001941	119.310	0.000000	0.168455
	constant	GB-5038	0.143532	0.020601	0.001800	0.29449	-0.00116	0.182503
		NW-5038	0.791557	0.626562	0.001112	23.489	0.038190	-1.04415
BUS	No constant	GB-5038	0.984012	0.968281	0.001814	457.896	0.000000	1.894026
		NW-5038	0.978101	0.956682	0.002120	331.275	0.000000	2.607324
	constant	GB-5038	0.528764	0.279591	0.001856	5.433	-0.00324	2.525907
		NW-5038	0.428443	0.183564	0.001975	3.148	0.004916	1.301008

For example, in TABLE 6-7, the prediction models for all vehicle types and locations show significantly better fit without an intercept constant (B0= zero) where the F value is significantly high in comparison to its value when utilising an intercept coefficient, and the R Square and Multiple R are also significantly higher without an intercept coefficient.

TABLE 6-8: SSE results based on existing GB and NW data as \hat{y}

Vehicle Type Proportion	Data Type	SSE for 5038 data as y and NW and GB data as \hat{y}
PC Proportion	5038 set-GB	0.007640
	5038 set-NW	0.022349
HGV Proportion	5038 set-GB	0.001379
	5038 set-NW	0.000547
LGV Proportion	5038 set-GB	0.014355
	5038 set-NW	0.021551
MC Proportion	5038 set-GB	0.014828
	5038 set-NW	0.011012
BUS Proportion	5038 set-GB	0.000386
	5038 set-NW	0.000633

6.3.5.3 Data validation step two:

The author found a linear or monotonic relationship between the registration data and the AADF data for road A5038. The author utilised correlation methods of Pearson, Spearman, and Kendall's Tau methods. The results in TABLE 6-9 show a high positive correlation between the GB registration set and the AADF set of vehicle type PC, LGV, and Bus, while it shows a high positive correlation between the NW and AADF sets. The higher correlation of the NW set than the GB set of HGVs with the AADF set is due to the local registration of HGVs with the Liverpool port.

TABLE 6-9: Correlation analysis by Pearson, Spearman, and Kendall's tau_b methods

Vehicle Type Proportion	Data Type	Pearson Correlation	Spearman's Rho Correlation	Kendall's tau_b Correlation
PC Proportion	5038 set-GB	0.607*	0.676**	0.517**
	5038 set-NW	-0.397	-0.685**	-0.450*
HGV Proportion	5038 set-GB	0.479	0.232	0.117
	5038 set-NW	0.730**	0.635**	0.467*
LGV Proportion	5038 set-GB	0.846**	0.858**	0.731**
	5038 set-NW	-0.168	-0.267	-0.149
MC Proportion	5038 set-GB	0.418	0.585*	0.436*
	5038 set-NW	-0.826**	-0.839**	-0.756**
BUS Proportion	5038 set-GB	0.529*	0.509*	0.367*
	5038 set-NW	0.428	0.468	0.333

where ** Correlation is significant at the 0.01 level (2-tailed)

* Correlation is significant at the 0.05 level (2-tailed)

6.3.5.4 Data validation step three

The results in TABLE 6-10 and TABLE 6-11 show the annual average daily traffic flow for ATC and AADF data for road A5036, respectively. The TF by ATC for road A5036 road for an average day in TABLE 6-10 show higher daily traffic volumes for HGVr and HGVA than in the AADF data in TABLE 6-11 by 44.09% and 11.8%, respectively.

TABLE 6-10: Annual average traffic flow for the year 2015 by ATC data for road A5036 at road link of A5038-A5207

Annual Average Working Day (Excluding weekends)	A5036 (link A5038-A5207)	TF	≥5.2m	5.21-6.6m	6.61-11.6m	>11.6m	All HGVs
	The year 2015	20543	12706	4921	1093	1824	2917
	Percentage	100%	61.85%	23.95%	5.32%	8.88%	14.2%
Annual Average Day (Including Weekends)	A5036 (link A5038-A5207)	TF	≥5.2m	5.21-6.6m	6.61-11.6m	>11.6m	All HGVs
	The year 2015	18967	12482	4260	855	1371	2226
	Percentage	100%	65.81%	22.46%	4.51%	7.23%	11.74%

TABLE 6-11: Annual Average Day for the year 2015 by AADF for road A5036 at road link of A5038-A5207 and road A5038 at road link of A566-A5036

Road A5036, link (A5038-A5207)	Total Flow	Motorcycles	Car/Taxi	Bus/Coach	LGV	HGVr	HGVa	All types Of HGVs
Flow volume	19648	104	14670	111	3078	478	1209	1686
Percentage	100%	0.53%	74.67%	0.56%	15.67%	2.43%	6.15%	8.58%
Road A5038, link (A566-A5036)	Total Flow	Motorcycles	Cars/Taxis	Buses/Coaches	LGV	HGVr	HGVa	All types of HGVs
Flow volume	12445	48	10061	118	1915	193	111	303
Percentage	100%	0.38%	80.85%	0.95%	15.39%	1.55%	0.89%	2.43%

As mentioned before, the AADF data for road A5036 is only available for the period 2000-2015. It means that the author utilised the AADF data for A5038 in 2015-2018 to predict traffic flow in A5036, with additional help from ATC data. To do so, the data of AADF for A5038 predicted values for road A5036 at an average day. In addition, the author utilised regression curve fitting to determine the right conversion factors for the four vehicle types in the ATC data, as in TABLE 6-12 and TABLE 6-13.

TABLE 6-12: Results for curve fitting by utilising four different regression methods with no constant (no line interception)

Vehicle Type	Regression factors	Linear	Quadratic	Cubic	Power
Motorcycle	R ²	0.937	0.961	0.963	0.997
	b1	1.278	2.161	3.037	1.061
	b2	-	-0.005	-0.016	-
	b3	-	-	0.3427E-4	-
Car/Taxi	R ²	0.996	0.998	0.998	1
	b1	1.355	2.075	1.72	1.031
	b2	-	-0.3225E-4	0	-
	b3	-	-	-7.294E-10	-
Bus/Coach	R ²	0.952	0.972	0.972	0.999
	b1	0.763	1.352	1.725	0.957
	b2	-	-0.002	-0.005	-
	b3	-	-	0.5395E-5	-
LGV	R ²	0.99	0.993	0.993	1
	b1	1.702	2.223	3.444	1.069
	b2	-	0	-0.001	-
	b3	-	-	1.431E-07	-
HGVr	R ²	0.98	0.982	0.982	1
	b1	2.94	3.767	3.42	1.176
	b2	-	-0.002	0	-
	b3	-	-	-0.2022E-5	-
HGVa	R ²	0.927	0.993	0.993	0.997
	b1	13.233	28.247	32.289	1.525
	b2	-	-0.076	-0.123	-
	b3	-	-	0	-

TABLE 6-13: Change in ATC traffic flow composite daily traffic volumes because of overlapping for road A5036 (link A5038-A5207)

The year 2015	Total Flow	≥5.2m	5.21-6.6m	6.61-11.6m	>11.6m	All HGV
Average Day	18967	12482	4260	855	1371	2226
Average Working Day	20543	12706	4921	1093	1824	2917
Average Day Adjusted	18951	12614	4463	477	1397	1874
Average Working Day Adjusted	20572	12874	5206	610	1882	2492
Conversion factors	-	1.021	1.166	1.2788	1.347	-

6.3.5.5 Data validation step four

According to the analysis of step 1-3, the registration data and the AADF show high correlation and regression match. Therefore, the results validate the overlap information that the author has collected from vehicle registration and compensate for the overlap effect. The author has corrected the ATC data and implemented the model's change, as shown in TABLE 6-14. The author implemented the correction factors in TABLE 6-14 in the SDM to compensate for the vehicle categorisation in ATC data's hourly traffic volume.

TABLE 6-14: ATC data correction by compensating for the overlap effect

The year 2015	≥5.2m	5.21-6.6m	6.61-11.6m	>11.6m
Average Working Day	12706	4921	1093	1824
Overlap correction factors	1.08	0.84	0.42	1.03
Corrected ATC Data	13722	4134	459	1879

6.4 MODEL SYSTEM VALIDATION

The author has validated the model's output to be an adequate representation of the real system. The author has chosen to validate the estimated capacity and VtCR of the DAS method against the capacity and VtCR of the SF method because experts already validate it and widely used in the world (TRB 2010). The author has utilised the RMSE as in (6-1), RMSPE as in (6-2), ME as in (6-3), MPE as in (6-4), SSE as in (6-5). Their's inequality coefficient, as in (6-6), (6-7), (6-8), (6-9), and (6-10), Chi-Sq-GF method as in (6-11), and Pearson's correlation (Toledo 2004; Wasserman 2005; Wetherill 1981; Dalglish 2008; Cady 2017).

$$RMSE = \sqrt{\frac{1}{N} \sum_{h=1}^{h=24} (V_{DASH} - V_{SFh})^2} \quad (6-1)$$

$$RMSPE = \sqrt{\frac{1}{N} \sum_{h=1}^{h=24} \left(\frac{V_{DASH} - V_{SFh}}{V_{SFh}} \right)^2} \quad (6-2)$$

where,

N is the total number of intervals

V_{DASH} is the value of the estimated variable based on the DAS method per hour

V_{SFh} is the value of the estimated variable based on the SF method per hour

h is the time in hours

$$ME = \frac{1}{N} \sum_{h=1}^{h=24} (V_{DASH} - V_{SFh}) \quad (6-3)$$

$$MPE = \frac{1}{N} \sum_{h=1}^{h=24} \left(\frac{V_{DASH} - V_{SFh}}{V_{SFh}} \right) \quad (6-4)$$

$$SSE = \sum_{h=1}^{h=24} (V_{DASH} - V_{SFh})^2 \quad (6-5)$$

where,

- N is the total number of intervals
- V_{DASH} is the value of the estimated variable based on the DAS method per hour
- V_{SFh} is the value of the estimated variable based on the SF method per hour
- h is the time in hours

$$U_1 = \frac{RMSE}{\sqrt{\left(\frac{1}{N} \sum_{h=1}^{h=24} V_{DASH}^2\right) + \left(\frac{1}{N} \sum_{h=1}^{h=24} V_{SFh}^2\right)}} \quad (6-6)$$

$$U_M = \frac{(AV_{DASH} - AV_{SFh})^2}{RMSE^2} \quad (6-7)$$

$$U_S = \frac{(STD_{DAS} - STD_{SF})^2}{RMSE^2} \quad (6-8)$$

$$U_C = \frac{2 \times (1-\rho) \times STD_{DAS} \times STD_{SF}}{RMSE^2} \quad (6-9)$$

$$U_2 = \sqrt{\frac{\frac{1}{N} \sum_{h=1}^{h=24} (V_{DASH} - V_{SFh}) / V_{SFh-1}}{\frac{1}{N} \sum_{h=1}^{h=24} (V_{SFh} - V_{SFh-1}) / V_{SFh-1}}} \quad (6-10)$$

where,

- N is the total number of intervals
- V_{DASH} is the value of the estimated variable based on the DAS method per hour
- V_{SFh} is the value of the estimated variable based on the SF method per hour
- h is the time in hours
- U is Theil's inequality coefficient
- U_M is Theil's inequality coefficient for bias
- U_S is Theil's inequality coefficient for variance
- U_C is Theil's inequality coefficient for convergence
- STD_{DAS} is the standard deviation of the variable estimated based on the DAS method
- STD_{SF} is the standard deviation of the variable estimated based on the SF method
- AV_{DASH} is the average value of samples of the variable estimated based on the DAS method
- AV_{SFh} is the average value of samples of the variable estimated based on the SF method
- ρ is the correlation coefficient between variables of SF and variable of DAS methods

The purpose of (6-10) is to determine whether Theil's method is effective in validating the model or not. If the result of (6-10) is less than 1, then Theil's method is suitable, and if the result is higher than 1, then it is not suitable.

This is because the Chi-Sq-GF depends on the X^2 value in (6-11), and the higher the value is, the lower the p-value, and if the p-value is less than α ($\alpha = 0.05$), then the null hypothesis will be rejected, and when it is higher than α the null hypothesis will be accepted (good fit) and the higher the p-value (up to 1) the better the fit.

$$X^2 = \sum_{h=1}^{h=24} \frac{(V_{DASH} - V_{SFh})^2}{V_{SFh}} \quad (6-11)$$

where,

- V_{DASH} is the value of the estimated variable based on the DAS method per hour
- V_{SFh} is the value of the estimated variable based on the SF method per hour
- h is the time in hours

Since that the ATS is the main contributor to the estimation of the C_{DAS} , PCE_{DAS} , TF_{PCE} , and $VtCR_{DAS}$, the author has utilised decided to accept an RMSE and RMSPE of up to 9.4% while the desired values should be equal to or lower than 5.72%, and it is due to the ATC data average error, as in TABLE 4-3. The ME, MPE, SSE, U_1 , U_M , and the U_S should be at their lowest level, and the U_C , Chi-Sq-GF's p-value, and the correlation should be the closest possible to one.

The validation method is to assess the goodness of fit between the results of the current SF system, including the ATC's ATS with the model estimation results, and the selected values are $VtCR$, Capacity, and ATS latter variables are for BR. The data categorisation is according to a range of conditions that involve varying the ABCL, RT, and HGV vehicle's weights, as in TABLE 6-15.

TABLE 6-15: Model scenarios of RT and GM

Scenario	ABCL	MR	ENE	HGV's Drivers Fatigue	RT of HGVa' driver	All HGVs' GM in the percentage of MAM
1	50%	0.45	0.5	0.4	2.81	100% of MAM
2	50%	0.45	0.5	0.4	2.81	60% of MAM
3	50%	0.45	0.5	0	2.41	60% of MAM
4	50%	0.45	0	0	1.91	60% of MAM
5	50%	0	0	0	1.46	60% of MAM
6	75%	0.45	0.5	0.4	2.45	100% of MAM
7	75%	0.45	0.5	0.4	2.45	60% of MAM
8	75%	0.45	0.5	0	2.05	60% of MAM
9	75%	0.45	0	0	1.55	60% of MAM
10	75%	0	0	0	1.10	60% of MAM
11	100%	0.45	0.5	0.4	2.08	100% of MAM
12	100%	0.45	0.5	0.4	2.08	60% of MAM
13	100%	0.45	0.5	0	1.68	60% of MAM
14	100%	0.45	0	0	1.18	60% of MAM
15	100%	0	0	0	0.73	60% of MAM

The author has utilised the Pearson correlation method to assess the correlation between methodologies in TABLE 6-16-TABLE 6-21. The Pearson's correlation factor can be in a range of values from +1 to -1. A value of 0 indicates that there is no association between the two variables. If the correlation factor is positive, then it means that if the value of one variable increases, the value of the other variable also increases. If the correlation factor is negative, then it means that if the value of one variable increases, the value of the other variable decreases.

The author has obtained the RMSE, RMSPE, ME, MPE, U_1 , U_M , U_S , U_C , U_2 , and Chi-Sq-GF by applying equations (6-1) to (6-11). The results for C_{DAS} BR (C_{DASb}) in TABLE 6-16 provided an acceptable RMSE and RMSPE values at an RT=1.46s and an ABCL=50%, at an RT=1.55s at an ABCL=75%, and an RT=1.68s at an ABCL=100%. The average RT was equal to 1.57s. However, the C_{DAS} AR (C_{DASa}) for approach one and two have failed to provide

acceptable RMSE and RMSPE values, and it is because the C_{SF} method is based on capacity level traffic flow, as shown in FIGURE 6-14, FIGURE 6-15, and FIGURE 6-16.

TABLE 6-16: Results of the goodness of fit of the C_{DAS} estimation at the hours of 1.00-24.00 BR and AR

Before Rescheduling												
Scenario	RMSE	RMSPE	ME	MPE	SSE	U_1	U_M	U_S	U_C	U_2	Chi-Sq-GF	Correlation
1	-333	0.263	-333	-0.21	2810732	0.16	0.61	0.13	0.07	1.07	0.00	0.42
2	-347	0.267	-347	-0.23	3017406	0.16	0.67	0.11	0.04	4.47	0.00	0.63
3	-347	0.264	-347	-0.23	3010372	0.16	0.70	0.10	0.03	4.95	0.00	0.73
4	-156	0.121	-156	-0.08	639464	0.07	0.42	0.29	0.16	0.66	0.56	0.80
<u>5</u>	<u>78</u>	<u>0.068</u>	<u>78</u>	<u>0.11</u>	<u>167474</u>	<u>0.03</u>	<u>2.15</u>	<u>0.35</u>	<u>0.98</u>	<u>0.78</u>	<u>0.19</u>	<u>0.78</u>
6	222	0.170	-176	-0.13	1182375	0.10	0.626	0.21	0.16	0.80	0.00	0.57
7	222	0.166	-189	-0.14	1186425	0.10	0.721	0.18	0.10	0.78	0.00	0.70
8	222	0.165	-194	-0.15	1187161	0.09	0.762	0.15	0.09	1.09	0.00	0.77
<u>9</u>	<u>98</u>	<u>0.093</u>	<u>38</u>	<u>0.038</u>	<u>232666</u>	<u>0.04</u>	<u>0.147</u>	<u>0.23</u>	<u>0.63</u>	<u>0.58</u>	<u>0.00</u>	<u>0.78</u>
10	331	0.295	319	0.279	2632248	0.12	0.930	0.00	0.07	1.93	0.00	0.68
11	127	0.110	-37	-0.02	384546	0.05	0.088	0.304	0.61	1.39	0.83	0.62
<u>12</u>	<u>111</u>	<u>0.091</u>	<u>-43</u>	<u>-0.03</u>	<u>293879</u>	<u>0.05</u>	<u>0.154</u>	<u>0.285</u>	<u>0.56</u>	<u>1.16</u>	<u>0.97</u>	<u>0.73</u>
13	104	0.083	-50	-0.03	259435	0.04	0.230	0.239	0.53	1.08	0.99	0.78
14	252	0.220	237	0.203	1518966	0.10	0.891	0.000	0.11	3.26	0.00	0.70
15	615	0.542	609	0.533	9068010	0.21	0.983	0.000	0.02	20.50	0.00	0.22
After rescheduling by applying approach one												
Scenario	RMSE	RMSPE	ME	MPE	SSE	U_1	U_M	U_S	U_C	U_2	Chi-Sq-GF	Correlation
1	398	0.271	-364	-0.17	3794915	0.18	0.51	0.38	0.02	1.40	0.00	0.72
2	400	0.270	-362	-0.17	3831793	0.18	0.51	0.38	0.01	1.46	0.00	0.72
3	400	0.269	-363	-0.18	3837818	0.18	0.52	0.37	0.01	1.48	0.00	0.72
4	233	0.166	179	-0.01	1303659	0.10	0.20	0.83	0.12	1.47	0.00	0.86
5	140	0.173	39.38	0.2	468502	0.06	0.60	1.93	0.50	1.95	0.00	1.00
6	286	0.238	-188	-0.09	1957115	0.14	0.433	0.52	0.05	1.65	0.00	0.96
7	285	0.237	-178	-0.08	1955553	0.13	0.388	0.55	0.06	1.77	0.00	0.96
8	286	0.231	-182	-0.09	1962606	0.14	0.404	0.53	0.06	3.42	0.00	0.96
9	210	0.304	36	0.110	1055887	0.10	0.029	0.77	0.20	3.97	0.00	0.98
10	363	0.536	300	0.375	3167568	0.15	0.683	0.26	0.06	8.15	0.00	0.94
11	191	0.242	-54	0.026	874210	0.08	0.079	0.754	0.17	1.42	0.00	0.96
12	207	0.258	-37	0.041	1027496	0.09	0.032	0.791	0.18	1.61	0.00	0.94
13	205	0.241	-42	0.029	1006298	0.09	0.041	0.774	0.19	1.60	0.00	0.93
14	299	0.435	228	0.287	2152642	0.12	0.582	0.323	0.10	2.95	0.00	0.89
15	616	0.791	585	0.648	9120355	0.22	0.900	0.093	0.01	5.54	0.00	0.96
After rescheduling by applying approach two												
Scenario	RMSE	RMSPE	ME	MPE	SSE	U	U^M	U^S	U^C	U_2	Chi-Sq-GF	Correlation
1	398	0.27	-364	-0.17	3794915	0.18	0.51	0.38	0.02	0.90	0.00	0.98
2	400	0.27	-362	-0.17	3831793	0.18	0.51	0.38	0.01	1.31	0.00	0.98
3	400	0.27	-363	-0.18	3831198	0.18	0.52	0.37	0.01	1.43	0.00	0.98
4	230	0.16	-173	-0.01	1269272	0.10	0.20	0.80	0.11	1.72	0.00	0.96
5	145	0.19	51	0.21	507635	0.06	0.58	1.45	0.38	2.37	0.00	0.94
6	286	0.238	-188	-0.09	1957115	0.14	0.433	0.52	0.05	1.67	0.00	0.96
7	282	0.232	-178	-0.09	1911036	0.14	0.398	0.54	0.06	1.62	0.00	0.96
8	281	0.224	-181	-0.09	1895166	0.11	0.416	0.53	0.06	1.60	0.00	0.96
9	189	0.284	35	0.110	861140	0.09	0.034	0.77	0.20	4.00	0.00	0.98
10	341	0.529	300	0.399	2792697	0.15	0.772	0.17	0.05	6.38	0.00	0.98
11	188	0.232	-60	0.020	844693	0.08	0.101	0.74	0.16	0.94	0.00	0.97
12	193	0.239	-40	0.035	892160	0.08	0.043	0.78	0.18	1.45	0.00	0.96
13	189	0.222	-44	0.025	856650	0.08	0.053	0.76	0.19	1.42	0.00	0.95
14	271	0.416	222	0.296	1768122	0.12	0.669	0.24	0.10	2.95	0.00	0.94
15	607	0.843	593	0.742	8832329	0.24	0.957	0.04	0.01	6.74	0.00	0.96

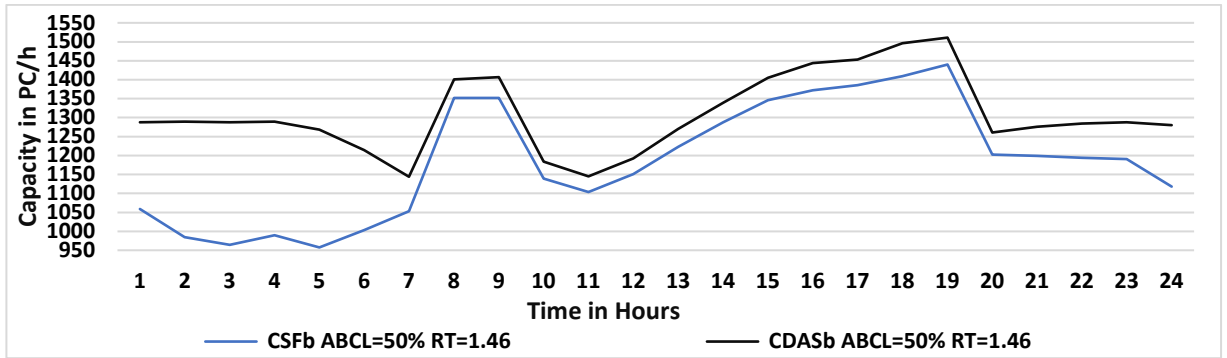


FIGURE 6-14: C_{DAS} estimation BR in comparison to C_{SF} at the hours of 1.00-24.00 at an ABCL of 50% and RT of 1.46s

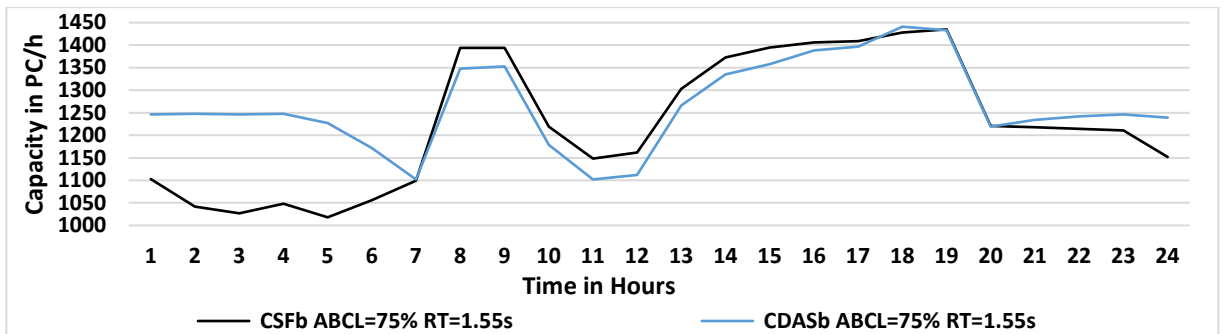


FIGURE 6-15: C_{DAS} estimation BR in comparison to C_{SF} at the hours of 1.00-24.00 at an ABCL of 75% and RT of 1.55s

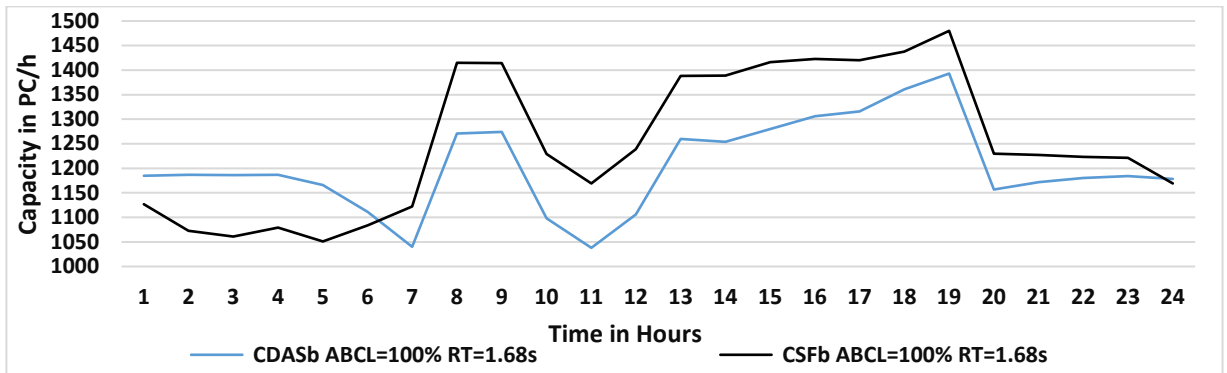


FIGURE 6-16: C_{DAS} estimation in comparison to C_{SF} at the hours of 1.00-24.00 BR at an ABCL of 100% and RT of 1.68s

Therefore, the author decided to repeat the test only for hours 8.00-19.00 (12h) to determine the effectiveness of the C_{DAS} with comparison to the C_{SF} method at capacity level, as in TABLE 6-17. The C_{DASb} has achieved the desirable levels of RMSE and RMSPE at ABCL=50% and 75% and provided an acceptable level at ABCL=100%. The results showed a significant improvement in the C_{DASa} test results, and the C_{DASa} has succeeded in providing

the desired fit at an ABCL of 50% BR and AR. However, at ABCL of 75%, the results showed a desirable fit BR and acceptable fit AR, and the results at ABCL of 100% showed acceptable fit BR and AR.

TABLE 6-17: Results of the goodness of fit of the C_{DAS} estimation at the hours of 8.00-19.00 BR and AR

Before Rescheduling												
Scenario	RMSE	RMSPE	ME	MPE	SSE	U_1	U_M	U_s	U_C	U_2	Chi-Sq-GF	Correlation
1	393	0.29	-390	-0.29	3710466	0.17	0.98	0.00	0.02	1.10	0.00	0.93
2	405	0.29	-403	-0.29	3930732	0.17	0.99	0.00	0.01	6.20	0.00	0.91
3	402	0.29	-401	-0.29	3882310	0.17	0.99	0.00	0.00	8.31	0.00	0.92
4	192	0.14	-191	-0.14	882826	0.08	0.99	0.00	0.02	0.66	0.138	0.96
<u>5</u>	<u>66</u>	<u>0.05</u>	<u>57</u>	<u>0.04</u>	<u>104825</u>	<u>0.02</u>	<u>0.75</u>	<u>0.03</u>	<u>1.37</u>	<u>0.26</u>	<u>1.00</u>	<u>0.96</u>
6	286	0.21	-286	-0.21	983150	0.12	1.00	0.00	0.002	4.08	0.00	0.95
7	287	0.21	-286	-0.21	985766	0.12	1.00	0.00	0.003	4.01	0.00	0.94
8	285	0.20	-285	-0.20	976590	0.11	1.00	0.00	0.003	4.00	0.00	0.94
9	<u>35</u>	<u>0.03</u>	<u>-29.5</u>	<u>-0.02</u>	<u>14836</u>	<u>0.01</u>	<u>0.70</u>	<u>0.14</u>	<u>0.165</u>	<u>0.53</u>	<u>1.00</u>	<u>0.99</u>
10	269	0.21	265	0.21	870718	0.10	0.97	0.03	0.001	4.28	0.00	1.00
11	133	0.10	-131	-0.10	213361	0.05	0.97	0.01	0.02	2.30	0.71	0.97
<u>12</u>	<u>125</u>	<u>0.09</u>	<u>-124</u>	<u>-0.09</u>	<u>187630</u>	<u>0.05</u>	<u>0.98</u>	<u>0.01</u>	<u>0.02</u>	<u>1.59</u>	<u>0.80</u>	<u>0.98</u>
<u>13</u>	<u>124</u>	<u>0.09</u>	<u>-122</u>	<u>-0.09</u>	<u>183455</u>	<u>0.05</u>	<u>0.97</u>	<u>0.01</u>	<u>0.02</u>	<u>1.53</u>	<u>0.82</u>	<u>0.98</u>
14	188	0.14	183	0.14	425488	0.07	0.94	0.05	0.01	2.01	0.13	0.99
15	562	0.47	560	0.47	3790038	0.19	0.99	0.01	0.00	26.52	0.00	0.96
After rescheduling by applying approach one												
Scenario	RMSE	RMSPE	ME	MPE	SSE	U_1	U_M	U_s	U_C	U_2	CHI-SQ-GF	Correlation
1	483	0.31	-485	-0.32	5589202	0.19	1.01	0.00	0.00	8.84	0.00	0.99
2	488	0.31	-491	-0.32	5708301	0.19	1.01	0.00	0.00	9.11	0.00	0.99
3	488	0.31	-492	-0.32	5715713	0.19	1.01	0.00	0.00	9.20	0.00	0.99
4	286	0.19	-289	-0.20	1960467	0.11	1.02	0.00	0.02	3.38	0.00	0.98
<u>5</u>	<u>58</u>	<u>0.04</u>	<u>-62</u>	<u>-0.05</u>	<u>80561</u>	<u>0.02</u>	<u>1.13</u>	<u>0.14</u>	<u>0.66</u>	<u>0.70</u>	<u>0.998</u>	<u>0.98</u>
6	360	0.24	-359	-0.24	1551804	0.16	0.99	0.00	0.003	3.60	0.00	0.96
7	363	0.24	-361	-0.24	1576848	0.15	0.99	0.00	0.007	3.62	0.00	0.96
8	363	0.24	-362	-0.24	1579276	0.16	0.99	0.00	0.006	15.32	0.00	0.96
9	<u>129</u>	<u>0.09</u>	<u>-125</u>	<u>-0.09</u>	<u>198233</u>	<u>0.05</u>	<u>0.94</u>	<u>0.03</u>	<u>0.027</u>	<u>2.95</u>	<u>0.79</u>	<u>0.98</u>
10	152	0.11	146	0.11	278197	0.06	0.92	0.05	0.043	1.59	0.51	0.94
11	199	0.14	-197.33	-0.14	476396	0.07	0.98	0.00	0.02	2.30	0.12	0.98
12	200	0.14	-198.42	-0.14	481741	0.07	0.98	0.00	0.02	2.05	0.12	0.98
13	201	0.14	-198.58	-0.14	482565	0.07	0.98	0.01	0.01	2.29	0.11	0.98
<u>14</u>	<u>94</u>	<u>0.07</u>	<u>83.58</u>	<u>0.06</u>	<u>105975</u>	<u>0.03</u>	<u>0.79</u>	<u>0.14</u>	<u>0.07</u>	<u>1.12</u>	<u>0.98</u>	<u>0.96</u>
15	445	0.34	443.08	0.34	2375701	0.14	0.99	0.00	0.01	71.79	0.00	-0.79
After rescheduling by applying approach two												
Scenario	RMSE	RMSPE	ME	MPE	SSE	U_1	U_M	U_s	U_C	U_2	Chi-Sq-GF	Correlation
1	482	0.31	-485	-0.32	5589202	0.19	1.01	0.00	0.00	1.80	0.00	0.98
2	487	0.31	-491	-0.32	5708300	0.19	1.01	0.00	0.00	8.79	0.00	0.98
3	488	0.31	-492	-0.32	5715713	0.19	1.01	0.00	0.00	9.11	0.00	0.98
4	285	0.19	-288	-0.20	1960467	0.11	1.02	0.00	0.01	2.59	0.00	0.96
<u>5</u>	<u>57</u>	<u>0.04</u>	<u>-54</u>	<u>-0.04</u>	<u>78109</u>	<u>0.02</u>	<u>0.91</u>	<u>0.05</u>	<u>0.62</u>	<u>0.54</u>	<u>0.999</u>	<u>0.94</u>
6	360	0.24	-358.63	-0.24	1551804	0.16	0.99	0.00	0.003	4.75	0.00	0.96
7	363	0.24	-361.47	-0.24	1576848	0.16	0.99	0.00	0.003	4.19	0.00	0.96
8	363	0.24	-361.78	-0.24	1579276	0.14	0.99	0.00	0.009	4.73	0.00	0.96
9	<u>123</u>	<u>0.09</u>	<u>-120.33</u>	<u>-0.09</u>	<u>182838</u>	<u>0.05</u>	<u>0.95</u>	<u>0.01</u>	<u>0.027</u>	<u>2.80</u>	<u>0.83</u>	<u>0.98</u>
10	167	0.13	163.33	0.13	333376	0.06	0.96	0.02	0.020	2.24	0.30	0.98
11	199	0.14	-197.42	-0.14	476815	0.07	0.98	0.00	0.02	2.19	0.12	0.98
12	198	0.14	-196.42	-0.14	471613	0.07	0.98	0.00	0.02	1.92	0.12	0.98
13	198	0.14	-196.58	-0.14	472375	0.07	0.98	0.00	0.01	2.13	0.12	0.98
14	<u>100</u>	<u>0.07</u>	<u>93.25</u>	<u>0.07</u>	<u>120511</u>	<u>0.04</u>	<u>0.87</u>	<u>0.09</u>	<u>0.05</u>	<u>1.08</u>	<u>0.96</u>	<u>0.98</u>
15	488	0.42	487.58	0.42	2859335	0.17	1.00	0.00	0.00	8.16	0.00	0.97

As shown in FIGURE 6-17, FIGURE 6-18, and FIGURE 6-19, the RT values of the desirable and acceptable fits at ABCL of 50%, 75%, and 100% are 1.46s, 1.55s, and 1.68s BR and 1.18s AR for both approaches, respectively.

Therefore, the average RT for desirable and acceptable fit BR is 1.57s, and AR is 1.4s. The result implies that the minimum RT at the capacity level must be 1.4s.

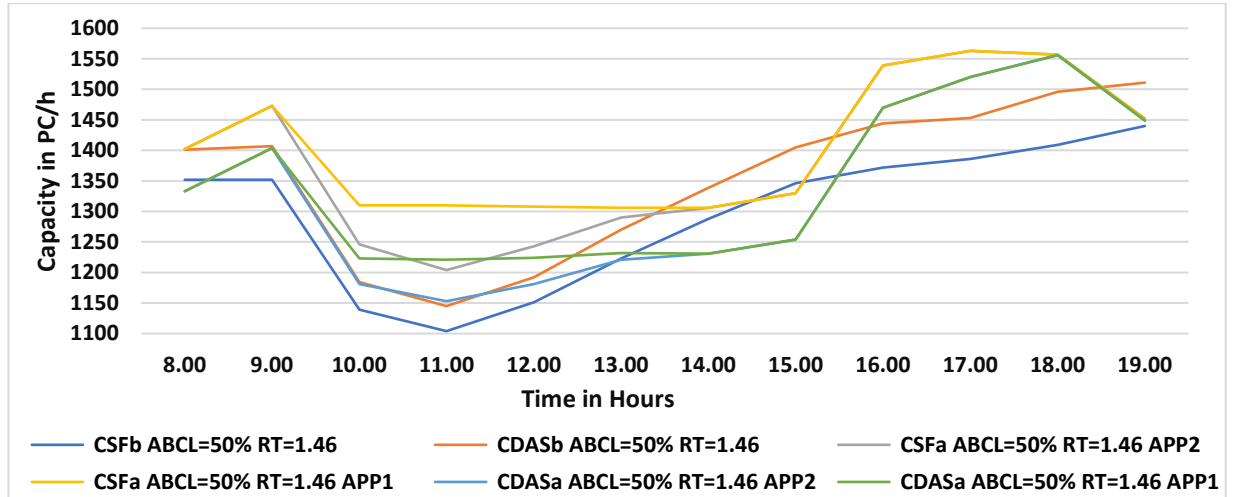


FIGURE 6-17: CDAS estimation BR and AR in comparison to CSF at the hours of 8.00-19.00 at an ABCL of 50% and RT of 1.46s

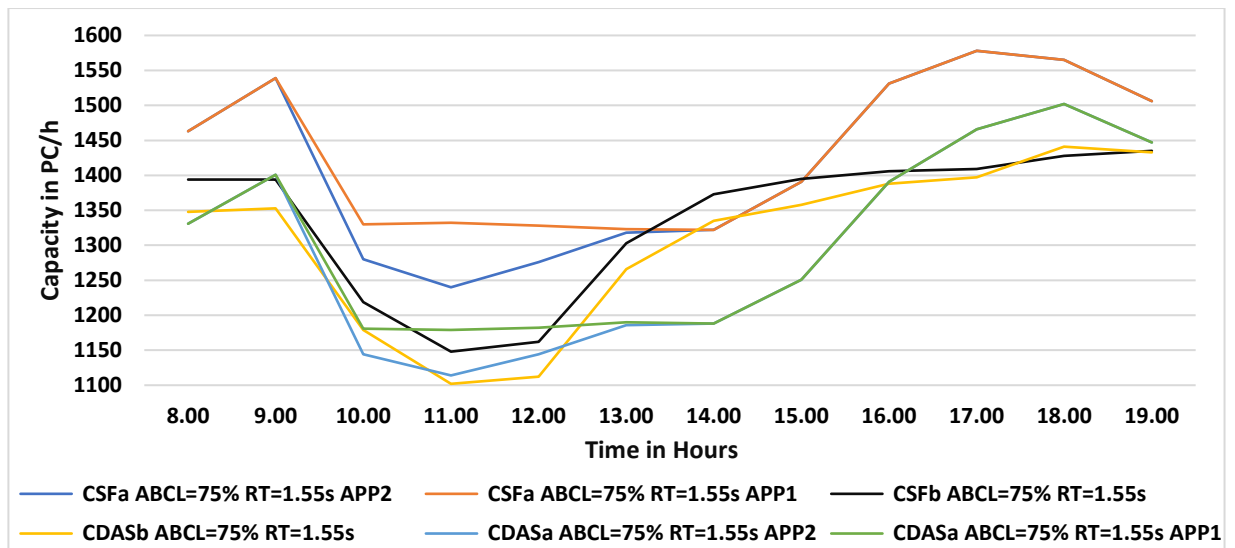


FIGURE 6-18: CDAS estimation BR and AR in comparison to CSF at the hours of 8.00-19.00 at an ABCL of 75% and RT of 1.55s

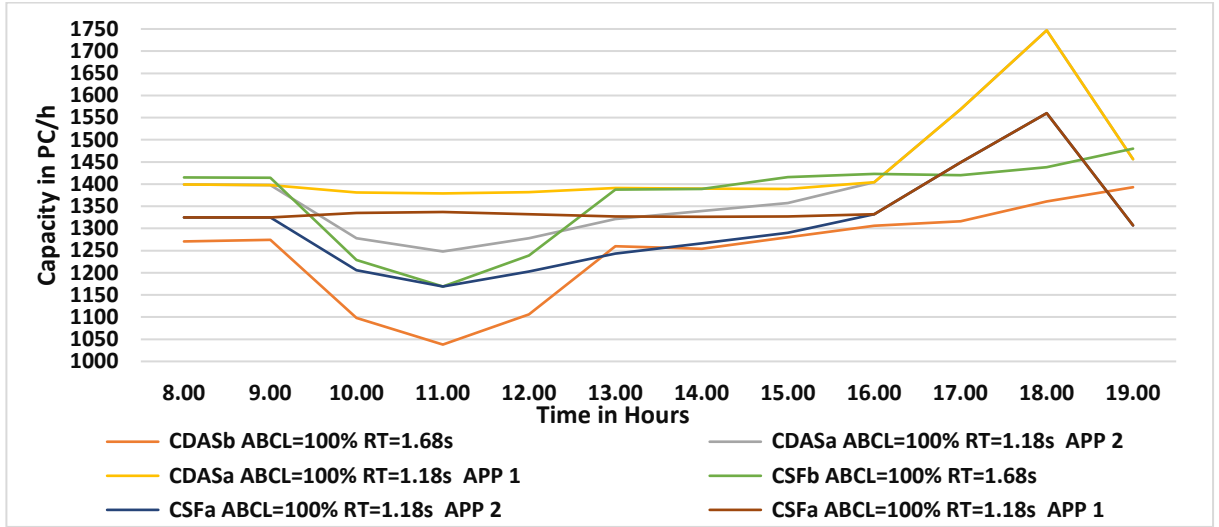


FIGURE 6-19: CDAS estimation BR and AR in comparison to CSF at the hours of 8.00-19.00 at an ABCL of 100% and RT of 1.18-1.68s

The results of the $VtCR_{DAS}$ in TABLE 6-18 showed acceptable fit BR at all ABCL levels at an average RT of 1.25s. However, the test failed to provide acceptable fit AR at an ABCL of 50% for both approaches and at an ABCL of 75% for approach two, as shown in FIGURE 6-20 and FIGURE 6-21. The scenario in FIGURE 6-22, where the ABCL=100% and the RT=1.18s, show acceptable fit BR and AR.

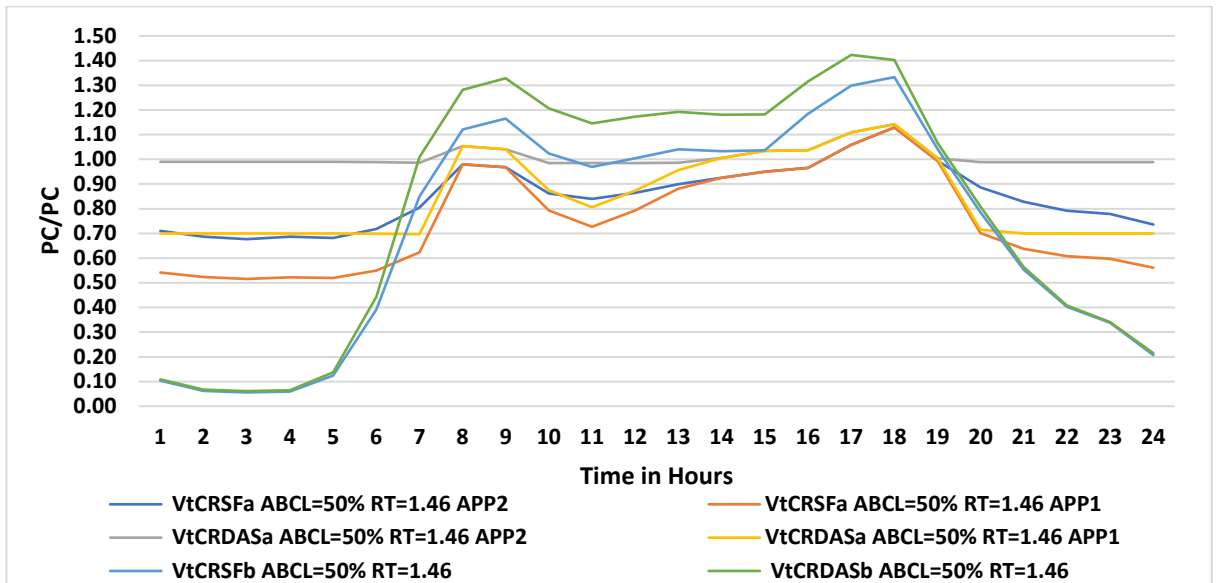


FIGURE 6-20: $VtCR_{DAS}$ estimation BR in comparison to $VtCR_{SF}$ at the hours of 1.00-24.00 at an ABCL of 50% and RT of 1.46s

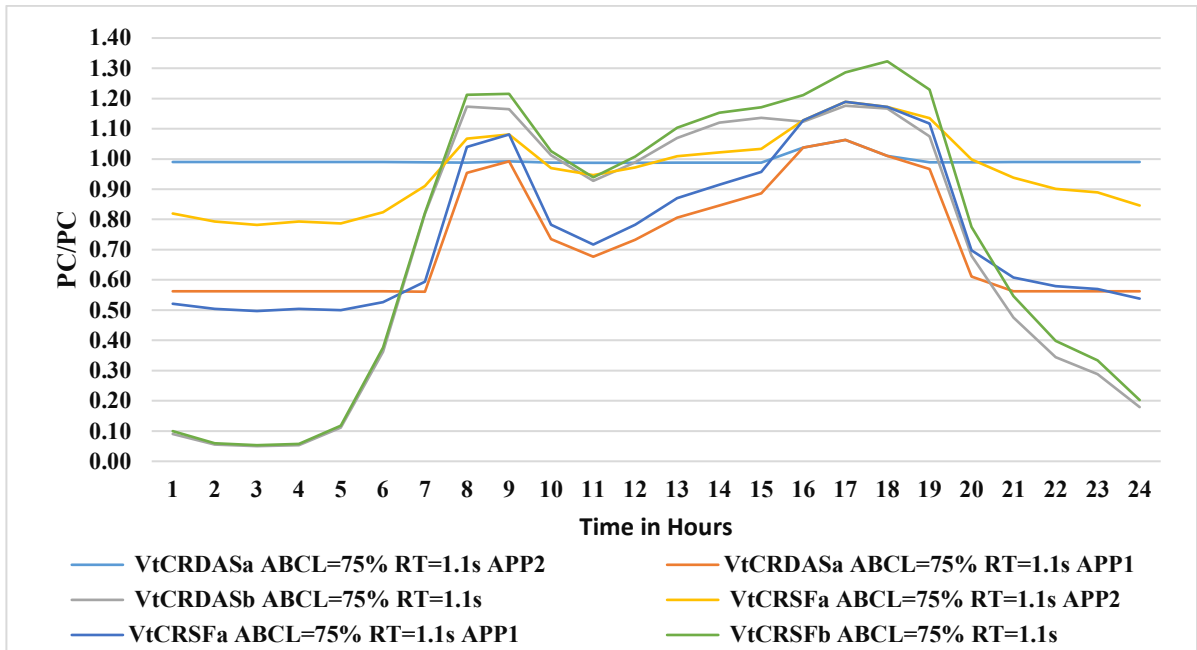


FIGURE 6-21: VtCR_{DAS} estimation BR and AR in comparison to VtCR_{SF} at the hours of 1.00-24.00 at an ABCL of 75% and RT of 1.1s

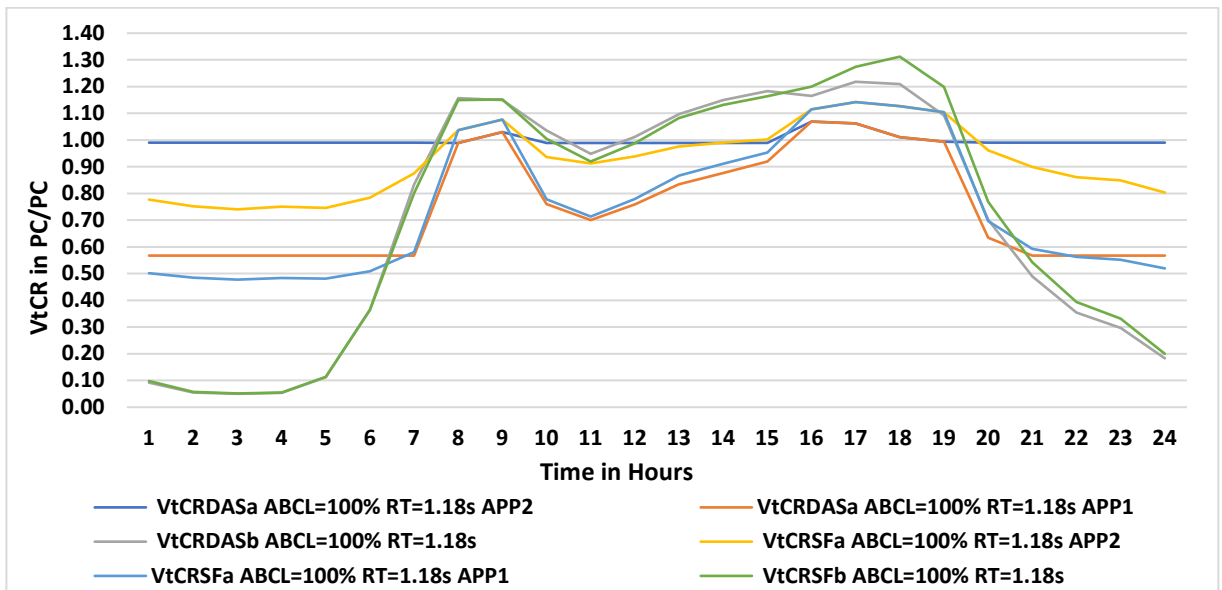


FIGURE 6-22: VtCR_{DAS} estimation in comparison to VtCR_{SF} at the hours of 1.00-24.00 BR and AR at an ABCL of 100% and RT of 1.18s

TABLE 6-18: Results of the goodness of fit of the VtCR_{DAS} estimation at the hours of 1.00-24.00 BR and AR

Before Rescheduling												
Scenario	RMSE	RMSPE	ME	MPE	SSE	U ₁	U _M	U _S	U _C	U ₂	Chi-Sq-GF	Correlation
1	0.60	0.59	0.53	0.30	8.73	0.27	0.61	0.28	0.01	1.46	0.00	0.99
2	0.55	0.55	0.48	0.13	7.35	0.26	0.59	0.27	0.01	1.35	0.00	0.99
3	0.52	0.53	0.46	0.09	6.60	0.25	0.59	0.27	0.01	1.30	0.00	1.00
4	0.29	0.29	0.25	0.57	1.98	0.15	0.63	0.29	0.02	0.75	0.00	1.00
5	0.09	0.09	0.07	0.54	0.21	0.05	0.75	0.39	0.20	0.28	0.84	1.00
6	0.39	0.44	0.32	0.42	3.74	0.20	0.66	0.31	0.01	1.03	0.00	0.99
7	0.35	0.40	0.29	0.39	2.97	0.18	0.67	0.31	0.00	0.93	0.00	1.00
8	0.33	0.39	0.27	0.38	2.61	0.17	0.68	0.30	0.01	0.89	0.00	1.00
9	0.14	0.15	0.11	0.14	0.45	0.08	0.61	0.29	0.02	0.37	0.24	1.00
10	0.06	0.08	-0.04	-0.07	0.10	0.04	0.50	0.14	0.17	0.12	1.00	1.00
11	0.24	0.26	0.19	0.24	1.38	0.13	0.64	0.31	0.06	0.63	0.00	0.993
12	0.21	0.23	0.16	0.22	1.01	0.11	0.64	0.31	0.05	0.54	0.00	0.995
13	0.19	0.21	0.15	0.20	0.84	0.11	0.65	0.30	0.05	0.50	0.00	0.996
14	0.04	0.06	-0.01	-0.03	0.04	0.02	0.12	0.01	0.95	0.08	1.00	0.996
15	0.22	0.24	-0.18	-0.23	1.11	0.13	0.68	0.29	0.03	0.46	0.00	0.997
After rescheduling by applying approach one												
Scenario	RMSE	RMSPE	ME	MPE	SSE	U ₁	U _M	U _S	U _C	U ₂	Chi-Sq-GF	Correlation
1	0.43	0.59	0.42	0.00	4.34	0.23	1.11	0.00	0.03	3.99	0.00	0.94
2	0.42	0.56	0.41	0.57	4.14	0.22	1.10	0.00	0.02	3.76	0.00	0.94
3	0.41	0.55	0.41	0.54	4.07	0.22	1.10	0.00	0.02	3.69	0.00	0.95
4	0.23	0.31	0.23	0.54	1.27	0.13	1.20	0.01	0.04	3.14	0.00	0.97
5	0.08	0.11	0.07	0.32	0.14	0.05	1.56	0.23	0.23	1.18	0.19	0.98
6	0.37	0.64	0.36	0.57	3.31	0.20	0.93	0.03	0.21	3.21	0.00	0.88
7	0.31	0.51	0.31	0.47	2.37	0.18	0.97	0.00	0.09	3.96	0.00	0.95
8	0.30	0.48	0.29	0.45	2.10	0.17	0.97	0.00	0.03	3.56	0.00	0.97
9	0.13	0.23	0.12	0.19	0.41	0.08	0.87	0.05	0.08	1.46	0.01	0.98
10	0.08	0.09	-0.04	-0.03	0.14	0.05	0.24	0.58	0.15	0.46	0.99	0.99
11	0.25	0.43	0.23	0.36	1.49	0.14	0.86	0.09	0.05	3.53	0.00	0.91
12	0.19	0.32	0.18	0.28	0.84	0.11	0.92	0.03	0.05	2.33	0.00	0.97
13	0.17	0.30	0.17	0.26	0.71	0.10	0.93	0.02	0.05	1.97	0.00	0.98
14	0.06	0.09	-0.01	0.01	0.09	0.04	0.01	0.68	0.31	0.45	1.00	0.99
15	0.19	0.21	-0.17	-0.20	0.90	0.13	0.75	0.24	0.01	1.06	0.00	0.99
After rescheduling by applying approach two												
Scenario	RMSE	RMSPE	ME	MPE	SSE	U ₁	U _M	U _S	U _C	U ₂	Chi-Sq-GF	Correlation
1	0.43	0.59	0.42	0.07	4.34	0.23	1.11	0.00	0.03	3.99	0.00	0.94
2	0.42	0.56	0.41	0.00	4.14	0.22	1.10	0.00	0.02	3.76	0.00	0.94
3	0.41	0.56	0.41	0.57	4.12	0.22	1.10	0.00	0.02	3.72	0.00	0.94
4	0.26	0.34	0.26	0.54	1.65	0.14	1.24	0.03	0.04	4.41	0.00	0.90
5	0.13	0.17	0.11	0.54	0.43	0.07	1.42	0.41	0.13	3.25	0.00	0.78
6	0.37	0.64	0.36	0.57	3.31	0.20	0.93	0.03	0.22	3.21	0.00	0.88
7	0.34	0.54	0.34	0.50	2.83	0.19	0.95	0.01	0.15	4.74	0.00	0.91
8	0.34	0.52	0.33	0.49	2.75	0.18	0.96	0.01	0.11	4.76	0.00	0.91
9	0.22	0.31	0.19	0.26	1.12	0.12	0.79	0.15	0.23	3.79	0.00	0.78
10	0.12	0.14	0.04	0.05	0.36	0.06	0.09	0.78	1.38	2.16	0.38	0.55
11	0.17	0.19	0.16	0.19	0.33	0.08	0.97	0.01	0.04	2.30	0.02	0.73
12	0.16	0.19	0.16	0.18	0.32	0.08	0.97	0.01	0.04	2.36	0.03	0.83
13	0.16	0.18	0.16	0.18	0.31	0.08	0.97	0.01	0.03	2.22	0.03	0.84
14	0.06	0.06	-0.02	-0.02	0.05	0.03	0.12	0.58	1.10	1.08	0.99	0.61
15	0.25	0.20	-0.24	-0.19	0.76	0.11	0.91	0.09	0.42	4.93	0.00	-0.68

However, the author has utilised the same approach of narrowing the test window from the hours 1.00-24.00 to 8.00-19.00 to determine its effectiveness for the VtCR_{DAS} validation, but the results in TABLE 6-19, FIGURE 6-

23, FIGURE 6-24, and FIGURE 6-25 show that the best scenario has changed from scenario 14 to 10 with ABCL=75% and RT=1.1.s that provided an acceptable fit BR and AR for both approaches.

TABLE 6-19: Results of the goodness of fit of the VtCR_{DAS} estimation at the hours of 8.00-19.00 BR and AR

Before Rescheduling												
Scenario	RMSE	RMSPE	ME	MPE	SSE	U ₁	U _M	U _S	U _C	U ₂	Chi-Sq-GF	Correlation
1	0.77	0.68	0.76	0.25	7.05	0.26	1.00	0.01	0.01	5.98	0.00	0.92
2	0.70	0.63	0.69	0.06	5.91	0.25	0.96	0.02	0.01	5.40	0.00	0.95
3	0.66	0.60	0.66	0.06	5.29	0.24	0.96	0.02	0.01	5.15	0.00	0.96
4	0.37	0.33	0.36	0.67	1.61	0.15	1.01	0.01	0.02	3.01	0.00	0.96
5	0.12	0.11	0.11	0.63	0.18	0.05	1.26	0.01	0.13	1.41	0.24	0.92
6	0.53	0.50	0.52	0.50	3.35	0.20	0.97	0.01	0.02	4.12	0.00	0.94
7	0.47	0.46	0.47	0.45	2.68	0.18	0.98	0.01	0.01	3.80	0.00	0.96
8	0.44	0.43	0.44	0.43	2.33	0.18	0.98	0.01	0.01	3.59	0.00	0.96
9	0.18	0.18	0.18	0.17	0.40	0.08	0.95	0.00	0.05	1.77	0.02	0.94
<u>10</u>	<u>0.08</u>	<u>0.06</u>	<u>-0.06</u>	<u>-0.05</u>	<u>0.08</u>	<u>0.04</u>	<u>0.61</u>	<u>0.17</u>	<u>0.22</u>	<u>0.90</u>	<u>0.98</u>	<u>0.92</u>
11	0.32	0.31	0.31	0.30	1.22	0.13	0.96	0.00	0.03	2.82	0.00	0.91
12	0.28	0.27	0.27	0.26	0.91	0.11	0.97	0.00	0.02	2.43	0.00	0.94
13	0.25	0.25	0.25	0.24	0.76	0.11	0.97	0.00	0.04	2.38	0.00	0.94
<u>14</u>	<u>0.05</u>	<u>0.04</u>	<u>-0.01</u>	<u>-0.01</u>	<u>0.03</u>	<u>0.02</u>	<u>0.07</u>	<u>0.40</u>	<u>0.51</u>	<u>0.60</u>	<u>1.00</u>	<u>0.93</u>
15	0.29	0.23	-0.28	-0.23	0.99	0.13	0.94	0.05	0.02	1.94	0.00	0.98
After rescheduling by applying approach one												
Scenario	RMSE	RMSPE	ME	MPE	SSE	U ₁	U _M	U _S	U _C	U ₂	Chi-Sq-GF	Correlation
1	0.44	0.48	0.44	0.00	2.32	0.20	0.94	0.01	0.00	4.48	0.00	0.99
2	0.43	0.48	0.43	0.48	2.26	0.20	0.93	0.01	0.00	4.40	0.00	0.99
3	0.43	0.48	0.43	0.48	2.22	0.20	0.93	0.01	0.00	4.36	0.00	0.99
4	0.23	0.26	0.23	0.47	0.66	0.12	1.02	0.00	0.01	2.76	0.00	0.98
<u>5</u>	<u>0.06</u>	<u>0.07</u>	<u>0.06</u>	<u>0.25</u>	<u>0.05</u>	<u>0.03</u>	<u>1.06</u>	<u>0.06</u>	<u>0.10</u>	<u>0.87</u>	<u>0.97</u>	<u>0.98</u>
6	0.29	0.34	0.29	0.34	1.03	0.14	0.99	0.00	0.01	3.42	0.00	0.98
7	0.29	0.34	0.29	0.33	0.99	0.14	0.99	0.00	0.01	3.35	0.00	0.99
8	0.28	0.33	0.28	0.33	0.97	0.14	0.99	0.00	0.01	3.42	0.00	0.99
9	0.10	0.12	0.10	0.11	0.12	0.05	0.95	0.01	0.04	1.26	0.69	0.98
<u>10</u>	<u>0.09</u>	<u>0.09</u>	<u>-0.09</u>	<u>-0.09</u>	<u>0.11</u>	<u>0.05</u>	<u>0.84</u>	<u>0.11</u>	<u>0.05</u>	<u>0.79</u>	<u>0.87</u>	<u>0.99</u>
11	0.17	0.19	0.16	0.19	0.33	0.08	0.97	0.01	0.04	2.30	0.02	0.98
12	0.16	0.19	0.16	0.18	0.32	0.08	0.97	0.01	0.04	2.36	0.03	0.98
13	0.16	0.18	0.16	0.18	0.31	0.08	0.97	0.01	0.03	2.22	0.03	0.98
<u>14</u>	<u>0.06</u>	<u>0.06</u>	<u>-0.02</u>	<u>-0.02</u>	<u>0.05</u>	<u>0.03</u>	<u>0.12</u>	<u>0.58</u>	<u>1.10</u>	<u>1.08</u>	<u>0.99</u>	<u>0.99</u>
15	0.25	0.20	-0.24	-0.19	0.76	0.11	0.91	0.09	0.42	4.93	0.00	1.00
After rescheduling by applying approach two												
Scenario	RMSE	RMSPE	ME	MPE	SSE	U ₁	U _M	U _S	U _C	U ₂	Chi-Sq-GF	Correlation
1	0.44	0.48	0.44	0.11	2.32	0.20	0.94	0.01	0.00	4.48	0.00	0.99
2	0.43	0.48	0.43	0.00	2.26	0.20	0.93	0.01	0.00	4.40	0.00	0.99
3	0.43	0.48	0.43	0.48	2.22	0.20	0.93	0.01	0.00	4.36	0.00	0.99
4	0.23	0.26	0.23	0.48	0.66	0.12	1.03	0.00	0.01	2.86	0.00	0.98
<u>5</u>	<u>0.06</u>	<u>0.07</u>	<u>0.06</u>	<u>0.47</u>	<u>0.05</u>	<u>0.03</u>	<u>1.45</u>	<u>0.24</u>	<u>0.13</u>	<u>1.53</u>	<u>0.87</u>	<u>0.93</u>
6	0.29	0.34	0.29	0.34	1.03	0.14	0.99	0.00	0.01	3.42	0.00	0.98
7	0.29	0.34	0.29	0.33	0.99	0.14	0.99	0.00	0.01	3.35	0.00	0.99
8	0.28	0.33	0.28	0.33	0.97	0.14	0.99	0.00	0.01	3.42	0.00	0.99
9	0.12	0.13	0.11	0.12	0.16	0.06	0.90	0.05	0.05	1.92	0.44	0.94
<u>10</u>	<u>0.09</u>	<u>0.08</u>	<u>-0.06</u>	<u>-0.05</u>	<u>0.09</u>	<u>0.04</u>	<u>0.47</u>	<u>0.39</u>	<u>0.14</u>	<u>1.59</u>	<u>0.94</u>	<u>0.71</u>
11	0.31	0.52	0.27	0.43	2.23	0.17	0.81	0.12	0.07	2.34	0.00	0.96
12	0.26	0.39	0.24	0.34	1.62	0.14	0.86	0.09	0.05	4.35	0.00	0.96
13	0.25	0.37	0.24	0.33	1.54	0.14	0.86	0.09	0.05	4.21	0.00	0.96
14	0.14	0.18	0.08	0.10	0.47	0.07	0.29	0.59	0.11	2.42	0.05	0.72
15	0.19	0.15	-0.14	-0.11	0.83	0.09	0.56	0.43	0.01	2.86	0.02	-0.61

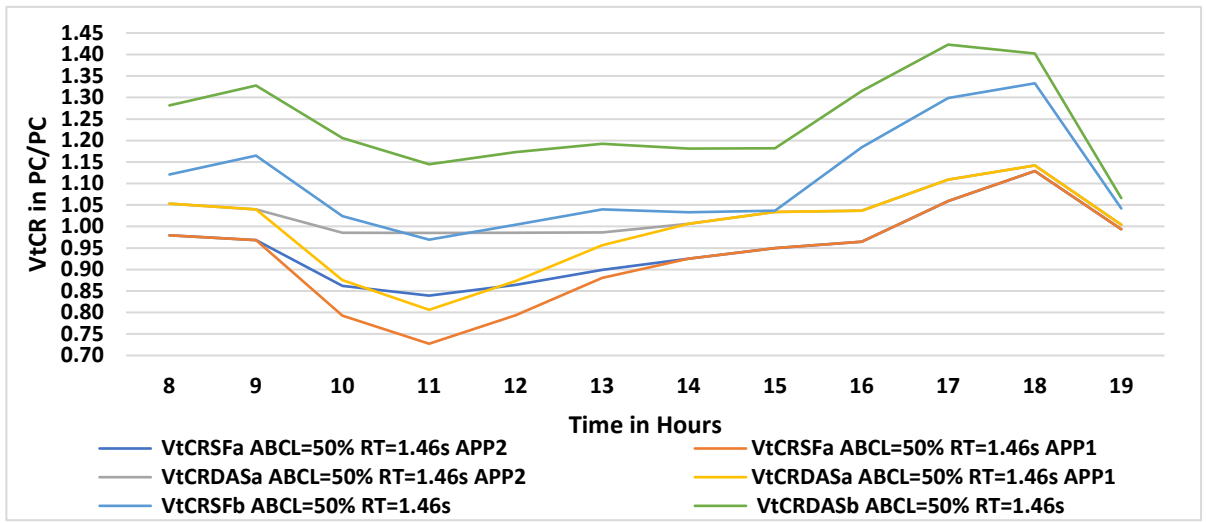


FIGURE 6-23: VtCR_{DAS} estimation in comparison to VtCR_{SF} at the hours of 8.00-19.00 BR and AR at an ABCL of 50% and RT of 1.46s

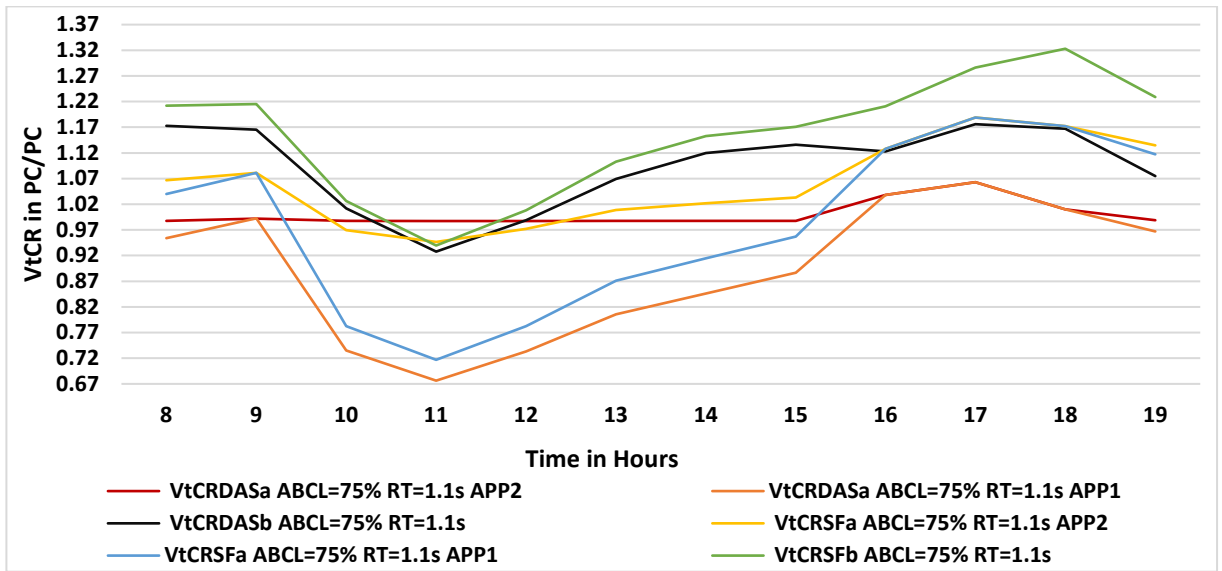


FIGURE 6-24: VtCR_{DAS} estimation BR and AR in comparison to VtCR_{SF} at the hours of 8.00-19.00 at an ABCL of 75% and RT of 1.1s

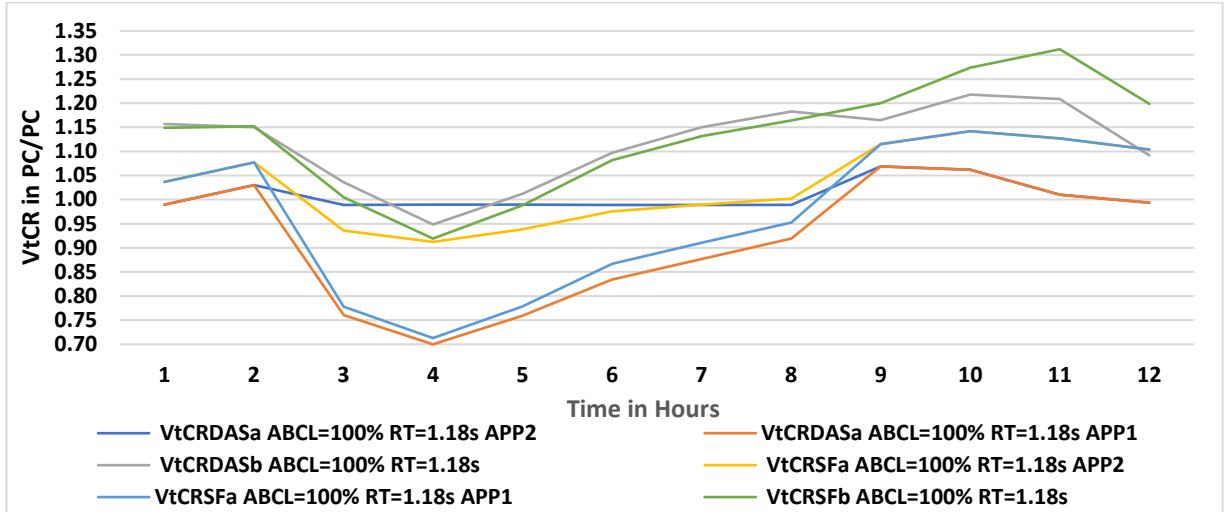


FIGURE 6-25: $VtCR_{DAS}$ estimation BR and AR in comparison to $VtCR_{SF}$ at the hours of 8.00-19.00 at an ABCL of 100% and RT of 1.18s

The author has already validated the ATS_{SDE} in chapter four by evaluating thirteen types of speed prediction methods and choosing one, and develop it by including the acceleration performance impact of non-PC vehicles on the ATS when the traffic density exceeds the maximum level. However, the author utilised only the RMSE and SSE methods in the validation process. Therefore, the author has validated the ATS_{DAS} again by utilising more methods, as in TABLE 6-20, FIGURE 6-26, FIGURE 6-27, and FIGURE 6-28.

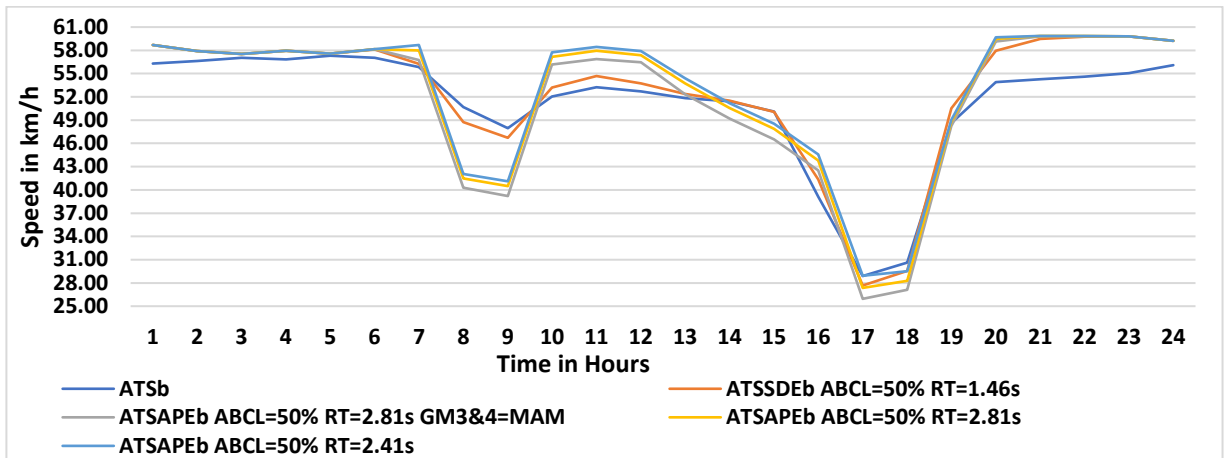


FIGURE 6-26: ATS_{SDE} and ATS_{APE} estimation BR and AR fit in comparison to ATS obtained from the ATC at the hours of 1.00-24.00 at an ABCL= 50% and an RT=1.46s for the ATS_{SDE} and an RT=2.41-2.81s for the ATS_{APE}

TABLE 6-20: Results of the goodness of fit of the ATS estimation methods at the hours of 1.00-24.00 BR

Prediction of ATS by utilising the speed-density estimation method												
Scenario	RMSE	RMSPE	ME	MPE	SSE	U ₁	U _M	U _S	U _C	U ₂	Chi-Sq-GF	Correlation
1	2.58	0.06	0.87	0.01	159	0.025	0.11	0.42	0.46	0.38	1.00	0.98
2	2.52	0.05	1.21	0.02	153	0.024	0.23	0.33	0.43	0.36	1.00	0.98
3	2.48	0.05	1.36	0.02	148	0.024	0.30	0.26	0.43	0.35	1.00	0.98
4	2.41	0.05	1.36	0.02	140	0.023	0.32	0.21	0.47	0.33	1.00	0.98
5	2.36	0.05	1.34	0.02	134	0.023	0.32	0.17	0.51	0.31	1.00	0.98
6	2.49	0.053	1.15	0.02	149	0.023	0.21	0.329	0.46	0.35	1.00	0.98
7	2.49	0.051	1.42	0.02	149	0.0237	0.33	0.248	0.43	0.35	1.00	0.98
8	2.48	0.049	1.58	0.03	148	0.0236	0.41	0.178	0.42	0.34	1.00	0.98
9	2.43	0.047	1.61	0.03	142	0.0231	0.44	0.130	0.43	0.32	1.00	0.98
10	2.39	0.045	1.60	0.03	138	0.0228	0.45	0.098	0.46	0.32	1.00	0.98
11	2.45	0.050	1.297	0.021	143	0.023	0.281	0.260	0.47	0.34	1.00	0.98
12	2.47	0.049	1.670	0.031	146	0.023	0.459	0.085	0.45	0.34	1.00	0.98
13	2.51	0.049	1.831	0.035	151	0.024	0.534	0.048	0.41	0.34	1.00	0.98
14	2.48	0.048	1.826	0.035	147	0.024	0.544	0.036	0.42	0.34	1.00	0.98
15	2.45	0.047	1.785	0.035	144	0.023	0.532	0.035	0.43	0.33	1.00	0.98
Prediction of ATS by utilising the acceleration performance estimation method												
Scenario	RMSE	RMSPE	ME	MPE	SSE	U ₁	U _M	U _S	U _C	U ₂	Chi-Sq-GF	Correlation
1	4.13	0.08	0.62	0.01	409	0.040	0.02	0.30	0.67	0.56	1.00	0.92
2	4.01	0.08	1.27	0.02	386	0.038	0.10	0.22	0.68	0.54	1.00	0.92
3	4.04	0.08	1.67	0.03	391	0.038	0.17	0.14	0.68	0.53	1.00	0.92
4	6.00	0.14	4.80	0.11	864	0.056	0.64	0.06	0.30	0.96	0.65	0.88
5	8.82	0.24	6.75	0.16	1868	0.080	0.59	0.31	0.10	1.55	0.00	0.80
6	4.32	0.093	3.08	0.06	449	0.041	0.51	0.000	0.50	0.64	0.99	0.92
7	4.81	0.106	3.69	0.08	555	0.045	0.59	0.006	0.41	0.72	0.97	0.91
8	5.24	0.120	4.12	0.09	658	0.049	0.62	0.024	0.36	0.80	0.91	0.90
9	8.47	0.229	6.58	0.15	1722	0.077	0.60	0.274	0.12	1.46	0.00	0.81
10	10.95	0.325	7.66	0.19	2878	0.099	0.49	0.393	0.12	2.05	0.00	-0.32
11	6.435	0.163	5.028	0.114	994	0.059	0.610	0.155	0.24	1.07	0.37	0.87
12	7.669	0.205	5.935	0.137	1411	0.070	0.599	0.235	0.17	1.37	0.04	0.83
13	8.220	0.222	6.354	0.148	1622	0.075	0.597	0.263	0.14	1.47	0.01	0.81
14	10.932	0.324	7.648	0.188	2868	0.099	0.489	0.394	0.12	2.05	0.00	-0.31
15	11.078	0.327	7.787	0.191	2945	0.100	0.494	0.382	0.12	2.08	0.00	-0.40

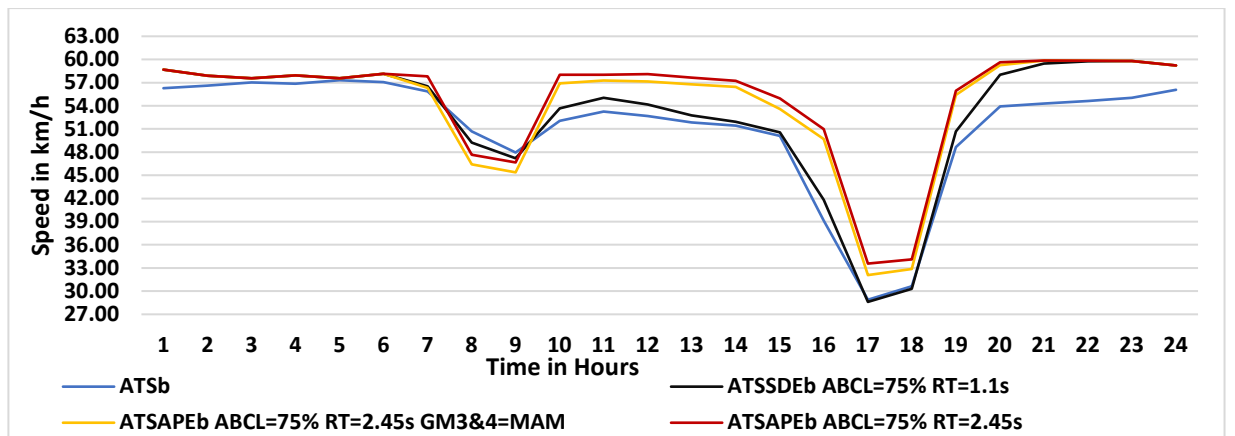


FIGURE 6-27: ATSSDE and ATSAPE estimation BR and AR in comparison to ATS obtained from the ATC at the hours of 1.00-24.00 at an ABCL= 75% and an RT=1.1s for the ATSSDE and an RT=2.45s for the ATSAPE

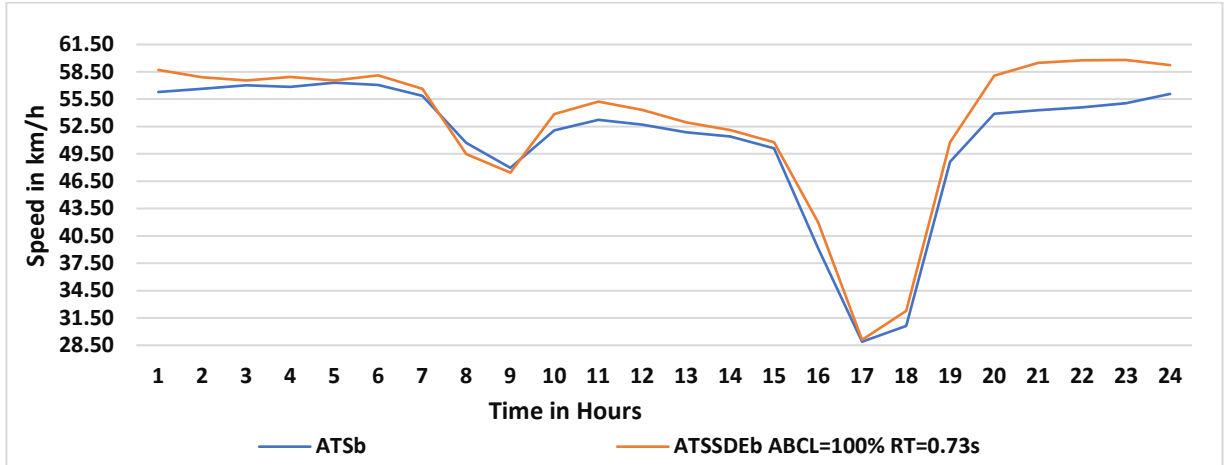


FIGURE 6-28: $ATSS_{SDE}$ estimation BR in comparison to ATS obtained from the ATC at the hours of 1.00-24.00 at an ABCL=100% and an RT=0.73s for the $ATSS_{SDE}$

The results in TABLE 6-21 have shown that the $ATSS_{SDE}$ provided the desired fit at all levels of ABCL and at an average RT of 1.1s. The $ATSA_{PE}$ method has provided an acceptable fit at an ABCL of 50% and an RT of 1.91s, 2.41s, and 2.81s with an average of 2.38s. After narrowing the test window, the results in TABLE 6-21, FIGURE 6-29, FIGURE 6-30, and FIGURE 6-31 showed a significant improvement in the RMSE, RMSPE, ME, MPE, and SSE values of the $ATSS_{SDE}$. However, the results for $ATSA_{PE}$ showed an increased RMSE and RMSPE values and a decrease in the ME, MPE, and SSE values, and the test provided an acceptable fit at an ABCL of 75% and an RT of 2.41s.

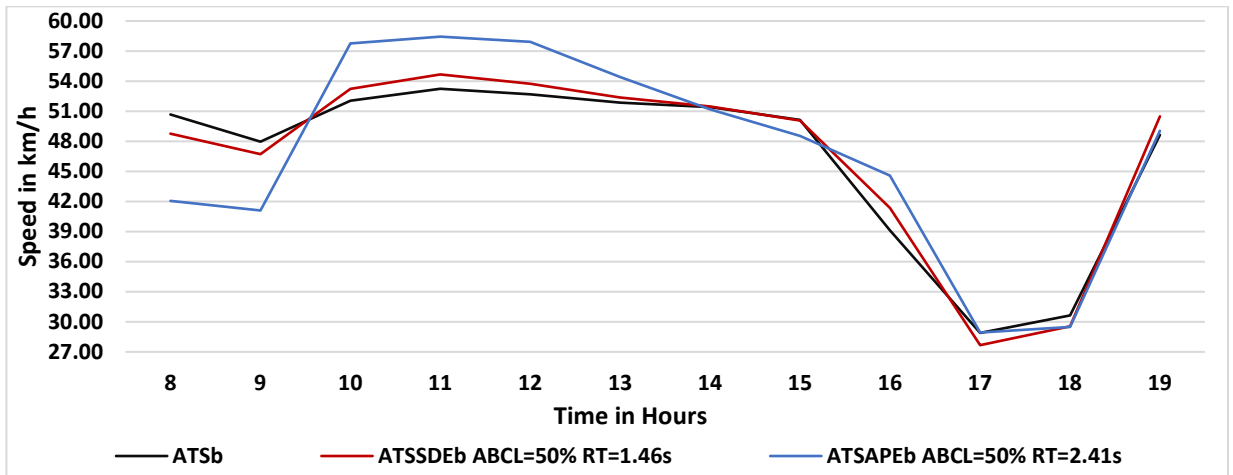


FIGURE 6-29: $ATSS_{SDE}$ estimation BR in comparison to ATS obtained from the ATC at the hours of 8.00-19.00 at an ABCL=50% and an RT=1.46s for the $ATSS_{SDE}$ and an RT=1.46s for the $ATSA_{PE}$

TABLE 6-21: Results of the goodness of fit of the ATS estimation methods at the hours of 8.00-19.00 BR

Prediction of ATS by utilising the speed-density estimation method												
Scenario	RMSE	RMSPE	ME	MPE	SSE	U	U ^M	U ^S	U ^C	U ₂	Chi-Sq-GF	Correlation
1	2.00	0.06	-0.66	-0.02	48	0.04	0.11	0.41	0.63	4.97	0.00	0.98
2	1.82	0.05	-0.03	-0.01	40	0.02	0.00	0.47	0.67	0.26	1.00	0.99
3	1.69	0.05	0.26	0.00	34	0.02	0.02	0.39	0.70	0.24	1.00	0.99
4	1.48	0.04	0.28	0.00	26	0.02	0.03	0.27	0.95	0.21	1.00	0.99
5	<u>1.33</u>	<u>0.03</u>	<u>0.23</u>	<u>0.00</u>	<u>21</u>	<u>0.01</u>	<u>0.03</u>	<u>0.15</u>	<u>1.23</u>	<u>0.18</u>	<u>1.00</u>	<u>0.99</u>
6	1.74	0.05	-0.13	-0.01	36	0.02	0.01	0.42	0.56	0.22	1.00	0.99
7	1.70	0.04	0.37	0.00	35	0.02	0.05	0.40	0.54	0.21	1.00	0.99
8	1.66	0.04	0.68	0.01	33	0.02	0.17	0.28	0.55	0.20	1.00	0.99
9	1.51	0.03	0.73	0.01	27	0.02	0.23	0.16	0.58	0.17	1.00	0.99
10	<u>1.40</u>	<u>0.03</u>	<u>0.72</u>	<u>0.01</u>	<u>24</u>	<u>0.01</u>	<u>0.27</u>	<u>0.06</u>	<u>0.65</u>	<u>0.15</u>	<u>1.00</u>	<u>0.99</u>
11	1.59	0.04	0.15	0.00	30	0.02	0.01	0.36	0.66	0.20	1.00	0.99
12	1.62	0.04	0.86	0.02	31	0.02	0.28	0.05	0.66	0.19	1.00	0.99
13	1.72	0.04	1.16	0.03	36	0.02	0.46	0.02	0.52	0.21	1.00	0.99
14	1.64	0.04	1.16	0.03	32	0.02	0.50	0.00	0.51	0.19	1.00	0.99
15	<u>1.56</u>	<u>0.04</u>	<u>1.08</u>	<u>0.02</u>	<u>29</u>	<u>0.02</u>	<u>0.48</u>	<u>0.00</u>	<u>0.51</u>	<u>0.18</u>	<u>1.00</u>	<u>0.99</u>
Prediction of ATS by utilising the acceleration performance estimation method												
Scenario	RMSE	RMSPE	ME	MPE	SSE	U	U ^M	U ^S	U ^C	U ₂	Chi-Sq-GF	Correlation
1	4.83	0.10	-1.37	-0.03	280	0.10	0.08	0.14	0.49	0.15	1.00	0.93
2	4.56	0.10	-0.21	-0.01	249	0.05	0.01	0.11	0.54	4.97	0.00	0.94
3	<u>4.55</u>	<u>0.09</u>	<u>0.51</u>	<u>0.01</u>	<u>249</u>	<u>0.05</u>	<u>0.00</u>	<u>0.15</u>	<u>0.62</u>	<u>0.41</u>	<u>0.88</u>	<u>0.93</u>
4	7.74	0.19	6.78	0.16	720	0.08	0.77	0.01	0.29	0.38	0.92	0.92
5	11.98	0.34	10.66	0.27	1723	0.12	0.79	0.16	0.88	0.38	0.93	0.89
6	5.15	0.12	3.56	0.08	319	0.05	0.48	0.01	0.52	0.57	0.79	0.91
7	5.89	0.14	4.63	0.11	417	0.06	0.62	0.00	0.38	0.66	0.58	0.91
8	6.56	0.16	5.45	0.13	516	0.07	0.69	0.00	0.31	0.75	0.36	0.90
9	11.46	0.32	10.31	0.25	1577	0.11	0.81	0.13	0.06	1.45	0.00	0.89
10	15.09	0.45	12.48	0.32	2733	0.14	0.68	0.27	0.04	2.07	0.00	-0.48
11	8.48	0.22	7.44	0.18	862	0.08	0.77	0.06	0.17	1.04	0.02	0.88
12	10.29	0.28	9.08	0.22	1270	0.10	0.78	0.11	0.11	1.36	0.00	0.85
13	11.09	0.31	9.86	0.24	1477	0.11	0.79	0.13	0.08	1.46	0.00	0.86
14	15.07	0.45	12.45	0.32	2723	0.14	0.68	0.27	0.05	2.06	0.00	-0.48
15	15.28	0.46	12.73	0.33	2800	0.14	0.69	0.27	0.04	2.09	0.00	-0.45

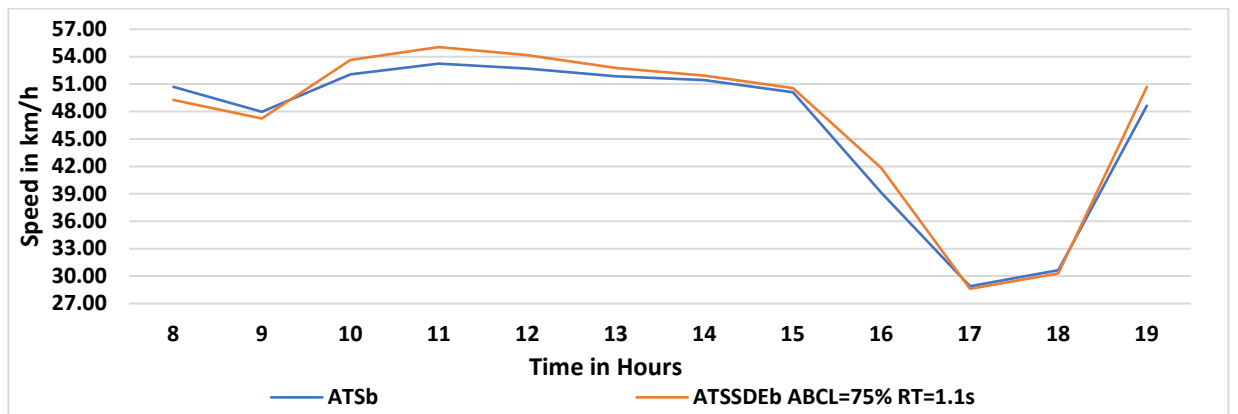


FIGURE 6-30: ATSSDE estimation BR in comparison to ATS obtained from the ATC at the hours of 8.00-19.00 at an ABCL=75% and an RT=1.1s for the ATSSDE

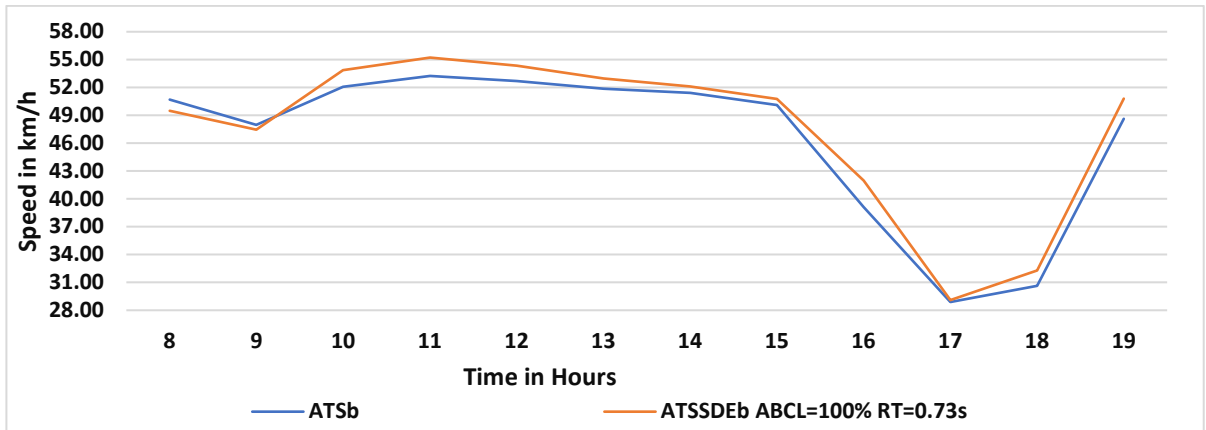


FIGURE 6-31: $ATSS_{SDE}$ estimation BR in comparison to ATSp obtained from the ATC at the hours of 8.00-19.00 at an ABCL=1000% and an RT=0.73s for the $ATSS_{SDE}$

All the results that provided an acceptable and desirable fit had good values of RMSE, RMSPE, ME, MPE, SSE, correlation, and CHI-SQ-GF, and these values were significantly improved after narrowing the test window to cover only high traffic density hours. However, Theil's method did not fulfil its usefulness with all the acceptable and desirable fit cases because of the U_2 of less or equal to one at nine out of 39 cases of acceptable and desirable fit scenarios.

CHAPTER SEVEN: CONCLUSIONS AND FUTURE WORK

7.1 Conclusions

In this research, the author has developed eight novel methods for estimating the HGVs' impact on the traffic flow operation's safety and logistics. The author has based the main methodology on the deceleration and acceleration performance of the vehicle along with the driver's BCL. The methods of estimating the PCE and capacity of the road are the PCE_{DAS} and C_{DAS} . Predicting ATS is important for traffic operation management, rescheduling, and planning. Therefore, the author has developed two speed's prediction methods, the method ATS_{SDE} considers the speed-density relationship, and it is suitable to predict the change ATS due to the change in traffic volumes (such as rescheduling). In contrast, the method ATS_{APE} considers the vehicle's acceleration performance along with the AAG on the road, and it is suitable for predicting ATS and individual vehicle's speed to facilitate road designing and accessibility restrictions.

The author has proposed four novel LoS methods that estimate the risk of having an accident and the risk of sustaining a severe injury or death to pedestrians. The LoS method considers the available reaction time and available stopping distance. It is essential to target the costs of accidents to reduce the number of fatalities and severe injuries, which reduces the cost of accidents. The LoS methods are unique because they target the type of vehicle and not the whole traffic mix. Therefore, such methods can limit access to some roads due to poor safety record or deny access to roads near schools by drivers with poor behaviour record or penalty points.

The author has utilized the vehicle's size, GM, traffic flow volume, the braking system, the ATS, EP, WS, road's grade, road friction, weather conditions, and the drivers' RT and BCL to calculate the deceleration and acceleration performance of vehicles and determine their impact on the traffic flow capacity. In addition, the out of the box approach of vehicle displacement provides realistic roadway availability calculation for the capacity estimation method because the ATS is inversely proportional to the TF.

The model analysis showed that the RT is inversely proportional to capacity and PCE value, and the BCL is directly proportional to capacity and inversely proportional to the headway and PCE value, and the vehicle' headway is directly proportional to the ATS, vehicle' length, weight, driver' RT and inversely proportional to capacity, and

that the PCE value is directly proportional to the traffic ATS, weight, and congestion, and inversely proportional to EP, driver's BCL, and capacity. Therefore, the increase in HGV's PCE will adversely impact capacity and congestion.

The author has found that the currently adopted 2s gap may not always be sufficient, and the current working RT is 1.46-1.68s. The results showed that the required time gap to keep a safe distance between the following vehicle and the leading vehicle depends on the driver's BCL of 100-50% is 1.64-2.37s, 1.64- 3.04 s, 1.89-3.74s, and 1.99-3.94s for PCs, LGVs, HGVr, and HGVa respectively at 64.37km/h (40mi/h). The results also showed that the PCE_{DAS} for HGVs at 64.4km/h with BCL of 100%-50% is 1.32-1.65, and 2.41-2.77 for HGVr HGVa, respectively.

The results also show that the headway distance at a BCL of 100%-50% should be 34.8m-47.6 m, 36m-61m, 45.4 m-78.4m, and 52.1m-86.9m for PC, LGV, HGVr, and HGVa, respectively. Also, the PCE_{DAS} value of HGVa with a BCL of 100% is less than the PCE_{DAS} value of that with a low BCL driver by 0.7. Thus, maintaining the safety gaps will prevent accidents, save lives and money, and allow enough time and space for drivers to decelerate to a standstill and prevent rear-end vehicle collision.

The rescheduling results show how it is possible to meet both of Mersey ports' targets for Liverpool's container port by either building an extra lane of an HGV access only or building HGVa access only two-lane roads in parallel to the current road. However, to improve the traffic flow operation and safety, the second choice will be better because it will keep the ATS above the optimum speed of the road at all times.

7.2 Future Work

The research needs to be extended to cover areas that are out of the scope of this thesis:

- 1- The current model design is microscopic, and in future work, the authors will develop the model to assess a wider area by connecting road links and must include roundabouts, tunnels, and side road.
- 2- Conduct extensive surveys on AEB gap and headways with the use of modern vehicles and the effect of vehicle's size on the reaction time
- 3- Extensively research drivers' behaviour for small and large vehicles, such as long HGVs and high Q container carriers, tankers, and cryogenic container tank carriers.

- 4- Extensively research the road accidents and the risk of drivers and pedestrians sustaining an injury and different ages and sizes of people
- 5- Determine the impact of the congestion on the environment and the driver's behaviour and driving habits effect on fuel consumption
- 6- cover all the aerodynamics of road transportation in extensive research and implement it in the model, such as the impact of snow, ice, and rain on the deceleration and acceleration performance and safety. Also, the road grade, tyre condition, and crosswind resistance and balance
- 7- The effect of re-routing HGVs on the road traffic operation

REFERENCES

- AASHTO, 2001. A Policy on Geometric Design of Highways and Streets. Washington: American Association of State Highway and Transportation Officials.
- AASHTO, 2004. A Policy on Geometric Design of Highway and Streets, Washington, DC: American Association of State.
- AASHTO, 2011. A Policy on Geometric Design of Highways and Streets. s.l.:American Association of State Highway and Transportation Officials (AASHTO).
- Abbas, K., 1990. The use of System Dynamic in Modelling Transportation systems with respect to new cities in Egypt. Masachussets, USA, Systems Dynamics Society, pp. 16-30.
- Abbas, K., 1994. System Dynamics Applicability to Transportation Modeling. *Transport Research*, 28(5), pp. 373-400.
- Adnan, M., 2014. Passenger Car Equivalent Factors in Heterogeneous Traffic Environment-Are we using the right numbers?. *Procedia Engineering*, Volume 77, pp. 106-113.
- Aerde, M. V. & Yagar, S., 1984. Capacity, speed and platooning vehicle equivalents for two-lane rural highways. s.l.:TRB.
- Akelik, R. & Besley, M., 2001. Acceleration and deceleration models. Melbourne, Australia, AAtraffic, p. 9.
- Albin, S., 1997. Build a System Dynamics Model Part 1: Conceptualization, Massachusetts: Massachusetts Institute of Technology (MIT).
- Al-Kaisy, A., 2006. Passenger car equivalents for heavy vehicles at freeways and multilane highways: some critical issues. *ITE Journal*, 76(3), pp. 40-43.
- Al-Kaisy, A. F., Hall, F. L. & Reisman, E. S., 2002. Developing passenger car equivalents for heavy vehicles on freeways during queue discharge flow. *Transportation Research Part A: Policy and Practice*, 36(8), pp. 725-742.
- Al-Kaisy, A. & Jung, Y., 2004. Examining the effect of heavy vehicles during congestion using passenger car equivalents. Johannesburg, South Africa, Document Transformation Technologies, pp. 1-10.
- Al-Kaisy, A., Jung, Y. & Rakha, H., 2005. Developing passenger car equivalency factors for heavy vehicles during congestion. *Journal of transportation engineering*, 131(7), pp. 514-523.
- Allen, J., 2012. The Role of Urban Consolidation Centres in Sustainable Freight Transport. *Transport Reviews*, 32(4), pp. 473-490.
- Allen, J., 2014. A Review of Urban Consolidation Centres in the Supply Chain Based on a Case Study Approach. *The International Journal of Supply Chain Forum*, 15(4), pp. 100-112.
- Ando, K., Sawase, K. & Takeo, J., 2002. Analysis of tight corner braking phenomenon in full-time 4WD vehicles. *JSAE review*, 23(1), pp. 83-87.
- Anon., 2006. Chapter 2: Sensor Technology. In: *Traffic Detector Handbook*. 3rd edition ed. s.l.:s.n.

- Aschauer, G., 2015. Modelling interrelationships between logistics and transportation operations a system dynamics approach. Emerald Group Publishing Limited: Logistics and Transport Operation, 38(5), pp. 505-539.
- Belhocine, A. & Bouchetara, M., 2013. Investigation of temperature and thermal stress in ventilated disc brake based on 3D thermomechanical coupling model. Ain Shams Engineering Journal, 4(3), pp. 475-483.
- Bellucci, P. & Cipriani, E., 2010. Data accuracy on automatic traffic counting: the SMART project results. European Transport Research Review, 2(4), pp. 175-187.
- Benekohal, R. F. & Zhao, W., 2000. Delay-based passenger car equivalents for trucks at signalized intersections. Transportation Research Part A: Policy and Practice, 34(6), pp. 437-457.
- Bester, C. J. & Varndell, P. J., 2002. The effect of a leading green phase on the start-up lost time of opposing vehicles. South Africa, 21st Annual South African Transport Conference.
- Brittany Ferries, 2020. Freight routes to Ireland. [Online]
- Available at: <https://www.brittanyferriesfreight.co.uk/ferry-routes/ireland>
- [Accessed 02 July 2020].
- Browne, M., Woodburn, A. & Allen, J., 2007. Evaluating the potential for urban consolidation centres. European Transport, Issue 35, pp. 46-63.
- Bullas, J. C., 2004. Tyres, road surfaces and reducing accidents-a review, Hampshire, UK: AA Foundation for road safety research.
- Butcher, L., 2009. Lorry sizes and weights. London: House of Commons Briefing SN/BT/654.
- Cady, F., 2017. The Data Science Handbook. s.l.:WILEY.
- Caliskanelli, S. P., Atasever, F. C. & Tanyl, S., 2017. Start-up Lost Time and its effect on signalized intersections in Turkey. Traffic and Transportation, 29(3), pp. 321-329.
- Carwow Ltd, 2020. Audi A4 sizes and dimensions guide. [Online] Available at: <https://www.carwow.co.uk/blog/audi-a4-dimensions-0364> [Accessed June 2020].
- Chandra, S. & Sikdar, P. K., 2000. Factors affecting PCU in mixed traffic situations on urban roads. Road and transport research, 9(3), pp. 40-50.
- Chang, M., Messer, C. J. & Santiago, A. J., 1985. Timing Traffic Signal Change Intervals Based on Driver Behavior. Transportation Research Record, Issue 1027, pp. 20-30.
- Chen, Y., 2016. Speed-Density Model of Interrupted Traffic Flow Based on Coil Data. Hindawi Mobile Information Systems, p. 12.
- Consiglio, W., 2003. Effect of cellular telephone conversations and other potential interference on reaction time in a braking response. Accident Analysis and Prevention, Volume 35, pp. 495-500.
- Cummins, 2017. Cummins Engines for Heavy-Duty Truck. [Online] Available at: <https://www.cummins.com/>
- Cunagin, W. D. & Chang, E. C., 1982. Effects of Trucks on Freeway Vehicle Headways Under Off-Peak Flow Conditions. Transportation Research Record, Issue 869, pp. 54-59.

- Cunagin, W. D. M. C. J., 1983. Passenger-Car Equivalents for Rural Highways. Washington District of Columbia, United States, Transportation Research Board, pp. 61-68.
- Dalglish, M. & Hoose, N., 2008. Highway Traffic Monitoring and Data Quality. 1st ed. London: Artech House.
- David Quarmby, P. C., 2016. Safety Management on the MRN, a major road network for ENGLAND: Supporting Document 8, s.l.: Rees Jeffreys.
- Del Castillo, J., 2012. Three new models for the speed-density relationship: Derivation and testing for freeway and urban data. *Transportmetrica*, Volume 6, p. 443-465.
- Del Castillo, J. M. & BENITEZ, F. G., 1995. On the functional form of the speed-density relationship-I: General Theory. *Transportation Research B*, 29B(5), pp. 373-38.
- DfT, 2018. Statistical data set, Port freight (PORT02): Port freight statistics tables. [Online] Available at: <https://www.gov.uk/government/statistical-data-sets/port-and-domestic-waterborne-freight-statistics-port>
- DfT, 2002. Design Manual for Roads and Bridges: Part 1: Volume 6 Road Geometric: TD 9/93 - Amendment NO 1: Highway Link Design. [Online] Available at: <http://www.standardsforhighways.co.uk/ha/standards/dmrb/vol6/section1.htm>
- DfT, 2003. Lorries Types and Weights Guide, London: Department for Transport (DfT).
- DfT, 2010. Guidance: HGV maximum weights. [Online]
Available at: <https://www.gov.uk/government/publications/hgv-maximum-weights/hgv-maximum-weights>
- DfT, 2015. The Highway Code, Stopping Distance, rule 126. [Online] Available at: <https://www.gov.uk/guidance/the-highway-code/general-rules-techniques-and-advice-for-all-drivers-and-riders-103-to-158>
- DfT, 2015. TRIS – User Guide Revision 3: Highway England-Data.gov.uk-Journey Time and Traffic Flow Data April 2015 onward User guide. London: Department for Transport.
- DfT, 2015. Working Together to Build a Safer Road System. [Online] Available at: https://assets.publishing.service.gov.uk/government/uploads/system/uploads/attachment_data/file/487704/british_road_safety_statement_print.pdf
- DfT, 2016. Free Flow Vehicle Speed Statistics: Great Britain 2015, London: Department for Transport (DfT).
- DfT, 2016. UK Port Freight Statistics: 2016 (revised). [Online] Available at: https://assets.publishing.service.gov.uk/government/uploads/system/uploads/attachment_data/file/646188/port-freight-statistics-2016-revised.pdf
- DfT, 2017. Information Sheet Maximum Length of Vehicles used in Great Britain. London: Department for Transport.
- DfT, 2017. Traffic Counts. [Online] Available at: <http://www.dft.gov.uk/traffic-counts/> [Accessed 23 April 2018].
- DfT, 2017. UK Port Freight Statistics: July to September 2017 (Quarter 3). [Online] Available at: <https://www.gov.uk/government/statistics/port-freight-statistics-july-to-september-2017>
- DfT, 2018. Accidents, casualties, and costs in UK. [Online] Available at: <https://www.gov.uk/government/statistical-data-sets/ras60-average-value-of-preventing-road-accidents>

- DfT, 2018. Traffic Statistics Methodology Review: Overview. [Online] Available at: https://assets.publishing.service.gov.uk/government/uploads/system/uploads/attachment_data/file/722511/traffic-statistics-methodology-review.pdf
- DfT, 2018. UK Port Freight Statistics: January to March 2018 (Quarter 1). [Online] Available at: https://assets.publishing.service.gov.uk/government/uploads/system/uploads/attachment_data/file/715517/port-freight-statistics-january-to-march-2018.pdf
- DfT, 2020. Road Traffic Statistics. London: DfT.
- DfT, 2020. Statistical data set: Heavy Goods Vehicles (VEH05). [Online] Available at: <https://www.gov.uk/government/statistical-data-sets/veh05-licensed-heavy-goods-vehicles> [Accessed 30 July 2017].
- Disney, S. M., Potter, A. T. & Gardner, B. M., 2003. The impact of vendor managed inventory on transport operations. *Transportation Research Part E*, 39(5), pp. 363-380.
- DMV, 2005. Commercial Driver's License Manual: Section 2: Driving Safely, State of California: Department of Motor Vehicles.
- DMV, 2005. Commercial Driver's License Manual: Section 5: Air Brakes, State of California: Department of Motor Vehicles.
- Drake, J. S., Schofer, J. L. & May Jr, A. D., 1967. A Statistical Analysis of Speed-Density Hypotheses. *Highway Research Record*, Issue 154, pp. 112-117.
- Drew, D. R. & Keese, C. J., 1965. Freeway Level of Service as Influenced by Volume and Capacity Characteristic, Texas: TEXAS TRANSPORTATION INSTITUTE.
- Easa, S. M., 1982. Selecting Two-Regime Traffic-Flow Models. *Transportation Research Record*, Issue 869, pp. 25-36.
- Edie, L. C., 1961. Car Following and Steady-State Theory for Non-Congested Traffic.. *Operations Research*, 9(1), pp. 66-76.
- Elefteriadou, L., Torbic, D. & Webster, N., 1997. Development of passenger car equivalents for freeways, two-lane highways, and arterials. *Transportation Research Record*, Issue 1572, pp. 51-58.
- Ericksen, E. L., Greenshields, B. D. & Schapiro, D., 1947. Traffic performance at urban street intersections. In: *Traffic Quarterly*. Saugatuck, Connecticut: The Eno Foundation for Transportation for Highway Control, pp. 254-267.
- Fambro, D. B., Fitzpatrick, K. & Koppa, R. J., 1997. NCHRP Report 400: Determination of stopping sight distances, Texas: Transportation Research Board.
- Fan, H. S. L., 1990. Passenger car equivalents for vehicles on Singapore expressways. *Transportation Research Part A: General*, 24(5), pp. 391-396.
- Fishwick, 1995. *Simulation Model Design and Execution*. 1st ed. London: Prentice-Hall.
- Forda, A. & Flynn, H., 2005. Statistical Sncreeing of system dynamics models. *System Dynamics Review*, 21(4), pp. 273-303.
- Forrester, J. W., 1961. *Industrial Dynamics*. 1st ed. Massachusetts: MIT.

- Forrester, J. W., 1980. Information Sources for Modeling the National Economy. *Journal of the American Statistical Association*, 75(371), pp. 555-566.
- Fosu, G. O., Akweitley, E., Opong, J. M. & Otoo, M. E., 2020. Vehicular traffic models for speed-density-flow relationship. *Journal of Mathematical Modeling*, 8(3), pp. 241-255.
- Freightliner, 2018. Departures and Arrivals. [Online]
- Available at: <https://www.freightliner.co.uk/intermodal/departures-and-arrivals/>
- Gaddam, H. K. & Rao, K. R., 2019. Speed–density functional relationship for heterogeneous traffic data: a statistical and theoretical investigation. *Journal of Modern Transport*, 27(1), pp. 61-74.
- Gautam, A. D. A. R. K. R. a. T. G., 2016. Estimation of PCE values for hill roads in heterogeneous traffic conditions. *Transportation Letters*, pp. 1-9.
- Geometrics and Operations Unit Traffic and Safety, 2015. Sight Distance Guidelines. s.l.:Michigan Department of Transportation (MDOT).
- Georgiadis, P., Vlachos, D. & Iakovou, E., 2005. A system dynamics modelling framework for the strategic supply chain management of food chains. *Journal of Food Engineering*, 70(3), pp. 351-364.
- Gillespie, T., 1992. *Fundamentals of Vehicle Dynamics*. 2nd ed. s.l.:Society of Automotive Engineers.
- Giuffrè, O. G. A. M. L. T. ., S. A., 2018. Capacity-based calculation of passenger car equivalents using traffic simulation at double-lane roundabouts. *Simulation Modelling Practice and Theory*, Volume 81, pp. 11-30.
- Giuffrè, O. & G. A. T. M. L. S. A., 2017. Estimation of Passenger Car Equivalents for single-lane roundabouts using a microsimulation-based procedure. *Expert Systems With Applications*, Volume 79, pp. 333-347.
- GmbH, R. B., 2011. *Bosch, Automotive Handbook*. 8th ed. s.l.:Wiley-Blackwell.
- GOV.UK, 2017. The Drink Drive Limit. [Online] Available at: <http://www.gov.uk/drink-drive-limit>
- GOV.UK, 2020. <https://www.gov.uk/government/news/vital-routes-for-supplies-and-people-kept-open-through-coronavirus-support-package>. [Online] Available at: <https://www.gov.uk/government/news/vital-routes-for-supplies-and-people-kept-open-through-coronavirus-support-package> [Accessed 01 July 2020].
- Government Office of Science, 2019. A time of unprecedented change in the transport system, London: Government Office of Science.
- Greenberg, H., 1959. An Analysis of traffic Flow. *Operation Research*, Volume 7, pp. 78-85.
- Green, M., 2000. "How Long Does It Take to Stop?" Methodological Analysis of Driver Perception-Brake Times. *Transportation Human Factors*, 2(3), pp. 195-216.
- Greenshields, B. D., 1935. A Study of Traffic Capacity. *Highway Research Board*, Volume 14, pp. 448-447.
- Greibe, P., 2007. *Braking distance, friction and behaviour*, Lyngby, Denmark: Trafitec.
- Guofa, L. et al., 2020. Influence of traffic congestion on driver behavior in post-congestion driving. *Accident Analysis and Prevention*, Volume 141.
- Gwynn, D. W., 1968. Truck equivalency. *Eno Transportation Foundation*, 22(2), pp. 225-236.

- Hammache, M., Michaelian, M. & Browand, F., 2002. Aerodynamic forces on truck models, including two trucks in tandem, California state: SAE Technical Paper.
- HE, 2017. A5036 Port of Liverpool access scheme. [Online] Available at: <https://highwaysengland.citizenspace.com/he/a5036-port-of-liverpool-access-scheme/> [Accessed 2021].
- HE, 2017. Available Data Sources. [Online] Available at: <http://tris.highwaysengland.co.uk/> [Accessed 30 May 2018].
- Heisler, H., 2002. Advanced vehicle technology. 2nd ed. London: Elsevier.
- HGV Direct, 2017. HGV Direct Parts. [Online] Available at: <https://www.hgvdirect.co.uk/>
- Highway Code, 2019. The Highway Code. [Online] Available at: <https://www.highwaycodeuk.co.uk/control-of-the-vehicle.html>
- Hill, T. B. F. S. R. J. R. C., 1984. Properties of Dynamic Simultaneous Equations Models. In: Advanced Econometric Methods. New York: s.n., pp. 530-552.
- HSE, 2020. How much space am I entitled to at work?. [Online] Available at: <https://www.hse.gov.uk/contact/faqs/roomspace.htm> [Accessed 2020].
- Huber, M. J., 1982. Estimation of Passenger-Car Equivalents of trucks in Traffic stream. Transportation Research Record, Issue 869, pp. 60-70.
- ICCT, 2019. European Vehicle Market Statistics: Pocketbook 2019/20. 2019 ed. Berlin, Germany: The International Council of Clean Transportation.
- iContainers, 2020. Guide to shipping container dimensions. [Online] Available at: <https://www.icontainers.com/the-different-types-of-containers/> [Accessed 02 July 2020].
- Ishak, A. B. B. T. O., 2016. Brake torque analysis of fully mechanical parking brake system: Theoretical and experimental approach. Measurement, Volume 94, pp. 487-497.
- Johansson, G. & Rumar, K., 1971. Drivers' brake reaction times. Human Factors, 13(1), pp. 23-27.
- Johansson, H. & Bjorklund, M., 2017. Urban consolidation centres; retail stores demands for UCC services. International Journal of Physical Distribution & Logistics Management (IJPDL), 47(7), pp. 646-662.
- Justyna Lemke, M. Ł., 2013. Validation of System Dynamics Models a Case Study. Journal of Entrepreneurship Management and Innovation (JEMI), 9(2), pp. 45-59.
- Kang, N. H., 2016. An Analysis of Heavy Vehicle Impact on Roundabout Entry Capacity in Japan. Transportation Research Procedia, ISEHP 2016. International Symposium on Enhancing Highway Performance, Volume 15, p. 308-318.
- Katrakazas, C., 2021. Prediction of rear-end conflict frequency using multiple-location traffic parameters. Accident Analysis and Prevention, 152(106007), pp. 1-9.
- Keller, E. L. S. J. G., 1984. Passenger car equivalents from network simulation. Journal of Transportation Engineering, 110(4), pp. 397-411.
- Kettlson & Associates, 2008. TRAFFIC SIGNAL TIMING MANUAL. Texas: The Federal Highway Administration.

- Kirkwood, 2013. *System Dynamics Methods: A Quick Introduction*. 2nd ed. s.l.: Ventana Systems.
- Kirkwood, C. W., 1998. *System Dynamics Methods: A Quick Introduction*. 1st ed. Arizona State: College of Business Arizona State University.
- Krammes, R. & Crowley, K., 1986. Passenger car equivalents for trucks on level freeway segments. *Transportation Research Record*, Issue 1091, pp. 10-17.
- Kroyer, H. R. G., 2015. Is 30 km/h a 'safe' speed? Injury severity of pedestrians struck by a vehicle and the relation to travel speed and age. *IATSS Research*, Volume 39, pp. 42-50.
- Kutz, M., 2004. *Handbook of transportation engineering*. 1st ed. New York: McGraw-Hill.
- Layton, R. & Dixon, K., 2012. *Stopping Sight Distance*, Corvallis, Oregon State: The Kiewit Center for Infrastructure and Transportation.
- Lee, H. Y. & Lee, H. W. K. D., 1998. Origin of synchronized traffic flow on highways and its dynamic phase transitions. *Physical Review Letter*, 81(5), p. 1130–1133.
- Lerner, N. D., 1993. Brake Perception-Reaction Times of Older and Younger Drivers. s.l., s.n., pp. 206-210.
- Lloyd, L. W. C. B. J., 2015. A collection of evidence for the impact of the economic recession on road fatalities in Great Britain. *Accident Analysis & Prevention*, Volume 80, pp. 274-285.
- LTP Support Unit, 2011. *The third Local Transport Plan for Merseyside, Annex 4:Freight Strategy*, Liverpool, UK: LTP Support Unit.
- Macioszek, E., 2019. The Passenger Car Equivalent Factors for Heavy Vehicles on Turbo Roundabouts. *Frontiers in Built Environment*, 5(68), p. 13.
- MacNicholas, M., 2008. A simple and pragmatic representation of traffic flow. Woods Hole MA, United States, *Greenshields 75 Symposium*, pp. 161-177.
- Makki, A. A., 2019a. Utilizing Automatic Traffic Counters to Predict Traffic Flow Speed. 12th International Conference on Developments in eSystems Engineering (DeSE), Kazan, Russia, pp. 823-830.
- Makki, A. A., 2019b. The effect of the increase of container carrier heavy goods vehicles on traffic flow operation and congestion. Liverpool, Liverpool John Moores University.
- Makki, A. A., 2020. Estimating Road Traffic Capacity. *IEEE Access*, Volume 8, pp. 228525 - 228547.
- Makki, A. A., Nguyen, T. T. & Ren, J., 2019c. A New Level of Service Method for Roads Based on Available Perception Time and Risk of Sustaining Severe Injury or Death, 5th International Conference on Transportation Information and Safety (ICTIS), Liverpool, UK, pp. 1031-1036.
- Mannering, F. L. & Washburn, S. S., 2013. *Principles of Highway Engineering and Traffic Analysis*. s.l.:WILEY.
- Maritime UK, 2019. Peel Ports. [Online] Available at: <https://www.maritimeuk.org/national-impact-award-2018/shortlist/peel-ports/>[Accessed 08 June 2021].
- Mardani, M. N., Chandra, S. & Ghoshc, B., 2015. Passenger Car Unit of Vehicles on Undivided Intercity Roads in India. *Procedia Computer Science*, Volume 52, pp. 926-931.
- Martin, V. H. S. H. D., 2013. *Econometric Modelling with Time Series*. Cambridge: Cambridge University Press.

- Mathew, T. V., 2014. Transportation Systems Engineering. 1st ed. s.l.:s.n.
- Matsoukis, E. & Efstathiadis, S., 2013. An investigation of the variability of start-up lost times and departure headways at signalized intersections in urban areas. Transactions on State of the Art Science and Engineering: Intersection Control and Safety, Volume 66, pp. 53-62.
- Maurya, A. K. & Bokare, P. S., 2012. Study of deceleration behaviour of different vehicle types. International Journal for Traffic & Transport Engineering, 2(3), p. 253 – 270.
- Meadows, E., 2018. Freight Rail Capacity, Liverpool: Freedom of Information.
- Mehar, A., Chandra, S. & Velmurugan, S., 2013. Speed and Acceleration Characteristics of Different Types of Vehicles on Multi-Lane Highways. European Transport, Issue 55, p. 12.
- Merseytravel, 2015. Liverpool City Region (LCR) Freight Sites, Liverpool: Merseytravel.
- Merseytravel, 2018. Freight Sites Neighbouring the Liverpool City Region, Liverpool, UK: Merseytravel.
- MIT, 1935. Report of the Massachusetts Highway Accident Survey, State of Massachusetts: Massachusetts Institute of Technology (MIT).
- Moderation, 2017. Blood Alcohol Content (BAC) Tables. [Online] Available at: <http://www.moderation.org/bac/bac-men.html> and <http://www.moderation.org/bac/bac-women.html>
- Molina, C. J., Messer, C. J. & Fambro, D. B., 1987. Development of passenger car equivalencies for large trucks at signalized intersections. ITE Journal, 57(11).
- Mustapha, N. H. N. H. N. N. W. N., 2016. Outflow of traffic from the national capital Kuala Lumpur to the north, south and east coast highways using flow, speed and density relationships. Journal of Traffic and Transportation Engineering (English edition), 3(6), pp. 540-548.
- MyCarDoesWhat.org, 2019. Automatic Emergency Braking. [Online] Available at: <https://mycardoeswhat.org/safety-features/automatic-braking/>
- National Infrastructure Commission, 2019. National Infrastructure Commission: Future of Freight Demand FINAL REPORT, s.l.: MDS TRANSMODAL LIMITED.
- Network Rail, 2018. The timetable. [Online] Available at: <https://www.networkrail.co.uk/running-the-railway/the-timetable/>
- Newell, G., 1961. Nonlinear effects in the dynamics of car following. Operation Research, 9(2), pp. 209-229.
- NHTSA, 2000. A Review of the Literature on the Effects of Low Doses of Alcohol on Driving-Related Skills, Washington: USA Department of Transport: National Highway Traffic Safety Administration (NHTSA).
- NHTSA, 2004. Class 8 Truck Tractor Braking Performance Improvement Study, Report 1: Straight Line Stopping Performance on a High Coefficient of Friction Surface, Washington: National Highway Traffic Safety Administration (NHTSA).
- NHTSA, 2004. Laboratory Test Procedure for FMVSS 121 Air Brake System, Washington: US Department of Transportation.
- NHTSA, 2005. Laboratory test on FMVSS 135 Light Vehicle Brake System, Washington: NHTSA.

- Nielsen, L. D., Jespersen, P. H., Petersen, T. & Hansen, L. G., 2003. Freight transport growth—a theoretical and methodological framework. *European Journal of Operational Research*, 144(2), p. 295–305.
- Norman, O. K., 1953. Braking distance of vehicles from high speed. *Highway Research Board*, Volume 32, pp. 421-436.
- Obiri-Yeboah, A. A., Tuffour, Y. A. & Salifu, M., 2014. Passenger Car Equivalents for Vehicles at Signalized Intersections within the Kumasi Metropolis in Ghana. *IOSR Journal of Engineering*, 4(4), pp. 24--9.
- O'Flaherty, C. et al., 2006. *Transport Planning and Traffic Engineering*. 1st ed. London: ELSEVIER.
- Oudat, E., Mousa, M. & Claudel, C., 2015. Vehicle Detection and Classification Using Passive Infrared Sensing. Dallas, TX, USA, IEEE, pp. pp. 443-444.
- Pajecki, R., 2019. Estimating Passenger Car Equivalent of Heavy Vehicles at Roundabout Entry Using Micro-Traffic Simulation. *Frontiers in Built Environment*, 5(77), pp. 1-11.
- Paul H. Wright, R. J. P., 1987. *Highway Engineering*. 5th ed. s.l.: John Wiley & Sons.
- Peel Ports, 2011. *Mersey Ports Master Plan: A 20 year Strategy for Growth*, Liverpool, UK: Peel Ports.
- Peel Ports, 2018. Peel Ports Launches First Rail Freight Service. [Online] Available at: <https://www.peelports.com/news/2018/peel-ports-launches-first-rail-freight-service>
- Peugeot, 2019. Eight-Seater Cars. [Online] Available at: <http://www.peugeot.co.uk>
- Pipes, L. A., 1967. Car Following Models and the Fundamental Diagram of Road Traffic. *Transportation Research*, Volume 1, pp. 21-29.
- Podoprigora, N. D. V. P. A. L. V., 2017. Methods of Assessing the Influence of Operational Factors on Brake System Efficiency in Investigating Traffic Accidents. *Transportation Research Procedia*, Volume 20, pp. 516-522.
- Porciatti, V. & Fiorentini, A. M. M. C. B. D. C., 1999. The effects of ageing on reaction times to motion onset. *Vision Research*, 39(12), pp. 2157-2164.
- Potter, A. & Lalwani, C., 2008. Investigating the impact of demand amplification on freight transport. *Transportation Research Part E*, 44(5), pp. 835-846.
- Qiu, Y. S. X. S. C., 2015. A System Dynamics Model for Simulating the Logistics Demand Dynamics of Metropolitans: A Case Study of Beijing, China. *Journal of Industrial Engineering and Management*, 3(8), pp. 783-803.
- Rahman, M. & Nakamura, F., 2005. Measuring passenger car equivalents for non-motorized vehicle (rickshaws) at mid-block sections. *Journal of the Eastern Asia Society for Transportation Studies*, Volume 6, pp. 119-126..
- Rakha, H., 2001. Vehicle dynamics model for predicting maximum truck acceleration levels. *Journal of transportation engineering*, 127(5), pp. 418-425.
- Right Driver, 2020. How wide are roads?. [Online] Available at: <https://mocktheorytest.com/resources/how-wide-are-roads/> [Accessed 2020].
- Road Safety Authority, 2015. *Guidelines on Maximum Weights and Dimensions of Mechanically Propelled Vehicles and Trailers, Including Manoeuvrability Criteria*, s.l.: Road Safety Authority.

- Roberts, N. et al., 1997. Introduction to Computer Simulation: A system dynamics modelling approach. Journal of Operational Research Society, Issue 48, p. 1145.
- Roess, R. P., Linzer, E. M., McShane, W. R. & Pignataro, L. J., 1980. A revised procedure for the capacity analysis of basic freeway sections. Transportation Research Part A: General, 14(1), pp. 1-11.
- Roess, R. P. M. C. J., 1983. Passenger car equivalents for uninterrupted flow: revision of the circular 212 values. Transportation Research Record, Issue 971, pp. 7-13.
- Rogers, M. E. B., 2016. Highway Engineering. 3rd ed. London: Wiley Blackwell.
- Rooijen, T. V. & Quak, H., 2010. Local impacts of a new urban consolidation centres the case of Binnenstadservice.nl. Social and Behavioral Sciences, 2(3), pp. 5967-5979.
- Ryus, P. et al., 2011. Highway Capacity Manual (HCM) Summary mini-feature. Washington: Transportation Research Board.
- Sabhash Chand, N. J. G. S. V., 2017. Development of Saturation Flow Model at Signalized Intersection for Heterogeneous Traffic. Transportation Research Procedia, Volume 25, pp. 1662-1671.
- Seguin, E. L., Crowley, K. W. & Zweig, W. D., 1982. Passenger car equivalents on urban freeways, Washington DC: US Federal Highway Administration, Offices of Research and Development.
- Sharp, C. & Jennings, A., 1972. More Powerful Engines for Lorries? An Exercise in Cost-Benefit Analysis. Journal of Transport Economics and Policy, 6(2), pp. 154-166.
- Shawky, M. A.-G. A., 2016. Start-up delay Estimation at Signalized Intersections: Impact of Left-Turn Phasing Sequences. International Journal of Engineering and Applied Sciences (IJEAS), 3(11), pp. 7-12.
- Shepherd, S., 2012. Toll Competition and Dynamic Toll-Setting Strategies. International Journal of Sustainable Transportation, 7(3), pp. 186-203.
- Sivak, M., Olson, P. L. & Farmer, K. M., 1982. Radar-Measured Reaction Times of Unalerted Drivers to Brake Signals. Perceptual and Motor Skills, 55(2), p. 594.
- St John, A. D., 1976. Nonlinear Truck Factor for Two-Lane Highways, Kansas City, Missouri: Midwest Research Institute.
- St John, A. D. & Kobett, D. R., 1978. Grade Effects on Traffic Flow Stability and Capacity, Kansas City, Missouri: National Cooperative Highway Research Program.
- Sterman, J., 2000. Business Dynamics: Systems thinking and modelling for a complex world. 1st ed. s.l.: McGraw-Hill Higher Education.
- Sumner, R. H. D. S. S., 1984. Segment passenger car equivalent values for cost allocation on urban arterial roads. Transportation Research Part A: General, 18(5-6), pp. 399-406.
- System Dynamics Society, 2019. Origin of System Dynamics:. [Online] Available at: <https://www.systemdynamics.org/origin-of-system-dynamics> [Accessed 2019].
- TAC-Drink Driving Statistics, 2017. Drink Driving Statistics, Melbourne, Australia: Transport Accident Commission (TAC).
- TAC-Effects of Alcohol, 2017. Effects of Alcohol, Melbourne, Australia: Transport Accident Commission (TAC).

- TAC-Fatigue statistics, 2017. Fatigue statistics, Melbourne, Australia: Transport Accident Commission (TAC).
- Talati, F. & Jalalifar, S., 2009. Analysis of heat conduction in a disk brake system. *Heat and mass transfer*, 45(8), p. 1047–1059.
- Tata Steel, 2013. Technical Information Sheet: Axle weights and load distribution, s.l.: Tata Steel.
- Tefft, B. C., 2013. Impact speed and a pedestrians risk of severe injury or death. *Accident Analysis & Prevention*, Volume 50, pp. 871-878.
- Thatcham Research, 2016. Autonomous Emergency Braking (AEB): Frequently Asked Questions. [Online] Available at: <https://news.thatcham.org/documents/aeb-frequently-asked-questions-52213> [Accessed 2017].
- The Independent Transport Commission (ITC), 2017. How can we improve urban freight distribution in the UK? Challenges and solutions. [Online] Available at: <https://www.theitc.org.uk/wp-content/uploads/2017/05/ITC-Urban-Distribution-report-May-2017.pdf>
- The Inland Waterways Association (IWA), 2013. IWA Policy on Freight on Inland Waterways. [Online] Available at: https://www.waterways.org.uk/pdf/freight_policy
- Toledo, T. & Koutsopoulos, H. N., 2004. Statistical Validation of Traffic Simulation Models. *Transportation Research Record Journal of the Transportation Research Board*, 1(1876), pp. 142-150.
- Tournier, C. C. P. T. H. C. L. C. L. H. M., 2014. A few seconds to have an accident, a long time to recover: Consequences for road accident victims from the ESPARR cohort 2 years after the accident. *Accident Analysis and Prevention*, Volume 72, pp. 422-432.
- TrafficTechnology, 2021. Tube. [Online] Available at: <https://trafficttechnology.co.uk/blog/portfolio/pneumatic-tube-counter/> [Accessed 2021].
- TRB, 2000. Highway Capacity Manual (HCM). 4th ed. Washington, DC: Transportation Research Board.
- TRB, 2010. Highway Capacity Manual (HCM). 5th ed. Washington, DC: Transportation Research Board.
- TRB, 2020. Highway Capacity Manual, A Guide for Multimodal Mobility Analysis. 6th edition ed. Washington DC: Transportation Reseach Board.
- U.S. Department of Transportation, 2017. Traffic Signal Timing Manual. Washington, DC: U.S. Department of Transportation, Federal Highway Administration, Office of Operation.
- UKessays, 2010. Effect of Alcohol on Reaction Times: Experiment. [Online] Available at: <https://www.ukessays.com/essays/sciences/alcohol-reaction-time.php?vref=1>
- Umama, A. & Mecit, C., 2017. Impacts of heavy vehicles on inter-vehicle interactions and passenger car equivalents for tunnel traffic. *Case Studies on Transport Policy*, Volume 5, pp. 580-586.
- Underwood, R. T., 1961. Speed, Volume, and Density Relationships: Quality and Theory of Traffic Flow, Pennsylvania State, United States: Yale Bureau of Highway Traffic.
- Volvo, 2017. Volvo Trucks. [Online] Available at: <http://www.volvotrucks.com>
- Volvo, 2017. Volvo Trucks Range whatever your needs, we have a truck suited to you, London, UK: Volvo.
- Wang, H., 2011. Logistic modeling of the equilibrium speed–density relationship. *Transportation Research Part A*, Volume 45, p. 554–566.

- Wasserman, L., 2005. All of Statistics : A Concise Course in Statistical Inference. 1st Edition ed. Pittsburgh, USA: Springer Texts in Statistics.
- Webster, N. & Elefteriadou, L., 1999. A simulation study of truck passenger car equivalents (PCE) on basic freeway sections. *Transportation Research Part B: Methodological*, 33(5), pp. 323-336.
- Werner, A. I. & Morrall, J. F., 1976. Passenger car equivalencies of trucks, buses, and recreational vehicles for two-lane rural highways. *Transportation Research Record*, Issue 615, pp. 10-17.
- Wetherill, G. B., 1981. *Intermediate Statistical Methods*. 1st Edition ed. New York, USA: Chapman and Hall.
- Wilson, M. C., 2007. The impact of transportation disruptions on supply chain performance. *Transportation Research Part E: Logistics and Transportation Review*, 43(4), pp. 295-320.
- Windmill Software Ltd, 2019. Vehicle Sensing: Ten Technologies to Measure Traffic. [Online] Available at: <https://www.windmill.co.uk/vehicle-sensing.html> [Accessed 2021].
- Wortman, R. H. & Matthias, J. S., 1983. Evaluation of Driver Behavior at Signalized Intersections. *Transportation Research Record*, Issue 904, pp. 10-20.
- Zwahlen, H. T., 1976. The effect of alcohol on driving skills and reaction times. *Journal of Occupational Accidents*, 1(1), pp. 21-38.

APPENDIX A: INTRODUCTION

A.1 AUTOMATIC RAIL TIMETABLE

To maintain and develop freight rail operations, the author has explored utilizing ARTT that can dynamically adapt to the events that occur at the rail tracks, ports, or UCCs and provide solutions to the problems facing the network. ARTT can maintain undisrupted rail flow by managing the timetables according to passenger and freight demand (Network Rail 2018).

- ARTT can help to an increase in the frequency of freight rail dispatches with expansion in infrastructure by making use of the communication and collaboration of rail and logistics operators
- ARTT can reduce HGVs, congestion and pollution on urban roads
- ARTT could have embedded scenarios in case of an emergency by having an alternative route and even dictate train speeds to reduce congestion
- ARTT can provide a clear path for freight trains because they do not stop at passenger rail stations
- ARTT can dynamically feed on the information hub that contains the communication between rail operators, suppliers, and retailers and adapt to the change in demand for freight deliveries
- ARTT can ensure the safety of the products and the crew by avoiding accidents
- ARTT can ensure the safety of passengers and the public at the rail station
- ARTT can reduce congestion and pollution trains on rail tracks, and reduce the cost of delivery and avoid any delivery deadline charges

However, to develop an ARTT solution, the author had to consider several problems associated with rail timetables.

These problems are as follows:

- Speed limits: The speed limit changes on parts of the same track, e.g., it varies at bends and over points.
- Number of trains for every section: Only one train can occupy a given track section at any single time

- Signalling infrastructure: The signalling infrastructure varies across the network in the UK; therefore, what is considered a safe distance between two trains at one location can be different from other locations in the UK.
- Minimum time gap: The trains operating at the same platform need to maintain at least the minimum time gap between each other to avoid crashes
- Train conductors can underestimate the speed of the train or overestimate the braking power, which leads to second rate accidents; however, these kinds of accidents do not cause fatalities
- Stopping or non-stopping trains: usually a passenger train makes many stops until it reaches its destinations (pick-up and drop-off passengers), while freight rail usually can continue on its path and speed until it reaches its destination
- Knock-on effects: If an event occurs at one location of the national network, it could cause a delay effect that would continue for a day or more and affect more vast regions and disrupt transportation. ARTT can reduce transportation delay caused by the knock-on effect by removing some trains from a track or arranging for alternative routes to maintain traffic flow and reduce delay
- Rail accidents and fatalities: Accidents that occur on the track or inside the trains could lead to fatalities and require police, ambulance, and social care attention. These events usually cause lengthy delays. ARTT can reduce rail accidents by maintaining the proper distance and time gap between trains on the same track. Facilitating alternative routes: In case of a disruption, delay, or congestion, the rail operators need to find alternative routes to deliver essential products and services and utilise the information of the speed limit change on rail tracks
- The collaboration and communication between all rail operators of passenger trains and freight trains: The difficulty of collaboration and communication between rail operators causes delays and low-quality service

A.2 INLAND WATERWAY FREIGHT OPERATIONAL BARRIERS

There are other operational barriers than what is in chapter one (IWA 2013):

- Lack of appropriate continuing development of waterway infrastructure, such as raising bridge headroom to facilitate the use of container barges
- Lack of operational experience in many types of industry, where transport managers are unfamiliar with processes, availability and costs
- Lack of knowledge about water-freight operational issues
- Inadequate promotion of waterborne freight
- Lack of immediate availability of suitable vessels or trained crew in some cases
- A planning system that does not adequately take account of waterway freight transport infrastructure needs at national, regional or local levels
- Lack of co-ordination between Government departments

APPENDIX B: ATC IMPUTED DATA

TABLE B- 1: Average working day of ATC data for 2015

Hour	TF	PC	LGV	HGVr	HGVa	Speed
1	121	81	4	2	19	57.47
2	70	42	3	2	16	57.62
3	58	32	4	1	14	57.61
4	60	34	4	1	13	57.98
5	117	65	6	3	29	58.08
6	382	228	19	12	73	57.96
7	887	563	53	27	128	56.86
8	1475	1024	86	50	128	52.41
9	1523	1051	87	55	143	49.70
10	1187	774	80	65	125	52.30
11	1109	716	80	62	112	53.53
12	1180	774	79	62	113	53.11
13	1283	864	75	57	117	51.81
14	1337	903	81	59	123	51.14
15	1418	955	87	63	131	49.72
16	1632	1111	101	70	140	37.97
17	1763	1235	93	51	143	28.20
18	1829	1356	60	30	119	30.50
19	1488	1159	42	17	53	48.89
20	940	729	25	9	36	54.66
21	664	513	17	5	27	55.20
22	476	369	11	3	20	55.87
23	385	296	7	4	18	55.71
24	242	175	7	3	22	56.68

TABLE B- 2: Average working day of ATC data for the year 2016

Hour	TF	PC	LGV	HGVr	HGVa	Speed
1	108	86	4	2	16	56.29
2	61	42	3	1	14	56.63
3	54	35	4	2	13	57.03
4	59	41	4	1	13	56.85
5	118	78	6	4	30	57.31
6	391	284	18	13	77	57.06
7	894	685	51	27	132	55.85
8	1519	1238	90	53	138	50.69
9	1582	1283	95	59	144	47.96
10	1187	914	83	66	124	52.06
11	1091	831	84	62	114	53.24
12	1174	914	84	62	115	52.69
13	1282	1029	80	55	117	51.85
14	1343	1079	85	58	120	51.42
15	1409	1128	90	64	128	50.12
16	1639	1327	105	71	135	39.11
17	1793	1509	96	47	140	28.89
18	1854	1644	61	30	118	30.64
19	1475	1358	45	16	56	48.64
20	926	852	27	8	39	53.90
21	651	600	17	5	29	54.28
22	471	433	12	4	22	54.61
23	395	364	8	4	19	55.05
24	228	195	6	3	23	56.08

TABLE B- 3: Average working day of ATC data for the year 2017

Hour	TF	PC	LGV	HGVr	HGVa	Speed
1	118	75	19	5	19	63.39
2	64	36	10	4	14	63.42
3	54	31	9	4	11	63.35
4	58	31	11	5	11	64.01
5	103	55	16	7	25	64.45
6	347	189	65	15	78	64.73
7	835	458	199	43	134	64.25
8	1387	848	348	66	124	60.49
9	1458	883	360	81	133	57.12
10	1113	619	280	97	117	59.46
11	1042	581	257	93	111	60.18
12	1113	640	271	89	113	59.84
13	1203	712	293	82	117	58.97
14	1267	744	309	90	123	59.08
15	1333	774	335	93	130	58.72
16	1550	913	403	96	139	51.05
17	1749	1065	459	80	144	35.02
18	1777	1177	439	51	111	38.94
19	1447	1013	341	36	56	55.84
20	917	667	196	20	35	61.62
21	620	458	121	14	26	62.48
22	436	328	82	8	18	62.29
23	342	258	63	6	15	62.26
24	210	150	34	8	19	62.83

TABLE B- 4: Average working day of ATC data for the year 2018

Hour	TF	PC	LGV	HGVr	HGVa	Speed
1	95	74	4	2	15	57.82
2	57	40	3	2	12	57.56
3	48	34	3	1	9	57.68
4	55	40	4	1	10	58.39
5	119	81	7	5	26	58.29
6	388	278	23	14	73	58.51
7	869	663	61	30	116	57.57
8	1387	1119	101	48	120	53.96
9	1417	1127	105	55	130	51.32
10	1099	837	91	64	108	53.82
11	1048	796	88	60	104	54.72
12	1127	876	88	59	105	54.28
13	1220	968	88	55	109	53.16
14	1283	1014	93	59	116	52.68
15	1359	1074	103	62	121	51.62
16	1552	1243	116	64	128	41.63
17	1718	1424	115	47	132	30.89
18	1756	1535	87	29	104	34.70
19	1382	1250	63	18	51	50.81
20	864	786	36	8	34	55.49
21	555	508	20	4	23	56.02
22	377	348	11	3	15	56.04
23	301	276	10	3	13	56.12
24	187	162	6	3	16	56.67

TABLE B- 5: Average working day of ATC data for the year 2015-2018

Hour	TF	PC	LGV	HGVr	HGVa	Speed
1	111	79	8	3	18	58.74
2	63	40	5	2	14	58.81
3	53	33	5	2	12	58.92
4	58	36	6	2	12	59.31
5	114	70	9	5	28	59.54
6	377	245	31	14	75	59.56
7	871	592	91	32	127	58.63
8	1442	1057	156	54	127	54.39
9	1495	1086	162	63	137	51.53
10	1146	786	134	73	119	54.41
11	1073	731	127	69	110	55.42
12	1149	801	130	68	111	54.98
13	1247	893	134	62	115	53.95
14	1307	935	142	67	121	53.58
15	1380	983	154	71	127	52.55
16	1593	1149	181	75	136	42.44
17	1756	1308	191	56	140	30.75
18	1804	1428	162	35	113	33.69
19	1448	1195	123	22	54	51.05
20	912	759	71	11	36	56.42
21	622	520	44	7	26	56.99
22	440	370	29	5	19	57.20
23	356	298	22	4	16	57.28
24	217	170	13	4	20	58.06

TABLE B- 6: Average day of ATC data for the year 2015

Hour	TF	PC	LGV	HGVr	HGVa	Speed
1	160	112	27	5	16	64.83
2	95	63	16	4	12	64.18
3	75	48	13	4	10	64.35
4	74	45	14	5	11	64.64
5	121	70	20	6	24	64.80
6	317	180	61	14	62	65.32
7	681	389	156	34	102	64.75
8	1050	649	253	51	98	62.08
9	1133	701	270	63	99	60.10
10	990	593	235	74	88	61.30
11	1018	631	232	71	83	61.41
12	1132	724	255	69	84	60.99
13	1241	812	278	65	87	60.30
14	1294	846	289	69	90	60.34
15	1324	856	304	71	93	60.05
16	1445	926	349	71	99	54.73
17	1558	1013	382	60	102	44.98
18	1561	1073	367	41	80	47.96
19	1272	915	286	29	43	58.32
20	859	643	173	17	26	62.34
21	598	454	111	12	21	63.19
22	422	324	75	8	14	63.21
23	322	248	56	6	12	63.32
24	225	167	37	6	15	63.44

TABLE B- 7: Average day of ATC data for the year 2016

Hour	TF	PC	LGV	HGVr	HGVa	Speed
1	134	114	5	2	13	59.15
2	84	69	4	1	10	58.29
3	68	56	4	1	7	58.42
4	69	55	4	1	9	59.15
5	124	90	7	4	22	59.08
6	335	247	18	11	58	59.35
7	702	538	47	23	94	58.76
8	1077	873	76	36	91	56.12
9	1140	918	80	43	99	54.53
10	990	787	73	48	83	56.01
11	1032	835	73	46	78	56.25
12	1148	950	75	45	79	55.62
13	1253	1054	76	42	81	54.63
14	1301	1090	80	45	85	54.33
15	1325	1106	84	46	88	53.50
16	1445	1212	93	47	93	46.84
17	1550	1328	92	35	95	39.78
18	1560	1390	72	23	75	42.36
19	1226	1123	52	14	38	53.73
20	820	756	31	7	26	56.87
21	548	508	18	4	18	57.10
22	364	339	10	3	12	57.07
23	297	276	9	3	10	57.35
24	200	178	7	3	12	57.98

TABLE B- 8: Average day of ATC data for the year 2017

Hour	TF	PC	LGV	HGVr	HGVa	Speed
1	142	119	5	2	16	58.79
2	89	70	4	1	13	58.27
3	70	53	4	1	12	58.29
4	64	49	4	1	10	58.56
5	101	71	5	3	22	58.62
6	279	198	15	10	57	58.69
7	613	448	41	21	103	58.19
8	985	783	65	37	100	54.96
9	1055	837	68	42	108	52.94
10	914	705	64	50	95	54.42
11	927	731	64	48	84	55.01
12	1024	829	64	47	84	54.61
13	1122	931	62	43	86	53.59
14	1168	969	65	45	90	53.13
15	1192	981	69	47	95	52.30
16	1301	1073	77	51	100	44.48
17	1372	1159	72	38	103	37.31
18	1396	1236	49	24	87	38.59
19	1124	1036	35	14	40	51.97
20	749	691	22	8	28	56.00
21	536	494	15	5	21	56.46
22	379	351	10	3	15	56.93
23	302	279	7	3	13	56.89
24	209	184	6	3	16	57.68

TABLE B- 9: Average day of ATC data for the year 2018

Hour	TF	PC	LGV	HGVr	HGVa	Speed
1	145	125	4	2	14	56.81
2	91	74	4	1	12	57.23
3	75	58	4	2	12	57.37
4	73	56	4	1	12	57.33
5	127	92	6	4	26	57.69
6	337	251	15	11	60	57.68
7	728	561	41	22	105	56.98
8	1168	952	69	39	108	53.51
9	1239	1013	73	46	107	51.62
10	1045	836	67	50	93	54.12
11	1063	861	68	48	86	54.66
12	1183	982	67	48	85	54.13
13	1306	1110	66	43	87	53.38
14	1347	1144	69	45	90	52.96
15	1380	1167	72	48	94	52.06
16	1522	1293	81	51	98	44.47
17	1610	1402	73	35	100	37.67
18	1627	1472	49	23	83	38.92
19	1286	1196	36	13	41	51.21
20	869	809	23	7	30	55.03
21	617	575	15	5	22	55.33
22	439	408	10	4	17	55.67
23	365	340	7	3	15	55.99
24	229	203	6	3	17	56.72

TABLE B- 10: Average day of ATC data for the year 2015-2018

Hour	TF	PC	LGV	HGVr	HGVa	Speed
1	145	118	10	3	15	59.90
2	90	69	7	2	12	59.49
3	72	54	6	2	10	59.61
4	70	51	7	2	10	59.92
5	118	81	10	4	24	60.05
6	317	219	27	12	59	60.26
7	681	484	71	25	101	59.67
8	1070	814	116	41	99	56.67
9	1142	867	123	48	103	54.80
10	985	730	110	55	90	56.46
11	1010	765	109	53	83	56.83
12	1122	871	115	52	83	56.34
13	1231	977	121	48	85	55.47
14	1278	1012	126	51	89	55.19
15	1305	1027	132	53	92	54.48
16	1428	1126	150	55	97	47.63
17	1522	1226	155	42	100	39.94
18	1536	1293	134	28	81	41.96
19	1227	1067	102	17	40	53.81
20	824	725	62	10	27	57.56
21	575	508	40	6	21	58.02
22	401	356	27	4	15	58.22
23	321	286	20	4	12	58.39
24	216	183	14	4	15	58.95